VOL. 689 NO. 2 13 JANUARY 1995
THIS ISSUE COMPLETES VOL. 689

JOURNAL OF CHROMATOGRAPHY A

INCLUDING ELECTROPHORESIS AND OTHER SEPARATION METHODS

ELSEVIER

JOURNAL OF CHROMATOGRAPHY A

INCLUDING ELECTROPHORESIS AND OTHER SEPARATION METHODS

Scope. The *Journal of Chromatography A* publishes papers on all aspects of **chromatography, electrophoresis** and related methods. Contributions consist mainly of research papers dealing with chromatographic theory, instrumental developments and their applications. In the *Symposium volumes*, which are under separate editorship, proceedings of symposia on chromatography, electrophoresis and related methods are published. *Journal of Chromatography B: Biomedical Applications* —This journal, which is under separate editorship, deals with the following aspects: developments in and applications of chromatographic and electrophoretic techniques related to clinical diagnosis or alterations during medical treatment; screening and profiling of body fluids or tissues related to the analysis of active substances and to metabolic disorders; drug level monitoring and pharmacokinetic studies; clinical toxicology; forensic medicine; veterinary medicine; occupational medicine; results from basic medical research with direct consequences in clinical practice.

Submission of Papers. The preferred medium of submission is on disk with accompanying manuscript (see *Electronic manuscripts* in the Instructions to Authors, which can be obtained from the publisher, Elsevier Science B.V., P.O. Box 330, 1000 AH Amsterdam, Netherlands). Manuscripts (in English; *four* copies are required) should be submitted to: Editorial Office of *Journal of Chromatography A*, P.O. Box 681, 1000 AR Amsterdam, Netherlands, Telefax (+31-20) 485 2304, or to: The Editor of *Journal of Chromatography B: Biomedical Applications*, P.O. Box 681, 1000 AR Amsterdam, Netherlands. Review articles are invited or proposed in writing to the Editors who welcome suggestions for subjects. An outline of the proposed review should first be forwarded to the Editors for preliminary discussion prior to preparation. Submission of an article is understood to imply that the article is original and unpublished and is not being considered for publication elsewhere. For copyright regulations, see below.

Publication information. *Journal of Chromatography A* (ISSN 0021-9673): for 1995 Vols. 683–714 are scheduled for publication. *Journal of Chromatography B: Biomedical Applications* (ISSN 0378-4347): for 1995 Vols. 663–674 are scheduled for publication. Subscription prices for *Journal of Chromatography A*, *Journal of Chromatography B: Biomedical Applications* or a combined subscription are available upon request from the publisher. Subscriptions are accepted on a prepaid basis only and are entered on a calendar year basis. Issues are sent by surface mail except to the following countries where air delivery via SAL is ensured: Argentina, Australia, Brazil, Canada, China, Hong Kong, India, Israel, Japan, Malaysia, Mexico, New Zealand, Pakistan, Singapore, South Africa, South Korea, Taiwan, Thailand, USA. For all other countries airmail rates are available upon request. Claims for missing issues must be made within six months of our publication (mailing) date. Please address all your requests regarding orders and subscription queries to: Elsevier Science B.V., Journal Department, P.O. Box 211, 1000 AE Amsterdam, Netherlands. Tel.: (+31-20) 485 3642; Fax: (+31-20) 485 3598. Customers in the USA and Canada wishing information on this and other Elsevier journals, please contact Journal Information Center, Elsevier Science Inc., 655 Avenue of the Americas, New York, NY 10010, USA, Tel. (+1-212) 633 3750, Telefax (+1-212) 633 3764.

Abstracts/Contents Lists published in Analytical Abstracts, Biochemical Abstracts, Biological Abstracts, Chemical Abstracts, Chemical Titles, Chromatography Abstracts, Current Awareness in Biological Sciences (CABS), Current Contents/Life Sciences, Current Contents/Physical, Chemical & Earth Sciences, Deep-Sea Research/Part B: Oceanographic Literature Review, Excerpta Medica, Index Medicus, Mass Spectrometry Bulletin, PASCAL-CNRS, Referativnyi Zhurnal, Research Alert and Science Citation Index.

US Mailing Notice. *Journal of Chromatography A* (ISSN 0021-9673) is published weekly (total 52 issues) by Elsevier Science B.V., (Sara Burgerhartstraat 25, P.O. Box 211, 1000 AE Amsterdam, Netherlands). Annual subscription price in the USA US$ 5389.00 (US$ price valid in North, Central and South America only) including air speed delivery. Second class postage paid at Jamaica, NY 11431. **USA POSTMASTERS**: Send address changes to *Journal of Chromatography A*, Publications Expediting, Inc., 200 Meacham Avenue, Elmont, NY 11003. Airfreight and mailing in the USA by Publications Expediting.

See inside back cover for Publication Schedule, Information for Authors and information on Advertisements.

0021-9673/95/$09.50

Printed in the Netherlands

CONTENTS

(Abstracts/Contents Lists published in Analytical Abstracts, Biochemical Abstracts, Biological Abstracts, Chemical Abstracts, Chemical Titles, Chromatography Abstracts, Current Awareness in Biological Sciences (CABS), Current Contents/Life Sciences, Current Contents/Physical, Chemical & Earth Sciences, Deep-Sea Research/Part B: Oceanographic Literature Review, Excerpta Medica, Index Medicus, Mass Spectrometry Bulletin, PASCAL-CNRS, Referativnyi Zhurnal, Research Alert and Science Citation Index)

REGULAR PAPERS

Column Liquid Chromatography

Gas Chromatography

Electrophoresis

(Continued overleaf)

Contents (continued)

BOOK REVIEWS

ELSEVIER

Journal of Chromatography A, 689 (1995) 177–187

JOURNAL OF CHROMATOGRAPHY A

Performance of an ethoxyethylacrylate stationary phase for open-tubular liquid chromatography

Remco Swart, Johan C. Kraak*, Hans Poppe

Laboratory for Analytical Chemistry, University of Amsterdam, Nieuwe Achtergracht 166, 1018 WV Amsterdam, Netherlands

First received 27 June 1994; revised manuscript received 8 September 1994

Abstract

Fused-silica capillaries of I.D. ca 11.4 μm were coated with polyacrylate layers. The layers consisted of copolymers of silicone acrylate and ethoxyethylacrylate which were polymerized in situ by UV irradiation. Capillaries with phase ratios up to 0.9 were prepared. This results in very high mass loadabilities so that solute amounts suitable for UV detection can be injected without overloading the stationary phase. This is illustrated by the separation of various mixtures containing phenolic and aromatic compounds. The retention behaviour and the kinetic performance were studied with both UV and laser-induced fluorescence detection. On a 5-m column more than 10^6 plates could be generated for anthracene. Further, the possibility of on-column preconcentration and the effect of temperature on the kinetic performance were investigated on this stationary phase.

1. Introduction

In chromatography, the highest separation efficiency and speed can be obtained with open-tubular columns. For liquid chromatography, these attractive features can only be realized by using columns with internal diameters in the range 1–10 μm. In contrast to gas chromatography, where capillary columns are now applied almost exclusively, all routine liquid chromatographic separations are still performed in packed columns. The full exploration of open-tubular liquid chromatography (OT-LC) is hampered mainly by two facts: (i) the lack of sensitive, universal detectors capable of detecting picogram amounts of solute in 40–200-pl peak volumes and (ii) problems encountered with the immobilization of a uniform stationary phase layer on the inside surface of the capillary with sufficient sample capacity to avoid overloading. Although there has been some progress in the development of miniaturized detection systems, mainly initiated by the interest in capillary zone electrophoresis, detection in OT-LC is still the main bottleneck. In order partly to circumvent this detection problem, it is advantageous to apply a thick stationary phase by which larger solute concentrations can be injected and detection is simplified.

Several methods have been utilized to realize a retentive layer, of which the static coating procedure [1,2] and the creation of a porous structure inside the capillary [3–5] have been studied most thoroughly. One of the most promising procedures in terms of phase ratio and success rate is in situ photopolymerization of acrylates.

In this paper, we describe the results of an investigation to prepare a thick silicone acrylate–

* Corresponding author.

0021-9673/95/$09.50
SSDI 0021-9673(94)00887-6

ethoxyethylacrylate (SiA–EEA) stationary phase in 10-μm capillaries for reversed phase OT-LC.

2. Experimental

2.1. Apparatus

The OT-LC set-up used for the chromatographic measurements is depicted in Fig. 1. It consisted of an HPLC pump (Spectroflow 400; Kratos, Rotterdam, Netherlands), a splitting device used to reduce the flow from ml/min to μl/min and a second splitting device used to diminish the injection volume. The volume of the applied injection valve was 0.2 μl; splitting ratios ranged from 5 in the preconcentration experiments to 1250 under normal conditions. The pressure was monitored with a digital pressure sensor (Type 4041A200; Kistler, Winterthur, Switzerland) combined with a current amplifier (Type 4061; Kistler) and a recorder (Model BD111; Kipp & Zonen, Delft, Netherlands). Two on-column detection systems were employed, a UV absorbance detector (Kratos Model 757) using a laboratory-built on-column detection cell with adjustable slit [6] (the detector rise time was set to 0.1 s) and a helium–cadmium laser (λ_{ex} = 325 nm) (Model 356 XM; Omnichrome, Chino, CA, USA) used as a light source for laser-induced fluorescence detection (LIF) with emission wavelength set at 380 nm. The fluorescence yield was measured with a photomultiplier tube (Type 6225 S; EMI, Hayes, UK).

2.2. Materials

Fused-silica capillaries with I.D. ca. 11.4 μm, having an acrylate outside protective coating, were a kind gift from Philips Research Laboratories (Eindhoven, Netherlands). The outside acrylate coating possessed sufficient UV transparency for in situ photopolymerization. To initiate the polymerization reaction α,α-dimethoxy-α-phenylacetophenone (DMPA) was used (Irgacure 651; Ciba-Geigy, Basle, Switzerland).

HPLC-grade methanol was obtained from Janssen (Beerse, Belgium), ethoxyethylacrylate (EEA) and 3-(methacryloxy)propyltrimethoxysilane (γ-MPS) from Fluka (Buchs, Switzerland) and silicone acrylate (SiA) (Tegomer V-Si2150) from Goldsmidt (Essen, Germany).

2.3. Coating procedure

The photopolymerization of acrylates to immobilize a polymer film in fused-silica capillaries has been described before [7]. Briefly, the procedure consists of the following successive steps: etching of the fused silica surface to enlarge the number of silanol groups; silylation of the surface with a silyl reagent containing an acrylate group (γ-MPS), (the acrylate group on the surface is needed to anchor the polymer layer);

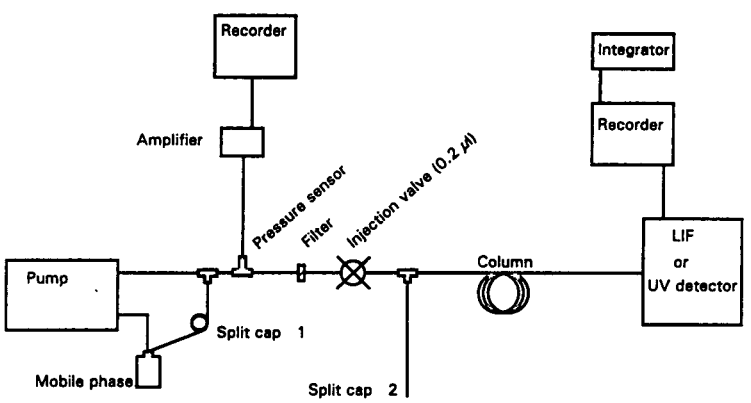

Fig. 1. Schematic diagram of the OT-LC system.

Table 1
Experimental coating conditions and dimensions of the fused-silica columns

Capillary	L (cm)	Monomer (%, v/v)	d_c (μm)	d_f (μm)	V_s/V_m
1	110.3	10% EEA–10% SiA	8.26	1.56	0.90
2	494.0	10% EEA–10% SiA	8.38	1.51	0.85

DMPA concentration, 3.0 mg ml^{-1} for both monomer solutions; solvent, acetone–pentane (1:1); light intensity, 0.14 mW; irradiation time, 350 s; d_c = column diameter; d_f = film thickness; V_s/V_m = phase ratio.

filling the capillary with a mixture of SiA and EEA monomers in acetone–pentane (1:1) containing a photoinitiator, then irradiating the capillary with UV radiation to initiate the polymerization; evaporation of the solvent; and curing at elevated temperature.

Capillaries of length ca. 1 m (capillary 1) and 5 m (capillary 2) were treated according to the aforementioned procedure. The I.D.s of the capillaries were calculated with the Poiseuille equation by measuring the holdup time of an unretained solute. The polymer film thickness, needed to calculate the phase ratio, was determined by subtracting the radius of the coated capillary from the initial capillary radius. The coating conditions and capillary characteristics are given in Table 1.

2.4. Chromatography

Pure methanol, acetonitrile or their mixtures were used as mobile phases. Solutes were dissolved in methanol, except in the preconcentration experiments, where they were dissolved in water. The chromatographic results were evaluated as described previously [7].

3. Results and discussion

3.1. Solvent evaporation

Previously we have reported some problems that can occur during the evaporation step with other acrylate phases [7]. With the present phase such difficulties did not occur during the preparation of the two columns under study, or during the preparation of columns with smaller diameters. The removal of the solvent from a capillary in time can in principle be derived from Poiseuille's law, resulting in [8]

$$L_c = Cd_c\sqrt{t} \quad (1)$$

where L_c = length of the capillary, C = constant, d_c = I.D. of the capillary and t = time.

The evaporation of the solvent from capillary 2 was followed as a function of time. In Fig. 2 the positions of the meniscus at different time intervals in the evaporation process are plotted against elapsed time. The solid line represents an empirical relationship. For this curve the constant C in Eq. 1 was adapted for the first two

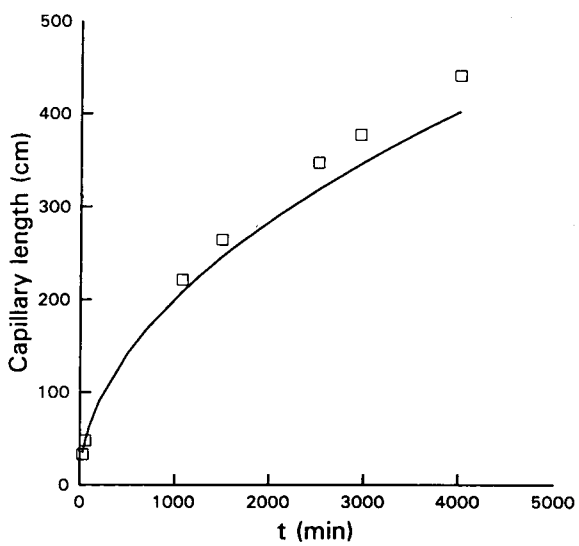

Fig. 2. Evaporation process in capillary 2. The capillary length refers to the part of the capillary from which the solvent has been evaporated. □ = Experimental data. The solid line is an empirical relationship based on the first two data points.

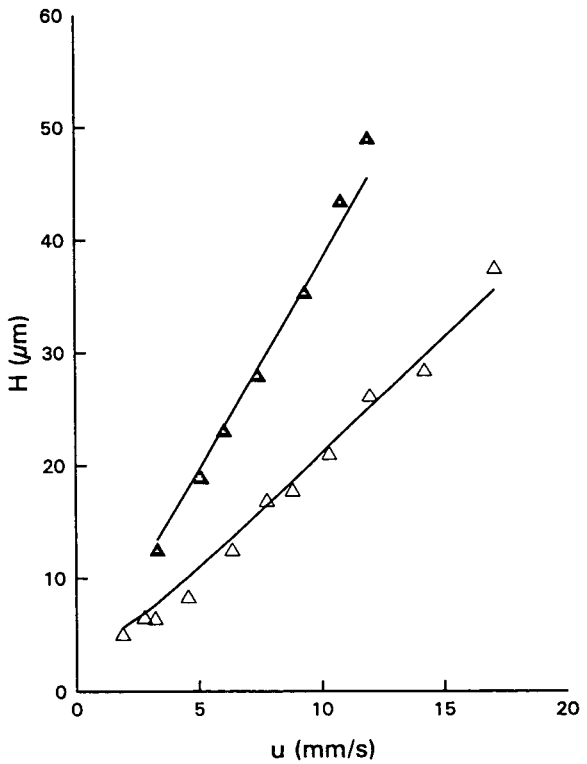

Fig. 3. Experimental and theoretical plate-height curves of anthracene on capillary 2. Mobile phase: ▲ = methanol; △ = acetonitrile. Solid lines represents theoretical Golay curves.

experimental data points. There is good agreement between the curve and the experimental data points. As can be seen from Fig. 2, it takes ca. 3.5 days to empty capillary 2. Eqn. 1 can be used to predict the evaporation time reasonably well. For instance, the complete evaporation of the solvent from a 10 m × 8.4 μm I.D. capillary under identical conditions will take about 14 days. The same time is predicted to remove the solvent from a 5 m × 4.2 μm I.D. capillary.

Table 2
Diffusion coefficients (10^{-10} m^2 s^{-1}) of anthracene derivatives in SiA–EEA stationary phases using methanol as mobile phase

Compound	Capillary	
	1	2
Anthracenemethanol	0.62	0.85
Anthracenecarbonitrile	0.95	1.40
Anthracene	1.40	2.20
Fluoranthene	1.10	1.40
9-Phenylanthracene	0.73	0.90
1,2-Benzanthracene	1.10	1.20

3.2. Kinetic performance

The theoretical plate height (H) in OT-LC can be calculated with the extended Golay equation according to

$$H = \frac{2D_m}{u} + \frac{(1 + 6k' + 11k'^2)d_c^2 u}{96D_m(1 + k')^2} + \frac{2k'd_f^2 u}{3D_s(1 + k')^2} \quad (2)$$

where u = linear velocity of the mobile phase, d_c = I.D. of the capillary, d_f = film thickness of the stationary phase, D_m = diffusion coefficient in the mobile phase, D_s = diffusion coefficient in the stationary phase and k' = capacity factor.

In the kinetic studies, reliable H values were obtained by using LIF and split injection, leading to negligible extra-column effects and sufficiently low concentrations. To obtain a high mass loadability and thus simplify detection in OT-LC, thick stationary phases have to be immobilized. However, with increasing film thickness the contribution of the third term in the extended Golay equation increases significantly. Therefore, in order to achieve efficient separations it is crucial to select a phase with a large diffusivity.

By fitting the experimental plate heights with the extended Golay equation, diffusion coefficients in the stationary phase, D_s, can be calculated as all other parameters in Eq. 1 are known or can be calculated. Diffusion coefficients in the mobile phase, D_m, were calculated with the Wilke–Chang equation. Fig. 3 shows H–u curves for anthracene obtained on column 2 using 100% methanol and 100% acetonitrile as mobile phases. The theoretical curves, calculated with the extended Golay equation, are included. Diffusion coefficients of anthracene used for the calculation of the Golay values are $2.2 \cdot 10^{-10}$ and $2.7 \cdot 10^{-10}$ m^2 s^{-1} applying methanol and acetonitrile, respectively. The contribution of the third term to the overall plate height is around 50% using acetonitrile and 45% using methanol

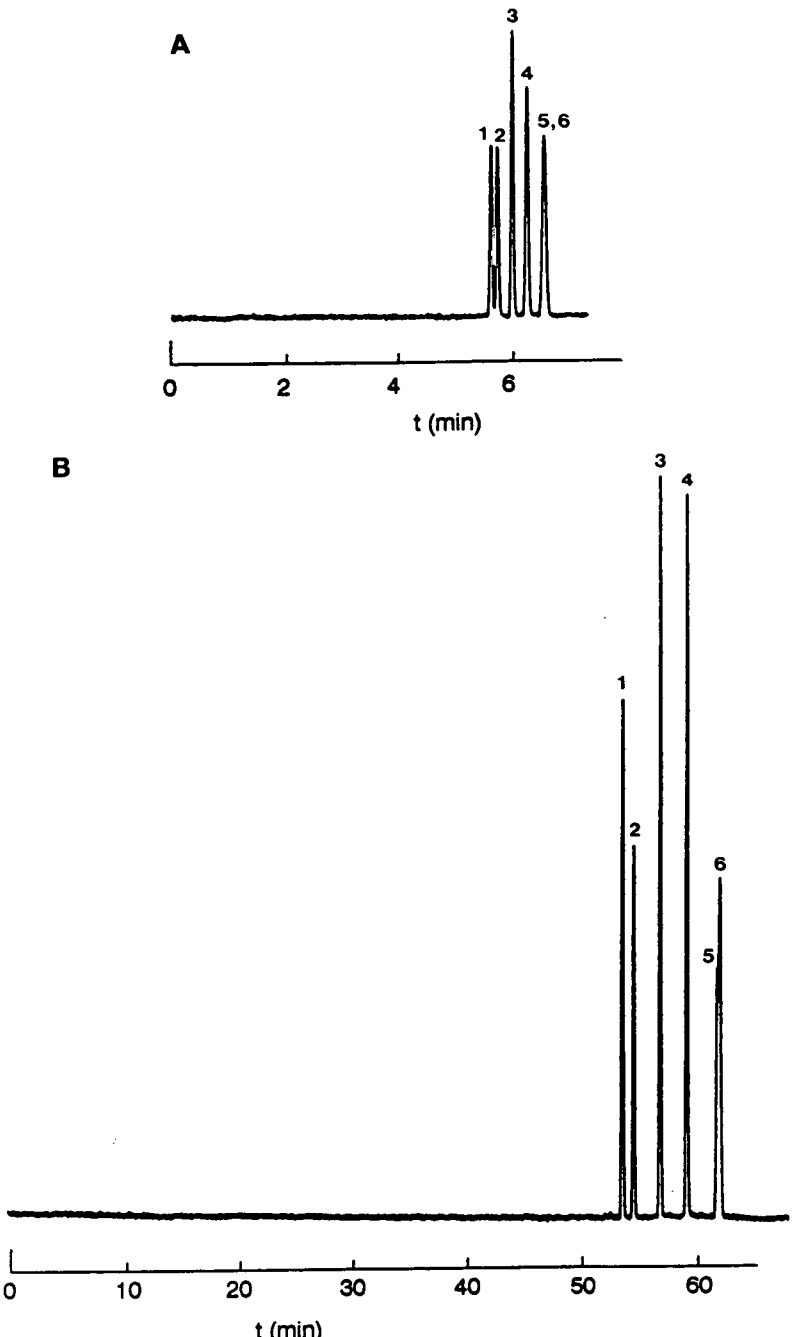

Fig. 4. Chromatograms of anthracene derivatives on column 2 at two mobile phase velocities, u: (A) 18.2; (B) 1.92 mm s^{-1}. Mobile phase: acetonitrile. Solutes: 1 = anthracenemethanol; 2 = anthracenecarbonitrile; 3 = anthracene; 4 = fluoranthene; 5 = 1,2-benzanthracene; 6 = phenylanthracene.

as mobile phase. There is good agreement between the extended Golay equation and the experimental data points. The diffusion coefficients calculated for various anthracene derivatives are given in Table 2.

Compared with previous immobilized stationary phases such as lauryl acrylate (LA), butyl acrylate (BA) and ethylhexyl acrylate (EHA) [7], the diffusion coefficients appear to be larger in the ethoxyethylacrylate polymer layer. On SiA–BA-coated capillaries a diffusion coefficient of $0.77 \cdot 10^{-10}$ m^2 s^{-1} was found for 1,2-benzanthracene using methanol as mobile phase, whereas a value of $1.15 \cdot 10^{-10}$ m^2 s^{-1} was found with SiA–EEA-coated capillaries.

An illustration of the performance of the 5-m capillary at two linear velocities can be seen in Fig. 4. Two solutes, 9-phenylanthracene and 1,2-benzanthracene, have similar capacity factors and cannot be separated at higher velocities (Fig. 4A). However, when the velocity of the mobile is reduced to near the optimum (Fig. 4B), a marginal separation between these compounds can be achieved. Under these conditions 784 000, 1 005 000 and 807 000 plates are generated for anthracenecarbonitrile, anthracene and fluoranthene, respectively.

3.3. Retention and selectivity

The retention behaviour of the SiA–EEA stationary phase was studied with several classes of compounds. The capacity factors of various anthracene derivatives remained constant for several weeks for all mobile phases. In this period a maximum fluctuation in capacity factors of 5% was observed. Within a day, the fluctuations of the capacity factors were usually 1–3%. As the capillaries were not thermostated, these fluctuations are acceptable. The distribution co-

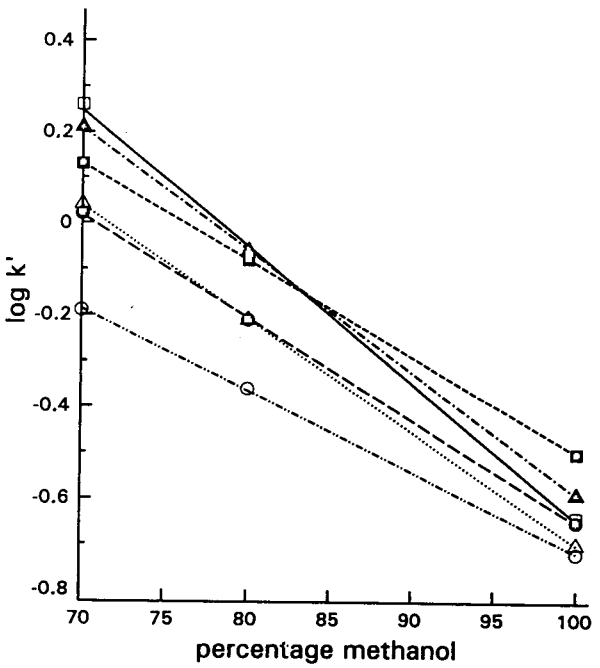

Fig. 5. Effect of the mobile phase composition on k' of phenolic compounds on capillary 2. ○ = Phenol; △ = 3-ethylphenol; □ = 2-*sec.*-butylphenol; ● = 2-methylphenol; ▲ = 3-chlorophenol; ■ = 2-nitrophenol.

Table 3
Distribution coefficients, K_i, and selectivity factors, $a_{i,j}$, of anthracene derivatives on SiA–EEA-coated capillaries

Compound	Methanol mobile phase				Acetonitrile mobile phase			
	Capillary 1		Capillary 2		Capillary 1		Capillary 2	
	K_i	$a_{j,i}$	K_i	$a_{j,i}$	K_i	$a_{j,i}$	K_i	$a_{j,i}$
Anthracenemethanol	0.41		0.42		0.29		0.29	
Anthracenecarbonitrile	0.71	1.72	0.75	1.76	0.33	1.14	0.32	1.08
Anthracene	0.78	1.10	0.83	1.11	0.38	1.18	0.38	1.19
Fluoranthene	0.99	1.27	1.06	1.28	0.45	1.17	0.44	1.16
9-Phenylanthracene	1.06	1.07	1.13	1.07	0.52	1.15	0.52	1.18
1,2-Benzanthracene	1.22	1.15	1.30	1.14	0.52	1.00	0.52	1.00

efficients, calculated from the capacity factor and phase ratio according to $K_i = k_i(V_m/V_s)$, and selectivity factors are listed in Table 3. The distribution coefficients with methanol are considerably larger than with acetonitrile, indicating the reversed-phase liquid chromatographic behaviour of the layer. Also, a significantly different selectivity is found with the two mobile phases, as is known from RP-HPLC. The small variations in retention on both columns indicate that the specific nature of the layers is constant.

In a previous paper [7] we reported the retention behaviour of anthracene derivatives on polyacrylate stationary phases using aqueous mobile phases. In this work the effect of the addition of water to the mobile phase on retention was studied with phenolic compounds. In Fig. 5 the logarithms of the capacity factors of phenolic compounds are plotted against the percentage of methanol in the mobile phase. The data points represent mean capacity factors of at least five measurements. As expected for RPLC, a linear relationship between the percentage of water and log k' was observed for all solutes. The correlation coefficients ranged from 0.9978 for 2-*sec.*-butylphenol to 0.9995 for 3-ethylphenol and 2-chlorophenol. Selectivity changes occur with increasing water content, resulting in a reversal of the elution order of some of the solutes.

3.4. Effect of temperature

According to the Golay equation, the contribution of the second and third terms to the overall plate height decreases when diffusion increases. Larger diffusion coefficients and consequently smaller plate heights can be realized by increasing the temperature, as has been shown by Liu and co-workers [9,10]. In addition, temperature will influence the capacity factors and selectivity.

The effect of temperature was investigated by measuring H–u curves for two phenolic compounds at 20 and 60°C with pure methanol as the mobile phase. For that purpose the OT-LC system represented in Fig. 1 was extended with a thermostated water-bath in which 95% of the capillary could be accommodated. The results of these measurements are shown in Fig. 6. Increasing the column temperature clearly decreases the plate heights. The total effect cannot fully be attributed to larger diffusion, however, since the capacity factors also decreases (by ca. 15% at 60°C).

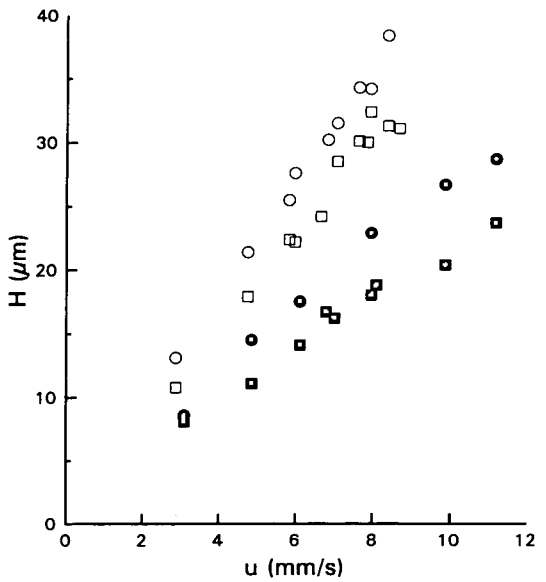

Fig. 6. Effect of temperature on the plate height for two phenolic compounds on capillary 2. □ = 2-Ethylphenol at 20°C; ○ = 2-*sec.*-butylphenol at 20°C; ■ = 2-ethylphenol at 60°C; ● = 2-*sec.*-butylphenol at 60°C.

The capacity factors appear to be more affected by temperature with aqueous mobile phases. Fig. 7 shows the effect of temperature on the separation of alkylphenols. The separation time can be shortened by about 30% at 60°C without significantly changing the resolution. Di-*tert.*-butylphenol showed the strongest decrease in k', of ca. 70%.

3.5. UV detection

The thick immobilized acrylate layers possess a high mass loadability, which opens the way to apply a less sensitive detection method, such as UV absorbance, without overloading the stationary phase. The use of UV detection will extend the applicability in OT-LC considerably.

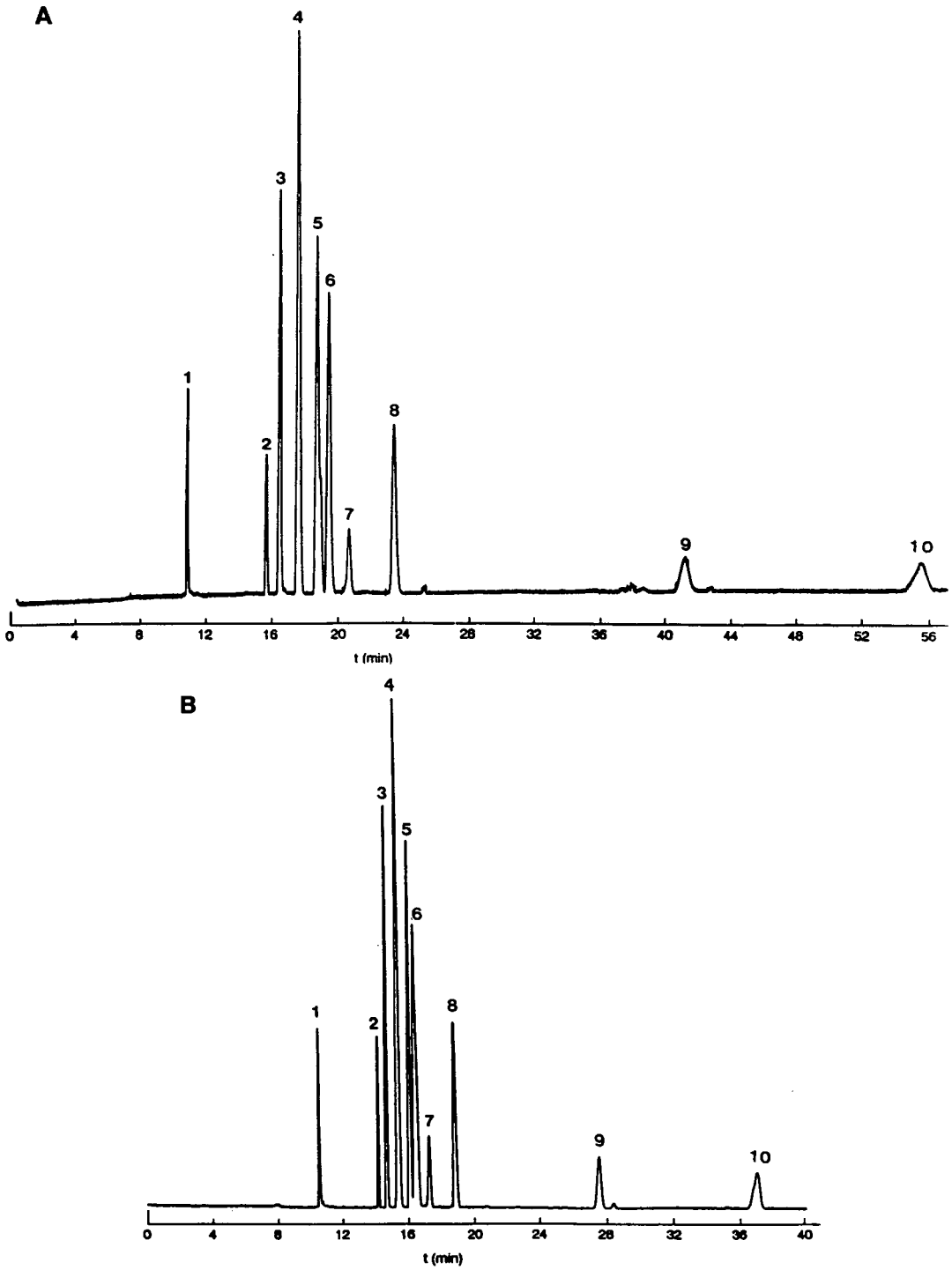

Fig. 7. Separation of a mixture of alkylphenols on capillary 2 at (A) 20 and (B) 60°C. Mobile phase: methanol–water (80:20). UV detection at 210 nm. Solutes: 1 = Salicylate; 2 = phenol; 3 = 3-methylphenol; 4 = 3-ethylphenol; 5 = 2-methylphenol; 6 = dimethylphenols; 7 = *n*-propylphenol; 8 = 2-*sec*.-butylphenol; 9 = di-*tert*.-butylphenol; 10 = tri-*tert*.-butylphenol.

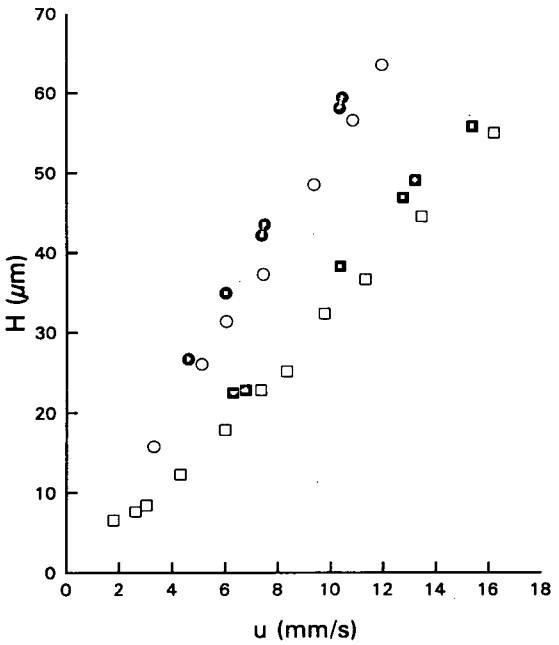

Fig. 8. Experimental plate heights for anthracenemethanol on column 2 using on-column UV and LIF detection. Mobile phase and detection: ● = methanol, UV; ○ = methanol, LIF; ■ = acetonitrile, UV; □ = acetonitrile, LIF.

In order to determine the performance with on-column UV detection, the efficiency obtained with LIF and UV detection was measured on capillary 2. Anthracenemethanol was chosen as the test compound because of its large molar absorptivity and native fluorescence. Fig. 8 shows H–u plots for anthracenemethanol using methanol and acetonitrile as mobile phases. Compared with LIF detection, an extra contribution to the plate height is found when UV detection is applied (solid symbols). If the time constant of the detector were responsible for the extra contribution, the deviation from the LIF data points would be more severe at higher mobile phase velocities, but this was not observed.

Also, the detector cell volume cannot be the cause of the increased plate heights. The solute band width of a peak with 100 000 plates on capillary 2 is 15.8 mm according to $\sigma_z^2 = HL$. As the window width of the detector cell is 1 mm, this cannot be the cause of the extra-column peak broadening. Although we have no explanation yet for this extra peak broadening, the 10%

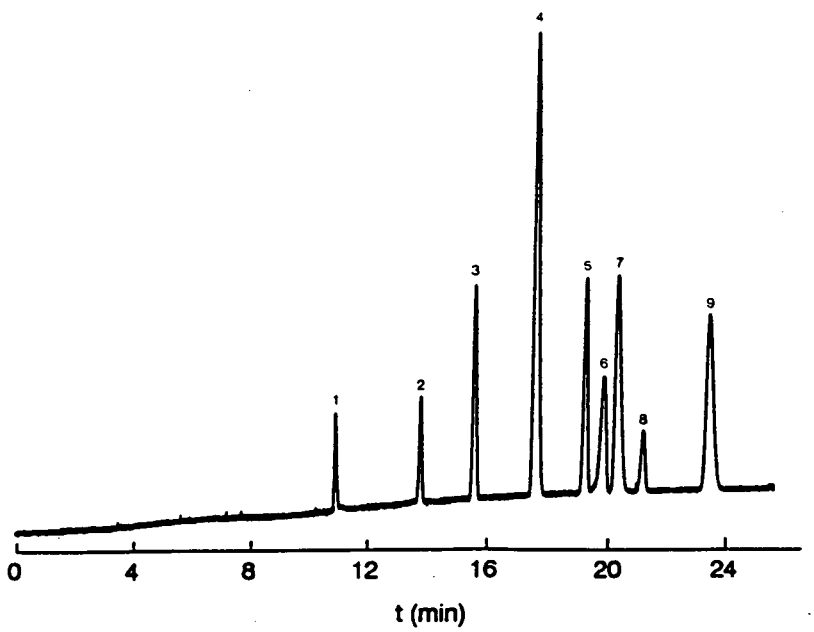

Fig. 9. Separation of a mixture of aromatic compounds using on-column UV detection. Mobile phase: methanol–water (80:20). Solutes: 1 = salicylate; 2 = phenylpropanol; 3 = phenol; 4 = 3-ethylphenol; 5 = methoxybenzene; 6 = 2-nitrophenol; 7 = 3-chlorophenol; 8 = toluene; 9 = 2-*sec.*-butylphenol.

extra broadening is acceptable in practice as the resolution changes with the square root of the plate height. In order to show the applicability of on-column UV detection, the separation of a mixture of aromatic compounds using UV detection is presented in Fig. 9.

3.6. Preconcentration

The justification for studying on-column preconcentration in OT-LC is twofold: on the one hand, the concentration detectability can be improved, and on the other, split injection, which may be less reproducible, could be avoided by using this technique.

For this preconcentration experiment, increasing volumes of solutions of phenol in water and in the mobile phase were injected and the plate numbers measured. The mean plate numbers of at least three measurements are given in Fig. 10 as a function of injected volume. It can be seen that when phenol is dissolved in the mobile phase, up to 160 pl can be injected without changing the plate number. With larger injection volumes the plate number decreases steeply. However, on injecting phenol dissolved in water, the plate number remains approximately constant up to 40 nl. Under these conditions a preconcentration factor of 250 can be realized for phenol. Larger preconcentration factors can be expected for less polar, more retained compounds.

Fig. 11 shows the separation of an aqueous solution containing catechol and phenol present at concentrations of $9.8 \cdot 10^{-4}$ and $8.5 \cdot 10^{-4}$ mol^{-1} l, respectively. These concentrations are approximately one order of magnitude above the detection limit. The injected solvent, 22.6 nl, fills the first 41 cm of the capillary while the solutes were concentrated at the head of the column.

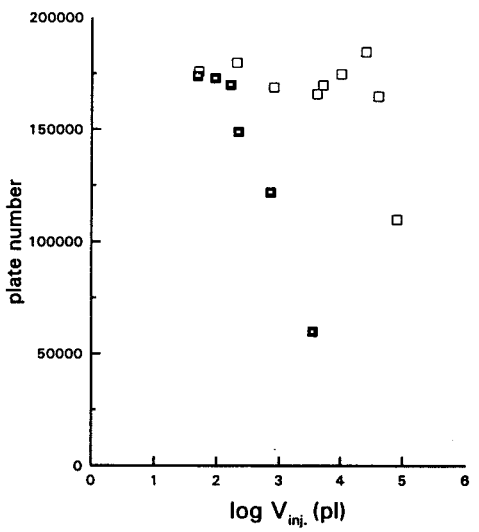

Fig. 10. Plate number versus injection volume on capillary 2, (□) with and (■) without preconcentration conditions. Mobile phase, methanol; UV detection at 210 nm; amount of phenol injected, 6.8 pmol.

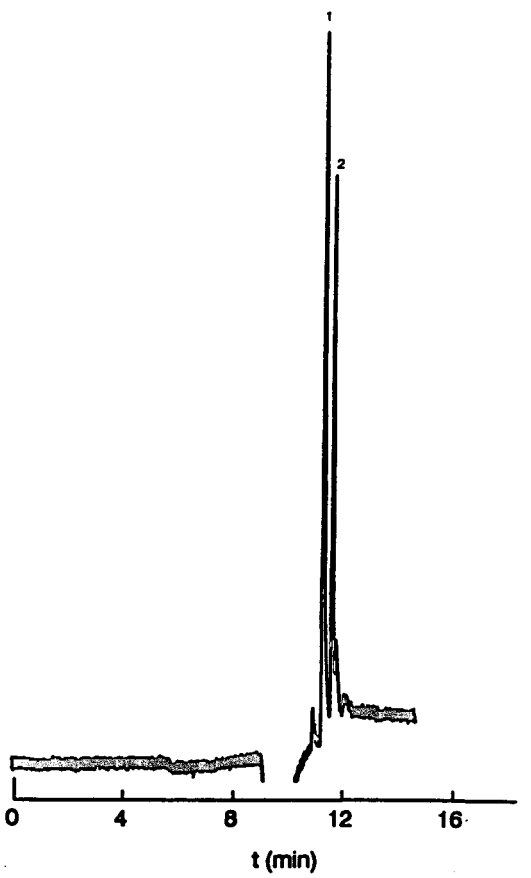

Fig. 11. Separation of (1) catechol ($9.8 \cdot 10^{-4}$ mol^{-1}) and (2) phenol ($8.5 \cdot 10^{-4}$ mol^{-1}). Mobile phase, methanol; UV detection at 210 nm; volume injected, 22.6 nl.

The water plug can be seen as a dip in the baseline.

References

[1] K. Göhlin and M. Larsson, *J. Microcol. Sep.*, 3 (1991) 547.
[2] K. Göhlin and M. Larsson, *J. Chromatogr.*, 645 (1993) 41.
[3] P.P.H. Tock, G. Stegeman, R. Peerboom, H. Poppe, J.C. Kraak and K.K. Unger, *Chromatographia*, 24 (1987) 617.
[4] P.P.H. Tock, C. Boshoven, H. Poppe, J.C. Kraak and K.K. Unger, *J. Chromatogr.*, 477 (1989) 95.
[5] A.L. Crego, J.C. Díez-Masa and M.V. Dabrio, *Anal. Chem.*, 65 (1993) 1615.
[6] G.J.M. Bruin, G. Stegeman, A.C. van Asten, X. Xu, J.C. Kraak and H. Poppe, *J. Chromatogr.*, 559 (1991) 163.
[7] R. Swart, J.C. Kraak and H. Poppe, *J. Chromatogr. A*, 670 (1993) 25.
[8] C.P.M. Schutjes, *Ph.D. Thesis*, Technical University, Eindhoven, 1983, p. 95.
[9] G. Liu, N. Djordjevic and F. Erni, *J. Chromatogr.*, 592 (1992) 239.
[10] G. Liu, L. Svenson, N. Djordjevic and F. Erni, *J. Chromatogr.*, 633 (1993) 25.

ELSEVIER

Journal of Chromatography A, 689 (1995) 189–193

JOURNAL OF CHROMATOGRAPHY A

Imprintable brush-type chiral stationary phase

Christopher J. Welch

Regis Technologies, Inc., 8210 Austin Avenue, Morton Grove, IL 60053, USA

First received 30 August 1994; revised manuscript received 21 October 1994; accepted 21 October 1994

Abstract

A chiral stationary phase (CSP) based upon a previously studied naphthamide atropisomer is described. Although CSPs based upon imprinted polymers have been known for some time, this naphthamide-derived CSP is the first reported example of an imprintable brush-type CSP. Deracemization of the racemic CSP using a soluble enantiopure imprint molecule affords a CSP which resolves the enantiomers of the imprint molecule and related compounds. A time-dependent HPLC study of the reversion of the imprinted stationary phase to the racemic form was performed, with a decrease in enantioselectivity being noted over a period of two weeks at room temperature, after which time the stationary phase was no longer capable of resolving enantiomers. Speculations about the potential utility of such CSPs are offered.

1. Introduction

The idea that a material could be somehow "imprinted" by a probe molecule so as to display at some later time an enhanced retention for that compound was originally conceived by Pauling [1], who suggested in 1940 that some such process might account for the ability of the immune system to mount an antibody response to an exceedingly wide variety of antigen structures. Realizing that a single polypeptide chain could exist in a multitude of low energy conformations, Pauling suggested that in the presence of different imprint molecules a single polypeptide chain could fold to form a variety of different antibody conformers, each with specific affinity for their imprint molecules. Later research showed that the diversity in immune response is in fact due to a more or less random splicing of bits of DNA coding for antibody structure, with a positive selection for those cells which produce antibodies which bind to the invading antigen [2,3]. Nevertheless, Pauling's hypothesis has given rise to a number of investigations of imprinted stationary phases for chromatographic separations [4–10]. Typically these stationary phases are produced by polymerizing a monomer in the presence of a imprint compound, milling and sizing the resulting polymer, and removal of the imprint compound by leaching (Fig. 1).

From the outset, much of the work in this field has focused on the production of chiral stationary phases (CSPs) for the chromatographic separation of enantiomers. Many of these CSPs have shown high levels of enantioselectivity, although the irregular nature of the stationary phase particles and the wide distribution of binding site affinities has historically resulted in poor chromatographic efficiency, particularly for the more retained enantiomer. Nevertheless, there has been continuing progress in producing more

0021-9673/95/$09.50
SSDI 0021-9673(94)01038-2

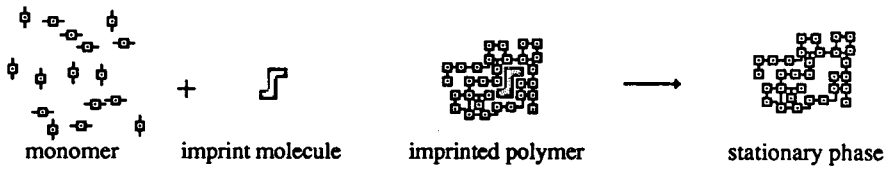

Fig. 1. Typical production of an imprinted polymer stationary phase involves polymerization of a monomer in the presence of an imprint compound followed by removal of the imprint compound by leaching.

efficient stationary phases. In the present study the first example of a silica-based imprintable brush-type CSP is presented.

A previous study of the chromatographic separation of the slowly interconverting enantiomers of a series of naphthamide atropisomers showed that separation factors in the range of 2–3 were obtained for many of these analytes using the Whelk-O 1 CSP (Fig. 2) [11]. This relatively high degree of enantioselectivity, combined with an enantiomer interconversion half life on the order of a day, permits a demonstration of enantioenrichment by on-column deracemization [11]. In this procedure, a racemic sample is applied to the CSP, the flow is stopped and several half lives allowed to elapse. The analyte is then eluted from the column, affording a sample which is enriched in the more retained enantiomer. The degree of enantioenrichment approaches the level of enantioselectivity observed in the chromatographic separation. A schematic depiction of the deracemization process is presented in Fig. 3.

The concept of reciprocity has been of great importance in the development of Pirkle-type CSPs [12]. Consequently, the design of a reciprocal CSP based upon the naphthamide atropisomer structure was a natural extension of the previously described study. Such a CSP cannot conveniently be prepared in enantiomerically pure form, owing to the relatively rapid racemization of the naphthamide enantiomers. However, the racemic CSP 1 (Fig. 4) (actually a mixture of two racemic diastereomers owing to the slow rate of rotation about both the $C_{(carbonyl)}$–$N_{(amide)}$ and the $C_{(carbonyl)}$–$C_{(aryl)}$ bonds [11]) is readily prepared by a simple extension of the procedure used in the previous study [11] (reaction of 2-methyl-1-naphthoyl

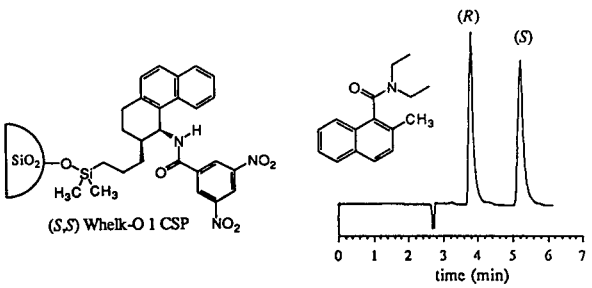

Fig. 2. Separation of the slowly interconverting enantiomers of *N,N*-diethyl-2-methyl-1-naphthylenecarboxamide on the Whelk-O 1 CSP. Mobile phase = ethyl acetate; flow rate = 1 ml/min; detection = UV 254. $k'_1 = 0.46$; $\alpha = 2.17$.

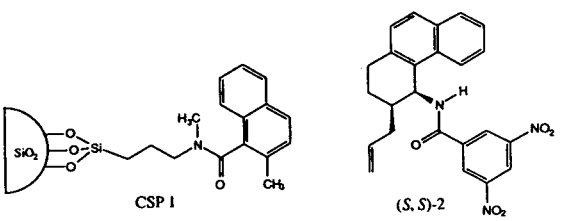

Fig. 4. The imprintable brush-type CSP 1 and the imprint molecule (*S,S*)-**2** used in its deracemization.

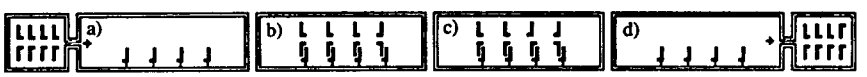

Fig. 3. On-column deracemization experiment. (a) racemate pumped onto column. (b) selective adsorption of one enantiomer leaves an excess of the opposite enantiomer in the mobile phase. (c) racemization of the analyte in the mobile phase. (d) column flushed to afford sample enriched in more retained enantiomer.

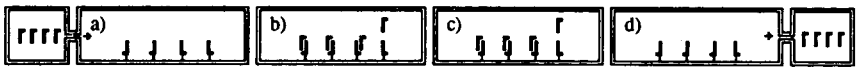

Fig. 5. Imprinting of CSP 1. (a) Enantiopure (*S*,*S*)-2 pumped onto column. (b) selective adsorbate formation with (*S*) form of CSP selector. (c) deracemization of CSP selector to favor (*S*) form. (d) column flushed to afford enantioenriched CSP.

chloride with the commercially available N-methyltrimethoxyaminopropyl silane followed by bonding of the resulting naphthamide silane to silica gel). This racemic CSP can be readily deracemized using (*S*,*S*)-**2**, a soluble analogue of the Whelk-O 1 CSP, as an imprint compound (Fig. 5).

2. Experimental

2.1. Apparatus

Chromatographic analysis was performed using a Kratos Spectroflow 400 pump, a Rheodyne Model 7125 injector fitted with either a 5-ml or a 20-μl sample loop, a Kratos Spectroflow 757 variable-wavelength absorbance monitor set at 254 or 280 nm, and a Hewlett-Packard HP 3394 integrating recorder.

2.2. Materials

The (*S*,*S*)-Whelk-O 1 CSP was obtained from Regis Technologies (Morton Grove, IL, USA). CSP 1 was prepared by reaction of 2-methyl-1-naphthoyl chloride (prepared by the method of Adams and Binder [13]) with N-methyltrimethoxyaminopropyl silane (Hüls America, Bristol, PA, USA), followed by bonding of the resulting silane on 5 μm/100 Å Rexchrom silica (Regis). Combustion analysis (C) revealed a selector surface coverage of $4.6 \cdot 10^{-4}$ mol/g (2.3 μmol/m^2). HPLC-grade ethyl acetate was obtained from EM Science (Gibbstown, NJ, USA). Racemic and (*S*,*S*)-**2** were prepared as described previously [14].

2.3. Deracemization of CSP 1 using (*S*,*S*)-2

Racemic CSP 1 was deracemized by first equilibrating the column with ethyl acetate at a flow-rate of 1 ml/min, then filling a 5-ml sample loop with a 20 mg/ml solution of (*S*,*S*)-**2** in ethyl acetate, and injecting this solution onto the column for a period of 4 min, at which time the flow was stopped, column end caps were inserted, and the column stored at room temperature for a period of 17 days. The column was then flushed with ethyl acetate at a flow-rate of 2 ml/min until a stable baseline was observed (3 h).

2.4. Evaluation of CSP 1

Separation of the enantiomers of a racemic sample of **2** spiked with 1,3,5-tri-*tert.*-butylbenzene as a void time indicator was studied on CSP 1 as a function of time at room temperature using a mobile phase of ethyl acetate at a flow-rate of 2 ml/min with 280 nm detection. During the course of the protracted study the column was intermittently stored in a freezer at −15°C, so as to effectively "freeze" the racemization process. This was done solely for operator convenience.

3. Results and discussion

Fig. 6 shows representative chromatograms which were obtained for the separation of the enantiomers of a racemic sample of **2** on the imprinted CSP 1. Independent injections allow identification of the less retained peak as (*R*,*R*)-**2** and the more retained peak as (*S*,*S*)-**2**. A relatively large separation factor is noted after 4 h ($\alpha = 2.54$) with a rapid decrease in enantioselectivity being observed until only one peak is observed at 119 h. A decrease in column flow-rate to 0.5 ml/min at 119 h revealed a marginal separation ($\alpha = 1.09$), which decreased over time until no trace of enantioseparation was seen at 194 h.

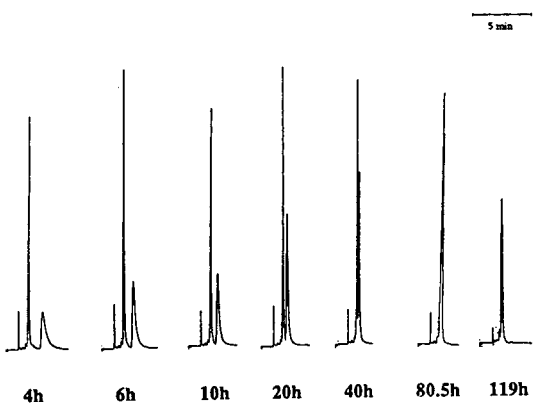

Fig. 6. Time dependent separation of the enantiomers of **2** on imprinted CSP 1. Conditions: Sample = racemic **2** spiked with 1,3,5 tri-*t*-butylbenzene; Column–CSP 1 following 17 day imprinting with 80 mg (*S,S*)-**2** in ethyl acetate; mobile phase = ethyl acetate; flow rate = 2.00 ml/min, detection = UV 254 nm; room temperature.

A plot of the time-dependent change in retention factors (k'_1, k'_2) for the two enantiomers of compound **2** on CSP 1 is shown in Fig. 7. As stated previously, the data after 119 h were collected at a flow-rate of 0.5 ml/min. In order to permit convenient data collection the column was periodically stored in a freezer at −15°C for the time periods marked with an asterisk. The results indicate that racemization of the CSP was almost completely suppressed at this temperature. The decrease in enantioselectivity can be seen to be almost entirely due to a decrease in the retention factor for the more retained enantiomer, a somewhat surprising result. A plot of the decrease in separation factor (α) for the two enantiomers of compound **2** on CSP 1 is shown in Fig. 8. Analysis of such data can reveal the kinetic parameters for enantiomer interconversion. In the present case, this analysis is somewhat complicated by the fact that CSP 1 contains four stereoisomeric components whose interconversion has been shown to be somewhat complex [11].

Several factors which influence the "charging" of an imprintable brush-type CSP can be identified or postulated. Under optimum circumstances, the limiting enantioenrichment obtained in the deracemization of the CSP can be expected to be roughly equivalent to the enantioselectivity observed for the enantiomers of the chiral selector by the imprinting agent. In the deracemization of CSP 1 by (*S,S*)-**2**, higher concentrations of the imprinter lead to a greater degree of CSP deracemization. This situation will be general, for the extent of deracemization is influenced by the position of the complexation equilibrium. Thus, a highly soluble imprint molecule which has both a high affinity for and a high enantioselectivity toward the CSP selector is preferred.

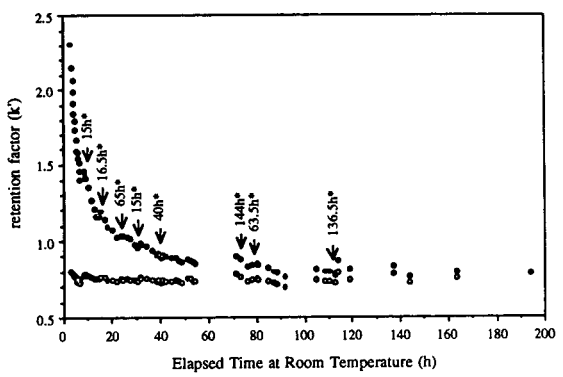

Fig. 7. Time dependent change in retention factors for separation of enantiomers of **2** on CSP 1. Conditions: as for Figure 6, except that data points greater than 120 h were collected at a flow rate of 0.5 ml/min. * denotes column storage time at −15°C.

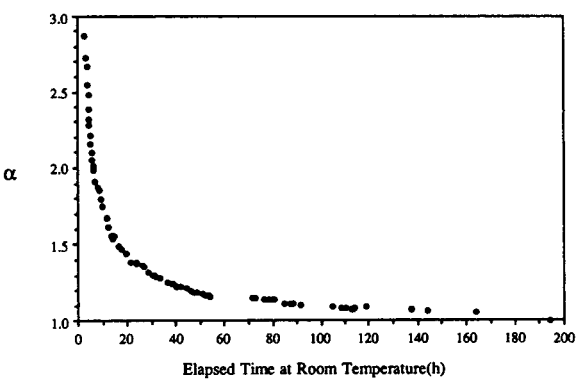

Fig. 8. Time dependent change in separation factor for separation of enantiomers of **2** on CSP 1. Conditions: as for Figure 7.

4. Conclusions

CSP 1 exhibits a number of undesirable properties which preclude its practical utility. Foremost among these is the rapidly changing characteristics of the column at room temperature and its relatively short lifespan once imprinted. However, longer lived analogues could be prepared by choice of a chiral selector with a slower rate of enantiomer interconversion, an approach which would also require increased time for the imprinting process. The time required to imprint such a CSP can be decreased by conducting the deracemization at an elevated temperature, where enantiomer interconversion is more rapid. However, owing to the fact that enantioselectivity typically decreases at higher temperatures, less enantioenrichment would be expected in the resulting CSP.

An interesting extension of this work, one that harkens back to Pauling's 1940 hypothesis, is the possibility of a general-purpose CSP which could accommodate a variety of imprint molecules. For example, a CSP structure containing only five slowly interconverting structural elements can exist in as many as 2^5 or 32 stereoisomeric forms, each of which could be expected to display differing levels of enantioselectivity for different racemates. By judicious choice of structure and appropriate disposition of interacting groups, an imprintable CSP with broad generality could perhaps be produced.

References

[1] L. Pauling, *J. Am. Chem. Soc.*, 62 (1940) 2643–2657.
[2] F.M. Burnet, *The Clonal Selection Theory of Acquired Immunity*, Vanderbilt Univ. Press, Nashville, TN, 1959.
[3] H.N. Eisen, *Immunology; an Introduction to Molecular and Cellular Principles of the Immune Responses*, Harper & Row, Philadelphia, PA, 1980.
[4] F.H. Dickey, *Proc. Natl. Acad. Sci. U.S.A.*, 35 (1949) 227–229.
[5] R. Curti and U. Colombo, *J. Am. Chem. Soc.*, 74 (1952) 3961.
[6] G. Wulff and W. Wesper, *J. Chromatogr.*, 167 (1978) 171.
[7] L. Andersson, B. Sellergren and K. Mosbach, *Tetrahedron Lett.*, 25 (1984) 5211.
[8] B. Sellergren, *Chirality*, 1 (1989) 63.
[9] B. Sellergren and K.J. Shea, *J. Chromatogr.*, 635 (1993) 31.
[10] O. Ranström, L.I. Andersson and K. Mosbach, *J. Org. Chem.*, 58 (1993) 7562.
[11] W.H. Pirkle, C.J. Welch and A.J. Zych, *J. Chromatogr.*, 648 (1993) 101.
[12] C.J. Welch, *J. Chromatogr. A*, 666 (1994) 3.
[13] R. Adams and L.O. Binder, *J. Am. Chem. Soc.*, 63 (1941) 2773.
[14] W.H. Pirkle and C.J. Welch, *J. Liq. Chromatogr.*, 15 (1992) 1947.

ELSEVIER

Journal of Chromatography A, 689 (1995) 195–201

JOURNAL OF CHROMATOGRAPHY A

Direct separation of carboxylic acid enantiomers by high-performance liquid chromatography with amide and urea derivatives bonded to silica gel as chiral stationary phases

Naobumi Ôi*, Hajimu Kitahara, Fumiko Aoki, Naoko Kisu

Sumika Chemical Analysis Service, Ltd., 3-1-135 Kasugade-naka, Konohana-ku, Osaka 554, Japan

First received 9 August 1994; revised manuscript received 12 September 1994

Abstract

For the separation of carboxylic acid enantiomers by HPLC, the chromatographic properties of four chiral amide and urea derivatives [N-3,5-dinitrobenzoyl-D-1-(α-naphthyl)glycine, 3,5-dinitrophenylaminocarbonyl-D-phenylglycine, 3,5-dinitrophenylaminocarbonyl-L-valine and 3,5-dinitrophenylaminocarbonyl-L-*tert.*-leucine] covalently bonded to 3-aminopropylsilanized silica gel as chiral stationary phases were examined. Direct separation of various carboxylic acid enantiomers was accomplished with these chiral stationary phases. The influence of the composition of the mobile phase in these enantiomer separations was shown. Amino acid enantiomers were also well resolved in the form of their derivatives containing a free carboxylic acid group, such as *tert.*-butoxycarbonyl (t-BOC), benzyloxycarbonyl (Z), 9-fluorenylmethoxycarbonyl (FMOC) and 5-dimethylamino-1-naphthalenesulfonyl (dansyl) derivatives.

1. Introduction

Carboxylic acids are one of the most important classes of chiral compounds, and it is well known that high-performance liquid chromatography (HPLC) with chiral stationary phases (CSPs) is useful for the separation of carboxylic acid enantiomers. Derivatives of cyclodextrin, cellulose and protein have been used as CSPs for this purpose [1–3]. Brush-type CSPs are unsuitable for the direct separation of racemic carboxylic acids and these compounds have usually been resolved in the form of amide derivatives [4,5]. We have found [6] that the direct separation of some aromatic carboxylic acids was possible with N-3,5-dinitrobenzoyl-D-phenylglycine bonded to silica gel (I), which is a typical brush-type CSP developed by Pirkle and Finn [7], but its enantioselectivity was inadequate. Recently, Pirkle and Welch [8] reported the excellent enantiomer separation of naproxen and other anti-inflammatory drugs with an improved brush-type chiral stationary phase using normal mobile phases, although the separation of aliphatic carboxylic acids was not described.

In this paper, we report the direct separation of a variety of carboxylic acids, both aromatic and aliphatic, with brush-type CSPs II–V (Fig. 1) using aqueous mobile phases. CSP II is a modification of phase I. We previously reported [9] that N-3,5-dinitrobenzoyl-D-1-(α-naphthyl)gly-

* Corresponding author.

0021-9673/95/$09.50
SSDI 0021-9673(94)00890-6

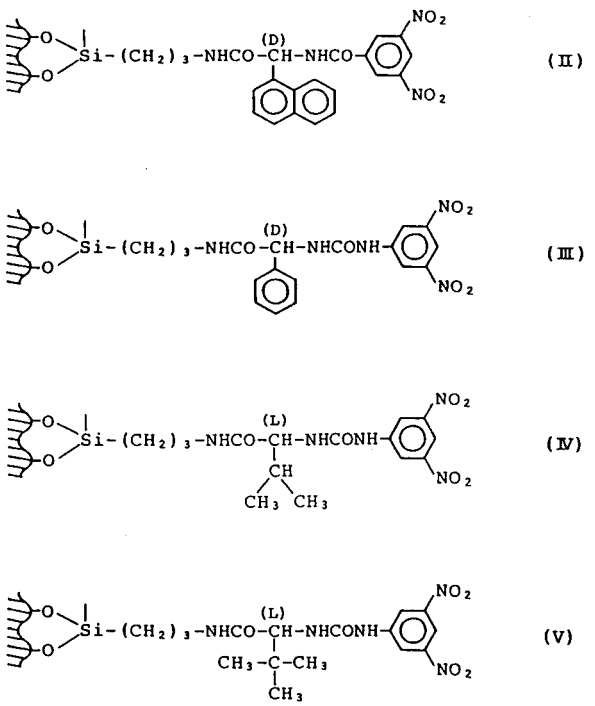

Fig. 1. Structures of CSPs.

cine ionically bonded to 3-aminopropylsilanized silica showed superior enantioselectivity to phase I in the separation of alcohol and ester racemates, but this phase was unsuitable for use under reversed-phase conditions. Therefore, we have prepared N-3,5-dinitrobenzoyl-D-1-(α-naphthyl)glycine covalently bonded to 3-aminopropylsilanized silica (II) for the separation of racemic carboxylic acids using aqueous mobile phases. CSP III is also a modification of phase I. We found previously [5,10] that various urea derivatives of amino acids bonded to silica gel were excellent CSPs for many racemic compounds, and this result showed that the urea group attached to the asymmetric carbon atom was effective in diastereomeric association for chiral recognition. Accordingly, we prepared a urea derivative (III) which contains the urea group instead of the amide group in phase I. Similar N-3,5-dinitrophenylurea derivatives (IV and V) derived from L-valine and L-*tert.*-leucine were also prepared. These CSPs are now commercially available as Sumichiral OA-2500 (CSP II), OA-3300 (CSP III), OA-3100 (CSP IV) and OA-3200 (CSP V).

2. Experimental

2.1. Chiral stationary phases

To prepare CSP II, N-3,5-dinitrobenzoyl-D-1-(α-naphthyl)glycine was synthesized by the procedure described previously [9]. It was covalently bonded to 3-aminopropylsilanized silica by the reported procedure [5].

CSP III was prepared using D-phenylglycine and 3,5-dinitrophenyl isocyanate instead of L-valine and alkyl isocyanate in the preparation of alkylurea derivatives of L-valine bonded to silica gel reported previously by paper [10]. 3,5-Dinitrophenyl isocyanate was obtained from 3,5-dinitroaniline (Aldrich, Milwaukee, WI, USA) by the reaction with phosgene.

CSPs IV and V were prepared as for CSP III but using L-valine and L-*tert.*-leucine, respectively, instead of D-phenylglycine.

Develosil-NH_2 (5 μm) (Nomura Chemical, Seto, Japan) was used as the starting silica gel. Grafting rates were calculated according to the C and N elemental analyses for each CSP: CSP II 0.42, CSP III 0.42, CSP IV 0.44 and CSP V 0.38 mmol/g.

2.2. Liquid chromatography

Stainless-steel columns (250 × 4.6 mm I.D.) were slurry packed with CSPs II–V using a conventional technique.

The experiments were carried out using a Waters Model 510 high-performance liquid chromatograph equipped with a variable-wavelength UV detector, operated at 230 and 254 nm. Solutes and solvents of analytical-reagent grade were purchased from Wako (Osaka, Japan). The structures of the racemic solutes used are shown in Fig. 2. Some compounds were kindly provided by Sumitomo Chemical (Osaka, Japan).

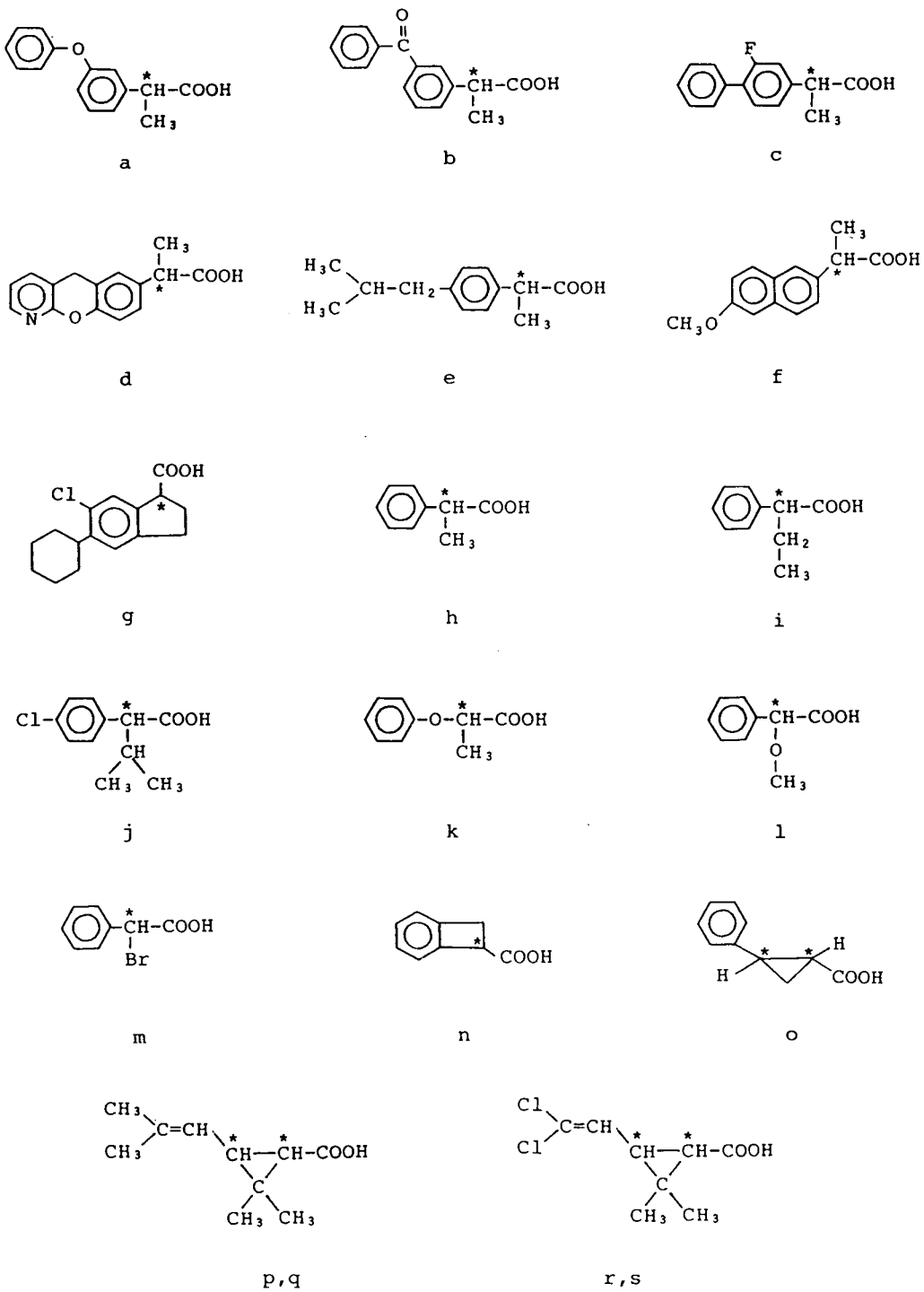

Fig. 2. Structures of racemic solutes.

3. Results and discussion

The chromatographic results are summarized in Table 1. A number of carboxylic acid enantiomers including pharmaceutical and agrochemical compounds were resolved directly with these CSPs under the reversed-phase conditions. Typical chromatograms of aromatic and aliphatic carboxylic acids are shown in Figs. 3 and 4.

Phase II shows superior enantioselectivity to phase I. This result showed that the naphthyl group of phase II plays a more effective role than the phenyl group of phase I for chiral recognition in racemic carboxylic acids and also in alcohol and ester enantiomers [9]. Phases III–V show very specific enantioselectivity and adequate separation was obtained for some carboxylic acids, such as clidanac (g), 2-(4-chlorophenyl)-3-methylbutyric acid (j), 2-phenoxypropionic acid (k), 1-benzocyclobutenecarboxylic acid (n) and *cis*-chrysanthemic acid (p). These carboxylic acid enantiomers were not or poorly resolved on phase II. These results show that the 3,5-dinitrophenylurea group attached to the asymmetric carbon atom is effective in the separation of carboxylic acid enantiomers and the effect of the structure of the amino acid moiety in chiral recognition is considerable.

Table 1
Enantiomer separation of carboxylic acids by HPLC

Compound	CSP II			CSP III			CSP IV			CSP V		
	k'_1	α	M	k'_1	α	M	k'_1	α	M	k'_1	α	M
(a) Fenoprofen	2.85	1.12	A	4.09	1.13	B	5.78	1.07	B	5.66	1.00	B
(b) Ketoprofen	2.27(−)	1.12	A	6.01	1.10	B	7.08	1.05	B	6.35	1.00	B
(c) Flurbiprofen	3.18	1.09	A	5.27	1.06	B	3.50	1.00	B	5.63	1.02	B
(d) Pranoprofen	4.46	1.14	A	10.84	1.04	A	16.60	1.00	B	12.84	1.07	B
(e) Ibuprofen	4.17	1.06	B	3.34	1.08	B	4.73	1.04	B	4.37	1.00	B
(f) Naproxen	5.25(−)	1.55	C	10.99	1.09	A	6.33	1.00	B	16.78	1.00	B
(g) Clidanac	4.22	1.03	A	4.42	1.17	B	6.85	1.56	B	5.26	1.55	B
(h) 2-Phenylpropionic acid	1.53	1.09	D	2.51	1.10	D	2.07	1.08	D	2.28	1.00	D
(i) 2-Phenylbutyric acid	2.01	1.08	D	3.54	1.13	D	3.20	1.10	D	3.21	1.07	D
(j) 2-(4-Chlorophenyl)-3-methylbutyric acid	3.10	1.00	D	9.91	1.16	D	5.40	1.06	D	7.35	1.00	D
(k) 2-Phenoxypropionic acid	1.15	1.00	D	2.58	1.34	D	2.14	1.00	D	2.34	1.05	D
(l) α-Methoxyphenylacetic acid	7.04	1.15	B	8.80	1.07	B	2.97	1.03	B	5.08	1.05	B
(m) α-Bromophenylacetic acid	6.22	1.11	B	5.48	1.00	B	2.08	1.06	B	3.48	1.05	B
(n) 1-Benzocyclobutene-carboxylic acid	5.87	1.00	B	6.03	1.07	B	2.12	1.10	B	3.28	1.10	B
(o) *trans*-2-Phenyl-1-cyclo-propanecarboxylic acid	4.68	1.08	B	4.37	1.00	B	1.94	1.00	B	2.49	1.00	B
(p) *cis*-Chrysanthemic acid	4.79	1.00	D	10.15	1.00	D	6.45(−)	1.05	D	7.45(−)	1.10	D
(q) *trans*-Chrysanthemic acid	3.88	1.06	D	6.11	1.16	D	3.81(−)	1.12	D	4.94(−)	1.16	D
(r) *cis*-3-(2,2-Dichlorovinyl)-2,2-dimethylcyclopropane-carboxylic acid	6.58	1.09	D	10.67	1.07	D	7.67	1.08	D	8.91	1.08	D
(s) *trans*-3-(2,2-Dichlorovinyl)-2,2-dimethylcyclopropane carboxylic acid	4.68	1.10	D	6.44	1.17	D	3.87	1.10	D	5.00	1.12	D

Mobile phase (M): A = 0.02 *M* ammonium acetate in methanol; B = 0.01 *M* ammonium acetate in methanol; C = 0.05 *M* ammonium acetate in methanol; D = 0.1 *M* ammonium acetate in water–tetrahydrofuran (60:40). A flow rate of 1.0 ml/min was typically used for the 250 × 4.6 mm I.D. column at room temperature. An injection volume of 1 μl (5 mg/ml) was typically used. k'_1, k'_2 = Capacity factors of first- and second-eluted isomers, respectively; α = separation factor (k'_2/k'_1).

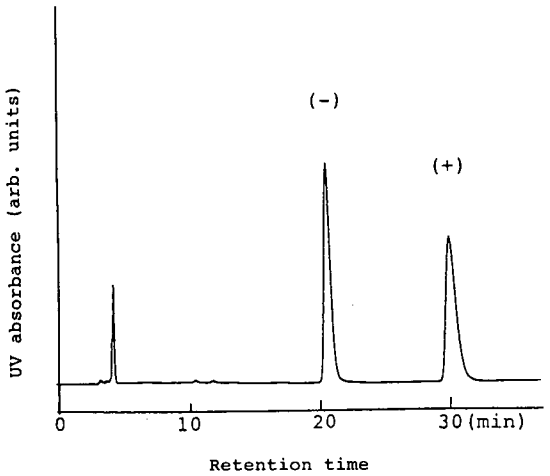

Fig. 3. Enantiomer separation of racemic naproxen (f) using a reversed mobile phase. Chromatographic conditions as in Table 1.

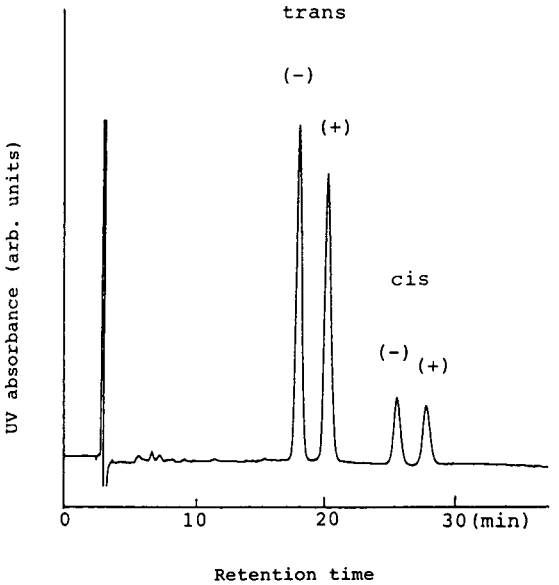

Fig. 4. Enantiomer separation of *cis*- and *trans*-chrysanthemic acid (p and q). Chromatographic conditions as in Table 1.

Table 2
Comparison of enantiomer separations using different mobile phase components

Compound	Stationary phase	k'_1	α	Mobile phase[a]
(b) Ketoprofen	CSP II	2.27	1.11	0.02 *M* NH_4AC in MeOH
		6.36	1.16	0.1 *M* NH_4AC in MeOH–H_2O (40:60)
		1.92	1.12	0.1 *M* NH_4AC in AN–H_2O (40:60)
		2.43	1.14	0.1 *M* NH_4AC in THF–H_2O (40:60)
		12.82	1.03	Hexane–DCE–EtOH–AA (190:9:1:1)
(f) Naproxen	CSP II	5.25	1.55	0.05 *M* NH_4AC in MeOH
		8.23	1.19	Hexane–DCE–EtOH–AA (190:9:1:1)
(g) Clidanac	CSP IV	6.85	1.56	0.01 *M* NH_4AC in MeOH
		4.01	1.19	Hexane–DCE–EtOH–AA (490:9:1:1)
(j) 2-(4-Chlorophenyl)-3-methylbutyric acid	CSP III	3.57	1.02	0.01 *M* NH_4AC in MeOH
		4.85	1.04	0.1 *M* NH_4AC in MeOH–H_2O (40:60)
		5.21	1.08	0.1 *M* NH_4AC in AN–H_2O (40:60)
		9.91	1.16	0.1 *M* NH_4AC in THF–H_2O (40:60)
		2.50	1.18	0.1 *M* NH_4AC in THF–H_2O (50:50)
		1.17	1.21	0.1 *M* NH_4AC in THF–H_2O (60:40)

A flow-rate of 1.0 ml/min was used for the 250 × 4.6 mm I.D. column at room temperature. An injection volume of 1 μl (5 mg/ml) was typically used. k'_1, k'_2 = Capacity factors of first- and second-eluted isomers, respectively; α = separation factor (k'_2/k'_1).

[a] NH_4AC = Ammonium acetate; MeOH = methanol; AN = acetonitrile; THF = tetrahydrofuran; DCE = 1,2-dichloroethane; EtOH = ethanol; AA = acetic acid.

It should be emphasized that these enantiomer separations were influenced by the composition of the mobile phase. Some of the data obtained are summarized in Table 2. An improvement of the separation was obtained by varying the aqueous mobile phase composition. For example, racemic 2-(4-chlorophenyl)-3-methylbutyric acid (j) was poorly resolved on phase III in methanol (containing 0.01 *M* ammonium acetate) or methanol–0.1 *M* ammonium acetate (40:60, v/v), but well resolved in tetrahydrofuran–0.1 *M* ammonium-acetate (40:60, v/v). Moreover, there was the increase in the separation factor as the tetrahydrofuran

Table 3
Enantiomer separation of amino acid derivatives by HPLC

Compound[a]	CSP III			CSP IV			CSP V		
	k'_1	α	M	k'_1	α	M	k'_1	α	M
N-Acetyl-									
alanine	2.30	1.12	A	3.71	1.00	B	3.16	1.12	A
valine	2.00	1.11	A	2.77	1.00	B	3.10	1.00	A
leucine	2.11	1.02	A	2.70	1.04	B	3.15	1.10	A
methionine	2.32	1.05	A	3.47	1.00	B	3.03	1.06	A
N-Benzoyl-									
valine	1.53	1.19	A	2.38	1.12	B	2.19	1.00	A
phenylalanine	2.41	1.17	A	4.12	1.07	B	2.83	1.06	A
glutamic acid	2.72	1.14	A	4.78	1.00	B	3.24	1.09	A
N-t-BOC-									
valine	1.04	1.10	A	1.09	1.00	A	2.32	1.00	A
leucine	1.13	1.09	A	0.99	1.00	A	2.45	1.04	A
phenylalanine	1.80	1.09	A	1.26	1.00	A	2.77	1.00	A
N-Z-									
alanine	2.77	1.05	A	4.14	1.04	B	3.33	1.16	A
valine	1.88	1.07	A	3.47	1.00	B	4.22	1.13	B
norvaline	2.19	1.09	A	4.00	1.00	B	4.61	1.13	B
leucine	2.10	1.07	A	3.85	1.05	B	3.23	1.17	A
serine	3.40	1.00	A	5.18	1.07	B	4.16	1.09	A
asparagine	5.68	1.00	A	6.60	1.12	B	9.94	1.11	B
N-FMOC-									
alanine	7.50(D)	1.17	A	3.18(D)	1.15	A	5.28(D)	1.19	A
valine	6.30	1.08	A	2.55	1.00	A	4.08	1.12	A
leucine	7.02	1.07	A	2.84	1.07	A	4.61	1.20	A
phenylalanine	8.76	1.08	A	3.52	1.00	A	5.41	1.10	A
N-Dansyl-									
valine	3.72	1.15	A	2.84(D)	1.21	A	5.21	1.28	A
norvaline	3.65	1.12	A	3.06(D)	1.15	A	6.58	1.24	A
threonine	4.59	1.18	A	4.09	1.17	A	8.42	1.15	A
Phenylalanine	5.65	1.12	A	4.53	1.17	A	8.34	1.27	A
tryptophan	15.92	1.12	A	9.41	1.16	A	16.93	1.16	A

Mobile phase (M): A = 0.01 *M* ammonium acetate in methanol; B = 0.005 *M* ammonium acetate in methanol; C = 0.03 *M* ammonium acetate in methanol. A flow-rate of 1.0 ml/min was used for the 250 × 4.6 mm I.D. column at room temperature. An injection volume of 1 μl (5 mg/ml) was typically used. k'_1, k'_2 = Capacity factors of first- and second-eluted isomers, respectively; α = separation factor (k'_2/k'_1).

[a] t-BOC- = *tert.*-Butoxycarbonyl-; Z- = benzyloxycarbonyl-; FMOC- = 9-fluorenylmethoxycarbonyl-; Dansyl- = 5-dimethylamino-1-naphthalenesulfonyl-.

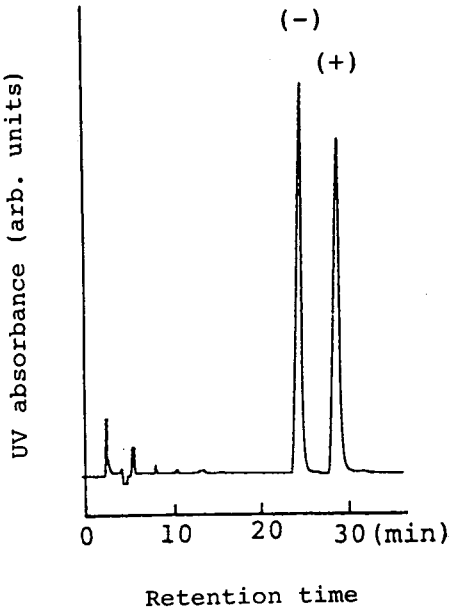

Fig. 5. Enantiomer separation of racemic naproxen (f) using a normal mobile phase. Chromatographic conditions as in Table 2.

content was increased in tetrahydrofuran–0.1 *M* ammonium acetate mobile phase. On the other hand, the influence was less in the separation of ketoprofen (b) enantiomers on phase II. The mechanism of the effect of the composition of the mobile phase is unclear and additional work is in progress. These CSPs were also effective using normal mobile phases. An example is shown in Fig. 5.

The results of the separation of amino acid enantiomers in the form of various derivatives containing free carboxylic acid groups are shown in Table 3. The enantiomer separation of *tert.*-butoxycarbonyl (t-BOC), benzyloxycarbonyl (Z) and 9-fluorenylmethoxycarbonyl (FMOC) derivatives of amino acid is significant for the peptide synthesis, and the separation of 5-dimethylamino-1-naphthalenesulfonyl (dansyl) derivatives of amino acids is valuable for the determination of small amounts of amino acids, as these derivatives show high sensitivity in UV or fluorescence detection. Hydroxy acid enantiomers were also resolved in the form of their derivatives containing free carboxylic acid groups.

These CSPs showed good durability under chromatographic conditions using the mobile phases shown in Tables 1 and 2. In conclusion, these novel amide and urea derivatives bonded to silica gel (CSPs II–V) are promising as chiral stationary phases for the separation of the enantiomers of various carboxylic acids and amino acids by HPLC.

Acknowledgement

The authors thank Sumitomo Chemical for providing some racemate samples.

References

[1] K.G. Feitsma, B.F.H. Drenth and R.A. de Zeeuw, *J. High Resolut. Chromatogr. Chromatogr. Commun.*, 7 (1984) 147–148.
[2] Y. Okamoto, R. Aburatani, Y. Kaida and K. Hatada, *Chem. Lett.* (1988) 1125–1128.
[3] T. Miwa, T. Miyakawa, M. Kagano and Y. Miyake, *J. Chromatogr.*, 408 (1987) 316–322.
[4] I.W. Wainer and T.D. Doyle, *J. Chromatogr.*, 284 (1984) 117–124.
[5] N. Ôi and H. Kitahara, *J. Liq. Chromatogr.*, 9 (1986) 511–517.
[6] N. Ôi, Y. Matsumoto, H. Kitahara and H. Miyazaki, *Bunseki Kagaku*, 35 (1986) 312–313.
[7] W.H. Pirkle and J.M. Finn, *J. Org. Chem.*, 46 (1981) 2935–2938.
[8] W.H. Pirkle and C.J. Welch, *J. Liq. Chromatogr.*, 15 (1992) 1947–1955.
[9] N. Ôi, H. Kitahara, Y. Matsumoto, H. Nakajima and Y. Horikawa, *J. Chromatogr.*, 462 (1989) 382–386.
[10] N. Ôi and H. Kitahara, *J. Chromatogr.*, 285 (1984) 198–202.

ELSEVIER

Journal of Chromatography A, 689 (1995) 203–210

JOURNAL OF CHROMATOGRAPHY A

Diol-bonded silica gel as a restricted access packing forming a binary-layered phase for direct injection of serum for the determination of drugs

Noriyuki Nimura*, Hiroko Itoh, Toshio Kinoshita

School of Pharmaceutical Sciences, Kitasato University, 9-1 Shirokane-5, Minato-ku, Tokyo 108, Japan

First received 25 April 1994; revised manuscript received 13 September 1994

Abstract

Direct serum injection for drug determinations can be achieved on a diol-bonded silica gel as a restricted access packing. The diol-bonded phase, 3-(2,3-dihydroxypropoxy)propylsilylsilica, contains two different functions, a hydrophilic function at the tip of the single chemical bond and a hydrophobic function on the inside part of the bond to form a "binary-layered phase" on the support surface. Proteins, as large molecules, contact only the hydrophilic surface of the diol phase, and they are eluted at the solvent front based on size-exclusion chromatography. On the other hand, small molecules such as synthetic drugs are retained on the internal hydrophobic function and separate based on reversed-phase chromatography. Accordingly, the diol-bonded silica gel performs as a restricted access packing for direct serum injection for the determination of relatively hydrophobic drugs.

1. Introduction

There have been a number of investigations concerned with protein separations by reversed-phase high-performance liquid chromatography (RP-HPLC). Separation mechanisms for proteins in RP-HPLC have also been proposed [1–10]. According to those studies, the behaviour of proteins on RP-HPLC columns is very different from that of small solutes. In RP-HPLC, the retention times of small molecules generally increase with increasing alkyl chain length of the chemically bonded phase on the chromatography support. In contrast, it is known that the retention of proteins is not seriously influenced by variations in alkyl chain length [5,11,12]. Consequently, it suggested that proteins interact only with the extreme top of the alkyl chains, and they scarcely penetrate into the chemically bonded phase under certain conditions.

Various types of restricted access packings [13,14] have previously been developed for analysis with direct serum injection. Yoshida and co-workers [15,16] first reported a protein (bovine serum albumin)-coated ODS column for that purpose. The external surface of the support was treated with a denatured protein, and the internal surface still retained the characteristics of the reversed-phase column for small molecules. Pinkerton's group [17–19] proposed internal-surface reversed phases (ISRP), which have been widely used in therapeutic drug monitoring.

* Corresponding author.

0021-9673/95/$09.50
SSDI 0021-9673(94)00896-5

Their material had both an external hydrophilic phase and an internal hydrophobic phase. Gisch et al. [20] prepared shielded hydrophobic phases (SHP), which had an external hydrophilic network that created a polyoxyethylene or polyethylene glycol. Hydrophobic zones such as phenyl groups were embedded in the polymer. Desilets et al. [21] reported semipermeable surfaces (SPS). Alkyl (C_8 and C_{18}) bonded phases were coated with Tween and Brij as non-ionic surfactants. Haginaka and co-workers [22,23] developed mixed functional phases (MFP) which had a phenyl phase as the hydrophobic phase and a diol phase as the hydrophilic phase on both external and internal pores. Thus the hydrophilic phases sterically prevent larger protein molecules from interacting with the hydrophobic zones, while small analytes are not hindered from interacting with the hydrophobic zones and are retained. Any restricted access packing has two functions: one restricts the access of large molecules to the hydrophobic bonded phase, and the hydrophobic function retains small molecules.

The above previous studies prompted us to consider a different restricted access separation system. We imagined that if a chemical bond on a support had two different parts at its top and bottom, a hydrophilic function in the upper part and a hydrophobic function in the lower part, such a chemically bonded phase should be usable as a restricted access packing material. A commercially available "diol phase", a glyceryl-propyl-bonded phase, consists of a hydrophilic ethanediol structure and a hydrophobic methoxypropyl structure at the upper part and the lower part, respectively. Therefore, it appeared that an internal hydrophobic layer hidden by an external hydrophilic layer existed on the support surface of the diol phase. Such a formation of the diol phase, called a "binary-layered phase", seemed to be suitable for use as a restricted access packing (Fig. 1).

In this study, we evaluated a conventional diol silica packing material as a restricted access packing with direct injection for the determination of drugs in human serum, and found it to be useful for that purpose. As a result, we propose the following concept: stationary phase(s) such as the diol phase that have two different functions at a single chemical bond on the support should be called "binary-layered phase packing(s)", and separation(s) on the binary-layered phase packing should be named "binary-layered phase liquid chromatography".

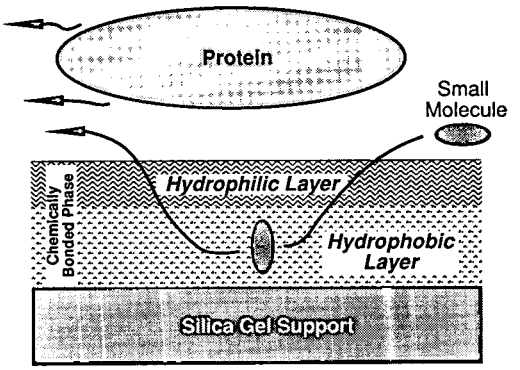

Fig. 1. Proposed conceptual model for binary-layered phase liquid chromatography using a binary-layered stationary phase as a restricted access packing.

2. Experimental

2.1. Reagents

Phenytoin sodium salt was purchased from Tokyo Kasei Kogyo (Tokyo, Japan). Other drugs and reagents were obtained from Wako (Osaka, Japan). HPLC-grade acetonitrile was from Kanto Chemical (Tokyo, Japan). Water was purified by passage through a Milli-R/Q system (Millipore, Bedford, MA, USA).

A diol silica packed cartridge column (LiChrospher 100 DIOL, 250 × 4 mm I.D., LiChroCART 250-4; Merck, Darmstadt, Germany) was obtained from Kanto Chemical. The mean particle diameter and pore size of this support were 5 μm and 10 nm, respectively.

2.2. HPLC apparatus and conditions

The HPLC system consisted of two Model 880-PU HPLC pumps (Jasco, Tokyo, Japan)

equipped with an ERC-3510 degasser (Erma, Tokyo, Japan), a Model 880-30 solvent mixing module (Jasco), a Model 7125 injector (Rheodyne, Cotati, CA, USA) and a Model 875-UV spectrophotometric detector (Jasco). An in-line filter unit, which had a changeable PTFE paper filter, was provided between the injector and the column to guard the column. Chromatograms were recorded and processed by a C-R6A Chromatopac integrator (Shimadzu, Kyoto, Japan).

The mobile phases, flow-rate and other chromatographic conditions used are given in the figure legends. All separations were performed at room temperature.

2.3. Sample preparation

Drugs were added to human serum at a known concentration and the resulting serum was filtered through a 0.22-μm membrane filter. An aliquot of the serum sample (a few to 20 μl) was then injected directly into the HPLC system.

3. Results and discussion

Many attempts have been made to apply direct serum injection in therapeutical drug monitoring using restricted access packings [13–23]. In these investigations, the procedure for sample pretreatment was extremely simple; the only filtration required used a membrane filter. The mobile phase composition in the separation systems was also uncomplicated. A mixture of a neutral buffer with an organic modifier such as acetonitrile was generally used as the mobile phase, and an acidic buffer or ion-pair technique was often used for the determination of ionic drugs. The content of the organic modifier was low, a few to 20%, because a high concentration of the organic solvent frequently caused precipitation of serum proteins. This study followed the previous examinations regarding the conditions for sample pretreatment and chromatographic separation.

Diol silica packings with macropores (mean pore diameter $\geq$30 nm) have been generally used for the size-exclusion separation of proteins [24]. In size-exclusion chromatography, it is a prerequisite that sample solutes have no direct interactions with the stationary phase on the support. Therefore, the proteins do not penetrate into the chemically bonded diol phase. Further, because the diol silica utilized here has micropores, the mean pore diameter being 10 nm, macromolecules such as proteins cannot permeate into the pores. Hence the proteins seem to be size-excluded and are eluted at the solvent front.

As a matter of course, extremely hydrophilic, water-attracting, small molecules such as amino acids and short-chain peptides were also separated according to the size-exclusion mode on the microporous diol phase eluted with an aqueous mobile phase without an organic modifier. However, relatively hydrophobic solutes behaved differently. In a preliminary examination, various amino acids and their homo-polypeptides were separated on the diol phase under aqueous elution conditions. Fig. 2 shows the relationship between the retention time of the solutes and the logarithm of their molecular mass. Glycine, alanine and their homo-polypeptides, which were relatively hydrophilic compounds, were separated based on the size-exclusion mode. However, the more hydrophobic leucine, phenylalanine and their polypeptides were eluted in reversed order. These retention data were replotted against Rekker's constant, which indicates the hydrophobicity of the compound (Fig. 3). For the phenylalanine derivatives, the retention time of the solute increased with increase in Rekker's constant. These observations suggest that the separation of hydrophobic solutes such as phenylalanine derivatives on the diol phase was based mainly on the reversed-phase mode. Further, simple series compounds, such as benzene, methylbenzene and ethylbenzene, were separated on the diol phase under various elution conditions. The correlation between the logarithm of the molecular mass of the benzene derivatives and their retention time is illustrated in Fig. 4. When an acetonitrile-rich (over 31.5%) mobile phase was used, the elution order of the compounds was based on the size-exclusion mode. It seems that, because the solutes were

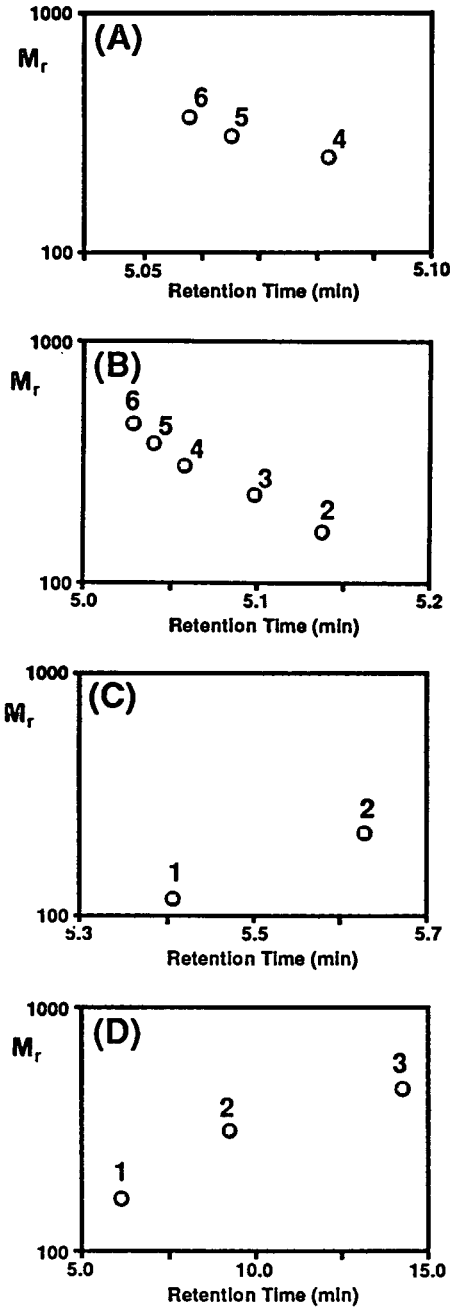

Fig. 2. Plot of molecular mass of the amino acid oligomers versus retention time on a diol silica gel column. Conditions: column, LiChrospher 100 DIOL (250 × 4 mm I.D.); eluent, 50 m*M* phosphate buffer (pH 6.9)–acetonitrile (91:9, v/v); flow-rate, 0.5 ml/min; column temperature, ambient; detection, UV at 215 nm. Samples, (A) $(Gly)_n$; (B) $(Ala)_n$; (C) $(Val)_n$; (D) $(Phe)_n$.

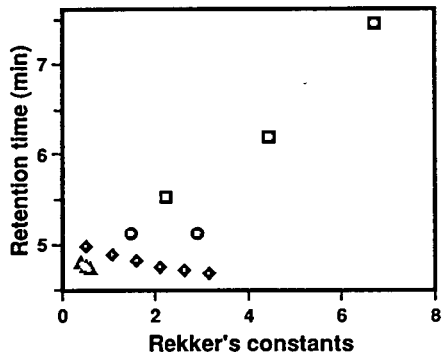

Fig. 3. Plot of retention time against Rekker's constants on diol silica gel column. Conditions as in Fig. 2. Samples, ▲ = $(Gly)_n$; ◆ = $(Ala)_n$; O = $(Val)_n$; and □ = $(Phe)_n$.

well solvated under these conditions, they had little interaction with the stationary phase. In contrast, the elution order was reversed by using an acetonitrile-poor mobile phase. Under these conditions, the solute compounds could penetrate into the hydrophobic layer of the chemically bonded diol phase and were retained based on the reversed-phase mode. These results suggest that such a diol-bonded phase behaves like two different types of packing materials considering

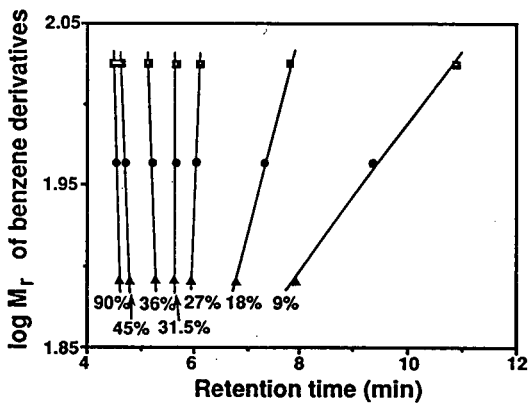

Fig. 4. Plot of logarithm of the molecular mass of the benzene derivatives against their retention times for different concentrations of acetonitrile in the mobile phase. Conditions: column, LiChrospher 100 DIOL (250 × 4 mm I.D.); eluent, 50 m*M* phosphate buffer (pH 6.9)–acetonitrile (percentages of acetonitrile are given below the lines); flow-rate, 0.5 ml/min; column temperature, ambient; detection, UV at 215 nm; injection volume, 2 μl. Samples: ▲ = benzene; O = methylbenzene; □ = ethylbenzene.

the state of the elution conditions or the physico-chemical characteristics of the solute compounds.

Next, standard human serum albumin and some small molecules such as synthetic drugs were injected into the diol column and were eluted with neutral phosphate buffer containing a small amount of acetonitrile. Chromatograms of the albumin and a mixture of theophylline and caffeine are shown in Fig. 5A and B, respectively. As expected, the albumin eluted at the solvent front, but the drugs were well retained and mutually separated from each other. The elution order of the drugs on the diol phase was almost the same as that on a conventional reversed-phase alkyl-bonded phase. Further, increasing the acetonitrile content in the mobile phase decreased the retention times of the drugs, and the drugs seemed to be separated mainly based on the reversed-phase mode. Strictly, the separation may be affected by some other physico-chemical interactions except for the hydrophobic interaction. As a result, it was found that the diol phase had two different layered functions to restrict the proteins and to retain the drugs. Therefore, the diol phase seemed to be suitable for a binary-layered phase packing as a restricted access packing material.

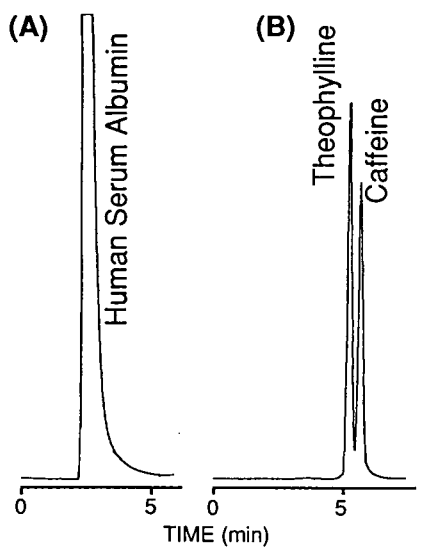

Fig. 5. Separations of (A) human serum albumin and (B) drugs on diol silica gel column. Conditions: column, LiChrospher 100 DIOL (250 × 4 mm I.D.); eluent, 50 m*M* phosphate buffer (pH 6.9)–acetonitrile (98.2:1.8, v/v); flow-rate, 0.6 ml/min; column temperature, ambient; detection, UV at 254 nm; injection volume, 20 μl. Samples: (A) human serum albumin (1%, w/v); (B) theophylline and caffeine (10 μg/ml each in water).

Fig. 6 shows chromatograms from the direct injection of human serum spiked with theophylline and caffeine on the diol silica column. Fig. 6A is for the serum bland and Fig. 6B for the spiked sample. The serum proteins were eluted in the void volume as the standard serum albumin, while the drugs followed the elution of the serum proteins, and these relatively hydrophilic compounds were well separated, as shown in Fig. 6B.

Fig. 7 shows a chromatogram from the direct injection of human serum containing phenobarbital, phenytoin and carbamazepine on the diol silica column. These relatively hydrophobic drugs were completely resolved within 10 min by increasing the acetonitrile content.

Fig. 8 shows the satisfactory separation of the acidic drugs acetylsalicylic and salicylic acid on the diol silica column with an acidic eluent.

When a macroporous diol silica gel (pore size ca. 30 nm) column was used for the same

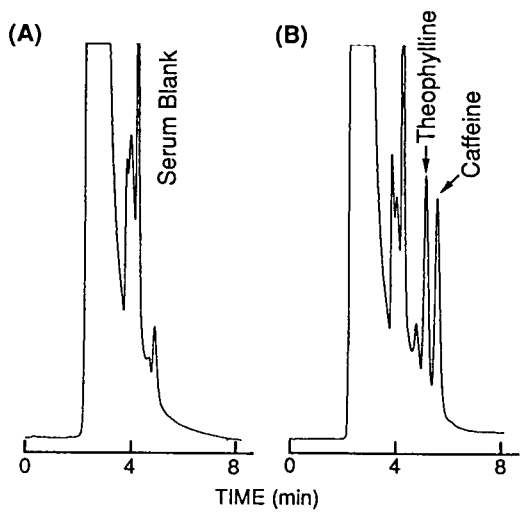

Fig. 6. Binary-layered phase liquid chromatographic analysis of (A) a serum blank and (B) serum spiked with drugs on a diol silica gel column. Chromatographic conditions as in Fig. 5. Samples: theophylline and caffeine (10 μg/ml each).

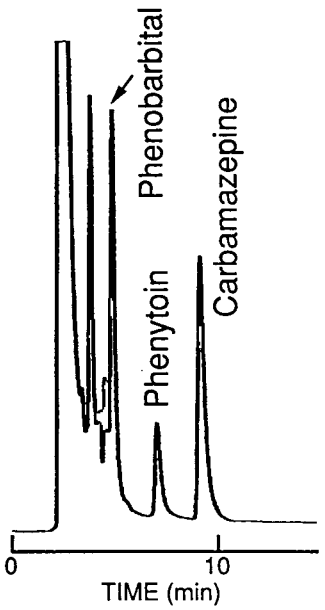

Fig. 7. Binary-layered phase liquid chromatographic separation of drugs in human serum by direct serum injection. Conditions: eluent, 50 m*M* phosphate buffer (pH 6.9)–acetonitrile (88:12, v/v); injection volume, 5 μl; other conditions as in Fig. 5. Samples: phenobarbital (18 μg/ml), phenytoin (20 μg/ml) and carbamazepine (18 μg/ml).

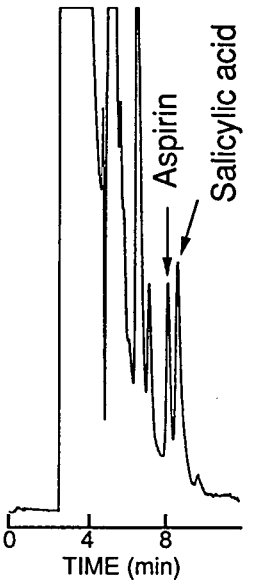

Fig. 8. Binary-layered phase liquid chromatographic separation of drugs in human serum by direct serum injection. Conditions: eluent, 50 m*M* phosphate buffer (pH 3.0)–acetonitrile (98.5/1.5, v/v); flow-rate, 0.5 ml/min; injection volume, 2 μl; other conditions as in Fig. 5. Samples: acetylsalicylic acid and salicylic acid (20 μg/ml each).

purpose, proteins also eluted before small molecules. However, small molecules such as drugs could not be sufficiently retained on the column to be mutually separated. The reason may be that the retention capacity of the macroporous diol silica is lower than that of microporous material based on the difference in their surface area. Although small hydrophobic solutes such as alkylbenzenes are naturally well retained on the macroporous diol silica column, it seens that these conditions are not practical for drug determinations.

As described above, diol columns have been used for the size-exclusion chromatography of the proteins. The recovery of the proteins on a diol column has also been investigated [25,26]. Schmidt et al. [25] reported that the recoveries of a number of proteins from a diol column were excellent when using 0.35 *M* sodium acetate (pH 5.0) and 0.1 *M* sodium sulfate as the mobile phase. Haginaka and Wakai [23] reported that serum proteins were almost completely eluted from a mixed functional phase containing a diol phase when 50–100 m*M* phosphate buffer over the pH range 3–7 was used as the eluent. The serum proteins seemed to be substantially recovered from the diol column used in the present study; the recovery of standard human serum albumin from the present diol column was nearly 100%.

When the PTFE paper filter of the column guard unit was changed after every 40th direct injection, the separation system with the same diol column maintained its performance for at least several hundred injections. Therefore, the binary-layered diol phase as a restricted access packing material seemed to be useful for direct serum injection for the determination of drugs.

As indicated above, it was found that the ethanediol layer if the diol-bonded phase restricted the access of proteins into the stationary

phase, and the methoxypropyl layer of the diol packing had sufficient hydrophobicity to retain small molecules such as synthetic drugs. As the hydrophobicity in the diol phase is lower than that for other previous restricted access packings, hydrophilic drugs such as theophilline eluted in the serum blank. However, this should not interfere with the quantitative analysis. Fig. 9 shows a suggested illustration of binary-layered phase liquid chromatographic separation on the diol-bonded silica column. In addition, diol-bonded silica gel was useful as a restricted access packing for the direct injection analysis of serum for the determination of both hydrophobic and hydrophilic drugs over the pH range of the eluent that is employed with ordinary siloxane-bonded silica material.

Fig. 10 shows schematic models of the restricted access packings. Previously reported models are based on the idea shown in model A, B or C. In model A, proteins were restricted by small pores from access to the internal hydrophobic bonded phase. This type of packing has two different functions on the internal surface and the external surface of the pores. Model B or C has a steric or shielding hydrophilic function that shielded the hydrophobic function to restrict protein access. These functions are introduced or localized without distinction regarding the internal or external location of the pores. In contrast, the present idea of a binary-layered phase is illustrated as model D. This is a new concept for a restricted access separation mechanism different from any idea of a multiple retention mechanism.

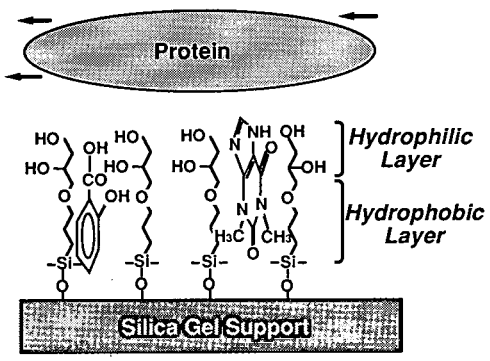

Fig. 9. Suggested illustration of the mechanism of the binary-layered phase liquid chromatographic separation of protein and synthetic drugs on the diol-bonded silica column.

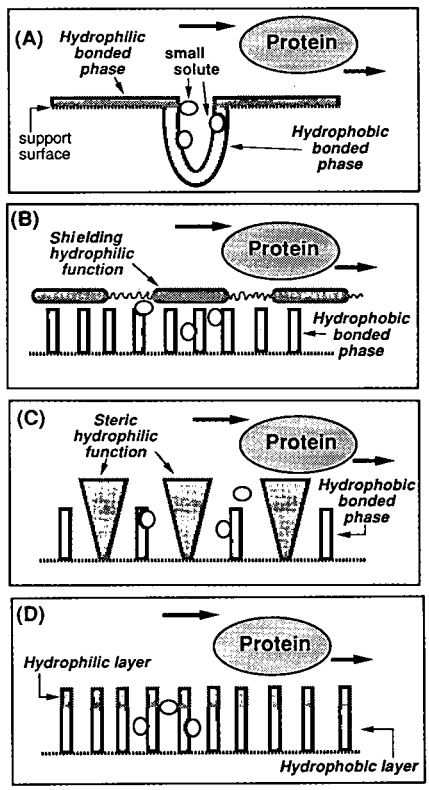

Fig. 10. Schematic models of various restricted access packings. (A) Internal-surface reversed phase; (b) shielded hydrophobic phase or semi-permeable surface; (c) mixed functional phase; (D) binary-layered phase.

Previously, many ideas have been reported for multiple retention mechanisms, and have been called "mixed-mode separation" [27], "multimode separation" [28], "bimodal separation" [29], and so on. These characteristic separations were carried out with various multi-functional stationary phases. For example, a long-chain alkylamine-coated alkylsilyl silica gel functioned as a hydrophobic anion exchanger, and the separations on this material were called mixed-mode separation. A polymer bead having a hydrophilic surface exhibited a negative hydrophobic effect owing to the constructional charac-

ter of the base gel, and the characteristic separations on the polymer gel were called multimode separation.

In contrast, the mechanism of the present multi-functional separation system can be clearly explained and discriminated from the abovementioned previous multiple retention mechanisms. Two different functional structures were obtained in one chemical bond forming a binary-layered phase on the support surface, and these intended functions were displayed in one chromatographic process. Following the present idea, various other combinations of the different functions can be designed to prepare a variety of binary-layered phase packing materials. We therefore propose the following concept [30]: stationary phase(s) such as the diol phase that have two different functions at a single chemical bond on the support should be called "binary-layered phase packing(s)", and separation(s) on the binary-layered phase packing should be named "binary-layered phase liquid chromatography".

References

[1] J.D. Pearson, N.T. Lin and F.E. Regnier, *Anal. Biochem.*, 124 (1982) 217.
[2] J.D. Pearson and F.E. Regnier, *J. Liq. Chromatogr.*, 6 (1983) 497.
[3] F.E. Regnier, *Science*, 222 (1983) 245.
[4] L.R. Snyder, M.A. Stadalius and M.A. Quarry, *Anal. Chem.*, 55 (1983) 1412A.
[5] X. Geng and F.E. Regnier, *J. Chromatogr.*, 296 (1984) 15.
[6] D.W. Armstrong and R.E. Boehm, *J. Chromatogr. Sci.*, 22 (1984) 378.
[7] M.A. Quarry, M.A. Stadalius, T.H. Mourey and L.R. Snyder, *J. Chromatogr.*, 358 (1986) 1.
[8] M.A. Stadalius, M.A. Quarry, T.H. Mourey and L.R. Snyder, *J. Chromatogr.*, 358 (1986) 17.
[9] N. Nimura, H. Itoh, T. Kinoshita, N. Nagae and M. Nomura, *J. Chromatogr.*, 585 (1991) 207.
[10] H. Itoh, N. Nimura, T. Kinoshita, N. Nagae and M. Nomura, *Anal. Biochem.*, 199 (1991) 7.
[11] G. Jilge, R. Janzen, H. Giesche, K.K. Unger, J.N. Kinkel and M.T.W. Hearn, *J. Chromatogr.*, 397 (1987) 71.
[12] H. Itoh, N. Nagae, T. Kinoshita and N. Nimura, *Chromatography*, 14 (1993) 89R.
[13] T.C. Pinkerton, *J. Chromatogr.*, 544 (1991) 13.
[14] K.K. Unger, *Chromatographia*, 31 (1991) 507.
[15] H. Yoshida, I. Morita, T. Masujima and H. Imai, *Chem. Pharm. Bull.*, 30 (1982) 2287.
[16] H. Yoshida, I. Morita, G. Tamai, T. Masujima, T. Tsuru, N. Takai and H. Imai, *Chromatographia*, 19 (1984) 466.
[17] I.H. Hagestam and T.C. Pinkerton, *Anal. Chem.*, 57 (1985) 1757.
[18] I.H. Hagestam and T.C. Pinkerton, *J. Chromatogr.*, 351 (1986) 239.
[19] S.E. Cook and T.C. Pinkerton, *J. Chromatogr.*, 368 (1986) 233.
[20] D.J. Gisch, B.T. Hunter and B. Feibush, *J. Chromatogr.*, 433 (1988) 264.
[21] C.P. Desilets, M.A. Rounds and F.E. Regnier, *J. Chromatogr.*, 544 (1991) 25.
[22] J. Haginaka, J. Wakai and H. Yasuda, *J. Chromatogr.*, 535 (1990) 163.
[23] J. Haginaka and J. Wakai, *J. Chromatogr.*, 596 (1992) 151.
[24] L. Hagel, in J.-C. Janson and L. Ryden (Editors), *Protein Purification*, VCH, New York, 1989, p. 63–106.
[25] D.E. Schmidt, Jr., R.W. Giese, D. Conron and B.L. Karger, *Anal. Chem.*, 52 (1980) 177.
[26] K.K. Unger and P. Roumeliotis, *J. Chromatogr.*, 218 (1981) 535.
[27] L.W. Mclaughlin, *Chem. Rev.*, 89 (1989) 309.
[28] N. Hirata, M. Kasai, Y. Yanagihara and K. Noguchi, *J. Chromatogr.*, 434 (1988) 71.
[29] S.H.Y. Wong, *J. Pharm. Biomed. Anal.*, 7 (1989) 1011.
[30] N. Nimura, H. Itoh and T. Kinoshita, *Chromatography*, 13 (1992) 293; *C.A.*, 119 (1993) 85258p.

ELSEVIER

Journal of Chromatography A, 689 (1995) 211–218

JOURNAL OF CHROMATOGRAPHY A

High-throughput processing of proteins using a porous and tentacle anion-exchange membrane

Satoshi Tsuneda[a], Kyoichi Saito[a,*], Shintaro Furusaki[a], Takanobu Sugo[b]

[a]*Department of Chemical Engineering, Faculty of Engineering, University of Tokyo, Hongo, Tokyo 113, Japan*

[b]*Takasaki Radiation Chemistry Research Establishment, Japan Atomic Energy Research Institute, Takasaki, Gunma 370-12, Japan*

First received 16 May 1994; revised manuscript received 15 September 1994

Abstract

The immobilization of polymer chains containing a diethylamino (DEA) group on the pore surface of a porous hollow-fibre membrane is reported. This novel membrane can collect proteins at a high rate and high capacity because of convective transport and multi-layering of proteins. Overlapping of the breakthrough curves for different residence times of bovine serum albumin (BSA) solution demonstrates that the diffusional resistance of BSA to the DEA group anchored to the polymer chain was negligible. Membranes with a higher density of DEA groups exhibited a higher binding capacity for BSA. For example, a membrane with a DEA group density of 2.9 mol/kg had a BSA binding capacity of 490 g/kg, which was equivalent to eleven times the adsorption capacity of a monolayer. This vertical layering is due to holding of the BSA molecules in a tentacle-like manner by the graft chains extending from the pore surface towards the pore interior.

1. Introduction

Conventional ion-exchange beads used for protein collection and purifications allow proteins to diffuse into the bead interior, immobilizing the ion-exchange groups; in this case, a longer time is required for proteins of higher molecular mass to reach the ion-exchange groups. This diffusion-limited binding process also results in a lower degree of enrichment in a subsequent elution process.

Brandt et al. [1] prepared a porous affinity membrane for the purification of proteins and demonstrated that convective transport of the protein minimized the diffusional path to the ligand. Afeyan et al. [2] prepared a functionalized bead having pores through which a protein can be transported by convection and showed that diffusional resistance in the bead-packed bed could be neglected. These two methods of chromatography aided by convection were designated membrane chromatography and perfusion chromatography, respectively.

We have anchored affinity ligands and ion-exchange groups to polymer chains grafted on the pore surface of porous membranes [3–5]. Negligible diffusional resistance of the protein to the ligand and ion-exchange group could be attained by permeating the protein solution through the porous membrane; a higher permeation rate led to a higher collection rate of the protein.

* Corresponding author.

0021-9673/95/$09.50
SSDI 0021-9673(94)00911-2

Conventional ion-exchange beads exhibit a monolayer adsorption capacity for proteins, and therefore porous ion-exchange beads with a higher specific surface area have been used for preparative chromatography. On the other hand, Muller [6] suggested tentacle-type ion-exchange beads, which were prepared by chemical grafting of vinyl monomers originally containing ion-exchange groups. The ion-exchange group-containing polymer chains can thus hold the proteins three-dimensionally like a tentacle. Monomers and supporting materials for the tentacle polymer chains have been studied for various kinds of proteins [7]. In order to clarify the tentacle phenomenon capable of collecting proteins in multi-layers, the dependence of the degree of tentacle binding on the nature of the grafted polymer branches, such as length, number density and charge density of the polymer chain, should be elucidated.

In this study, we developed a novel "porous and tentacle" membrane that achieves protein processing at a high rate and high capacity. The porous membrane immobilizing the ion-exchange graft chain capable of tentacle binding can collect proteins at a high rate and high capacity because of convective transport and multi-layering of the proteins. Fig. 1 illustrates the principle of processing of proteins using the porous and tentacle membrane. A diethylamino (DEA) group [$-N(CH_2CH_3)_2$] as a weakly basic anion-exchange group was appended to a porous hollow-fibre membrane by radiation-induced graft polymerization and subsequent chemical modification. The DEA-containing anion exchanger has a wide applicability for protein collection [8–11]. Advantages brought about by the porous and tentacle membrane in protein collection were evaluated by permeating a protein solution through the pores of the resultant hollow fibre.

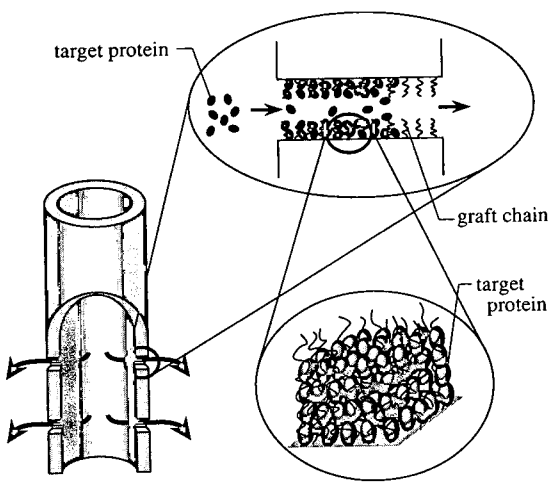

Fig. 1. Processing of proteins using the porous and tentacle ion-exchange membrane. Proteins are adsorbed on the ion-exchange group-containing polymer chain immobilized on the pore surface of the membrane. (a) Convection of the liquid across the hollow fibre through its pores minimizes the diffusion path of the proteins to the ion-exchange groups on the graft chain. (b) The graft chains extending towards the pore interior from the pore surface lead to vertical layering of proteins.

2. Experimental

2.1. Materials

A commercially available microfiltration hollow-fibre membrane (Asahi Chemical Industry, Tokyo, Japan) was used as a trunk polymer for grafting. This hollow fibre, made of polyethylene, has inner and outer diameters of 1.95 and 3.01 mm, respectively, with a nominal pore diameter of 0.34 μm and a porosity of 71%. Technical-grade glycidyl methacrylate [GMA, $CH_2=C(CH_3)COOCH_2CHOCH_2$] was purchased from Tokyo Kasei Industry (Tokyo, Japan) and used without further purification. Diethylamine [$NH(CH_2CH_3)_2$] and ethanolamine ($NH_2CH_2CH_2OH$) were obtained from Wako (Osaka, Japan). Lactoglobulin, bovine serum albumin and bovine γ-globulin were purchased from Sigma (St. Louis, MO, USA).

2.2. Preparation of diethylamino-containing membrane

Fig. 2 shows the preparation scheme for the DEA-containing hollow-fibre membrane. A 10-

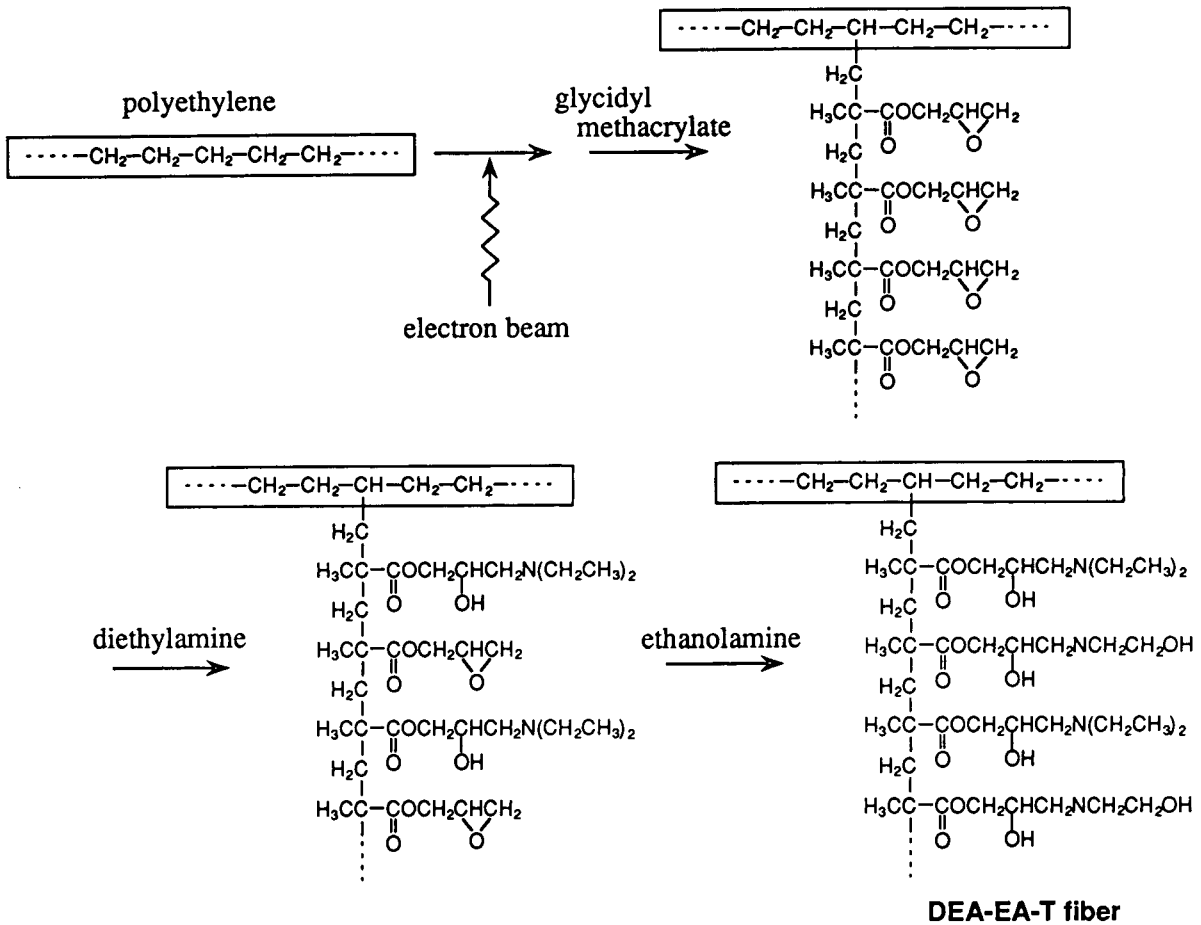

Fig. 2. Scheme of preparation of diethylamino-containing hollow-fibre membrane.

cm long hollow fibre was irradiated with an electron beam from an accelerator at ambient temperature under a nitrogen atmosphere. The total dose was 200 kGy. The irradiated hollow fibre was immersed at 313 K in 10% (v/v) solution of GMA in methanol which had previously been deaerated. The amount of GMA grafted on to the hollow fibre was expressed by the degree of grafting,

$$dg = 100[(M_1 - M_0)/M_0] \quad (1)$$

where M_0 and M_1 are the masses of the original and GMA-grafted hollow fibres, respectively. Here, dg was set at 200%.

The epoxy groups produced were converted into diethylamino (DEA) groups by immersing the GMA-grafted hollow fibre in 50% (v/v) aqueous diethylamine solution at 303 K. After the prescribed time, the hollow fibre was removed, washed repeatedly with deionized water and dried under reduced pressure. The remaining epoxy groups were subsequently converted into ethanolamino (EA) groups by soaking the hollow fibre in ethanolamine at 303 K for 6 h. The density of DEA groups was defined from the mass change as follows:

$$\text{density of DEA groups } (X) = [((M_2 - M_1)/73)/M_3] \quad (2)$$

where M_2 and M_3 are the masses of the DEA-

containing hollow fibre and DEA- and EA-containing hollow fibre, respectively. The constant 73 is the molecular mass of diethylamine.

2.3. Properties of membrane

The membrane volume V_m in the wet state was calculated from the equation

$$V_m = \pi L(d_o^2 - d_i^2)/4 \quad (3)$$

where d_i, d_o and L are the inner and outer diameters and the length of the hollow fibre, respectively. Prior to volume measurement, the hollow fibre was immersed in methanol for 10 min and subsequently replaced with water. The inner and outer diameters of the hollow fibre were measured under a microscope and the length with a scale.

After the hollow fibre had been dried under reduced pressure, the specific surface area was determined by the nitrogen adsorption method using Quantasorb (Yuasa Ionics, Tokyo, Japan). The pore structure was observed by scanning electron microscopy.

2.4. Adsorption and elution of proteins during permeation

The protein was dissolved in 0.02 *M* Tris–HCl buffer (pH 8.0). The feed concentration was 5 mg/ml. A hollow fibre was set in an I-configuration. The solution was forced to permeate from the inside to the outside of the hollow fibre at a constant flow-rate using an infusion syringe pump (ATOM-235, ATOM, Tokyo, Japan). The flow-rate ranged from 20 to 100 ml/h. The effluent penetrating the outside surface of the hollow fibre was collected using a fraction collector (Model 2110; Bio-Rad Labs., Richmond, CA, USA). The protein concentration of each fraction was determined by measuring the UV absorbance at 280 nm.

After adsorption equilibrium had been attained in the permeation mode, 10 ml of the protein-free buffer solution and 0.02 *M* Tris–HCl buffer solution containing 0.5 *M* NaCl were forced to permeate radially outwards to wash and elute the adsorbed protein, respectively. The elution percentage was defined as

$$\text{elution percentage} = 100[(\text{amount eluted})/(\text{amount adsorbed} - \text{amount washed})] \quad (4)$$

2.5. Evaluation of binding capacity of membrane

The corresponding binding capacity of the porous ion-exchange membrane, q, calculated by integrating the breakthrough curve, is as follows:

$$q = \int_0^{V_s} (C_0 - C)\, dV/M_3 \quad (5)$$

where C_0 and C are the protein concentrations of the feed and effluent, respectively, V is the effluent volume and V_s is the effluent volume when C reaches C_0.

The theoretical binding capacity q_t for protein adsorbed as a monolayer on the membrane is

$$q_t = a_v M_{rp}/(aN_A) \quad (6)$$

where a_v is the specific surface area of the membrane, a is the cross-sectional area occupied by a protein molecule with an end-on orientation, N_A is Avogadro's number and M_{rp} is the molecular mass of the protein.

3. Results

3.1. Preparation of diethylamino-containing fibre

A polymer chain containing epoxy groups was grafted on to a porous polyethylene hollow-fibre membrane by radiation-induced graft polymerization of GMA. Subsequently, part of the epoxy groups produced were converted into DEA groups and the remaining epoxy groups were converted into EA groups. The resultant hollow fibre is referred to as a DEA(X)-EA-T fibre, where X is the DEA group density and T stands for tubular shape. The DEA group density ranged from 0 to 2.9 mol per kilogram of the product by varying the reaction time. A uniform distribution of chloride ions captured by the

DEA group throughout the hollow fibre was observed using an electron probe X-ray microanalyser. The specific surface area of the DEA-EA-T fibre was constant at 5.0 m^2/g irrespective of the DEA group density. After grafting and subsequent chemical modification, the hollow fibre extended from 10 to 13 cm in length due to swelling. The DEA(2.9)-EA-T fibre swelled 3.2 times compared with the starting hollow fibre; therefore, the pore structure observed by scanning electron microscopy (SEM) was maintained.

3.2. Protein adsorption and elution during permeation

Bovine serum albumin (BSA) solution was forced to permeate through the DEA(1.7)-EA-T fibre at different flow-rates. Fig. 3 shows the breakthrough curve, i.e., BSA concentration as a function of effluent volume. The flow rate, ranging from 20 to 100 ml/h, corresponded to mean residence time, ranging from 165 to 33 s. The breakthrough curves overlapped irrespective of the residence time. Also, a sharp peak of the elution curve was obtained irrespective of the flow-rate.

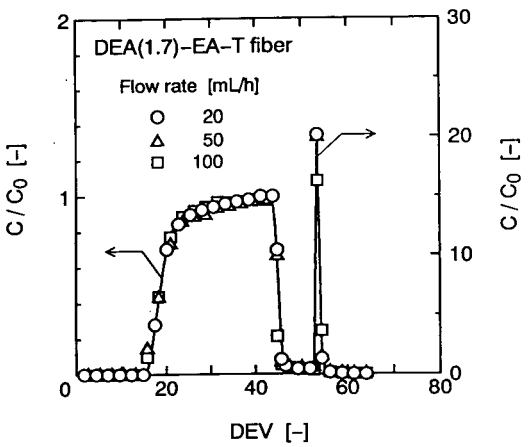

Fig. 3. Breakthrough and elution curves for the porous hollow-fibre membrane containing diethylamino (DEA) groups at different flow-rates: ○ = 20; △ = 50; □ = 100 ml/h. The ordinate C/C_0 is the concentration of the effluent relative to the feed; the abscissa is dimensionless effluent volume (DEV), defined as the effluent volume divided by the membrane volume.

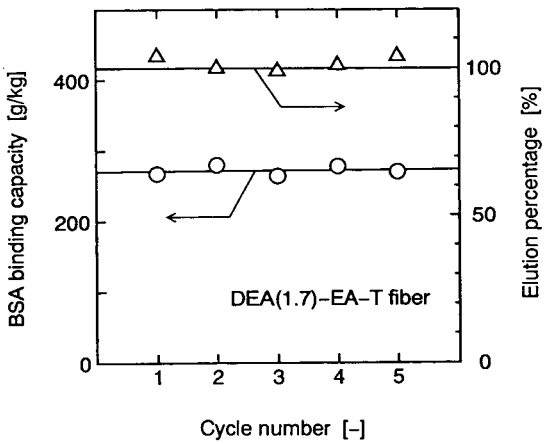

Fig. 4. Amount of BSA adsorbed and elution percentage vs. number of repeated uses.

3.3. Dependence of binding capacity and elution percentage on repeated use

Fig. 4 shows the amount of BSA adsorbed and the elution percentage in each cycle consisting of adsorption, washing and elution, in that sequence. BSA could be quantitatively eluted with Tris–HCl buffer solution containing 0.5 *M* NaCl. No deterioration of the physical strength or the binding capacity of the membrane was observed during five cycles of adsorption, washing and elution.

3.4. Dependence of binding capacity on DEA group density

Fig. 5 shows the binding capacity of the DEA(*X*)-EA-T fibre, q, calculated by integrating the breakthrough curves. The dashed line represents the theoretical binding capacity, q_t, for BSA adsorbed on the DEA(*X*)-EA-T fibre in a monolayer with an end-on orientation. A higher density of the DEA groups on the membrane led to a higher binding capacity for BSA. For example, the DEA(2.9)-EA-T fibre had a

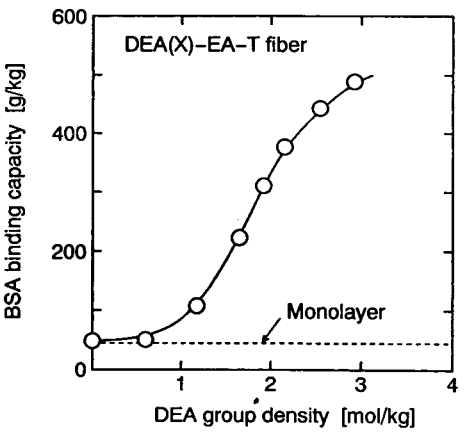

Fig. 5. BSA binding capacity as a function of DEA group density.

BSA binding capacity of 490 g/kg, which was eleven times higher than q_t.

3.5. Adsorption of various proteins

Three kinds of proteins, lactoglobulin (M_{rp} = 18 000, 3.6 × 3.6 × 3.6 nm, pI = 5.0) [12], bovine serum albumin (BSA, M_{rp} = 67 500, 4.0 × 4.0 × 11.5 nm, pI = 4.9) [13] and bovine γ-globulin (M_{rp} = 169 000, 4.4 × 4.4 × 23.5 nm, pI = 5.8–7.3) [14], were tested in the permeation mode, using the same buffer solution (pH 8). The binding capacities for the proteins bound to the DEA(1.7)-EA-T fibre are summarized in Table 1. The proteins tested were held in a tentacle-like manner by the graft chain.

4. Discussion

We succeeded in preparing a novel material in a hollow-fibre form that meets the three requirements for high-throughput processing of proteins: high rate, high capacity and high reproducibility. First, we aimed to transport the protein by convection through the pores of the hollow-fibre membrane immobilizing the ion-exchange group-containing graft chain. The protein solution was forced to permeate across the porous ion-exchange membrane. As a result, the breakthrough curve was independent of flow-rate, i.e., the residence time, because of negligible diffusional mass-transfer resistance. This means that a higher flow-rate of the protein

Table 1
Summary of properties and protein adsorption performance of tentacle-type ion exchangers

Support material			Grafting method	Monomer[a]	Protein	Monolayer adsorption (g/kg)[b]	Binding capacity (g/kg)	Ref.
Type	Shape	Structure						
Polyethylene	Hollow fibre	Porous	Radiation	GMA–DEA	Lactoglobulin	15	266	This work
					BSA	45	49–490	
					BGG	93	387	
Polyethylene	Hollow fibre	Porous	Radiation	GMA–SS	Lysozyme	18	40–200	[15]
Fractogel[c]	Bead	Non-porous	Chemical	DEAEAAm	BSA		70–140 g/l	[6]
				AAc	Haemoglobin		70–140 g/l	
				AMPS	Lysozyme		70–140 g/l	
Silica	Bead	Porous	Chemical	TMAEAAm	BSA		50	[7]

[a] DEAEAAm = Diethylaminoethylacrylamide; AAc = acrylic acid; AMPS = 2-acrylamide-2-methylpropanesulfonic acid; TMAEAAm = trimethylaminoethylacrylamide; GMA = glycidyl methacrylate; SS = sodium sulfide; DEA = diethylamine.
[b] Theoretical binding capacity for protein adsorbed as a monolayer with an end-on orientation on the ion exchanger.
[c] Copolymer of oligoethylene glycol, glycidyl methacrylate and pentaerythrol dimethacrylate.

solution through the membrane can result in a higher collection rate of the protein.

Second, the ion-exchange group-containing graft chains extended from the pore surface towards the pore interior owing to mutual electrostatic repulsion. A higher density of the ion-exchange groups was found to lead to a higher capacity for protein binding owing to the presence of three-dimensional adsorption sites for proteins. As a result, the DEA-containing membrane could hold an amount of bovine serum albumin eleven times greater than that which could be adsorbed as a monolayer on the interface.

Third, we designed the polymer chains grafted on to a porous membrane made of polyethylene in such a way that led to enhancement of the selective adsorption of the target proteins by the anion-exchange (DEA) groups and retardation of non-selective adsorption of the proteins by alcoholic hydroxyl (EA) groups. The EA group functioned as both an anion-exchange group and a hydrophilic group: the EA-containing fibre [DEA(0)-EA-T fibre], which was obtained via 90% conversion of the GMA-grafted fibre with ethanolamine, allowed monolayer BSA adsorption, as shown in the plot corresponding to a DEA group density of zero in Fig 5. As BSA could be quantitatively eluted from the DEA(0)-EA-T fibre, satisfactory quenching of the epoxy groups was realized. Quantitative elution of the protein by permeating a buffer solution containing 0.5 *M* NaCl was achieved for DEA-EA-T fibres whose DEA group density ranged up to 2.9 mol/kg. A higher rate of elution was also attained by convection of the adsorbed protein from the ion-exchange group to the bulk.

Vertical layering of the protein by the DEA-containing graft chain, i.e., tentacle binding, was confirmed for bovine γ-globulin, lactoglobulin and BSA. In a previous study [15], the combination of lysozyme and a sulfonic acid group-containing graft chain also exhibited a tentacle-like interaction. Table 1 summarizes the tentacle binding in previous studies [6,7,15]. Tentacle binding was found not to be an exceptional interaction between a protein and the ionizable graft chain.

Membrane chromatography [1] and perfusion chromatography [2] have been suggested as methods of protein processing aided by convective transport. Tentacle binding using chemically modified beads was reported by Muller [6]; however, the degree of tentacle binding has not previously been investigated as a function of the chemical structure of the graft chain. In this study, we realized simultaneously high-rate and high-capacity processing of proteins while retarding non-selective adsorption of the protein using a porous and tentacle ion-exchange membrane prepared by radiation-induced graft polymerization of the epoxy-containing monomer and subsequent modification into an anion-exchange moiety.

Acknowledgements

We thank Yoshizumi Inai of the Industrial Membrane Division of Asahi Chemical Industry for providing the starting hollow-fibre membrane. We are also grateful to Tsuyoshi Yoshida for preparing the schematic illustrations.

References

[1] S. Brandt, R.A. Goffe, S.B. Kessler, J.L. O'Connor and S.E. Zale, *Bio/Technology*, 6 (1988) 779.
[2] N.B. Afeyan, S.P. Fulton, N.F. Gordon, I. Mazsaroff, L. Varady and F.E. Regnier, *Bio/Technology*, 8 (1990) 203.
[3] H. Iwata, K. Saito, S. Furusaki, T. Sugo and J. Okamoto, *Biotechnol. Prog.*, 7 (1991) 412.
[4] M. Kim, K. Saito, S. Furusaki, T. Sugo and I. Ishigaki, *J. Chromatogr.*, 586 (1991) 27.
[5] H. Shinano, S. Tsuneda, K. Saito, S. Furusaki and T. Sugo, *Biotechnol. Prog.*, 9 (1993) 193.
[6] W. Muller, *J. Chromatogr.*, 510 (1990) 133.
[7] R. Janzen, K.K. Unger, W. Muller and M.T.W. Hearn, *J. Chromatogr.*, 522 (1990) 77.
[8] R.D. Whitley, R. Wachter, F. Liu and N.H.L. Wang, *J. Chromatogr.*, 465 (1989) 137.
[9] A.C.R. Tsuei and V.C. Yang, *Biomaterials*, 11 (1990) 734.
[10] J.X. Huang, J. Schudel and G. Guiochon, *J. Chromatogr. Sci.*, 29 (1991) 122.
[11] E.A. James and D.D. Do, *J. Chromatogr.*, 542 (1991) 19.

[12] A. Baszkin and D.J. Lyman, *J. Biomed. Mater. Res.*, 14 (1980) 393.
[13] P. Bagchi and S.M. Birnbaum, *J. Colloid Interface Sci.*, 83 (1981) 460.
[14] M.C. Wahlgren, T. Arnebrant and M.A. Paulsson, *J. Colloid Interface Sci.*, 158 (1993) 46.
[15] S. Tsuneda, H. Shinano, K. Saito, S. Furusaki and T. Sugo, *Biotechnol. Prog.*, 10 (1994) 76.

ELSEVIER

Journal of Chromatography A, 689 (1995) 219–226

JOURNAL OF CHROMATOGRAPHY A

Recognition of α-helical peptide structures using high-performance liquid chromatographic retention data for D-amino acid analogues: influence of peptide amphipathicity and of stationary phase hydrophobicity

S. Rothemund[a], E. Krause[a,*], M. Beyermann[a], M. Dathe[a], H. Engelhardt[b], M. Bienert[a]

[a]*Forschungsinstitut für Molekulare Pharmakologie, Alfred-Kowalke-Strasse 4, 10315 Berlin, Germany*
[b]*Angewandte Physikalische Chemie, Universität des Saarlandes, 66123 Saarbrücken, Germany*

First received 14 June 1994; revised manuscript received 21 September 1994

Abstract

The reversed-phase HPLC behaviour of double D-amino acid replacement sets of amphipathic and non-amphipathic helix-forming peptides consisting exclusively of leucine, lysine and alanine residues was studied on different polymer-encapsulated silica-based stationary phases. Plotting the retention times versus the position of D-amino acid substitution gives a characteristic pattern showing decreased retention times in the helical region. The retention time profile obtained using an amphipathic α-helix is caused by disturbance of the preferred binding domain of the stationary phase-bound peptide. However, the effect is similar but less pronounced using a non-amphipathic helical peptide that is unable to interact by a preferred binding site. The results demonstrate that reversed-phase HPLC data for peptide analogues provide an indication event of a non-amphipathic helical structure in peptides.

1. Introduction

In recent years, reversed-phase chromatography has become a useful tool for studying the structure of peptides induced by hydrophobic interactions [1]. Peptides consisting of more than 13–15 amino acid residues may form a secondary structure during RPC, influencing the retention behaviour [2]. The formation of an amphipathic α-helical structure with a hydrophobic binding domain causes a considerable increase in retention time in reversed-phase chromatography [3–6]. As incorporation of D-amino acids in α-helical peptides is known to decrease the helical content [7,8], D-amino acid replacement sets of KLALKLALKALKAALKLA-NH_2 and neuropeptide Y (NPY) were synthesized and used for the study of HPLC retention behaviour [9,10]. The results demonstrated that D-amino acid replacements destabilize the amphipathic α-helix leading to a decrease in hydrophobic interaction during reversed-phase HPLC. The effect is enhanced by substitution of two adjacent D-amino acids and correlates well with the circular dichro-

* Corresponding author.

0021-9673/95/$09.50
SSDI 0021-9673(94)00909-0

ism (CD)-determined helicity [9]. Thus, the "retention profile" that results from plotting the retention time versus the position of D-amino acid replacement provides an indication of amphipathic α-helical secondary structure in peptides. The effect of D-amino acid substitutions on the retention behaviour explained by disturbance of the hydrophobic binding site has so far been exclusively investigated by examining amphipathic helicies.

This study was carried out to evaluate the relationship between amphipathicity of a helical peptide and the effect of D-amino acid replacements on HPLC retention time. Non-amphipathic and amphipathic model peptides consisting exclusively of leucine, lysine and alanine having the same amino acid composition were synthesized and used in correlation studies of helicity versus HPLC retention time. In an attempt to investigate the influence of the stationary phase on the retention behaviour of the D-amino acid replacement sets, HPLC studies were carried out on polymer-encapsulated silica-based stationary phases with different hydrophobicities.

2. Experimental

2.1. Reversed-phase HPLC

Chromatographic measurements were performed on a Shimadzu LC-10A gradient HPLC system consisting of two LC-10AD pumps, a Sil-10A autoinjector, an SPD-M10A diode-array detector operating at 215 nm and a CLASS-LC10 software package. The sample concentration was 1 mg/ml peptide in 0.1% trifluoroacetic acid (TFA) with an injection volume of 10 μl. Runs were performed at ambient temperature and at a mobile phase flow-rate of 1 ml/min. Mobile phase A was 0.1% TFA in water and B was 0.1% TFA in acetonitrile–water (1:1, v/v), and the retention times of peptides were determined using a linear gradient from 30 to 95% B in 40 min.

2.2. Columns

Analytical runs were carried out on silica encapsulated with butyl acrylate (PolyEncap A300) (250 × 4.6 mm I.D., 5 μm) (Bischoff Analysentechnik, Leonberg, Germany), silica encapsulated with butylacrylamide (BAA) and silica encapsulated with octadecyl acrylate (ODA). The BAA and ODA phases were prepared by copolymerization of vinyl-derivatized silica (Nucleosil 5 μm, 300 Å pore diameter) with the corresponding acrylic acid derivatives as described previously [11]. By varying the acrylic acid derivatives it is possible to prepare different kinds of reversed-phase stationary phases. The relative hydrophobicity of these packings is BAA < PolyEncap < ODA. Columns (250 × 4.6 mm I.D.) were slurry packed using carbon tetrachloride–2-propanole (1:1, v/v).

2.3. Peptide synthesis and purification

The 18-mer model peptides and the corresponding D-amino acid analogues were synthesized automatically (Abimed AMS 422 multiple peptide synthesizer) by solid-phase methods using standard 9-fluorenylmethoxycarbonyl (Fmoc) chemistry (TentaGel S RAM resin, 0.21 mmol/g; Rapp Polymere, Tübingen, Germany), 2-(1H - benzotriazol - 1 - yl - oxy - 1,1,3,3 - bispentamethylene-uronium tetrafluoroborate (TBPipU) coupling [12] and deblocking with piperidine–dimethylformamide (20:80). The peptides were N-terminally acetylated with acetic anhydride–dimethylformamide–diisopropylethylamine (20:70:10, v/v/v) and the final cleavage was performed with trifluoroacetic acid–thioanisole–*m*-cresol (90:5:5, v/v/v) for 3 h at ambient temperature. Purification of the crude peptides was carried out by preparative HPLC on PolyEncap A300, 10 μm (250 × 20 mm I.D.) (Bischoff Analysentechnik) to give final products >95% pure by HPLC analysis. The peptides were characterized by matrix-assisted laser desorption ionization mass spectrometry (MALDI II; Kratos, Manchester, UK), which gave the expected $[M+H]^+$ mass

peaks and correct amino acid analyses (Biotronik-Eppendorf LC 3000).

2.4. Circular dichroism measurements

CD measurements were carried out on a Jasco Model 720 spectrometer in trifluoroethanol–water from 185 to 260 nm. Calculation of the percentage helicity content (h) was performed according to Chen et al. [13]:

$$h(\%) = ([\Theta]_{222} - [\Theta]^{0}_{222})/[\Theta]^{100}_{222}$$

where $[\Theta]_{222}$ is the determined mean residue ellipticity at 222 nm. The values of $[\Theta]^{0}_{222}$ and $[\Theta]^{100}_{222}$, corresponding to 0 and 100% helic content, respectively, at 222 nm, are estimated to be -2340 and $-30\,300°cm^2/dmol$, respectively. For precise determination of peptide concentrations, quantitative amino acid analysis was used.

3. Results and discussion

3.1. Design of α-helices with different amphipathicity

Derived from secondary structure-forming peptides which consisted of leucine, lysine and alanine [2], model peptides with 18 residues and identical amino acid composition were synthesized. Differences in the sequence lead to different distributions of hydrophobic and hydrophilic amino acids, as shown in the helical wheel projections in Fig. 1. In the amphipathic peptide KLLK the eight leucines are localized at one site, whereas in the peptide KLAL four leucines are clustered at two different places on the hydrophobic face of the helix. In both amphipathic peptides, KLLK and KLAL, the five hydrophilic lysines are exclusively located at one site of the helix. In contrast, the hydrophilic and hydrophobic amino acid residues of the non-amphipathic peptide KALK are well distributed around the α-helix. However, all peptides synthesized have a strong potential to form an α-helix according to the Chou–Fasman parameter [15]. Since acetylation of the N-terminus and amidation of the C-terminus are able to suppress unfavourable charge–dipole interactions of the helix and therefore increase the helix stability [16], the peptides were N-terminally acetylated and C-terminally amidated.

In order to cause a reliable destabilization along the helical peptide sequence, KLLK, KLAL and KALK analogues having successive replacements of two adjacent amino acids with the corresponding D-amino acids (DD-replacement set) were synthesized.

3.2. Determination of helicity by circular dichroism spectroscopy

The helical potential of the model peptides and of the double D-amino acid replacement sets was determined by circular dichroism. The fractional helicities (h) of KLLK, KLAL and KALK measured in acidic aqueous solutions (0.01 M H_3PO_4) remain less than 15%. As addition of 2,2,2-trifluoroethanol (TFE) is known to induce the formation of helical structures in peptides [17], CD spectroscopy were carried out in 0.01 M H_3PO_4–TFE mixtures. The maximum helical content of KLLK, KLAL and KALK was determined with 50% TFE to reach 79, 82 and 86%, respectively. Further, a change in peptide concentration from $5 \cdot 10^{-6}$ to $1 \cdot 10^{-3}$ M has no influence on CD, indicating that the three peptides consist mainly of monomeric helical structures in the presence of TFE. The CD spectra of some of the KLLK analogues are shown in Fig. 2 and the fractional helicities of the complete DD-replacement sets are summarized in Table 1. The results demonstrate that double D-amino acid substitutions in the amphipathic KLLK and KLAL and also in the non-amphipathic KALK decrease the fractional helicity, especially in the center of the helix. The influence of the position of double D-amino acid substitution on the helicity of the three model peptides is shown in Fig. 3. The obtained helicity profiles of the amphipathic and non-amphipathic peptides are similar and confirm a general destabilization of TFE-induced helical structures by double D-amino acid incorporation.

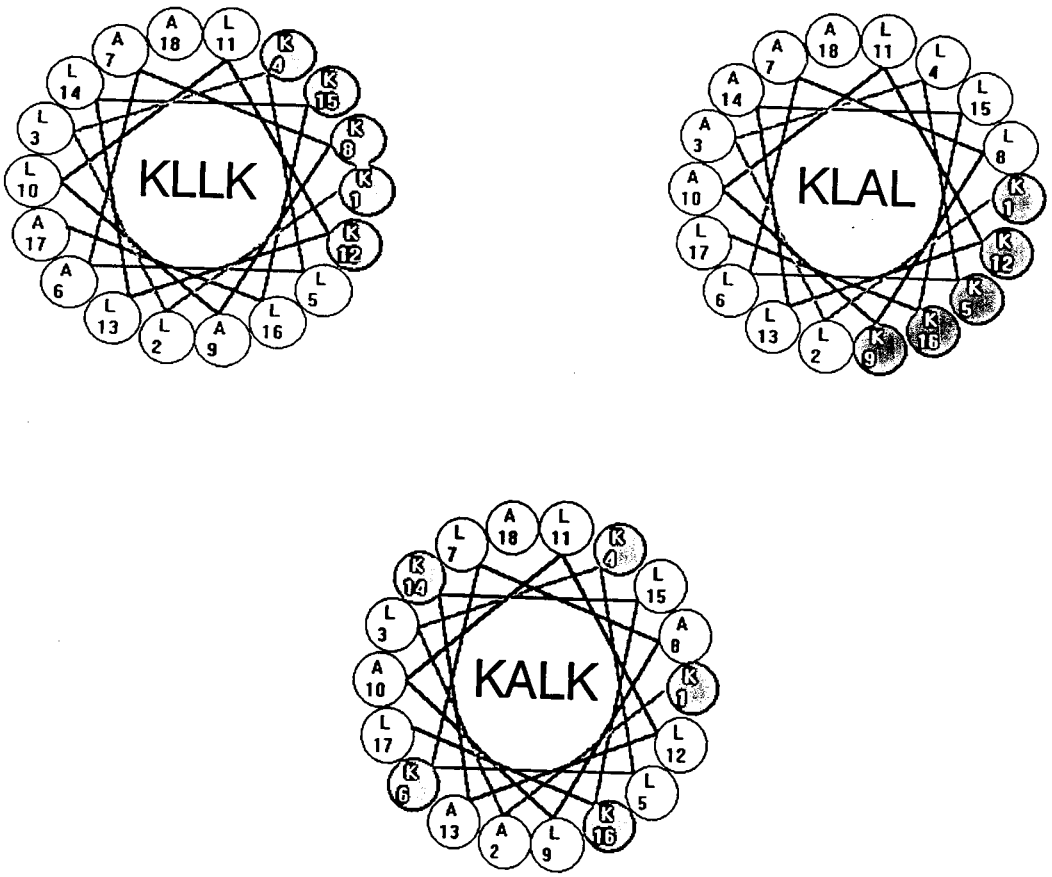

Fig. 1. Helical wheel projections [14] of KLLK, KLAL and KALK. The lysine residues are denoted by black circles.

3.3. Retention behaviour of the double D-amino acid replacement sets

The retention times of the model peptides and of the DD-replacement sets determined using a PolyEncap A300 column are given in Table 1. The order of the retention times of KLLK, KLAL and KALK (31.3, 29.4 and 19.0 min) correlates with the amphipathicity of the helices in line with Zhou et al. [5]. The more amphipathic the peptide, the longer is the retention time. These results indicate that the HPLC conditions are helix inducing and all of the model peptides are bound in a helical arrangement. Next, the effect of double D-amino acid replacement on the retention time was investigated. As shown in Fig. 4, the replacement of two amino acids by their D-isomers decreases the retention time in reversed-phase HPLC. This effect is stronger in the centre of the helix, whereas replacements close to either end have comparatively small effects because the lack of hydrogen bonds decreases the stability at the helix ends. A similar shape of a helix-destabilizing effect was described by Chakrabarty et al. [18] for a series of single alanine–glycine substitutions in a model helix. The results obtained with KLLK, KLAL and KALK confirm that the

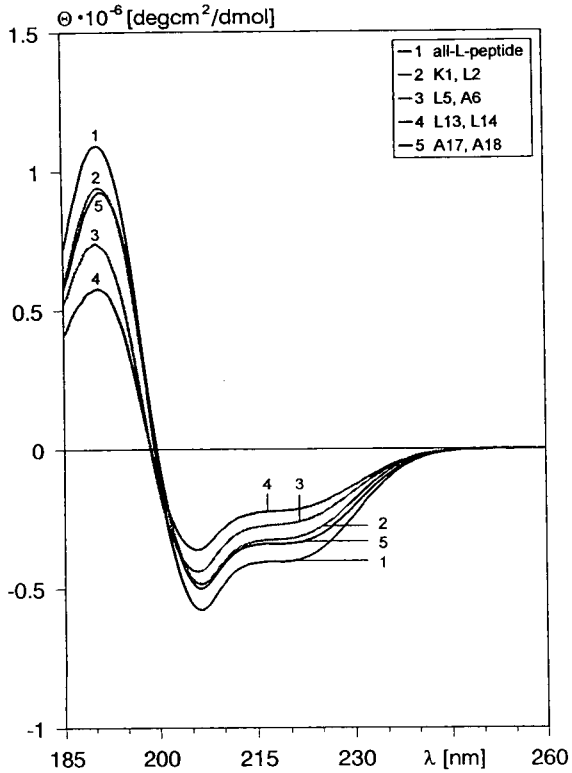

Fig. 2. CD spectra of KLLK and some of its analogues with double D-amino acid substitutions in TFE–0.01 *M* H_3PO_4 (1:1, v/v), $5 \cdot 10^{-5}$ mol/l.

differences in retention behaviour caused by DD-replacement correlate well with the helicity. It is remarkable that the replacement by double D-amino acids also in a non-amphipathic peptide, which is unable to form a preferred hydrophobic domain, leads to a characteristic retention time profile [Δ (retention time) versus substitution position]. Only the magnitude of the differences in retention times between all-L analogues and corresponding D-amino acid analogues is attributed to the disturbance of amphipathicity. Consequently, large differences (8–10 min) were obtained for the amphipathic peptides KLLK and KLAL, whereas the retention time profile of the DD-replacement of the non-amphipathic KALK which is caused exclusively by the destabilization of the helical structure is less pronounced (Fig. 4).

The formation of the energetically favoured helix structure during the chromatographic process depends on the hydrophobicity of the stationary phase [19] and therefore should be considered to examine secondary structure effects of peptides and proteins. Consequently, the retention time profiles of KLLK, KLAL and KALK were determined on different polymer-encapsulated silica-based stationary phases coated with butylacrylamide (BAA), butyl acrylate (PolyEncap A300) and octadecyl acrylate (ODA), as previous studies [20] have demonstrated that this kind of stationary phase is suitable for chromatographic separations of hydrophobic amphipathic peptides. The retention times of the all-L-peptides are given in Table 2. According to the relative hydrophobicity of these stationary phases, all peptides elute much later on ODA than on the less hydrophobic BAA column. Additionally, the retention times correlate on all three phases with the amphipathicity of the model peptides, e.g., the retention orders KLLK > KLAL > KALK were identical.

The retention time profiles resulting from the DD-replacement sets of KLLK, KLAL and KALK are shown in Fig. 5. Comparing the three stationary phases, the typical shapes with a significant decrease in the centre and only a slight effect at the ends are similar. Most interestingly, examining the non-amphipathic KALK, the largest retention time differences between all-L and D-amino acid analogues were obtained by using the less hydrophobic stationary phase BAA. The measurement on BAA leads to a more pronounced retention time profile, in which the retention times of peptides with N-terminal replacements in positions 1–4 are already reduced. An explanation for these findings might be that (i) the high ligand hydrophobicity of both ODA and PolyEncap leads to a stronger capability to induce and/or stabilize the helix and therefore equilize at least in part the effect of the D-amino acid substitutions and (ii) the less hydrophobic BAA is also able to induce a helical structure of the phase-bound KALK, but the

Table 1
Fractional helicity and retention times of D-amino acid analogues

Peptide sequence[a]	D-Amino acid substitution	Retention time[b] (min)	Helicity, h (%)
KLLK			
Ac-KLLKLAAKALLKLLKLAA-NH_2	None	31.3	79
Ac-<u>KL</u>LKLAAKALLKLLKLAA-NH_2	K1, L2	27.8	63
Ac-KL<u>LK</u>LAAKALLKLLKLAA-NH_2	L3, K4	24.9	53
Ac-KLLK<u>LA</u>AKALLKLLKLAA-NH_2	L5, A6	22.3	51
Ac-KLLKLA<u>AK</u>ALLKLLKLAA-NH_2	A7, K8	23.1	52
Ac-KLLKLAAK<u>AL</u>LKLLKLAA-NH_2	A9, L10	20.7	44
Ac-KLLKLAAKAL<u>LK</u>LLKLAA-NH_2	L11, K12	23.7	51
Ac-KLLKLAAKALLK<u>LL</u>KLAA-NH_2	L13, L14	23.9	42
Ac-KLLKLAAKALLKLL<u>KL</u>AA-NH_2	K15, L16	27.7	56
Ac-KLLKLAAKALLKLLKL<u>AA</u>-NH_2	A17, A18	28.6	69
KLAL			
Ac-KLALKLALKALKLALKLA-NH_2	None	29.4	82
Ac-<u>KL</u>ALKLALKALKLALKLA-NH_2	K1, L2	27.6	69
Ac-KL<u>AL</u>KLALKALKLALKLA-NH_2	A3, L4	24.3	52
Ac-KLAL<u>KL</u>ALKALKLALKLA-NH_2	K5, L6	21.8	46
Ac-KLALKL<u>AL</u>KALKLALKLA-NH_2	A7, L8	22.4	48
Ac-KLALKLAL<u>KA</u>LKLALKLA-NH_2	K9, A10	20.7	50
Ac-KLALKLALKA<u>LK</u>LALKLA-NH_2	L11, K12	19.1	45
Ac-KLALKLALKALK<u>LA</u>LKLA-NH_2	L13, A14	21.1	36
Ac-KLALKLALKALKLA<u>LK</u>LA-NH_2	L15, K16	22.7	53
Ac-KLALKLALKALKLALK<u>LA</u>-NH_2	L17, A18	27.4	68
KALK			
Ac-KALKLKLALALLAKLKLA-NH_2	None	19.0	86
Ac-<u>KA</u>LKLKLALALLAKLKLA-NH_2	K1, A2	19.3	85
Ac-KA<u>LK</u>LKLALALLAKLKLA-NH_2	L3, K4	19.6	80
Ac-KALK<u>LK</u>LALALLAKLKLA-NH_2	L5, K6	17.4	51
Ac-KALKLK<u>LA</u>LALLAKLKLA-NH_2	L7, A8	18.0	66
Ac-KALKLKLA<u>LA</u>LLAKLKLA-NH_2	L9, A10	16.3	59
Ac-KALKLKLALA<u>LL</u>AKLKLA-NH_2	L11, L12	15.2	61
Ac-KALKLKLALALL<u>AK</u>LKLA-NH_2	A13, K14	16.1	81
Ac-KALKLKLALALLAK<u>LK</u>LA-NH_2	L15, K16	17.9	73
Ac-KALKLKLALALLAKLK<u>LA</u>-NH_2	L17, A18	19.2	74

[a] The one-letter code of the D-amino acids is underlined.
[b] Retention times were determined on PolyEncap A300.

structure induction is not strong enough to compensate for the influence of substitutions.

4. Conclusions

This study has clearly demonstrated the good correlation between retention time profiles and the helical behaviour of the corresponding double D-amino acid replacement sets determined by CD. The decreased retention of analogues was expected for amphipathic peptides owing to reduced hydrophobic binding domains. However, similar characteristic retention time profiles were obtained also for the D-amino acid replacement set of a non-amphipathic peptide. As the non-amphipathic peptide should not interact with the hydrophobic phase by a preferred binding site, the characteristic retention time profile should be caused by disturbances of the

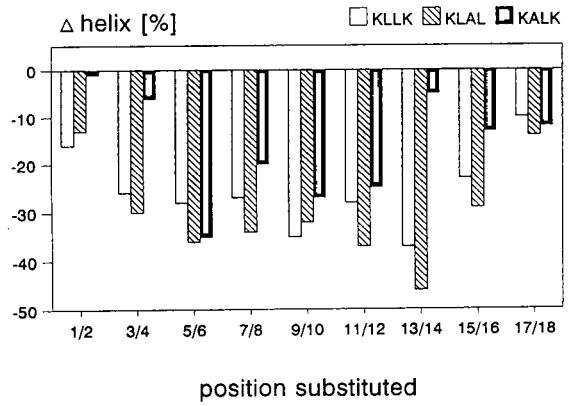

Fig. 3. Influence of the position of D-amino acid substitution on the helicity of KLLK, KLAL and KALK. The helical content of the corresponding all-L-peptides of KLLK, KLAL and KALK were 79, 82 and 86%, respectively. TFE–0.01 *M* H_3PO_4 (1:1, v/v), $5 \cdot 10^{-5}$ mol/l.

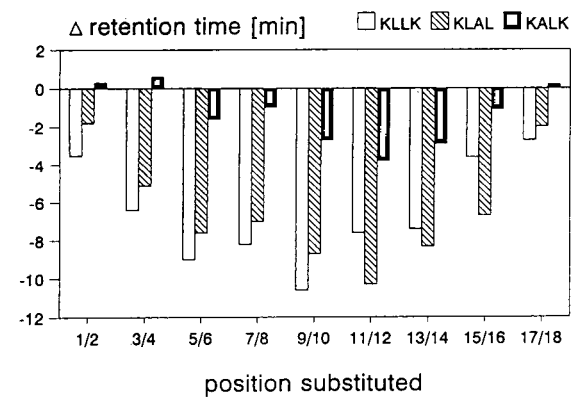

Fig. 4. Influence of the position of D-amino acid substitution on the HPLC retention time of KLLK, KLAL and KALK using PolyEncap A300 as stationary phase. The retention times of the corresponding all-L-peptides of KLLK, KLAL and KALK were 31.3, 29.4 and 19.0 min, respectively.

Table 2
HPLC retention times of KLLK, KLAL and KALK using BAA, PolyEncap A300 and ODA as stationary phases

Peptide	Retention time (min)		
	BAA	PolyEncap	ODA
KLLK	24.5	31.3	39.9
KLAL	23.7	29.4	37.5
KALK	16.5	19.0	24.4

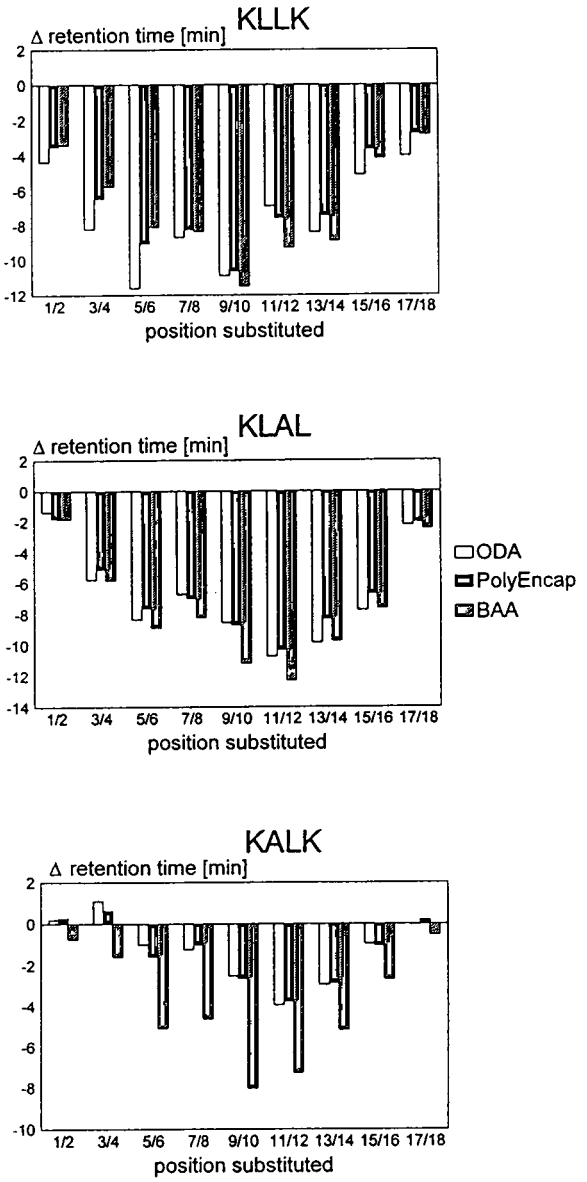

Fig. 5. HPLC retention behaviour of double D-amino acid replacement sets of KLLK, KLAL and KALK on polymer-encapsulated silica-based stationary phases with different hydrophobicities. The retention times of the related all-L-peptides are given in Table 2.

helix formation itself. The finding that BAA shows the influence of D-amino acid replacement more clearly for the non-amphipathic helix indicates that a less hydrophobic phase has a greater

sensitivity for the detection of the helix-destabilizing effect of D-amino acids. Further studies will be necessary to examine the influence of the simultaneous presence of amphipathic and non-amphipathic structure elements in one peptide on the HPLC behaviour of double D-amino acid replacement sets.

Acknowledgements

This work was supported by the Deutsche Forschungsgemeinschaft, Kr 1451/2-1. The authors thank Dr. P. Henklein for his assistance with peptide synthesis and H. Nikolenko and B. Pisarz for technical assistance.

References

[1] R. Houghten and S. Blondelle, *Biochemistry*, 31 (1992) 12688.
[2] V. Steiner, M. Schär, K. Börnsen and M. Mutter, *J. Chromatogr.*, 586 (1991) 43.
[3] J. Ostresh, K. Büttner and R. Houghten, in R. Hodges (Editor), *HPLC of Peptides and Proteins: Separation, Analysis and Conformation*, CRC Press, Boca Raton, FL, 1991, p. 633.
[4] K. Büttner, C. Pinilla, J. Appel and R. Houghten, *J. Chromatogr.*, 625 (1992) 191.
[5] N. Zhou, C. Mant and R. Hodges, *Pept. Res.*, 3 (1990) 8.
[6] M. Hanson, K. Unger, R. Hodges and C. Mant, *J. Chromatogr.*, 599 (1992) 65.
[7] H.-C. Chen, J.H. Brown, J.L. Morrel and C.-M. Huang, in J.E. Rivier and G.R. Marshall (Editors), *Peptides: Chemistry, Structure and Biology*, ESCOM, Leiden, 1990, p. 122.
[8] Y. Pounny and Y. Shai, *Biochemistry*, 31 (1992) 9482.
[9] E. Krause, M. Beyermann, M. Dathe, H. Wenschuh, S. Rothemund and M. Bienert, in R.S. Hodges and J.A. Smith (Editors), *Peptides: Chemistry, Structure and Biology*, ESCOM Science, Leiden, 1994, p. 247.
[10] M.I. Aguilar, S. Mougos, J. Boublik, J. Rivier and M.T.W. Hearn, *J. Chromatogr.*, 646 (1993) 53.
[11] H. Engelhardt, H. Löw, W. Eberhardt and M. Mauss, *Chromatographia*, 27 (1989) 535.
[12] P. Henklein, M. Beyermann, M. Bienert and R. Knorr, in E. Girald and D. Andreu (Editors), *Peptides 1990*, ESCOM, Leiden, 1991, p. 67.
[13] Y.H. Chen, J.T. Yang and H.M. Martinez, *Biochemistry*, 11 (1972) 4120.
[14] M. Schiffer and A.B. Edmundson, *Biophys. J.*, 7 (1967) 121.
[15] P.Y. Chou and G.D. Fasman, *Biochemistry*, 13 (1974) 211.
[16] K.R. Shoemaker, P.S. Kim, E.J. York, J.M. Stewart and R.L. Baldwin, *Nature*, 326 (1987) 563.
[17] F.D. Sönnichsen, J.E. Van Eyk, R.S. Hodges and B.D. Sykes, *Biochemistry*, 31 (1992) 8790.
[18] A. Chakrabarty, J.A. Schellman and R.L. Baldwin, *Nature*, 351 (1991) 586.
[19] M. Hanson, K.K. Unger, J. Schmid, K. Albert and E. Bayer, *Anal. Chem.*, 65 (1993) 2249.
[20] E. Krause, H. Wenschuh, M. Beyermann and M. Bienert, in C.H. Schneider and A.N. Eberle (Editors), *Peptides 1992*, Elsevier, Amsterdam, 1993, p. 469.

ELSEVIER

Journal of Chromatography A, 689 (1995) 227–234

JOURNAL OF CHROMATOGRAPHY A

Charged fusions for β-galactosidase retention in anion-exchange chromatography

Meng H. Heng, Charles E. Glatz*

Department of Chemical Engineering, Iowa State University, Ames, IA 50011, USA

First received 7 December 1993; revised manuscript received 3 May 1994

Abstract

The retention behavior of a series of negatively charged β-galactosidase fusion proteins carrying an additional 1 (designated BGCD1), 5 (BGCD5), 11 (BGCD11), and 16 (BGCD16) aspartate residues was studied. The added tails promoted protein retention in order of tail length and were most effective closer to the isoelectric point. The two parameters Z and I, obtained from the stoichiometric displacement model, were used to characterize the extent of binding between the protein and the ion-exchange surface. At pH 5.7, the Z number increased with tail length (charge) and was 11.5, 8.5, 6.9 and 5.3 for BGCD11, BGCD5, BGCD1 and wild type β-galactosidase (BGWT), respectively. At these conditions, the fusions had very similar I values which were five times smaller than that of BGWT. However, the increase in Z numbers outweighed the decrease in I values and retention was enhanced. When BGWT was brought to the same net charge (by increasing the mobile phase pH) as each of the fusions, the Z number was similar to that of the corresponding fusion. However, the I value decreased with increasing pH (net charge) and was lower than that of the corresponding fusion by factors of 25–500. Consequently, despite the similar Z numbers, the fusions still had higher retention.

1. Introduction

Protein separation based on ion-exchange adsorption is the most widely used step in downstream processing [1]. In principle, the unique electrostatic interactions of each protein with the stationary phase of the ion-exchange sorbent form the basis for separation. However, the amphoteric nature and three-dimensional structure of the proteins make their interaction with the ion-exchange surface very complex [2–5].

The three-dimensional structure and charge distribution of the protein determine the surface amino acid residues which are in position to interact with the ion-exchange sorbent. The surface area containing the amino acid residues participating in the interaction is referred to as the chromatographic contact region or footprint of retention [5]. A single amino acid variation in the chromatographic contact region can have a marked effect on protein retention [6]. The residues in the contact region may interact directly with the sorbent, or they may influence binding of other residues through electrostatic effects on the dissociation of neighboring residues and steric perturbation of hydrogen bonded water molecules [6]. In addition, the charged density of ion exchanger [7,8] and the type of displacing ions of mobile phase [2,9–11]

* Corresponding author.

0021-9673/95/$09.50
SSDI 0021-9673(94)00970-8

can affect retention, elution, resolution, selectivity and recovery.

Using recombinant DNA technology it is possible to produce genetically engineered proteins with charge characteristics specifically designed to facilitate purification [12–14] and/or to study chromatographic retention mechanisms [6]. Our previous work has taken advantage of negatively charged tails to enhance β-galactosidase recovery [14] and immobilization [15] using ion-exchange membranes. The tails were a series of polyaspartate fusions of the form: Gly–Asp–Pro–Met–Ala–$(Asp)_n$–Tyr adding 1, 5, 11, and 16 negative charges to β-galactosidase designated as BGCD1, BGCD5, BGCD11, and BGCD16, respectively. In this work we use the same series of fusion proteins to investigate the contributions of the high linear charge density region of the fusion tails to protein retention in anion-exchange chromatography. The concept of using fusions to alter charge is illustrative of a larger class of "purification fusions" that have added a wide variety of chromatographic binding regions to proteins [16].

The stoichiometric displacement model [17] based on the mass action law was used to characterize the retention. For this model, the ion-exchange "reaction" is represented by

$$S_o + Z \cdot D_b \Leftrightarrow S_b + Z \cdot D_o \quad (1)$$

The free solute (S_o) will displace multiple (Z) bound ions (D_b) when it is adsorbed (S_b) on the ion-exchange sorbent surface. The stoichiometry of the displacement process is determined by the number (Z) of displacing ions in solution (D_o) required to displace the solute from the sorbent. The equilibrium is expressed as

$$K_{eq} = \frac{[S_b]\,[D_o]^Z}{[S_o]\,[D_b]^Z} \quad (2)$$

where K_{eq} is a binding constant. For low protein coverage, the protein retention (as capacity factor k') can be related to the displacing ion concentration by [2,7]

$$k' = \frac{I}{[D_o]^Z} \quad (3)$$

The capacity factor, k', is related to protein retention by

$$k' = \frac{(t_R - t_O)}{t_O} \quad (4)$$

where t_R and t_O are the retention times of the solute at retained and non-retained conditions, respectively. I is independent of D_o and is given by the equation

$$I = K_{eq}\varphi[D_{bi}]^Z \quad (5)$$

where φ and $[D_{bi}]$ are phase ratio (ratio of stationary and mobile phase volumes) and the ionic capacity of the resin, respectively. Where Z is constant, I can be viewed in terms of K_{eq} which is the ratio of the rate constant for adsorption of protein from the mobile phase to that for desorption of bound protein from the stationary phase. Thus changes in I values have been explained [6,7] in terms of the number of chromatographic contact regions available for effective (i.e. leading to binding) collisions between these regions and the sorbent ($k_{adsorption}$) as well as the ease of solute desorption ($k_{desorption}$).

The two parameters, Z and I, are obtained using the linear form of Eq. (3),

$$\log k' = \log I + Z \log \frac{1}{[D_o]} \quad (6)$$

By measuring t_R for isocratic elution at a series of D_o levels, k' can be calculated from Eq. (4) and Z and I from the slope and intercept of the data plotted according to Eq. (6).

The model has been widely used to describe ion-exchange retention of nucleic acids [18] and proteins [2,6–8,19]. For example, Kopaciewicz et al. [2] found that increased protein retention was due to an increase in Z number. Others [6,7] reported that even proteins with similar Z numbers can have different retentions based on their I values. These latter studies found that the probability of an effective collision and, hence, the rate of adsorption of a solute is proportional to the number of chromatographic regions available for interaction with the ion-exchange sorbent.

The model has also been successfully applied to hydrophobic [20] and reversed-phase [5,21,22] chromatography of proteins. Mazsaroff et al. [19] have derived a similar model for preparative ion-exchange chromatography to investigate the effects of protein concentration on Z numbers.

The Z numbers obtained using this model provide some insight into the role of three-dimensional structure in ion-exchange chromatography. For small molecules such as oligonucleotides with less than 10 residues, Z is equivalent to the number of negative charges in the molecule [20]. For larger molecules such as proteins and oligonucleotides with more than 10 residues, due to steric limitations and charge asymmetry, the Z numbers are substantially lower than their net charges [2,10].

2. Experimental

2.1. Materials

All the BGCD fusions were purified from *Escherichia coli* cell extracts using ammonium sulphate precipitation followed by binding to an affinity matrix [14]. After elution from the affinity matrix, the protein was dialyzed against 100 mM, pH 7.0 potassium phosphate buffer containing 5 mM $MgCl_2.6H_2O$ and 1 mM 2-mercaptoethanol, freeze dried and stored desiccated at 4°C. Before use, the protein was redissolved in deionized water, filtered (0.2 μm cut-off) and checked for DNA content using the ratio of absorbance at 280 nm to 260 nm. In cases where high amounts of DNA ($>10\%$) were detected, the proteins were further purified using ion-exchange (ActiDisk with quaternary amine functionality, FMC Corp., Pine Brook, NJ, USA). For the ion exchange step, each fusion was first dialyzed against 25 mM, pH 5.7 bis-Tris buffer and loaded by syringe onto a new membrane preequilibrated with the same buffer. The effluent was collected and recirculated through the membrane (five times). The loaded membrane was then washed with 10 ml of the bis-Tris buffer followed by step gradient elution using NaCl steps (0.1 M, 0.2 M, . . . , 0.7 M, 1 M, 2 M) in the same buffer. Samples from each step were analyzed for A280/A260 nm ratio. Fractions (0.4 M and 0.5 M for BGCD1 and BGCD5; and 0.5 M and 0.6 M for BGCD11 and BGCD16) with ratios higher than 0.7 ($<10\%$ DNA) were pooled, dialyzed against 25 mM, pH 5.7 bis-Tris buffer and stored at 4°C until use. The wild type β-galactosidase (BGWT) and all reagents were purchased from Sigma Chemical Company, St. Louis, MO, USA. All solutions were prepared with deionized water (resistivity >16 M$\Omega \cdot$cm; NANOpure II, Barnstead, Boston, MA, USA) adjusted to the desired pH using HCl, and filtered (0.2 μm cut-off).

2.2. Chromatography

All chromatographic experiments were performed on a strong anion-exchange perfusion column with quaternized polyethyleneimine functionality (POROS Q, M Series, 30 mm × 2.1 mm I.D.; PerSeptive Biosystems, Cambridge, MA, USA). The chromatographic system consisted of a gradient mixer (Model 2360 Gradient Programmer, ISCO, Lincoln, NE, USA), pump (Model 2350 HPLC Pump, ISCO) and a variable wavelength detector (Beckman 165, Beckman Instruments, Berkeley, CA, USA). Data were collected and retention times determined using Dionex Advanced Interface and Software (Dionex Corp., Sunnyvale, CA, USA).

Retention data were obtained using gradient elution at a flow rate of 1 ml/min at room temperature (21°C). A 10-min linear gradient from 25 mM bis-Tris buffer (buffer A) to 2 M NaCl in buffer A (buffer B) at various pHs was used. At the end of the gradient, buffer B was held for 3 min before switching to buffer A to reequilibrate (at least 7 min) the column for subsequent injection. All samples were injected using a 20-μl sample loop.

Isocratic analyses were carried out at the same conditions: 1 ml/min, 21°C and 20-μl sample. Initial values of NaCl concentration for isocratic elution were obtained from the gradient elution. The NaCl concentration was adjusted using buffers A and B in the desired ratio. After each isocratic experiment the column was cleaned

using buffer B (5 min) and reequilibrated (at least 7 min). The retention time for the 2 *M* NaCl experiment was taken to be t_o.

3. Results and discussions

3.1. Retention maps

Fig. 1 shows the protein retention (as NaCl concentration required for elution, μ_{elute}) as a function of mobile phase pH for BGWT and all the BGCD fusions. For BGWT, BGCD1, and BGCD5, protein retention increased with increasing pH. This is expected of anion-exchange chromatography; retention generally increases as the surrounding environment becomes more basic and the protein becomes more negatively charged. However, BGCD11 and BGCD16 did not show significant variation in retention over the pH range studied. One possible explanation is that even at low pH, the fusion tail has provided sufficient charge for maximum retention and further increases in charge (by increasing pH) did not increase retention. At all the pH values, the fusion proteins are retained longer than BGWT and the order of retention increased with increasing tail length (charge).

In order to better understand the effect of the high linear charge density region on β-galactosidase retention, the retention data in Fig. 1 were replotted as a function of estimated net charge [14]. Fig. 2 shows that the protein retention increased with increasing net charge for BGWT (up to $Z_P \approx -75$), BGCD1 and BGCD5, confirming the previous observation that μ_{elute} increased with increasing pH is a direct consequence of the increase in net charge. On the other hand, the retentions of BGCD11 and BGCD16 did not vary significantly with the net charges. Fig. 2 also shows that at a given net charge, all the fusions show higher retention than the BGWT. This clearly demonstrates that the added tails promote protein retention and the increase parallels the tail length.

It is general practice in ion-exchange chromatography to vary the mobile phase pH and, hence, the protein net charge to obtain optimum

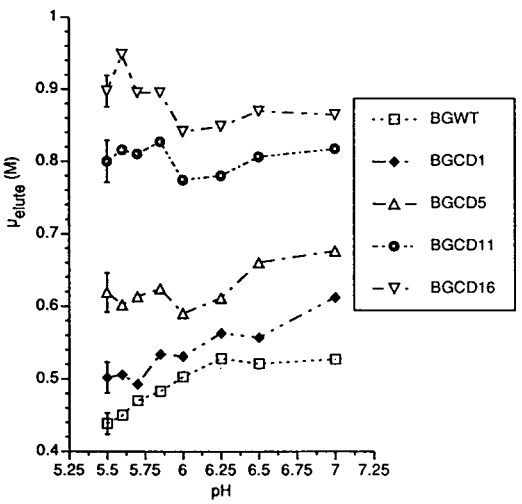

Fig. 1. Protein retention (measured as the NaCl concentration required to elute the protein, μ_{elute}) as function of pH for BGWT and BGCD fusions at 25 m*M* bis-Tris, 1 ml/min and 21°C. Each data point is the mean of at least three replicates. Error bar indicates the average standard deviation (pooled estimates for each protein over all pHs studied).

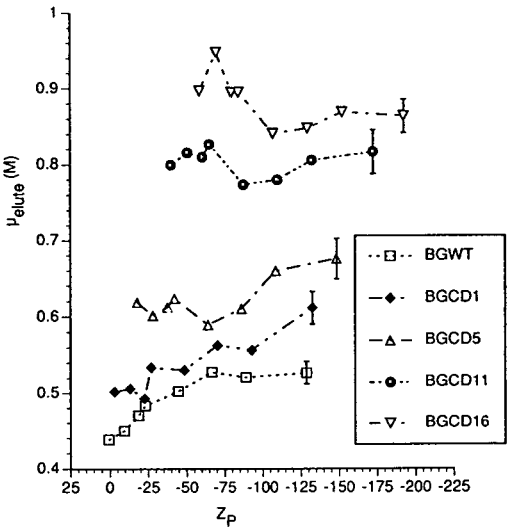

Fig. 2. Protein retention (measured as the NaCl concentration required to elute the protein, μ_{elute}) as function of estimated net charge (Z_P) for BGWT and BGCD fusions at 25 m*M* bis-Tris, 1 ml/min and 21°C. Each data point is the mean of at least three replicates. Error bar indicates the average standard deviation (pooled estimates for each protein over all pHs studied).

separation. Here protein net charge has been altered by adding charged tails to the protein. In order to correlate the dependence of μ_{elute} on the additional charge due to the added tail, linear regression plots of μ_{elute} versus the protein net charge at a various pHs were constructed and Fig. 3 shows a typical plot obtained at pH 5.5. The absolute value of the slope thus obtained, $|\Delta\mu_{elute}/\Delta Z_P|$, is a measure of the effectiveness of the additional charge due to the added tail in enhancing the β-galactosidase retention. Fig. 4 shows such slopes as a function of pH. The $|\Delta\mu_{elute}/\Delta Z_P|$ generally decreased until pH 6.0 and then remained relatively constant, indicating that the additional charges carried by the tails were best utilized (to enhance retention) at the low pH conditions. One possible explanation is that as the pH increases, the protein net charge also increases and the tail represents only a small portion of the total charge.

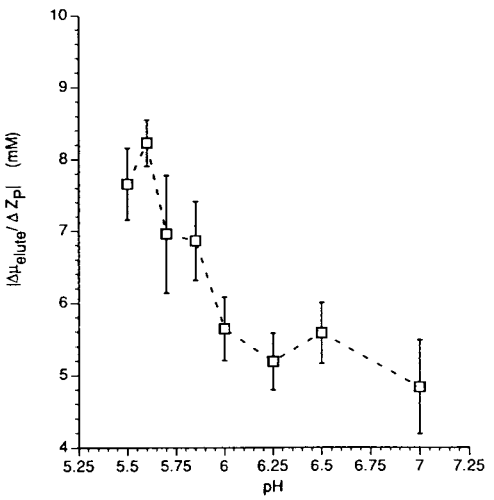

Fig. 4. Effectiveness of added tails for enhancing retention as a function of pH. The $|\Delta\mu_{elute}/\Delta Z_P|$ values were obtained from the slope of the plot in Fig. 3 at various pHs.

3.2. Stoichiometric displacement model

Eq. (6) was fitted using linear least-square regression (JMP version 2, Software for Statistical Visualization on the Apple Macintosh, SAS Institute, Inc.). The correlation coefficients (r) for all proteins, except for the BGCD1 ($r = 0.94$), are greater than 0.98. The Z numbers and I values obtained were used to characterize the strength of binding between the protein and the ion-exchange surface.

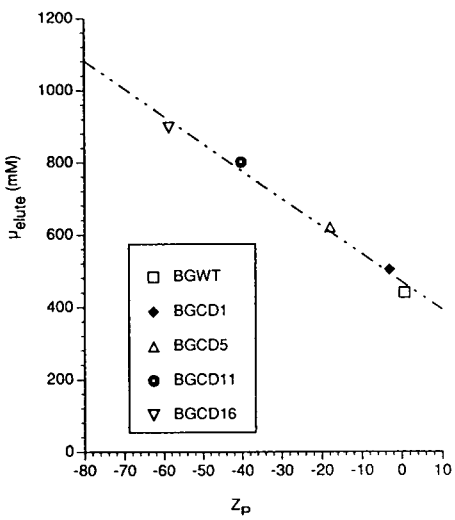

Fig. 3. NaCl concentration required for elution (μ_{elute}) versus estimated protein net charges (Z_P) at pH 5.5 with 25 mM, pH 5.5 bis-Tris buffer, 1 ml/min flow and 21°C. Results for other pHs are similar and all have linear correlation coefficients (r) greater than 0.98.

Effects of adding charged tails at constant pH

Fig. 5 shows the plots of log k′ at pH 5.7 versus log $1/[D_0]$ for BGWT, BGCD1, BGCD5, and BGCD11. The values of Z (i.e. the slope) increased with increasing tail length. They were 11.5, 8.5, 6.9 and 5.3 for BGCD11, BGCD5, BGCD1 and BGWT, respectively (see Fig. 6). The additional charges carried by the fusion tails result in a greater direct electrostatic contact between the protein and the ion exchanger. The Z number of each protein represents only a small fraction of the protein net charge: 0.28, 0.32, 0.23, and 0.19 for BGWT, BGCD1, BGCD5, and BGCD11, respectively. This is consistent with many early reports [2,6,7], which suggest that due to steric limitations only a small portion of the protein is participating in the interaction. It is particularly understandable for this large (M_r 460 000) tetrameric protein, where simulta-

After completion of this work, the BGWT net charge was estimated by using titration data above pH 6 and a pI value (4.8) approximated from the solubility data [23]. Based on these new charge estimates, the data of Fig. 6 would shift to lower values of Z_p with the BGWT points spanning a smaller range of Z_p. However, the above comparison of I values at similar Z number does not change as Z is independent of the estimate of Z_p. Overall then, despite the similar (or lower) Z numbers, each of the fusions studied has a higher I value and, hence, a higher μ_{elute} (Fig. 2).

There are two possible ways in which the added tails can enhance binding relative to the untailed protein of the same binding number (i.e. increase I at the same Z). First, the tails may orient or steer the protein into a position such that the chromatographic contact region can interact more favorably with the ion-exchange surface [2]. The more likely alternative, given the correspondence of Z and tail length, is that the tails serve as the chromatographic contact region. The flexibility and accessibility of the tails, relative to the more distributed surface contact region of the BGWT, would increase the probability of an effective interaction between the protein and the ion-exchange surface. In other words, the collisional efficiency of the binding step would be increased. Additionally, one could speculate that the rate of desorption would also be lower for the tailed case where displaced sections of the tail are kept positioned for resorption by those sections not yet displaced. Hence, desorption would require nearly simultaneous displacement of all the tail sites. Either effect would increase K_{eq} and, hence, I. At a given pH, the high linear charged density region fused to the β-galactosidase provided an effective way to enhance protein retention by increasing the Z numbers without greatly reducing the I values.

4. Conclusions

It was demonstrated that a high linear charge density tail fused to β-galactosidase can enhance protein retention in anion-exchange chromatography. The additional charges carried by the tails enhanced retention in the following order: BGCD16 > BGCD11 > BGCD5 > BGCD1 > BGWT. The added tails were most effective in enhancing retention at low pHs.

Two parameters, Z and I, obtained from the stoichiometric displacement model, were used to characterize the extent of binding between the protein and the ion-exchange surface. At pH 5.7, the Z number increased with tail length (charge) and was 11.5, 8.5, 6.9 and 5.3 for BGCD11, BGCD5, BGCD1 and BGWT, respectively. At these conditions, the fusions had very similar I values and those were five times smaller than that of BGWT. However, the increase in Z numbers outweighed the decrease in I values and an overall enhanced retention was observed. Similar Z numbers were obtained for the BGWT brought to the same approximate net charge (by varying the mobile phase pH) as each of the fusions. The I values of BGWT decreased with increasing pH (net charge) and were lower than that of the corresponding fusion. Consequently, despite the similar Z numbers, the fusions had a higher retention than the corresponding BGWT, demonstrating the effectiveness of the high charge density tail.

Acknowledgements

This material is based upon work supported by the National Science Foundation under Grant No. BCS-9108583. The Government has certain rights in this material.

Symbols and abbreviations

BGCD	β-galactosidase with carboxyl aspartate fusion peptide
BGWT	wild-type β-galactosidase
[D]	displacing ion concentration
$[D_{bi}]$	ionic capacity of ion-exchange resin
I	parameter in Eq. (5)
k'	capacity factor
K_{eq}	binding constant

[S]	solute (protein) concentration
t_R	retention time
t_o	retention time of solute at non-retained condition
Z	number of charge interactions
Z_P	protein estimated net charge
μ_{elute}	NaCl concentration required for elution
φ	phase ratio (ratio of stationary and mobile phase volumes)

subscripts for D and S

b	bound state
o	free state (in solution)

References

[1] J. Bonnerjea, S. Oh, M. Hoare and P. Dunnill, *Bio/Technol.*, 4 (1986) 954.
[2] W. Kopaciewicz, M.A. Rounds, J.L. Fausnaugh and F.E. Regnier, *J. Chromatogr.*, 266 (1983) 3.
[3] K.M. Gooding and M.N. Schmuck, *J. Chromatogr.*, 296 (1984) 321.
[4] X. Geng and F.E. Regnier, *J. Chromatogr.*, 332 (1985) 147.
[5] F.E. Regnier, *Science*, 238 (1987) 319.
[6] R.M. Chicz, and F.E. Regnier, *Anal. Chem.*, 61 (1989) 2059.
[7] R.R. Drager and F.E. Regnier, *J. Chromatogr.*, 406 (1987) 237.
[8] D. Wu and R.R. Walters, *J. Chromatogr.*, 589 (1992) 7.
[9] W. Kopaciewicz, M.A. Rounds and F.E. Regnier, *J. Chromatogr.*, 318 (1985) 157.
[10] M.A. Rounds and F.E. Regnier, *J. Chromatogr.*, 283 (1984) 37.
[11] S.J. Brewer and H.M. Sassenfeld, *Tibtech.*, 3 (1985) 119.
[12] H.M. Sassenfeld and S.J. Brewer, *Bio/Technol.*, 2 (1984) 76.
[13] W. Kopaciewicz and F.E. Regnier, *Anal. Biochem.*, 133 (1983) 251.
[14] M.H. Heng and C.E. Glatz, *Biotechnol. Bioeng.*, 42 (1993) 333.
[15] M.H. Heng and C.E. Glatz, *Biotechnol. Bioeng.*, submitted for publication (1993).
[16] C.F. Ford, I. Suominen, and C.E. Glatz, *Prot. Expr. Purif.*, 2 (1991) 95.
[17] N.K. Boardman and S.M. Partridge, *Biochem. J.*, 59 (1955) 543.
[18] R.R. Drager and F.E. Regnier, *J. Chromatogr.*, 359 (1986) 147.
[19] I. Mazsaroff, S. Cook and F.E. Regnier, *J. Chromatogr.*, 443 (1988) 119.
[20] J.L. Fausnaugh and F.E. Regnier, *J. Chromatogr.*, 359 (1986) 131.
[21] F.E. Regnier, *Science*, 222 (1983) 245.
[22] X. Geng and F.E. Regnier, *J. Chromatogr.*, 296 (1984) 15.
[23] J.R. Luther and C.E. Glatz, *Biotechnol. Bioeng.*, in press (1994).

ELSEVIER

Journal of Chromatography A, 689 (1995) 235–245

JOURNAL OF CHROMATOGRAPHY A

Alternative methods for the determination of trace amounts of 4-aminomorpholine in molsidomine and linsidomine

Andreas Körner*, Albert Peter

Cassella AG, Analytical and Physical Department, Pharma Quality Control, Hanauer Landstrasse 526, 60386 Frankfurt am Main, Germany

First received 28 December 1993; revised manuscript received 17 August 1994

Abstract

Different methods based on either ion chromatography with electrochemical detection or precolumn derivatization with *o*-phthaldialdehyde were developed to determine trace amounts of 4-aminomorpholine in molsidomine and linsidomine. Electrochemical detection combined with ion chromatographic separation revealed outstanding selectivity whereas derivatization with *o*-phthaldialdehyde turned out to be very sensitive using RP-HPLC and standard UV detection.

1. Introduction

The identification and determination of synthesis intermediates in drug substances is an important task in synthesis development, optimization and final quality control. Substituted hydrazines, e.g., 4-aminomorpholine are synthesis intermediates of pharmacologically active 3-dialkylaminosydnonimines used as anti-anginal agents. The scheme of their synthesis is presented in Fig. 1. Hydrazines may be present in trace amounts in the final product. The absence of π-bonding in these compounds has the consequence of low sensitivity for photometric detection. Conductivity detection in LC or separation by GC is not possible owing to the low conductivity of the hydrazines and thermal instability of the sydnonimines, respectively.

As all other potential by-products and degradation products of molsidomine and linsidomine hydrochloride have already been determined

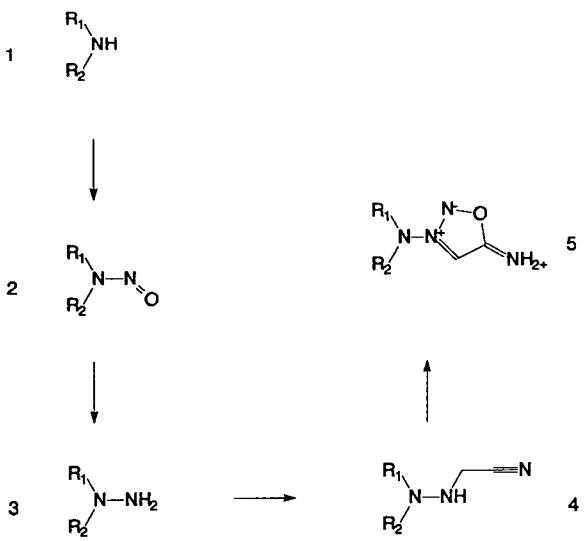

Fig. 1. Scheme of synthesis of 3-dialkylsydnonimines starting with the secondary amine (1) (e.g., morpholine). The hydrazine (3) (e.g., 4-aminomorpholine) is formed as a synthesis intermediate which is not isolated during synthesis.

0021-9673/95/$09.50
SSDI 0021-9673(94)00873-6

using a gradient HPLC method, we investigated the development of a suitable, very sensitive detection procedure for 4-aminomorpholine. Several structural closely related synthesis intermediates and potential degradation products had to be taken into account, demanding the highest selectivity (Fig. 2).

Many advances have been reported in the use of preinjection and postcolumn derivatization to generate photometrically or electrochemically active adducts [1]. Only the determination of morpholine in molsidomine using precolumn derivatization with dansyl chloride has been reported so far [2]. *o*-Phthaldialdehyde (OPA) is a well known derivatizing reagent for primary amines, amino alcohols, peptides and amino acids which fulfils the demands for highest sensitivity, as fluorescent products are formed [3]. It has not been used so far, to our knowledge, for the derivatization of hydrazines.

Precolumn derivatization of 4-aminomorpholine for separation by RP-HPLC and UV detection is discussed in this paper. Disturbances occurred when the method was transferred to linsidomine hydrochloride. Ion chromatographic separation followed by direct electrochemical detection was then performed. This mode of detection had already been applied to the determination of hydrazines [4]. We found that precolumn derivatization could not be transferred to other related hydrazines whereas electrochemical detection turned out to be very dependent on the pattern of substitution.

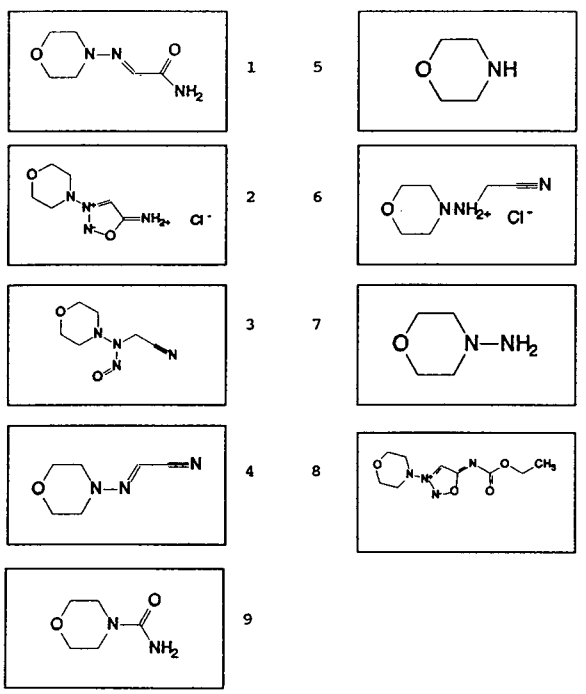

Fig. 2. Synthesis intermediates and some of the major decomposition products of molsidomine and linsidomine hydochloride. 1 = (4-Morpholinylimino)acetamide (SIN 1 C amide); 2 = 3-morpholinosydnonimine (linsidominehydrochloride); 3 = (4-morpholinylnitrosoamino)acetonitrile (SIN 1 A); 4 = (4-morpholinylimino)acetonitrile (SIN 1 C); 5 = morpholine; 6 = (4-morpholinylamino)acetonitrile (SIN 1 B); 7 = 4-aminomorpholine; 8 = molsidomine; 9 = 4-morpholinecarboxamide.

2. Experimental

2.1. Apparatus

Chromatographic analysis was performed using a HP 1090 LC system with an HP 79994A Chem Station (Hewlett-Packard, Waldbronn, Germany).

2.2. Precolumn derivatization

The chromatographic system was equipped with a photodiode-array detector set at 235 nm when precolumn derivatization was used. For derivatization, the injector programme was used. A 5-μl volume of the sample solution was sandwiched between two 5-μl volumes of derivatization reagent. The mixing volume was 10 μl and ten mixing cycles were applied. After a waiting time of 10 min, the whole sample was injected.

2.3. Electrochemical detection

An HP 1049A programmable electrochemical detector equipped with a solid silver/silver chloride reference electrode and a glassy carbon working electrode (Hewlett-Packard) was used. An HP 35900 dual-channel interface was used for digital conversion of the analogue signal

delivered by the electrochemical detector (Hewlett-Packard).

2.4. Chromatographic method

Precolumn derivatization

The column used was a Nucleosil 120 C_{18}, 3 μm (250 mm × 3 mm I.D.) stainless-steel column (Macherey–Nagel, Düren, Germany).

The solvents used were (A) 50 m*M* potassium dihydrogenphosphate, (B) methanol and (C) acetonitrile–water (80:20, v/v). The initial mobile phase was A–B–C (80:20:0, v/v/v). After injection, a stepwise gradient was applied as follows: (1) the initial mixture was maintained for 5 min; (2) B was increased to 80% (v/v) in 25 min with a linear gradient; (3) C was increased to 100% (v/v) with a linear gradient in 5 min; (4) the system was returned to the initial mobile phase in 5 min according to the following scheme:

0 min	80% A–	20% B–	0% C
5 min	80% A–	20% B–	0% C
30 min	20% A–	80% B–	0% C
35 min	0% A–	0% B–	100% C
40 min	80% A–	20% B–	0% C

The flow-rate was 0.5 ml/min.

Electrochemical detection

The column used was an OmniPac PCX-100 (10-32) (Dionex, Sunnyvale, CA, USA). The mobile phase was phosphate buffer (pH 4.0)–acetonitrile (75:25, v/v). The phosphate buffer was prepared by dissolving 6.9 g of sodium dihydrogenphosphate and 0.75 g of sodium chloride in 1000 ml of demineralized water. The pH of this solution was adjusted to 4.0 with orthophosphoric acid.

2.5. Chemicals

4-Aminomorpholine (analytical-reagent grade) was purchased from Fluka (Buchs, Switzerland). All other chemicals and solvents were obtained at the highest purity available from Riedel-de Haën (Seelze, Germany). Molsidomine, linsidomine hydrochloride and all potential impurities were manufactured at our plant and were fully characterized prior to use.

Water for HPLC analyses was demineralized water passed through a Milli-Q water-purification system (Millipore, Bedford, MA, USA).

2.6. Derivatization reagent

The reagent for derivatization was prepared by dissolving 50 mg of *o*-phthaldialdehyde in 1 ml of methanol. The solution was diluted to 10 ml with a solution containing 2 g of sodium tetraborate ($Na_2B_4O_7 \cdot 10H_2O$) in 100 ml of demineralized water, then 50 μl of 2-mercaptoethanol were added. After mixing thoroughly, the solution was filtered through a 0.45-μm filtration unit. The reagent was prepared freshly every day.

2.7. Precolumn derivatization

Preparation of standard solutions

Standards were prepared by dissolving 100.0 mg of 4-aminomorpholine reference standard in 100.0 ml of water–acetonitrile (80:20, v/v). A 100-μl volume of this solution and 100 μl of an internal standard solution containing 100 mg of 3-aminopropanol per 100 ml of water were mixed and diluted to 10.0 ml with water–acetonitrile (80:20, v/v) in a volumetric flask.

Sample preparation

A 100.0-mg amount of molsidomine was dissolved in 8 ml of water–acetonitrile (80:20) and 100 μl of the internal standard solution were added. The solution was diluted to 10.0 ml with demineralized water.

Selectivity and stability

The selectivity was tested by injecting solutions of the potential synthesis intermediates and/or degradation products SIN-1, SIN-1 A, SIN-1 B, SIN-1 C amide, morpholine and 4-morpholinecarboxamide at a concentration of 0.5% each, relative to molsidomine.

The stability of molsidomine with regard to the alkaline reagent was tested by dissolving the required amount of molsidomine in 0.1 *M* sodium hydroxide solution for the specified time (see chromatograms). The stability was also tested in 0.1 *M* hydrochloric acid. For testing the light

stability of molsidomine it was exposed to direct sunlight in a petri dish.

2.8. Electrochemical detection

Preparation of standard solutions

Standard solutions were prepared by dissolving 25.0 mg of 4-aminomorpholine reference standard, accurately weighed, in exactly 100.0 ml of demineralized water. A 100-μl amount of this solution was diluted to 10.0 ml with the mobile phase in a volumetric flask.

Sample preparation

A 250.0-mg amount of linsidomine hydrochloride, accurately weighed, was dissolved in 100.0 ml of the mobile phase in a volumetric flask.

Selectivity

The selectivity of the method was tested by injecting solutions of all synthesis intermediates and/or degradation products (4-morpholinecarboxamide, SIN-1 A, SIN-1 B, SIN-1 C, SIN-1 C amide and morpholine) using UV detection at 210 nm for the electrochemically inactive compounds and by increasing the potential to 1200 mV to obtain a signal for the electrochemically active compounds.

Hydrodynamic voltammograms were obtained with solutions of the reference standards of 4-aminomorpholine, *cis*-2,6-dimethylpiperidine and 3,3-dimethyl-4-aminothiomorpholine at a concentration of 0.25 mg per 100 ml each by increasing the potential stepwise from 0.3 to 1.2 V.

3. Results and discussion

3.1. Precolumn derivatization

A critical aspect of derivatizations, which dictates the usefulness of this analytical technique, is the selectivity and reproducibility with regard to the stability of the derivatives formed. The results presented here clearly show that problems of this kind could be overcome effectively. No interferences with any of the synthesis intermediates or decomposition products could be observed (Fig. 3).

The formation and stability of the derivatives were investigated by varying the time of derivatization. The peak height of the derivative of 3-aminopropanol decreased rapidly when the time of derivatization exceeded 2 min, whereas the amount of the derivative formed with 4-aminomorpholine could even be increased by lengthening the time of derivatization up to 8 min. A time of 1 min for derivatization was found to be suitable for obtaining sufficiently large peak areas for both compounds (Fig. 4).

The relative standard deviation of the results obtained in the test for precision was about 4% and the recoveries were in the range 90–110%. Linearity was satisfactory over the whole concentration range from 20 to 1000 ppm (Fig. 5).

It was also demonstrated that decomposition of molsidomine, which may take place in the alkaline medium of the derivatization reagent, does not disturb the determination of 4-aminomorpholine. No interfering peaks were observed after leaving a solution of molsidomine at pH 12 for 8 h (Fig. 6).

At a strongly acidic pH of 2, no 4-aminomorpholine was formed, which is in contradiction to earlier reports on the stability of molsidomine [5].

The derivatization product formed revealed no fluorescence, in contrast to the products formed with, e.g., primary amines, amino alcohols or amino acids which have been described so far. Identification is still in progress. The UV spectrum exhibited a shoulder at 220 nm and a maximum at 335 nm.

Absorption of the derivative of 4-aminomorpholine was found to be sufficiently high for the low limit of detection demanded. The limit of detection, defined by a signal-to-noise ratio of 3, was as low as 20 ppm, relative to molsidomine.

Linsidomine hydrochloride is the final synthesis intermediate of molsidomine but it is also used as an anti-anginal agent for injection solutions. As linsidomine hydrochloride obviously behaves as a primary amine and consequently reacts with *o*-phthaldialdehyde itself, the derivatization method could not be used for the

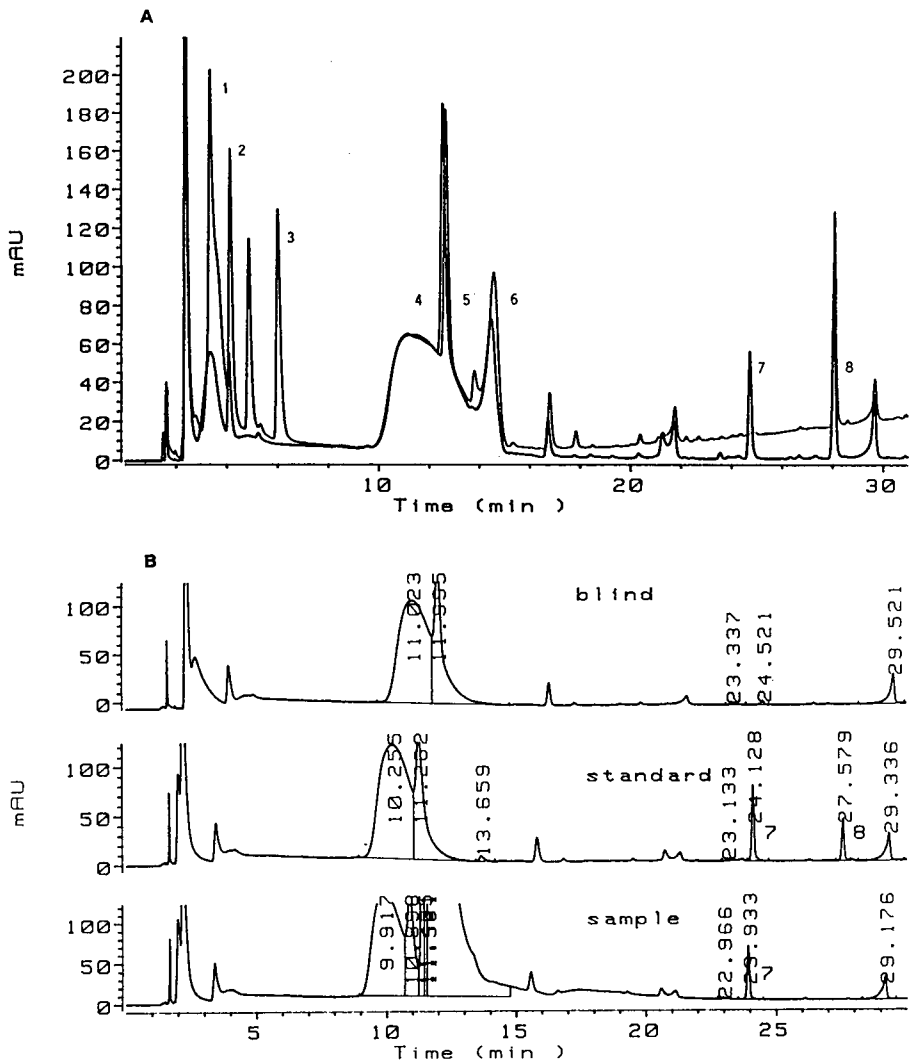

Fig. 3. Chromatograms demonstrating the selectivity of precolumn derivatization for molsidomine. (A) Overlay of a chromatogram obtained with a standard solution containing 0.1% of 4-aminomorpholine and the internal standard and a chromatogram of the potential byproducts without 3-aminopropanol. Peaks: 1 = SIN 1 C amide; 2 = SIN 1; 3 = SIN 1 A + C; 4–6 are from the derivatization reagent; 7 = 3-aminopropanol; 8 = 4-aminomorpholine. (B) Chromatogram of the solvent (top), the standard solution containing 3-aminopropanol and 4-aminomorpholine (middle) and a typical batch of molsidomine (bottom) (the content of 4-aminomorpholine is below the limit of detection). Retention time of molsidomine = 11 min.

detection of 4-aminomorpholine in this substance as a great excess of *o*-phthaldialdehyde would be necessary. Further, when we tried to transfer the method to related hydrazines which are of importance for the synthesis of new anti-anginal compounds, we found that substitution of the hydrazine also plays an important role, as the structurally analogous 4-amino-*cis*-2,6-dimethylpiperidine could not be derivatized satisfactorily.

Steric hindrance by the two methyl groups at positions 2 and 6 influences the reactivity to a great extent, as could also be confirmed by

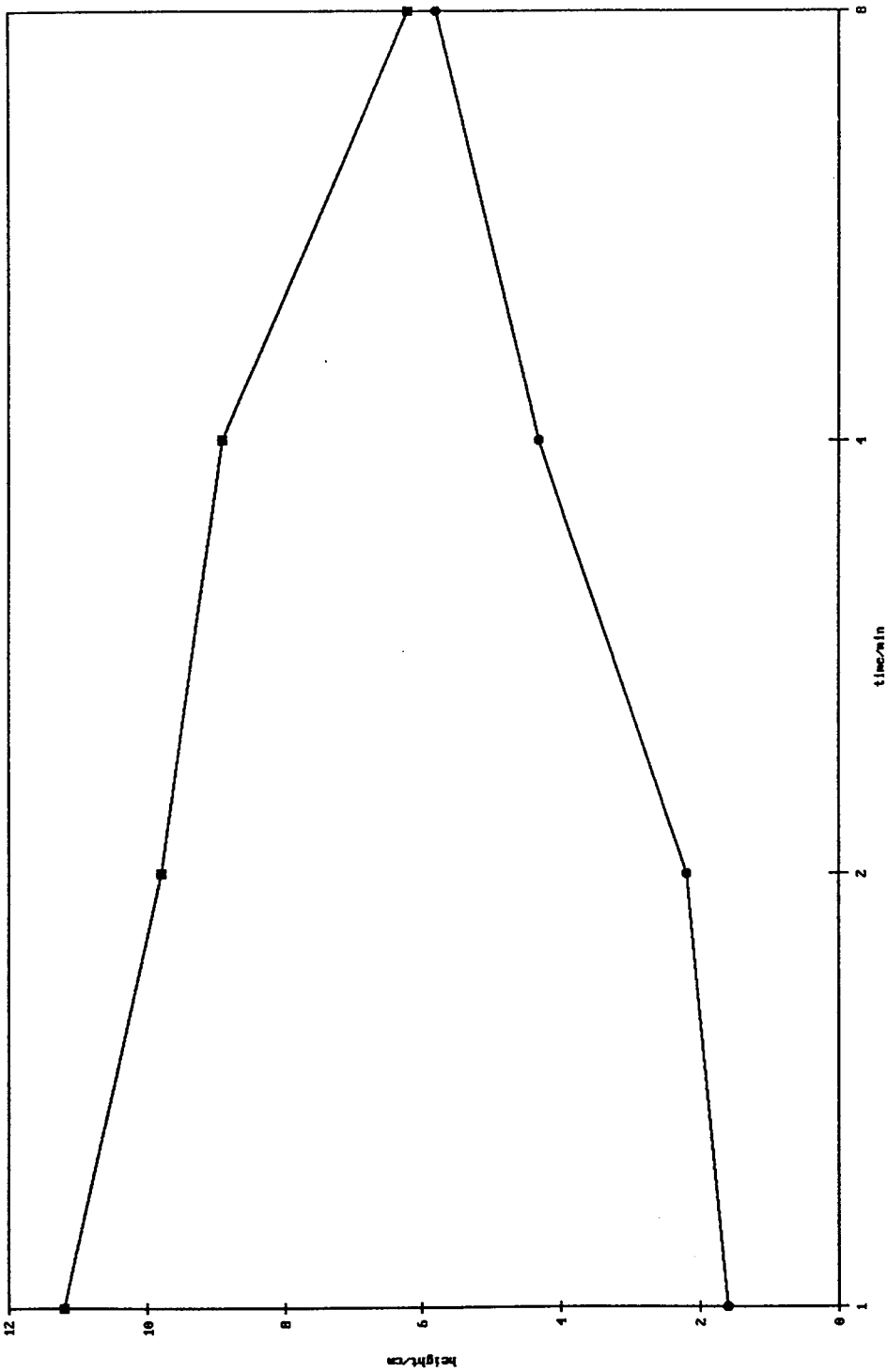

Fig. 4. Diagram showing dependence of peak areas on derivatization time for (●) 4-aminomorpholine and (■) internal standard 3-aminopropanol.

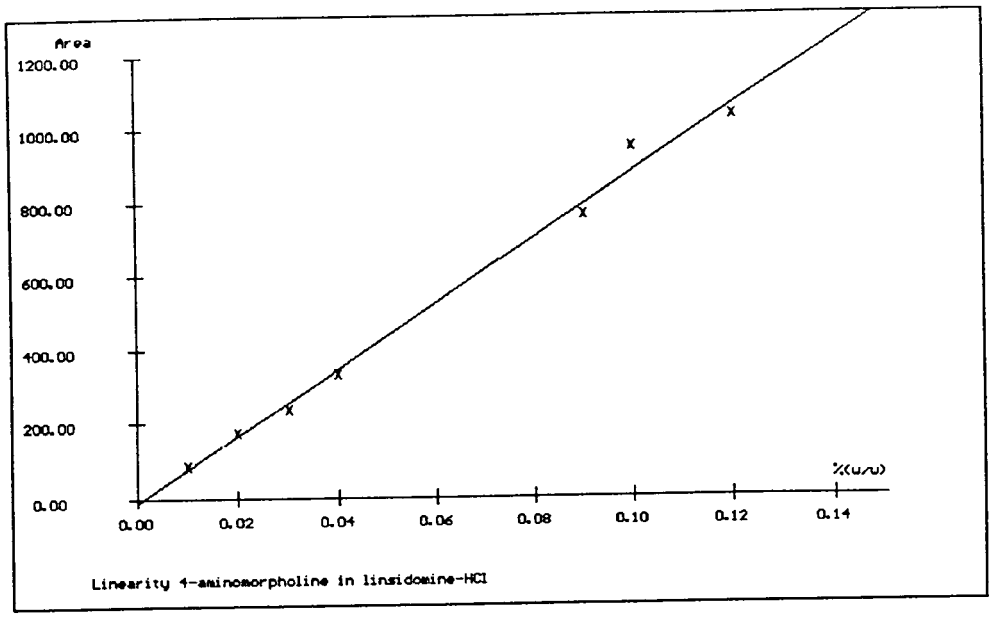

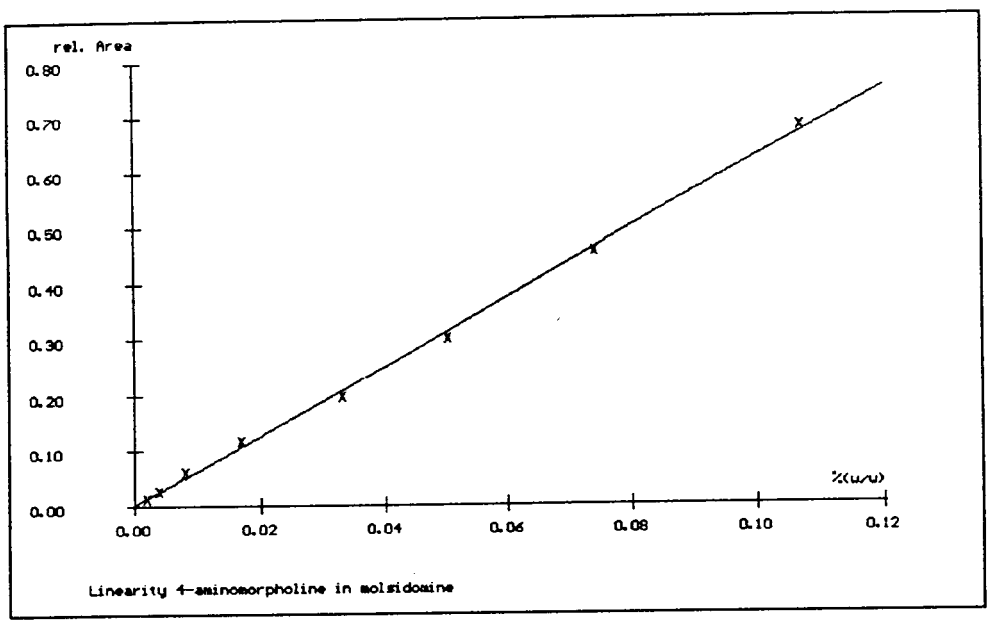

Fig. 5. Linearity shown for both methods, i.e., precolumn derivatization and electrochemical detection.

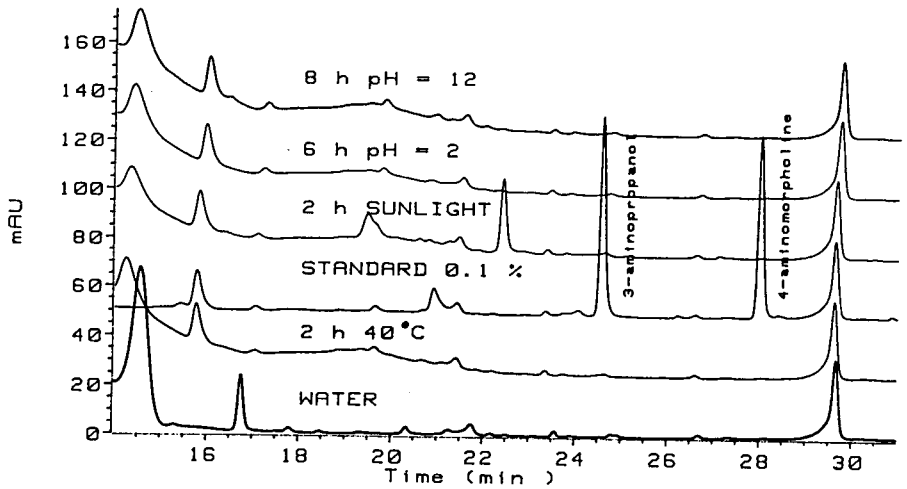

Fig. 6. Stability of molsidomine under different storage conditions. No 4-aminomorpholine was formed in the test solutions.

variation of the parameters for electrochemical detection.

3.2. Electrochemical detection

Oxidation of the strongly reducing hydrazines takes place under relatively mild conditions. A potential as low as 350 mV was found to be most suitable with respect to high sensitivity and maximum selectivity (Fig. 7). By-products were fully separated, as was shown by UV detection, and a potential as high as 1200 mV was needed to obtain a signal for other electrochemically active compounds (Fig. 8). The PCX-100 column turned out to be most convenient for chromatography as strong non-ionic interactions of the

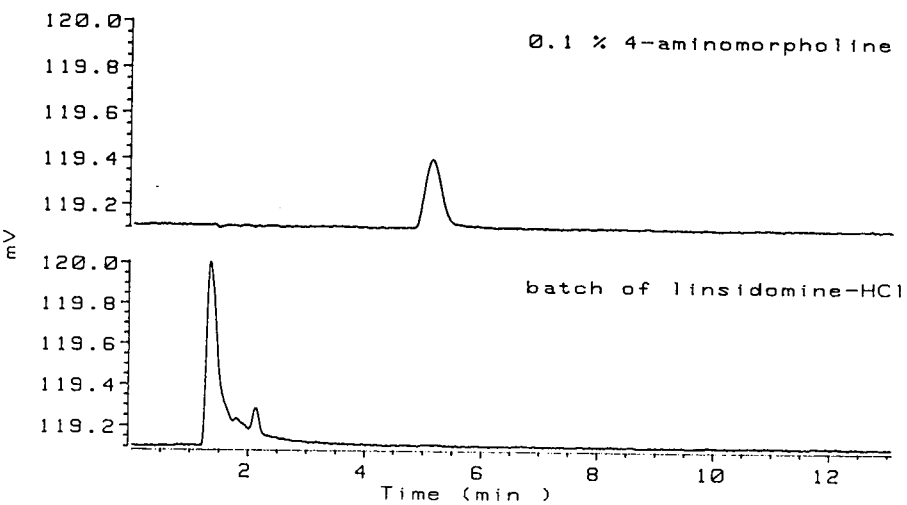

Fig. 7. Chromatograms of synthesis intermediate linsidomine hydrochloride and a standard solution of 4-aminomorpholine [0.1% relative to molsidomine (1 g l^{-1})].

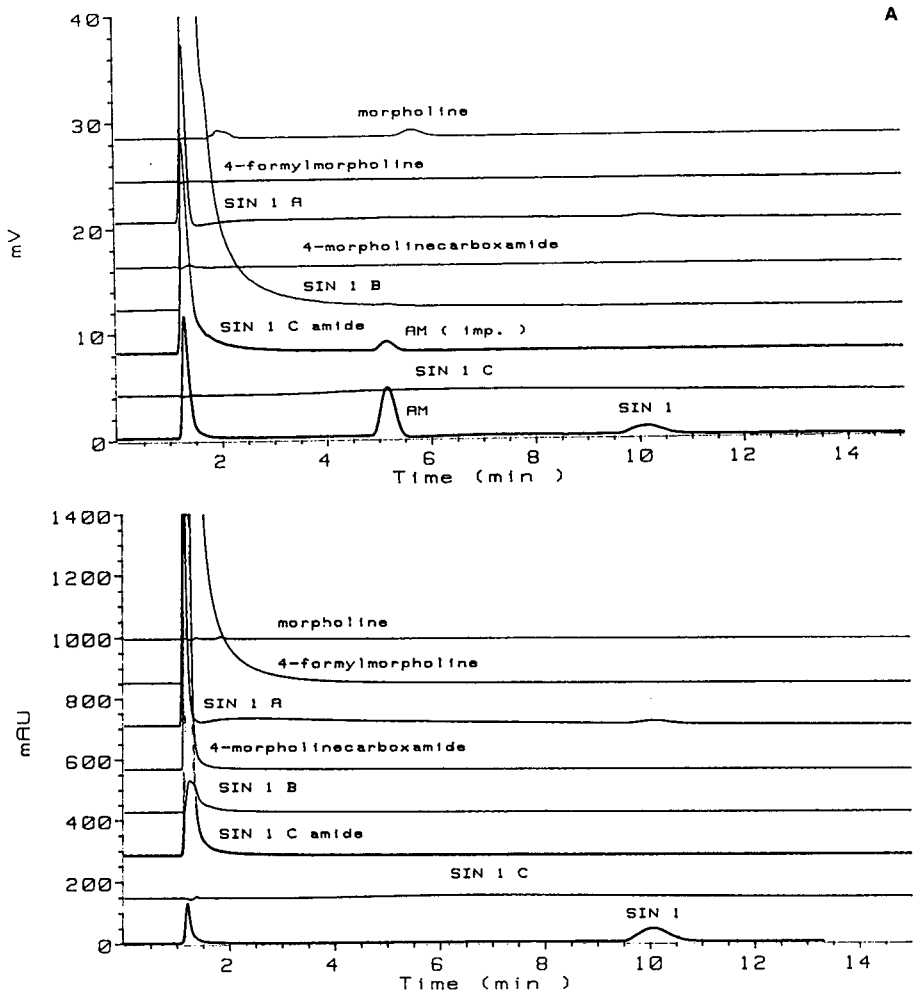

Fig. 8. Chromatograms demonstrating selectivity for the determination of 4-aminomorpholine in linsidomine. (A) Obtained by setting the potential at 1200 mV; (B) obtained by measuring at 210 nm. All by-products are well separated and are either only electrochemically active at the high potential of 1200 mV or inactive.

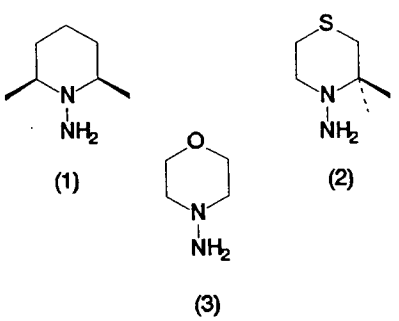

Fig. 9. Structures of the hydrazines investigated: 1 = *cis*-2,6-dimethylpiperidine; 2 = 3,3-dimethyl-4-aminothiomorpholine; 3 = 4-aminomorpholine.

ionized substances were observed on most cation-exchange stationary phases.

PCX-100 is a polymer-based stationary phase, resistant to organic solvents. Variation of the acetonitrile content in the mobile phase may easily be adjusted to influence the selectivity and to reduce non-ionic contributions to retention [6]. In addition, the pH of the mobile phase was adjusted to 4.0 so that degradation of linsidomine hydrochloride could be significantly reduced during analysis. Degradation of linsidomine hydrochloride and molsidomine was observed in alkaline solutions [5].

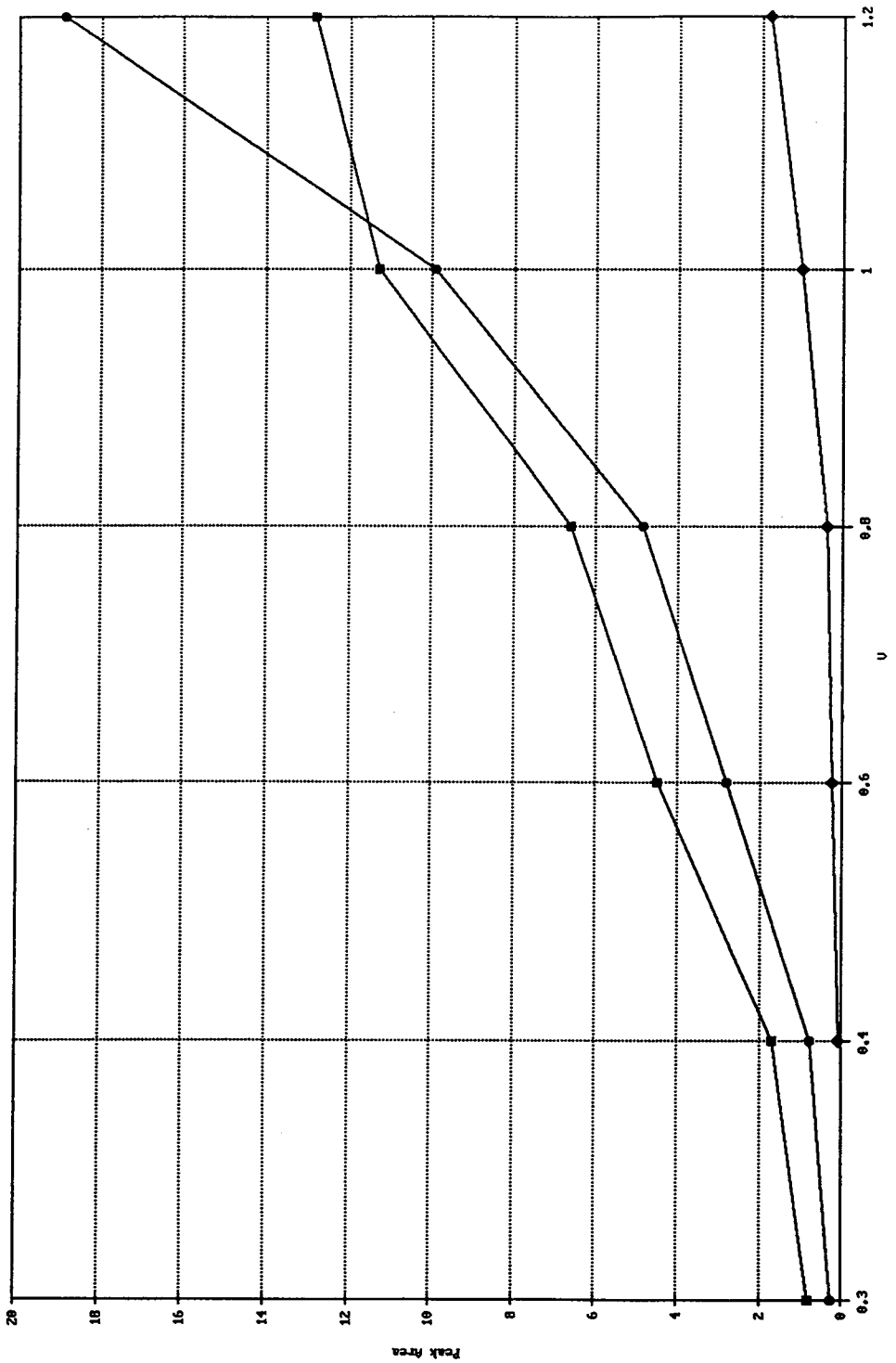

Fig. 10. Hydrodynamic voltammograms obtained for (◆) *cis*-2,6-dimethylpiperidine, (■) 3,3-dimethyl-4-aminothiomorpholine and (●) 4-aminomorpholine

The precision of the method at the limit of quantification (50 ppm) was sufficient (relative standard deviation = 7%) and no contamination of the working electrode surface could be observed, as was demonstrated by repetitive injections of the same solution without electrode pretreatment.

This mode of detection was applicable to the structurally similar 4-amino-*cis*-2,6-dimethylpiperidine and to 3,3-dimethyl-4-aminothiomorpholine (Fig. 9).

Hydrodynamic voltammograms for the three hydrazines investigated are shown in Fig. 10.

Low responses were observed for 4-amino-*cis*-2,6-dimethylpiperidine whereas similar responses were obtained for 4-aminomorpholine and 3,3-dimethyl-4-aminothiomorpholine. This may be explained by a greater steric hindrance due to the methyl groups for 4-amino-*cis*-2,6-dimethylpiperidine than for the others. We also found that the SIN 1 C analogous compound of 3,3-dimethyl-4-aminothiomorpholine yielded a good response, whereas its sulfoxide was electrochemically inactive, so oxidation obviously occurs at the sulfur atom.

4. Conclusions

Two methods suitable for routine pharmaceutical quality control for the determination of trace amounts of 4-aminomorpholine in molsidomine and linsidomine were presented, based on precolumn derivatization and ion chromatography–electrochemical detection.

The reactivity of some other hydrazines investigated was shown to be very dependent on their pattern of substitution.

Procolumn derivatization may be run on standard HPLC equipment with an appropriate autosampler. High sensitivity can be obtained using standard UV detection.

If high selectivity is required, electrochemical detection should be preferred but again the pattern of substitution has to be kept in mind when choosing suitable analytical conditions with respect to the pH value, the working potential and the stationary phase.

References

[1] I.S. Krull (Editor), *Post-Column Reaction Detectors in HPLC*, Marcel Dekker, New York, 1986.
[2] K. Thoma, *Pharm. Ind.*, 54 (1992) 630.
[3] P.K. Dasgupta, *J. Chromatogr. Sci.*, 27 (1989) 422.
[4] J.K. Wong, T.H. Joyce and T.H. Morrow, *J. Chromatogr.*, 385 (1987) 267.
[5] Y. Asahi, K. Shinozaki and M. Nagoaka, *Chem. Pharm. Bull.*, 19 (1971) 1079.
[6] J. Weiss, *Chromatographie*, 2 (1992) 67.

ELSEVIER

Journal of Chromatography A, 689 (1995) 247–254

JOURNAL OF CHROMATOGRAPHY A

Liquid chromatographic separation of diamino analogues of 2′- or 3′-deoxyadenosine from adenine on a poly(styrene–divinylbenzene) polymer column

G. Thoithi*, A. Van Schepdael, P. Herdewijn, E. Roets, J. Hoogmartens

Katholieke Universiteit Leuven, Laboratorium voor Farmaceutische Chemie en Analyse van Geneesmiddelen, Faculteit Farmaceutische Wetenschappen, Van Evenstraat 4, B-3000 Leuven, Belgium

First received 16 June 1994; revised manuscript received 1 September 1994

Abstract

A liquid chromatographic method that can separate each of a series of diamino analogues of 2′- or 3′-deoxyadenosine from their main degradation product, adenine, is described. A PLRP-S 1000 Å (8 μm) 250 mm × 4.6 mm I.D. column was used at 60°C. The method was developed by systematic evaluation of the influence of the mobile phase pH, the type and concentration of the organic modifier, the concentration of the ion-pairing agent and the buffer. The mobile phase consisted of tetrahydrofuran–0.2 *M* sodium octanesulphonate–0.2 *M* potassium phosphate buffer (pH 2.0)–water (15:25:30:30, v/v).

1. Introduction

Currently intensive research is focused on new drugs for the treatment of AIDS and a variety of nucleosides with activity against HIV have been discovered. Diamino analogues of 2′- or 3′-deoxyadenosine (**1–4**) (Fig. 1) were synthesized as part of a structure–activity relationship study of analogues of 2′,3′-dideoxyadenosine that are active against HIV, but none of them had substantial antiretroviral or cytostatic activity [1]. Although many studies have been published on the stability of normal deoxynucleosides, little is known about the stability of the amino-substituted congeners. We therefore considered it of interest to carry out stability studies on **1–4**. Knowledge of the stability might be useful when carrying out derivatization reactions with these nucleosides. In addition, compounds **1–4** are potential candidates for incorporation into oligodeoxynucleotides, serving as enzymatically stable substitutes for the natural deoxynucleosides. Stability studies on **1–4** necessitated an analytical method that could separate each of them from their main degradation product, adenine (A), and such a method had not previously been reported.

2. Experimental

2.1. Samples and reagents

The synthesis of compounds **1–4** has been described elsewhere [1]. Adenine, sodium octanesulphonate, methanol and acetonitrile were

* Corresponding author.

0021-9673/95/$09.50
SSDI 0021-9673(94)00856-6

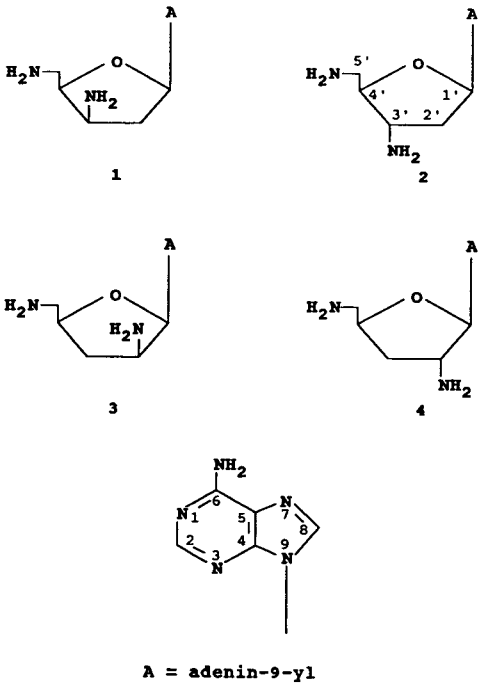

Fig. 1. Structures of diamino analogues of 2′- or 3′-deoxy adenosine.

purchased from Janssen Chimica (Beerse, Belgium). Methanol and acetonitrile were redistilled before use. HPLC-grade tetrahydrofuran was obtained from Rathburn (Walkerburn, UK). Water was distilled twice in glass apparatus. All other reagents were of analytical-reagent grade (Janssen Chimica).

2.2. Liquid chromatography

The liquid chromatographic apparatus consisted of an SP 8700 XR solvent-delivery system (Spectra-Physics, San Jose, CA, USA), used at a flow-rate of 1 ml/min, a Model CV-6UH-Pa-N-60 injector (Valco, Houston, TX, USA) equipped with a 20-μl loop, a Waters (Milford, MA, USA) Model 440 detector set at 254 nm and a Hewlett-Packard (Avondale, PA, USA) Model 3396 integrator. The stationary phases examined were RSil C_{18} LL (5 μm) (Alltech, Deerfield, IL, USA), Spherisorb ODS-1 (10 μm) (Phase Separations, Queensferry, UK), Chromspher C_8 (5 μm) (Chrompack, Middelburg, Netherlands), PRP-1 (7–9 μm) (Hamilton, Reno, NV, USA), Rogel 80 Å (8 μm) (Bio-Rad Labs., Richmond, CA, USA), PLRP-S 100 Å (8 μm), PLRP-S 300 Å (8 μm) and PLRP-S 1000 Å (8 μm) (Polymer Laboratories, Church Stretton, Shropshire, UK), all in 250 mm × 4.6 mm I.D. columns, equilibrated by means of a water-bath. The mobile phase consisted of tetrahydrofuran–0.2 *M* sodium octanesulphonate–0.2 *M* potassium phosphate buffer (pH 2.0)–water (15:25:30:30, v/v). Samples of **1** used for kinetic studies were prepared by diluting 0.1 ml of a $5 \cdot 10^{-3}$ *M* stock standard solution with 4.9 ml of 0.1 *M* glycine hydrochloride buffer (pH 1.15) and ionic strength 0.4 (adjusted with KCl before measuring the final pH). Aliquots (0.5 ml) of this solution were put in vials, capped and degraded in a Memmert (Schwabach, Germany) oven. The vials were removed and quenched with 0.5 ml of 0.1 *M* KOH to give a final concentration of $5 \cdot 10^{-5}$ *M* (the amount injected was 0.25 μg).

3. Results and discussion

Compound **1** was used to develop the method. Monoamino analogues of 2′- or 3′-deoxyadenosine have been well separated from adenine on a silica-based reversed-phase column with the use of a silanol-masking agent [2]. Similar studies were carried out for diamino analogues of 2′- or 3′-deoxyadenosine, whereby different types of silica-based reversed-phase columns, namely RSil C_{18} LL (5 μm), Spherisorb ODS-1 (10 μm), and Chromspher C_8 (5 μm), were tested using either a silanol-masking agent (tetramethylammonium phosphate) or an ion-pairing agent (sodium octanesulphonate). There was good resolution, but considerable peak tailing with these columns owing to the high interaction between the basic amino groups and the acidic silanol groups and so a poly(styrene–divinylbenzene) polymer [PLRP-S 1000 Å (8 μm)] column was chosen for further method development. By using an ion-pairing agent, there was good resolution between **1** and

adenine. Therefore, the emphasis in optimizing the mobile phase was on improving the peak symmetry, particularly that of the nucleoside, because kinetic calculations are based on the peak areas of **1–4**. The mobile phase was developed by systematic investigation of the influence of the pH, the type and concentration of the organic modifier and the concentration of the ion-pairing agent and the buffer.

The pK_a of adenine (N1) is 4.18 [3] but the pK_a values of **1–4** have not previously been reported. It is expected that the pK_a values of N1 of **1–4** would be in a similar range to those of monoamino analogues of 2′- or 3′-deoxyadenosine, some of which have been previously determined by NMR and are given in Table 1 (results from Ref. [4]). Fig. 2 shows the influence of the mobile phase pH on the chromatographic parameters of the separation of **1** and A. All

Table 1
pK_a values of some monoamino analogues of 2′- or 3′-deoxyadenosine (from Ref. [4])

Compound	pK_a (N1)	pK_a ($-NH_2$)
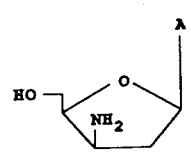	3.1	9.0
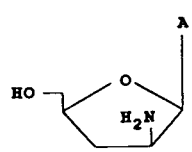	3.3	6.2
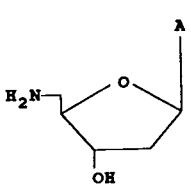	4.1	9.0

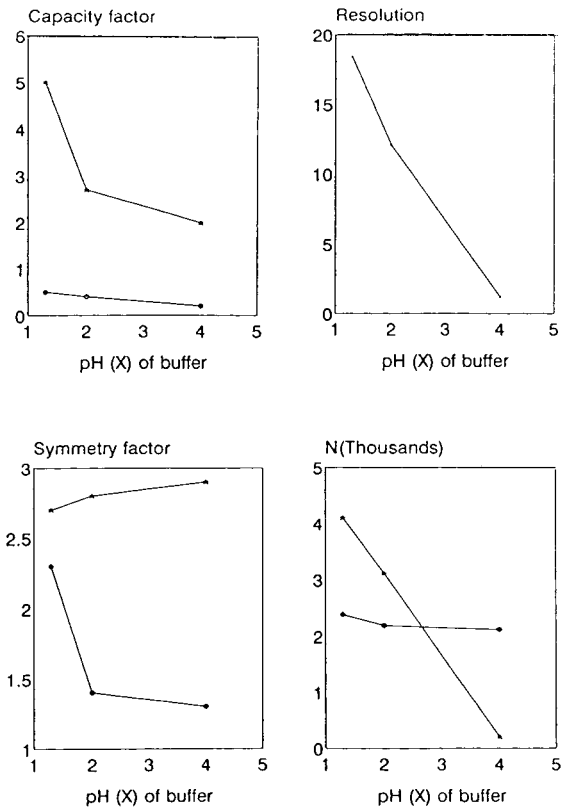

Fig. 2. Influence of mobile phase pH on the chromatographic parameters of separation of (○) adenine and (★) **1**. Mobile phase, acetonitrile–0.02 *M* sodium octanesulphonate–0.2 *M* potassium phosphate buffer–water (10:15:5:70, v/v). Column temperature, 70°C. N = plate number.

chromatographic parameters were calculated using equations from the European Pharmacopoeia [5]. At the low pH values used in this study, the sugar amino groups are fully protonated. There is an increase in the retention of **1** and A with decrease in pH owing to increased protonation of the heterocyclic ring and hence more ion pairing. The peak symmetry (A_s) of **1** at pH 2.0 is almost the same as that at pH 1.3, yet A_s of adenine is greatly improved at pH 2.0. Therefore, pH 2.0 was chosen for further work.

The column was heated to reduce the backpressure. When temperature was increased, there was an overall decrease in retention but little change in selectivity (results not shown). A temperature of 60°C was found to be the best

because it gave the best peak symmetry of **1** and it was used in all subsequent experiments.

The influence of organic modifiers and their concentrations on the chromatographic parameters of **1** and A was investigated. Methanol gave very poor peak shapes. Tetrahydrofuran produced a large improvement in peak symmetry compared with acetonitrile. Tetrahydrofuran (7%) was used for further work because it gave the best peak symmetry of adenine and **1**.

The effects of different concentrations of 0.02 *M* sodium octanesulphonate and 0.2 *M* potassium phosphate buffer (pH 2.0) on the chromatographic parameters of adenine and **1** are shown in Figs. 3 and 4, respectively. As expected, k' increases with increase in concentration of the ion-pairing agent owing to the reduced polarity of A and **1** after the formation of an ion pair. Increasing the buffer concentration increases the dissociation of the ion pairs, thereby causing a decrease in retention [6]. The effect of changing the ion-pairing agent and the buffer concentration on k' is much greater for **1** than for A. This is due to, amongst other factors, the fact that **1** has more protonation sites (and hence more potential pairing sites) than adenine [6]. The best results were obtained by use of 10% of 0.02 *M* sodium octanesulphonate and 5% of 0.2 *M* potassium phosphate buffer (pH 2.0).

Hence samples of **1–4** dissolved in water could

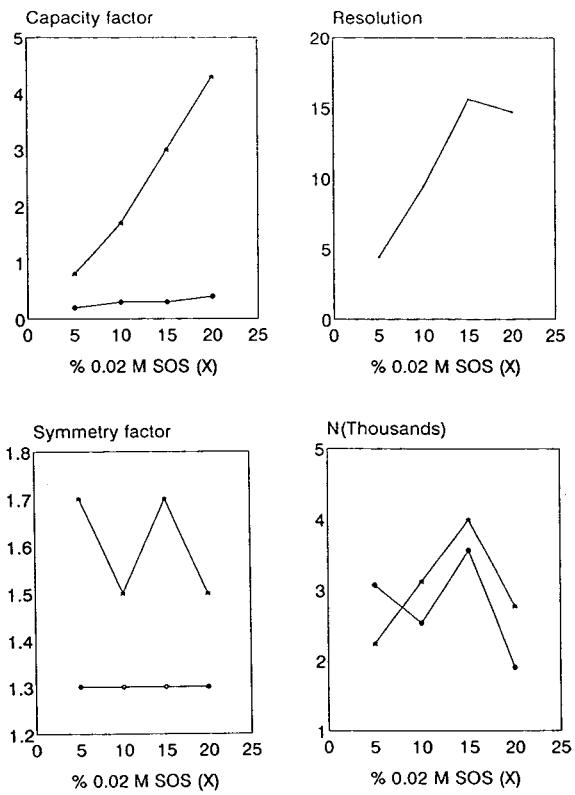

Fig. 3. Influence of proportion of 0.02 *M* sodium octanesulphonate on the chromatographic parameters of the separation of (O) adenine and (★) **1**. Mobile phase, tetrahydrofuran–0.02 *M* sodium octanesulphonate–0.2 *M* potassium phosphate buffer (pH 2.0)–water (7:*X*:5:88 − *X*, v/v); column temperature, 60°C. *N* = plate number; SOS = sodium octanesulphonate.

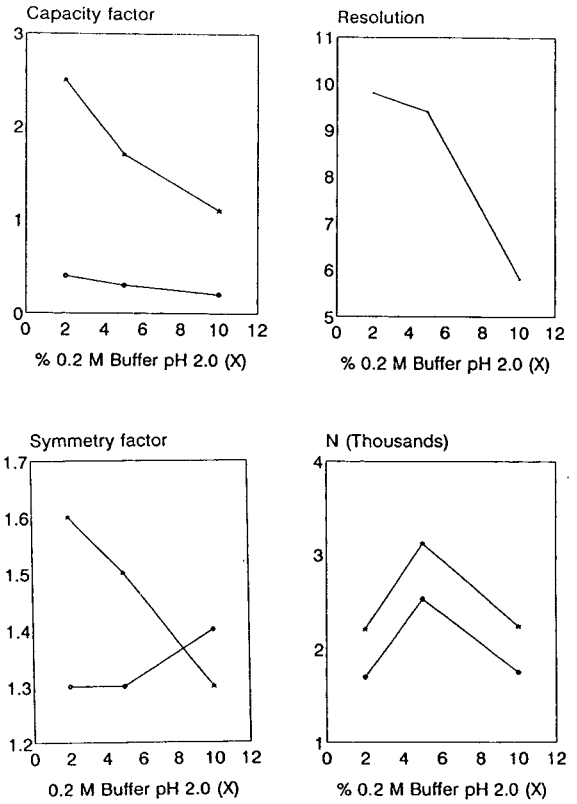

Fig. 4. Influence of proportion of 0.2 *M* potassium phosphate buffer on the chromatographic parameters of the separation of (O) adenine and (★) **1**. Mobile phase, tetrahydrofuran–0.02 *M* sodium octanesulphonate–0.2 *M* potassium phosphate buffer (pH 2.0)–water (7:10:*X*:83 − *X*, v/v); column temperature, 60°C. *N* = plate number.

be analysed on a PLRP-S 1000 Å (8 μm) column equilibrated at 60°C and a mobile phase consisting of tetrahydrofuran–0.02 *M* sodium octanesulphonate–0.2 *M* potassium phosphate buffer (pH 2.0)–water (7:10:5:78, v/v).

When a sample of **1** used for kinetic studies was analysed with the mobile phase developed above, there was a shoulder on the peaks (Fig. 5a). This is contrary to studies done on monoamino analogues of 2′- or 3′-deoxyadenosine, whereby a sample dissolved in water and one for kinetic studies could both be analysed on a Spherisorb ODS-1 column using a mobile phase containing acetonitrile–0.2 *M* tetramethylam-

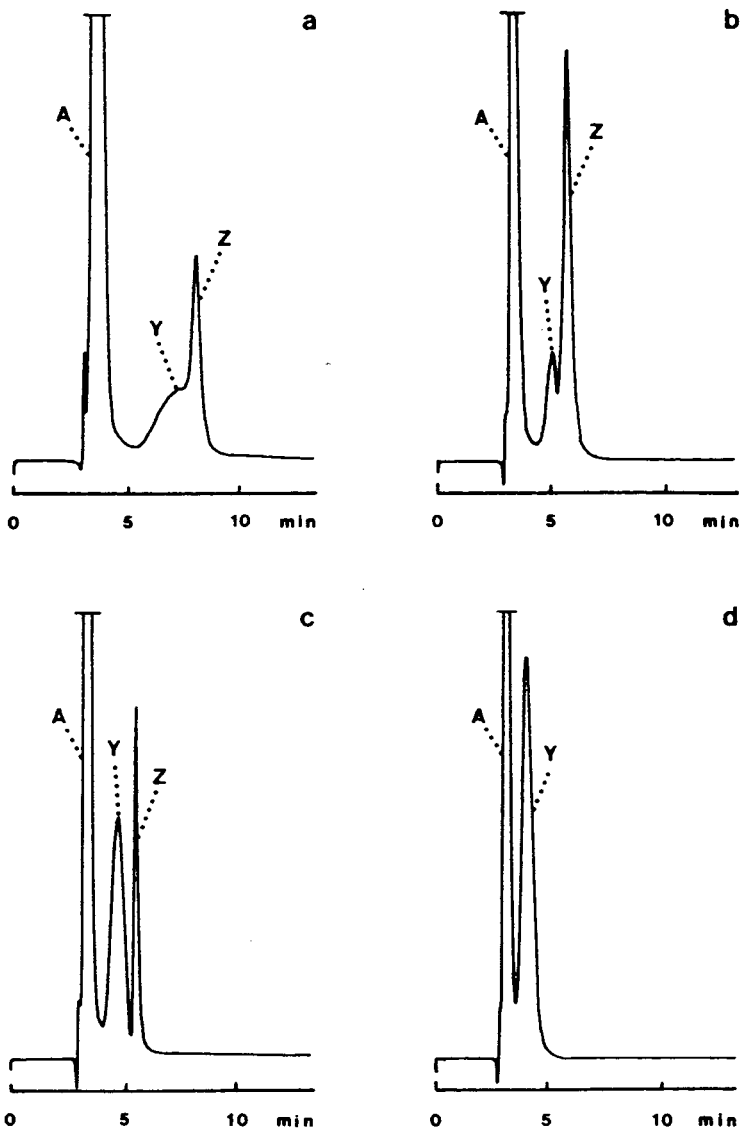

Fig. 5. Liquid chromatograms showing effect of buffer. Sample, **1** degraded at pH 1.15 and 100°C for 1.5 h; mobile phase, tetrahydrofuran–0.02 *M* sodium octanesulphonate–0.2 *M* potassium phosphate buffer (pH 2.0)–water (7:10:X:83 − X, v/v). X = (a) 5; (b) 15; (c) 20; and (d) 30. A = adenine.

monium phosphate (pH 6.0)–0.2 *M* potassium phosphate buffer (pH 6.0)–water (5:0.5:5:89.5, v/v) [2]. The appearance of shoulders on both the peaks corresponding to adenine and **1** suggested that the shoulders were due to chromatographic effects rather than the presence of other degradation products. Indeed, an undegraded sample of **1** also exhibited a similar shoulder on analysis with the mobile phase described above. Compounds **1–4** behaved similarly. It was suspected that the peak shoulders were due to insufficient buffering of the sample by the mobile phase. As the mobile phase buffer was increased to solve this problem, two distinct peaks (Y and Z) that corresponded to **1** were formed. As the buffer concentration increased, the size of peak Y increased while that of peak Z decreased until finally only one peak (Y) was left (Fig. 5b–d). In ion-pair systems, k' is determined mainly by reversed-phase and ion-pair processes. Increasing buffer concentration increases the total cation concentration, resulting in reduced ion pairing [6], and this coincides with decrease in the retention and size of peak Z. In addition, this causes a second process (most likely a reversed-phase mechanism), responsible for peak Y, to become more predominant. This phenomenon disappeared when, in addition to increasing the buffer concentration, the amount of ion-pairing agent was increased until the stationary phase was saturated.

The influence of higher concentrations of the ion-pairing agent on the chromatographic parameters for the separation of **1** and adenine are shown in Fig. 6. There is a linear increase in k' with increase in amount of the ion-pairing agent up to about 20% of 0.2 *M* sodium octanesulphonate, after which the graph flattens owing to saturation of the stationary phase. Below 25% of 0.2 *M* sodium octanesulphonate there are peak shoulders and split peaks. Different concentrations of the buffer were also investigated (data not shown). Use of 25% of 0.2 *M* sodium octanesulphonate and 30% of 0.2 *M* potassium phosphate buffer (pH 2.0) gave the best peak symmetry of adenine and **1**. The tetrahydrofuran concentration was then adjusted to give reasonable retention.

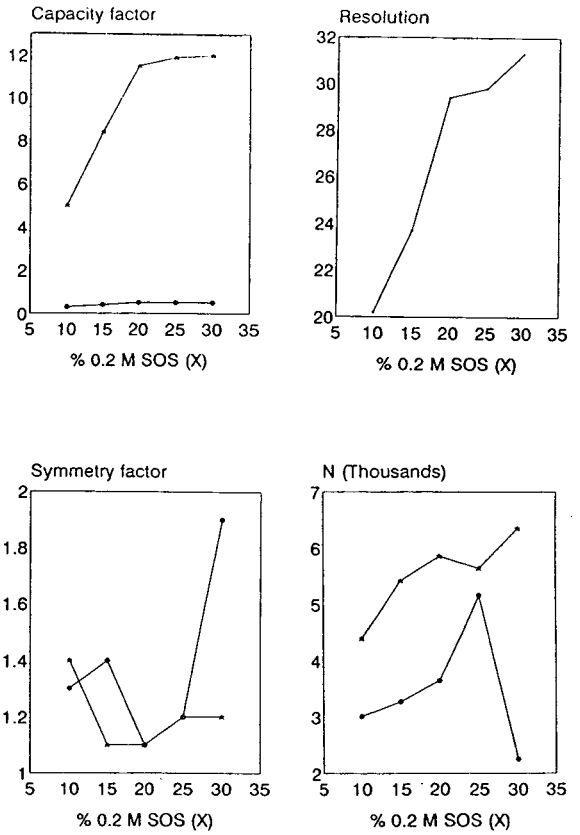

Fig. 6. Influence of proportion of 0.2 *M* sodium octanesulphonate on the chromatographic parameters of the separation of (○) adenine and (★) **1**. Mobile phase, tetrahydrofuran–0.2 *M* sodium octanesulphonate–0.2 *M* potassium phosphate buffer (pH 2.0)–water (10:*X*:30:60 – *X*, v/v); column temperature, 60°C. N = plate number; SOS = sodium octanesulphonate.

The best mobile phase for the analysis of samples used for kinetic studies consists of tetrahydrofuran–0.2 *M* sodium octanesulphonate–0.2 *M* potassium phosphate buffer (pH 2.0)–water (15:25:30:30, v/v).

The linearity of the detector response was tested in the range $5 \cdot 10^{-6}$ *M* (1.25 μg/ml) to 10^{-4} *M* (24.9 μg/ml) of **1** using four calibration points (twelve data points). The following relationship was obtained: $y = 14817x + 203$ (y = peak area/1000 and x = concentration injected in μg/ml); $r = 0.9988$; standard error of y

estimate = 243; standard deviation of slope = 252. The method was found to be repeatable (R.S.D. = 1.0%; $n = 4$). The limit of detection was 0.05 ng at a signal-to-noise ratio of 3. The limit of quantification was 5 ng ($n = 4$; R.S.D. = 14%).

Results obtained with this mobile phase and other columns are given in Table 2. Compound **1** tailed too much on the PLRP-S 300 Å (8 μm) column. On the PLRP-S 100 Å (8 μm) and Rogel 80 Å (8 μm) columns there was front tailing and this could cause inaccurate integra-

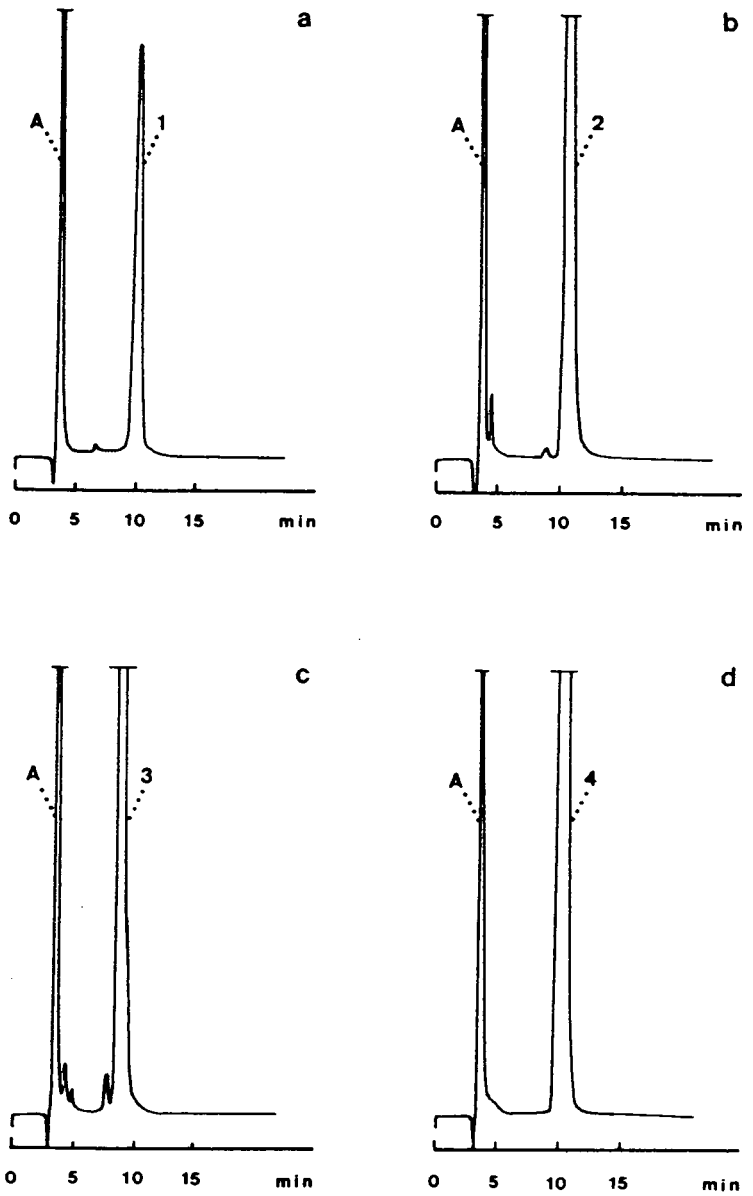

Fig. 7. Liquid chromatograms of **1–4** partially degraded at pH 1.15. Mobile phase: tetrahydrofuran–0.2 *M* sodium octanesulphonate–0.2 *M* potassium phosphate buffer (pH 2.0)–water (15:25:30:30, v/v).

Table 2
Chromatographic parameters of the separation of adenine and **1** on polymer columns from different manufacturers

Column	Capacity factor		Resolution, adenine/**1**	Peak Symmetry, **1**	Plate number	
	Adenine	**1**			Adenine	**1**
PLRP-S 1000 Å (8 μm)	0.3	3.2	13.6	1.3	1490	4530
PLRP-S 300 Å (8 μm)	0.5	6.1	10.4	3.4	1940	900
PLRP-S 100 Å (8 μm)	0.7	8.4	16.8	0.8	1670	2550
PRP-1 (7–9 μm)	0.8	10.5	25.6	1.3	2240	5720
RoGel 80 Å (8 μm)	1.1	13.6	23.3	0.8	1990	4300

Mobile phase, tetrahydrofuran–0.2 *M* sodium octanesulphonate–0.2 *M* potassium phosphate buffer (pH 2.0)–water (15:25:30:30, v/v); flow-rate, 1 ml/min; column temperature, 60°C; detection at 254 nm.

Table 3
Chromatographic parameters for the separation of adenine and **1–4**

Compound	Capacity factor		Resolution, adenine/N	Peak Symmetry, N	Plate number	
	Adenine	N			Adenine	N
1	0.3	3.2	13.6	1.3	1490	4530
2	0.3	3.4	15.0	1.5	1140	4290
3	0.3	2.6	12.3	1.5	960	4280
4	0.3	3.0	13.6	1.4	960	4550

Mobile phase, tetrahydrofuran–0.2 *M* sodium octanesulphonate–0.2 *M* potassium phosphate buffer (pH 2.0)–water (15:25:30:30, v/v); flow-rate, 1 ml/min; column, PLRP-S 1000 Å (8 μm); column temperature, 60°C, detection, 254 nm. N = nucleoside.

tion of the peaks. The PRP-1 (7–9 μm) column gave good symmetry of **1** and adenine, but high retention, and therefore the PLRP-S 1000 Å (8 μm) column was chosen for the analysis of **1–4**. Table 3 gives the results obtained and Fig. 7 shows typical chromatograms.

Acknowledgements

G.T. thanks the Belgian Administration for Development Cooperation (ABOS) for a scholarship. The authors are grateful to Mr. I. Quintens for graphical assistance.

References

[1] P. Herdewijn, J. Balzarini, R. Pauwels, G. Janssen, A. Van Aerschot and E. De Clercq, *Nucleosides Nucleotides*, 8 (1989) 1231.
[2] G. Thoithi, A. Van Schepdael, P. Herdewijn, E. Roets and J. Hoogmartens, *Chromatographia*, 35 (1993) 451.
[3] J. Clauwaert and J.Z. Stockx, *Z. Naturforsch., Teil B*, 23 (1968) 25.
[4] G. Thoithi, A. Van Schepdael, R. Busson, P. Herdewijn, E. Roets and J. Hoogmartens, *Nucleosides Nucleotides*, submitted for publication.
[5] *European Pharmacopoeia*, Maisonneuve, Sainte-Ruffine, 2nd ed., 1987, p. V.6.20.4.
[6] A.P. Goldberg, E. Nowakowska, P.E. Antle and L.R. Snyder, *J. Chromatogr.*, 316 (1984) 241.

ELSEVIER

Journal of Chromatography A, 689 (1995) 255–267

JOURNAL OF CHROMATOGRAPHY A

Comparison of chromatographic behaviour of oligoethylene glycol nonylphenyl ether non-ionic and anionic surfactants in reversed-phase high-performance liquid chromatography

P. Jandera[a,*], J. Urbánek[b]

[a]*Faculty of Chemical Technology, University of Pardubice, Nám. Legií 565, 532 10 Pardubice, Czech Republic*
[b]*BOHEMIACHEM, Tovární 63, Děčín XXXII, Czech Republic*

First received 9 May 1994; revised manuscript received 9 September 1994

Abstract

A simple retention mechanism is proposed to describe the retention behaviour of oligomeric sulphated and non-sulphated surfactants of the oligoethylene glycol nonylphenyl ether type in reversed-phase systems containing ion-pairing reagents in aqueous–organic mobile phases. The equations derived using this mechanism relate the capacity factors of the individual oligomers to the number of oxyethylene units and to the concentrations of the organic solvent (2-propanol) and of the ion-pairing reagent (cetyltrimethylammonium bromide) in the mobile phase. Most capacity factors calculated using the best-fit parameters of these equations agree with the experimental values with errors of less than ±5% relative. The capacity factors of the anionic surfactants with various degrees of polymerization on a C_{18} column reach maximum values in the mobile phases containing 0.02 mol/l cetyltrimethylammonium bromide, while the retention of the non-ionic surfactants decreases regularly with increasing concentration of the ion-pairing reagent. The concentration of propanol affects the retention of the anionic and non-ionic surfactants in the same way, but the anionic surfactants are more strongly retained. The composition of the mobile phase can be optimized so that the sulphated and non-sulphated oligoethylene glycol nonylphenyl ethers are distinguished into two groups of peaks and the separation of the individual oligomers in the two groups is possible in a single run.

1. Introduction

Oxyethylenated alcohols, carboxylic acids and phenols are common non-ionic surfactants and their sulphated derivatives are also widely used as anionic surfactants in various industrial and household applications. Efficient separations of oxyethylenated non-ionic surfactants can be achieved by high-performance liquid chromatography (HPLC) with both normal-phase [1–11] and reversed-phase [12–17] systems. Few reports have been published on the systematic investigation of their retention behaviour [18,19]. Much less work has been reported on the chromatographic separation of anionic sulphated derivatives than of their non-sulphated parent compounds. In addition to the separation of the sulphated from the non-sulphated fraction [20], ion-pair reversed-phase chromatography has been used to separate the individual oligomers in the sulphated and non-sulphated fractions [21–23]. Both non-sulphated and sulphated oligomers

* Corresponding author.

0021-9673/95/$09.50
SSDI 0021-9673(94)00892-2

are eluted in order of decreasing number of oligomeric oxyethylene units in reversed-phase systems, as in chromatography on a mixed-mode reversed-phase–ion-exchange column [24], but in contrast to chromatography in normal-phase systems. Separation of sulphated oxyethylenated surfactants has also been attempted by ion-exchange chromatography on silica gel-based stationary phases [25].

Recently, we have suggested equations for the description of the simultaneous effects of the degree of polymerization, n, and of the concentration of the stronger solvent in binary mobile phases on the retention in oligomeric series, in both reversed-phase [26,27] and normal-phase [28] systems. In this work, this theory was extended to reversed-phase ion-pair chromatographic systems and conditions were established for the separation of both non-ionic oligoethylene glycol nonylphenyl ethers (OEGNPEs) and their anionic sulphated derivatives in a single run.

2. Theoretical

Sulphated derivatives of OEGNPEs are completely ionized in aqueous–organic solutions and, like other organic and inorganic anions, are not retained in reversed-phase systems with non-polar adsorbents, unless ionic modifiers are added to the aqueous–organic mobile phase to increase the retention and make possible the separation of the ionized samples. Most common are modifiers with a large hydrophobic part and a small ionized functional group, carrying a charge opposite to that of the sample ions. The modifiers, often called ion-pairing reagents, usually show surface-active properties.

To describe chromatographic behaviour in aqueous–organic mobile phases containing ion-pairing additives, various retention models proposed so far have been reviewed recently [29]. The original "ion-pair chromatography" model based on the formation of the electroneutral associates (ion pairs) between the sample ion and the modifier ion of opposite charge [30] did not take into account the adsorption of the ionic modifier on the surface of the non-polar column packing material. This sorption was assumed to be controlled by a Langmuir isotherm in the "dynamic ion-exchange model" [31], which yielded the same formal mathematical description of the chromatographic behaviour as the "ion-pair" model. The so-called "ion-interaction model" does not rely on the formation of ion pairs in the mobile phase [32]. Instead, the ionic modifier was assumed to control the sorption of sample ions by means of its effect on the interfacial surface tension [33]. Finally, electrostatic models have been proposed that do not take into account the formation of stoichiometric ion associates in either the mobile or stationary phase. The effect on the retention of ionic samples is explained by the sorption of the ionic modifier followed by the formation of an electrical potential over a diffuse layer adjacent to the surface of the particles of column packing material and the retention of ionic samples is attributed to the electrostatic forces in the diffuse layer [34,35]. This model leads to equations describing the influence of the concentration of the ionic modifier on the retention of ionic solutes formally similar to those applying to ion-exchange systems.

In developing a model describing the effect of the number of oligomeric units and of the concentrations of the long-chain ionic modifier [cetyltrimethylammonium bromide (CTAB)] and of the organic solvent in water–2-propanol mobile phases on the retention of sulphated derivatives of oxyethylenated nonylphenols on a C_{18} column, we had to take into account the following main features of the experimental behaviour in the system investigated: the analytes are not retained in absence of CTAB and the dependences of their retention on the concentration of CTAB show pronounced maxima. To account for the experimental behaviour, we used an approach similar to that proposed by Knox and Hartwick [31] to describe the retention of analytes in the reversed-phase system studied. However, because of the character of the compounds investigated here, the present treatment differs from theirs as follows.

(1) The concentration of free (non-associated)

anionic analytes in the stationary phase was neglected as these compounds are eluted with the column dead volume in mobile phases that do not contain ionic additives.

(2) As the concentrations of CTAB used in this work were one order of magnitude higher than those commonly used in the ion-pair chromatography of small ions, adsorption of the cetyltrimethylammonium (CTA^+) cations on the surface of the non-polar column,

$$CTA_M \rightarrow CTA_S \quad (1)$$

is assumed to be better described by a Langmuir than by a linear isotherm, in agreement with the previous model [33]:

$$[CTA]_S = \frac{a[CTA]_M}{1 + b[CTA]_M} \quad (2)$$

where a (dimensionless) is the distribution ratio of CTA^+ ions in concentrations close to infinite dilution and b (l/mol) is related to the saturation capacity q_S of the column packing material for CTA^+ cations: $b = a/q_S$.

(3) As in the model of Knox and Hartwick [31], the formation of ion pairs of solute anions, X^-, with CTA^+ cations in the mobile phase was considered:

$$X_M + CTA_M \rightleftharpoons XCTA_M \quad (3)$$

characterized by the equilibrium constant K_{IM}:

$$K_{IM} = \frac{[XCTA]_M}{[X]_M[CTA]_M} \quad (4)$$

(4) Rather than real ion exchange between sulphated OEGNPEs and Br^- counter ions, the association of the solute anions X^- with CTA^+ cations already adsorbed in the stationary phase was assumed:

$$X_M + CTA_S \rightleftharpoons XCTA_S \quad (5)$$

characterized by the equilibrium constant K_{IS}:

$$K_{IS} = \frac{[XCTA]_S}{[X]_M[CTA]_S} \quad (6)$$

This association can be understood as ion-pair formation in the stationary phase. The retention is enhanced as the concentration of CTA^+ cations in the stationary phase increases. On the other hand, the formation of ion pairs in the mobile phase leads to a decrease in the retention proportional to the concentration of CTA^+ cations in the mobile phase. Because the concentration of CTA^+ cations in the stationary phase is proportional to the concentration in the mobile phase by means of the Langmuir isotherm, maximum retention is expected to occur at a certain concentration of CTA^+ cations in the mobile phase.

The capacity factor $k' = (V_R/V_M - 1)$ of the sample anions, A, is defined as

$$k' = \phi K_D = \phi \cdot \frac{[X]_S + [XCTA]_S}{[X]_M + [XCTA]_M} \approx \phi \cdot \frac{[XCTA]_S}{[X]_M + [XCTA]_M} \quad (7)$$

because the free anions X^- are not retained in the absence of the CTA^+ cations, so that $[X]_S = 0$. K_D in Eq. 7 is the distribution ratio, $\phi = V_S/V_M$ is the phase ratio in the column, i.e., the ratio of the volumes of the stationary and mobile phases, V_S and V_M, respectively, and V_R is the retention volume.

Combination of Eqs. 2, 4, 6 and 7 leads to the expression for k' as a function of the concentration of CTA^+ cations in the mobile phase, $[CTA]_M = c_M$:

$$k' = \frac{\phi \cdot \frac{K_{IS}}{K_{IM}} \cdot a}{(1 + bc_M)\left(1 + \frac{1}{K_{IM}c_M}\right)} = \frac{A}{1 + Bc_M + \frac{C}{c_M}} \quad (8)$$

where $A = \phi K_{IS} a/(K_{IM} + b)$, $B = K_{IM} b/(K_{IM} + b)$ and $C = 1/(K_{IM} + b)$.

According to Eq. 8, k' decreases as either Bc_M or C/c_M increases, i.e., it increases as the saturation capacity, $q_s = a/b$, of the bonded phase for CTAB increases and as the equilibrium constant of the sorption, K_{IS}, increases, while it decreases as the constant of the ion-pair formation, K_{IM}, in

the mobile phase increases. Eq. 8 predicts maximum retention to occur at $c_M = (C/B)^{1/2}$.

It is interesting that a maximum of retention as a function of c_M is not predicted if ion-pair formation in the mobile phase is not considered and if it is assumed that the true dynamic ion exchange, i.e., the exchange between the adsorbed sample anions and Br^- counter anions, controls the retention provided that the sorption of CTA^+ cations follows the Langmuir isotherm. In the absence of a buffer in the mobile phase (the sulphated OEGNPEs are ionized over a broad pH range including neutral solutions) and as the sample ions are present in low concentrations which can be neglected, the condition of electroneutrality requires that the concentration of the Br^- anions is the same as that of the CTA^+ cations both in the mobile and in the stationary phases and consequently c_M would be involved only in the denominator of the Langmuir equation (Eq. 2) and in the equation for k', so that a steady decrease of retention would be expected as the concentration of CTAB is increased in the chromatographic system.

To obtain appropriate retention and good separation in ion-pair reversed-phase systems, it is necessary to adjust the polarity of the mobile phase by controlling the concentration of the organic solvent as the second additive to the aqueous–organic mobile phase. In the chromatographic separation of oligomeric series such as that of sulphated OEGNPEs, the number of the repeat oligomeric units such as $-O-CH_2-CH_2-$ (oxyethylene) groups, is the most important structural factor. It has been found earlier that the dependence of the capacity factors of both non-sulphated and sulphated OEGNPEs on the number of oxyethylene groups, n, and on the volume fraction of 2-propanol, φ, in mobile phases consisting of CTAB, 2-propanol and water can be described by the equation [22]

$$\log k' = a_{0P} + a_{1P}n - (m_{0P} + m_{1P}n)\varphi \qquad (9)$$

where a_{0P}, a_{1P}, m_{0P} and m_{1P} are constants independent of n and φ and relate to 2-propanol as the component of the mobile phase.

Non-sulphated OEGNPEs cannot show ionic interactions with ionic modifiers and if a modifier such as CTAB contains a bulky non-polar part, it can affect the retention by modifying the polarity of the mobile phase and the properties of the stationary phase where it is sorbed in a similar way to the organic solvents in aqueous–organic mobile phases, so that the following equation can be assumed to apply:

$$\log k' = a_{0C} + a_{1C}n - (m_{0C} + m_{1C}n)c_M \qquad (10)$$

where c_M is the molar concentration of CTAB in the mobile phase and a_{0C}, a_{1C}, m_{0C} and m_{1C} are constants independent of n and c_M and relate to CTAB as the component of the mobile phase. (At the very low concentrations of ionic modifiers used in ion-pair reversed-phase chromatography, using molar concentrations is equivalent to but more convenient than working with volume fractions. Of course, the numerical values of a_{0C}, a_{1C}, m_{0C}, m_{1C} would be different when different concentration units are used.)

If the influence of the organic solvent on retention of non-sulphated OEGNPEs is independent of that of the ionic modifier, the following retention equation can be written to describe simultaneous effects of the two mobile phase additives:

$$\log k' = a_0 + a_1n - (m_{0P} + m_{1P}n)\varphi - (m_{0C} + m_{1C}n)c_M \qquad (11)$$

where m_{0P}, m_{1P}, m_{0C} and m_{1C} are constants of Eqs. 9 and 10 and relate to 2-propanol and CTAB, respectively, as the components of the mobile phase. The following relationships apply for the constants a_0 and a_1: $a_0 = a_{0P} + m_{0C}c_M = a_{0C} + m_{0P}\varphi$, $a_1 = a_{1P} + m_{1C}c_M = a_{1C} + m_{1P}\varphi$.

Unlike non-sulphated OEGNPs, their sulphated derivatives are affected primarily by ionic interactions with CTAB, which are assumed to be more important than the possible non-polar contribution of CTAB to the retention and, if the latter can be neglected, combination of Eqs. 8 and 9 results in the following relationship for the description of the dependence of the retention of sulphated OEGNPEs on the number of oxyethylene units, n, and concentrations of

CTAB, c_M, and 2-propanol, φ, in the mobile phase:

$$\log k' = a_0 + a_1 n - (m_{0P} + m_{1P} n)\varphi - \log\left(1 + Bc_M + \frac{C}{c_M}\right) \quad (12)$$

3. Experimental

Some experiments were performed using an M6000A pump, a U6K injector and an M440 UV detector operated at 254 nm (all from Waters, Milford, MA, USA), connected to a TZ 4241 line recorder and a CI 100 computing integrator (both from Laboratory Instrument Works, Prague, Czech Republic). An HP 1090M liquid chromatograph equipped with a UV diode-array detector, operated at 230 nm, an automatic sample injector, a 3DR solvent delivery system, a thermostated column compartment and a Series 7994A workstation was used for other experiments.

A stainless-steel column (300 × 3.8 mm I.D.) was packed in the laboratory with spherical octadecylsilica gel Silasorb SPH C_{18} (7.5 μm) (Lachema, Brno, Czech Republic) using a high-pressure slurry-packing technique.

Oligoethylene glycol nonylphenyl ethers (OEGNPEs) with various declared average stoichiometric ratios of oxyethylene units to nonylphenol were obtained from Servo (Delden, Netherlands) under the commercial names Serdox NNP 4, NNP 5 and NNP 8. Oligomeric anionic surfactants were prepared by sulphation of OEGNPEs and the products prepared contained both sulphated and non-sulphated oligomers. The samples were dissolved in the mobile phase in appropriate concentrations to yield good UV detector responses.

2-Propanol of spectroscopic grade was obtained from Lachema and CTAB from Serva (Heidelberg, Germany). Water was doubly distilled in glass with addition of potassium permanganate. All the solvents were filtered using a Millipore 0.45-μm filter and the mobile phases were prepared by mixing the components in the required ratios and degassed by ultrasonication before the use, or were prepared directly in the HP 1090M instrument from the components continuously stripped with a stream of helium.

Column dead volumes, V_M, were determined using methanol and ^2H_2O as dead volume markers and refractometric detection with an R 401 differential refractometer (Waters). The retention volumes, V_R, of the members of oligomeric series were measured at different mobile phase compositions. The mean values of V_R from three repeated experiments were used for calculations of the capacity factors, $k' = (V_R/V_M - 1)$, of the individual oligomers. The identification of the peaks was performed as discussed previously [19,22]. An Adstat software package and a 386 AT personal computer were used for linear and non-linear single- and multiple-parameter regression of the experimental sets of retention data as a function of the concentrations of the mobile phase components and of the number of oligomeric units.

4. Results and discussion

Sulphated OEGNPEs are not retained on a C_{18} column in mobile phases containing only 2-propanol and water and are eluted at the column dead volume in a single, unresolved peak, so that they can be separated from the parent non-sulphated oligomers, which are retained under these conditions. To make the separation of the individual sulphated oligomers possible, it is necessary to increase their retention by the addition of a cationic ion-pair reagent, such as CTAB. Experimental capacity factors of non-sulphated and sulphated OEGNPEs on a Silasorb SPH C_{18} column in aqueous–organic mobile phases with various concentrations of 2-propanol and CTAB are given in Tables 1 and 2, together with the values of k' calculated from Eqs. 11 and 12 fitted to the experimental data sets. The retention ($\log k'$) decreases regularly as the number of oxyethylene units in the oligomers increases, in agreement with earlier experiments on octylsilica and octadecylsilica columns [22]. The reversed order of elution of both sulphated and non-sulphated

Table 1
Capacity factors, k', of non-sulphated OEGNPEs with n oxyethylene units on a Silasorb SPH C_{18} (7.5 μm) column (300 × 3.8 mm I.D.) in mobile phases containing c_M mol/l CTAB and $\varphi \cdot 10^2$% (v/v) 2-propanol in water

n	Capacity factor[a]	$\varphi = 0.50$, $c_M = 0$	$\varphi = 0.50$, $c_M = 0.005$	$\varphi = 0.50$, $c_M = 0.02$	$\varphi = 0.50$, $c_M = 0.04$	$\varphi = 0.50$, $c_M = 0.08$	$\varphi = 0.35$, $c_M = 0.04$	$\varphi = 0.40$, $c_M = 0.04$	$\varphi = 0.45$, $c_M = 0.04$	$\varphi = 0.60$ $c_M = 0.04$
1	k'_e	3.69	3.47	3.14	2.81	2.16	9.76	6.46	4.24	1.30
	k'_c	3.63	3.51	3.18	2.78	2.13	9.22	6.18	4.15	1.25
2	k'_e	3.37	3.19	2.87	2.49	1.90	8.38	5.59	3.72	1.16
	k'_c	3.31	3.20	2.87	2.49	1.88	8.11	5.48	3.70	1.14
3	k'_e	3.06	2.88	2.58	2.20	1.65	7.18	4.85	3.27	1.03
	k'_c	3.02	2.91	2.60	2.24	1.66	7.14	4.85	3.29	1.03
4	k'_e	2.76	2.59	2.30	1.98	1.43	6.31	4.27	2.89	0.92
	k'_c	2.75	2.65	2.35	2.00	1.46	6.28	4.29	2.93	0.94
5	k'_e	2.52	2.37	2.08	1.76	1.26	5.54	3.76	2.57	0.83
	k'_c	2.51	2.41	2.12	1.80	1.29	5.53	3.80	2.61	0.85
6	k'_e	2.33	2.18	1.90	1.59	1.13	4.96	3.40	2.31	0.76
	k'_c	2.29	2.19	1.92	1.61	1.13	4.87	3.37	2.33	0.77
7	k'_e	2.14	2.01	1.75	1.43	1.02	4.48	3.11	2.11	0.69
	k'_c	2.09	1.99	1.74	1.45	1.00	4.28	2.98	2.08	0.70
8	k'_e	1.99	1.87	1.61	1.34	0.93	4.12	2.89	1.92	0.61
	k'_c	1.90	1.81	1.57	1.30	0.88	3.77	2.64	1.85	0.64

Column dead volume $V_M = 2.35$ ml.
[a] k'_e = Experimental capacity factors; k'_c = capacity factors calculated from the best-fit parameters of Eq. 11: $\log k' = 2.362 - 0.0671n - 3.523\varphi - 2.720c_M + 0.054\varphi n - 0.182c_M n$.

OEGNPEs is apparent from the shift of the maxima of the mass distribution to lower retention times with increasing nominal degree of polymerization in order Serdox NNP 4 — Serdox NNP 5 — Serdox NNP 8 in mobile phases containing 0.04 mol/l CTAB in 45% 2-propanol (Fig. 1).

Fig. 2 shows dependences of log k' of sulphated and non-sulphated OEGNPEs on the volume fraction, φ, of 2-propanol in aqueous–organic mobile phases containing 0.04 mol/l CTAB. The plots are well characterized by straight lines in the concentration range of 2-propanol investigated and the slopes of the individual oligomers within each series are very close to each other, which means that the oligomeric selectivity, α, is almost independent of the concentration of 2-propanol in the mobile phase. The values of α for the sulphated and non-sulphated OEGNPE series are very close to each other in a mobile phase of a given composition and the selectivity of separation of the individual oligomers increases slightly with decreasing concentration of 2-propanol in the mobile phase (Table 3). This is due to the same oxyethylene repeat structural unit in the two series. However, both the absolute values of k' and the slopes of the log k' versus φ plots are significantly higher with sulphated than with non-sulphated OEGNPEs. It has been demonstrated earlier [22] that the differences in the slopes, as characterized by the parameter m_{0p} in Eq. 9, increase with increasing size of the end-group in the oligomeric series. This is in agreement with the present experimental observations, as the end-group in sulphated OEGNPEs is much bulkier than that in the non-sulphated series, because it is contributed to not only by the sulpho group, but also by the associated bulky CTA^+ pairing cation.

The effect of the concentration of CTAB on the retention of sulphated OEGNPEs is very different from the effect on that of the non-sulphated parent series, as is demonstrated by the dependences of log k' on c_M in Figs. 3 and 4. The plots for non-sulphated oligomers in Fig. 3 show a linear decrease, in agreement with Eq. 10, much like the dependences of log k' on the

Table 2
Capacity factors, k', of sulphated OEGNPEs with n oxyethylene units on a Silasorb SPH C_{18} (7.5 μm) column (300 × 3.8 mm I.D.) in mobile phases containing c_M mol/l CTAB and $\varphi \cdot 10^2$% (v/v) 2-propanol in water

n	Capacity factor[a]	$\varphi = 0.50$, $c_M = 0.005$	$\varphi = 0.50$, $c_M = 0.02$	$\varphi = 0.50$, $c_M = 0.04$	$\varphi = 0.50$, $c_M = 0.08$	$\varphi = 0.40$, $c_M = 0.04$	$\varphi = 0.45$, $c_M = 0.04$	$\varphi = 0.60$, $c_M = 0.04$	$\varphi = 0.65$, $c_M = 0.04$
1	k'_e	–	–	7.85	6.61	26.72	14.37	2.58	1.48
	k'_c	6.36	9.04	8.24	6.31	25.84	14.59	2.63	1.48
2	k'_e	–	7.97	7.44	5.91	23.37	13.47	2.45	1.41
	k'_c	5.75	8.17	7.45	5.71	23.05	13.10	2.41	1.37
3	k'_e	4.83	7.57	6.76	5.23	20.53	12.15	2.26	1.28
	k'_c	5.19	7.39	6.73	5.16	20.55	11.76	2.21	1.26
4	k'_e	4.43	6.95	6.02	4.58	18.18	10.77	2.04	1.17
	k'_c	4.70	6.68	6.09	4.66	18.33	10.56	2.02	1.17
5	k'_e	4.09	6.30	5.41	3.99	15.95	9.54	1.85	1.08
	k'_c	4.25	6.04	5.50	4.22	16.34	9.48	1.85	1.08
6	k'_e	3.79	5.72	4.87	3.52	–	8.52	1.68	–
	k'_c	3.84	5.46	4.97	3.81	14.58	8.52	1.70	0.99
7	k'_e	3.59	5.24	4.42	3.16	–	7.65	1.56	–
	k'_c	3.47	4.93	4.50	3.44	13.00	7.65	1.56	0.92
8	k'_e	–	–	4.03	2.92	–	7.07	–	–
	k'_c	3.14	4.46	4.07	3.11	11.59	6.86	1.43	0.84
9	k'_e	–	–	3.71	2.57	–	6.33	–	–
	k'_c	2.84	4.03	3.67	2.82	10.34	6.16	1.31	0.78

Column void volume $V_M = 2.35$ ml.
[a] k'_e = Experimental capacity factors; k'_c = capacity factors calculated from the best-fit parameters of Eq. 12: $\log k' = 3.718 - 0.073n - 5.022\varphi + 0.059n\varphi - \log(1 + 15.379c_M + 0.0061/c_M)$.

volume fraction of 2-propanol in Fig. 2. This supports the idea that the role of CTAB in controlling the retention of non-ionic solutes in reversed-phase systems is principally based on modifying the polarity of the mobile phase and of the surface of the column packing material.

The agreement of the experimental capacity factors with the k' values calculated from Eq. 10 fitted to the experimental data proves suitability of this equation to describe the retention of non-sulphated OEGNPEs in the chromatographic system studied (the differences between the experimental and the calculated k' values exceed 5% relative for only three out of 72 values in Table 1 and the agreement for all the k' values is better than 10% relative). This precision of calculation allows unquestionable attribution of the calculated k' to the experimental peaks of the individual oligomers if the composition of the mobile phase is varied within the range investigated in this work.

As expected, the effect of the concentration of CTAB, c_M, on the retention of sulphated OEGNPEs is different from the effect on that of the parent non-sulphated oligomers. The plots of log k' of the individual oligomers show maxima in mobile phases containing approximately 0.02 mol/l ion-pairing reagent (Fig. 4). The points correspond to the experimental data and the curves were calculated using the best-fit parameters of the logarithmic form of Eq. 8. The differences between calculated and experimental k' values were 0.2 or less, i.e., the relative errors of the fitted data were less than 4%, which is comparable to the experimental errors in the determination of k' and demonstrates a good fit of Eq. 8 to the experimental data.

Such a maximum of retention as a function of c_M is predicted on the basis of the retention model described by Eqs. 8 and 12. Eq. 8 predicts no retention ($k' = 0$) for $c_M = 0$ and a maximum retention for $c_M = (K_{IM}b)^{-1/2}$. The occurrence of the maximum can be explained as follows: at low concentrations of CTAB, c_M, the concentration

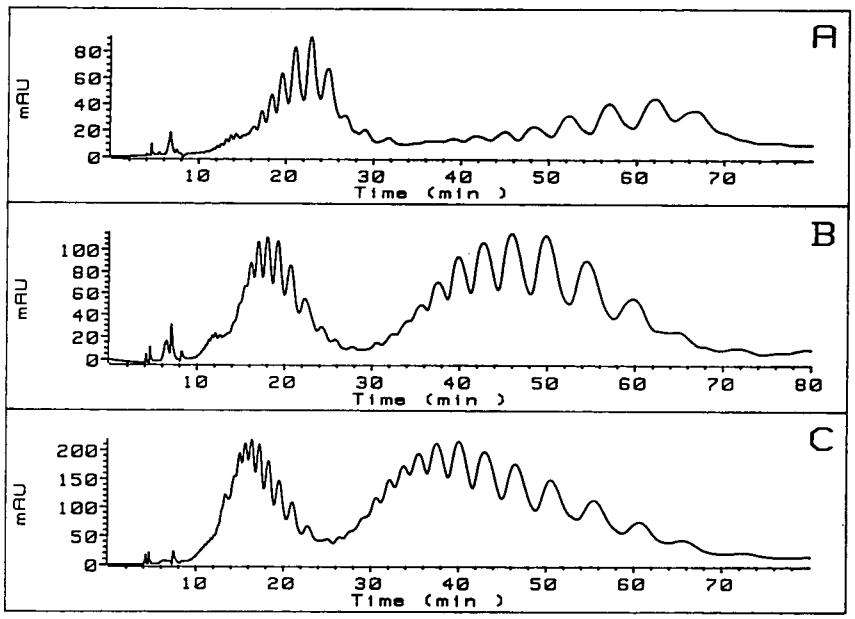

Fig. 1. Separation of partially sulphated samples of OEGNPEs with various nominal degrees of ethyoxylation, (A) Serdox NNP 4, (B) Serdox NNP 5 and (C) Serdox NNP 8, on a Silasorb C_{18} SPH (7.5 μm) column (300 × 3.8 mm I.D.) with aqueous–organic mobile phases containing 45% 2-propanol and 0.04 mol/l CTAB at a flow-rate of 0.5 ml/min. Detection, UV at 230 nm. The first group of peaks belongs to non-sulphated and the second group to sulphated OEGNPEs.

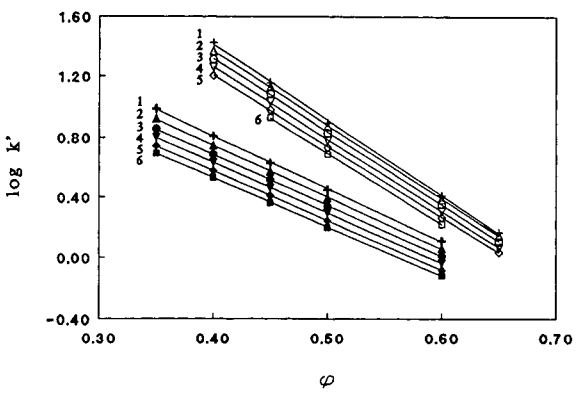

Fig. 2. Dependence of the retention (capacity factors, k') of non-sulphated (closed symbols) and sulphated (open symbols) OEGNPEs with various numbers of oxyethylene units (given by the numbers on the plots) on the volume fraction φ (10^{-2}% v/v of 2-propanol in aqueous–organic mobile phases containing 0.04 mol/l CTAB). Column as in Fig. 1. Points, experimental values; lines, dependences calculated from Eqs. 11 and 12 with the best-fit parameters.

of the ion-pairing reagent adsorbed in the stationary phase, c_S, increases approximately linearly with increase in c_M (steep part of the Langmuir isotherm) and the retention is enhanced because the amount of the sorbed ions of the analytes is proportional to the concentration of CTAB in the stationary phase. The increase of the amount of CTAB adsorbed with increase in c_M is less steep in the higher concentration range of CTAB, corresponding to the shallow part of the Langmuir isotherm, and its effect eventually becomes less important than the competition of CTA^+ cations in the mobile phase for the anionic solute, so that an increase in c_M causes a decrease in the retention.

The values of the parameters of Eq. 12 obtained from the best fit to the complete data set at various concentrations c_M and φ are given in Table 2, together with the capacity factors calculated using Eq. 12 and the best-fit parameters. The deviations of the calculated values from the experimental k' values are higher than those for the data obtained by fitting Eq. 8, because of an

Table 3
Parameters of the equation $\log k' = \log \beta + n\log \alpha$ for sulphated (series 1) and non-sulphated (series 2) OEGNPEs on a Silasorb SPH C_{18} (7.5 μm) column (300 × 3.8 mm I.D.) in aqueous mobile phases with various concentrations of 2-propanol (φ) and of CTAB (c_M)

c_M (mol/l)	φ (10^{-2}%, v/v)	Series 1			Series 2		
		Log β	Log α	R [a]	Log β	Log α	R [a]
0.005		0.778	−0.033	0.9968	0.578	−0.037	0.9985
0.02		0.985	−0.037	0.9984	0.538	−0.042	0.9986
0.04		0.949	−0.043	0.9984	0.487	−0.047	0.9979
0.08		0.870	−0.052	0.9985	0.379	−0.053	0.9971
	0.40	1.481	−0.056	0.9999	0.866	−0.059	0.9966
	0.45	1.217	−0.047	0.9974	0.671	−0.051	0.9983
	0.50	0.951	−0.043	0.9970	0.487	−0.047	0.9978
	0.60	0.460	−0.038	0.9970	0.154	−0.046	0.9986

[a] Correlation coefficient.

additional parameter, φ, included in Eq. 12, but are lower than 10% relative and the differences exceed 5% relative only for 10 values out of 57. This agreement suggests that Eq. 12 is suitable to describe the retention behaviour of sulphated OEGNPEs in the chromatographic system studied. As with non-sulphated OEGNPEs, the precision of calculation allows the calculated k' to be safely attributed to the experimental peaks in mobile phases with various concentrations of 2-propanol and CTAB (with the exception of the oligomers with 6–8 oxyethylene units in a mobile phase containing 0.08 mol/l of CTAB).

The fit of a retention equation to the set of experimental data alone does not prove the validity of the underlying theoretical model in the chromatographic system studied. However, there is some additional supporting evidence that can be extracted from the present experimental data.

The constants a and b of the Langmuir iso-

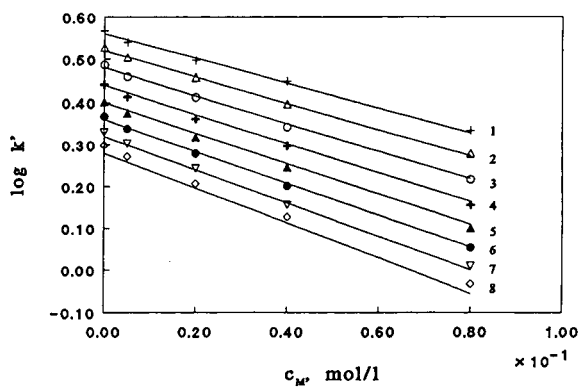

Fig. 3. Dependence of the retention (capacity factors, k') of non-sulphated OEGNPEs with various numbers of oxyethylene units (given by the numbers on the plots) on the molar concentration, c_M, of CTAB in aqueous–organic mobile phases containing 50% 2-propanol. Column as in Fig. 1. Points, experimental values; lines, dependences calculated from Eq. 11 with the best-fit parameters.

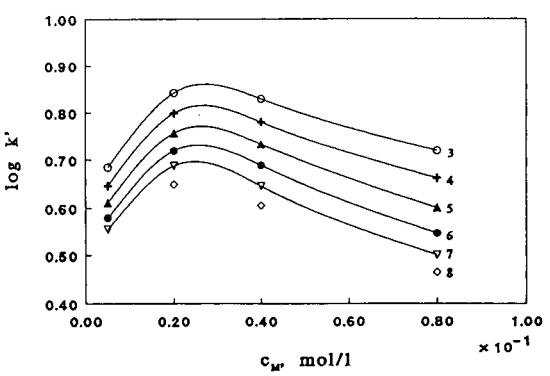

Fig. 4. Dependence of the retention (capacity factors, k') of sulphated OEGNPEs with various numbers of oxyethylene units (given by the numbers on the plots) on the molar concentration, c_M, of CTAB in aqueous–organic mobile phases containing 50% 2-propanol. Column as in Fig. 1. Points, experimental values; lines, dependences calculated from Eq. 8 with best-fit parameters.

therm are not expected to depend on the number of oxyethylene units in the molecule of the analyte. Further, as the distribution between the stationary and the mobile phases in reversed-phase systems is controlled principally by the polarity and size of the sample solutes, the number of oxyethylene units, n, is likely to affect much more significantly the equilibrium constant K_{IS} of the association of the sample anions with CTA^+ cations in the stationary phase than the equilibrium constant K_{IM} of the formation of ion pairs in the mobile phase, which is controlled by the electrostatic attraction forces and depends principally on the magnitude of the charges of the interacting ions. Consequently, the number of the oligomeric units, n, is expected to affect much more significantly the constant A of Eq. 8 than the parameters B and C. Also the concentration of 2-propanol in the mobile phase is likely to affect the equilibrium constant K_{IS} and the constant A more significantly than the constant K_{IM} or the constant b of the Langmuir isotherm and consequently the constants B and C of Eq. 8. The derivation of Eq. 12 is based on the above assumptions and it is possible to calculate the values of the constants K_{IM} and b from the parameters B and C of this equation. The present set of experimental data yielded the following values of the constants: $B = 15.4 \pm 2.6$, $C = 0.00605 \pm 0.00008$, $K_{IM} = 17 \pm 3$ and $b = 148 \pm 5$ l/mol. The constants B and C were calculated also from the experimental data sets for the individual oligomers and the calculated values were almost independent of the number of oxyethylene units, n. The value of b is in reasonable agreement with $b = 312$ l/mol ($a = 436$) determined by measuring the Langmuir sorption isotherm of CTAB on a C_8 column in 30% aqueous methanol, where the experimental data agreed with the values calculated from the Langmuir isotherm with relative errors between 1.4 and 5.4% in the CTAB concentration range $1 \cdot 10^{-3}$–$4 \cdot 10^{-3}$ mol/l [36].

The following supporting evidence for the validity of the assumptions accepted in the derivation of the present retention model can be found in the experimental data:

(1) Not only are the values of the oligomeric selectivities α in the non-sulphated and sulphated OEGNPE series in Table 3 very close to each other for mobile phases with a given concentration of 2-propanol, φ, but also the intercepts a_{1P} (0.067 and 0.073, respectively) and the slopes m_{1P} (0.054 and 0.059, respectively) of the dependences of log α on φ are almost identical in the two series (Tables 1 and 2). Also, the selectivities α in mobile phases with a given concentration of CTAB, c_M, are very similar for the sulphated and non-sulphated OEGNPE series (Table 3). This behaviour is possible only if the logarithmic term on the right-hand side of Eq. 12 and consequently the constants K_{IM} and b (and the parameters B and C) of Eq. 8 are independent of the number of oxyethylene units, n, and φ, otherwise the intercepts and slopes of the above dependences for the two series would have different values. On the other hand, the constant K_{IS} (Eq. 6) should depend on the concentration of 2-propanol, φ, and on the number of oxyethylene units, n, much in the same way as the distribution ratio (or the capacity factor) of non-sulphated OEGNPEs (especially in the quasi-linear part of the CTAB isotherm, where the ratio $[CTA]_S/[CTA]_M$ is constant), as both the K_{IM} and the distribution of non-sulphated oligomers are controlled mainly by the polarities of the stationary and mobile phases and by the size of the analytes. Consequently, the constant K_{IM} is contributed to by the parameters a_0, a_1, m_0 and m_1 of Eq. 14 essentially in the same way as k' of non-sulphated OEGNPEs by the constants a_{0P}, a_{1P}, m_{0P} and m_{1P}. Hence the similarity of the intercepts and slopes of the dependences of log α on φ is in agreement with the assumptions made in the derivation of the retention model.

(2) The logarithmic term in Eq. 12, $Y = \log(1 + Bc_M + C/c_M)$, calculated (a) from c_M and the constants B and C of Eq. 8 and (b) from the experimental k' and constants a_{0P}, a_{1P}, m_{0P} and m_{1P} have identical values within the limits of the experimental error (Table 4).

(3) The value of the term $a_0 - Y$ in Eq. 12 evaluated from the complete data set for the sulphated OEGNPEs ($3.72 - 0.25 = 3.47$, Tables 3 and 4) is in very good agreement with the value of the constant a_{0P} of Eq. 9 (3.46), calculated by fitting Eq. 9 to the limited data set acquired

Table 4
Comparison of the values of $Y = \log(1 + Bc_M + C/c_M)$ calculated (a) from c_M and the parameters B and C of Eq. 8 and (b) from the experimental k' and the parameters a_0, m_0, a_1 and m_1 of Eq. 12, $Y = a_0 + a_1 n - (m_0 + m_1 n)\varphi - \log k'$ [arithmetic means for various oligomers with different numbers of oxyethylene units, n, and concentrations of 2-propanol, φ (10^{-2}%, v/v), ± standard deviations] at various concentrations of CTAB in the mobile phase (c_M)

Parameter	c_M (mol/l)			
	0.005	0.02	0.04	0.08
Y (a)	0.36	0.21	0.25	0.36
Y (b)	0.37 ± 0.02 ($N = 5$)[a]	0.19 ± 0.02 ($N = 8$)[a]	0.25 ± 0.01 ($N = 35$)[a]	0.38 ± 0.02 ($N = 9$)[a]

[a] Number of calculated values of Y for different n and φ.

at a constant concentration of CTAB $c_M = 0.04$ mol/l.

(4) The concentration of CTAB at which the retention maxima occur, $c_M(\max)$, is independent of the number of oxyethylene units, n, in sulphated OEGNPEs (Fig. 4) and can be predicted from the parameters B and C of Eq. 12: $c_M(\max) = (C/B)^{1/2} = (K_{IM}b)^{-1/2} = 0.0198$ mol/l. This behaviour obviously follows from the independence of K_{IM} and b of the number of oxyethylene units assumed in the derivation of the retention model.

The selectivity of separation of the individual oligomers in both the sulphated and non-sulphated OEGNPE series increases very slightly with increasing concentration of CTAB and with decreasing concentration of 2-propanol in the mobile phase, and the absolute retention of non-sulphated OEGNPEs increases with decreasing concentrations of both CTAB and 2-propanol (Table 3). Because the absolute retention of sulphated OEGNPEs decreases with increasing concentration of 2-propanol, but shows a maximum at 0.02 mol/l CTAB, the best separation of the groups of sulphated and non-sulphated OEGNPEs and simultaneously good resolution of the individual oligomers in the two groups can be accomplished with mobile phases containing CTAB at a slightly higher concentration than that yielding maximum retention (i.e., 0.03–0.04 mol/l) and as low a concentration of 2-propanol as is acceptable from the point of view of the time of analysis (40–45%, v/v). Under these conditions, the separation of both sulphated and non-sulphated OEGNPEs in a sample mixture is possible in a single run on a C_{18} column, such as in the examples shown in Fig. 1.

The group of non-sulphated OEGNPEs is eluted in 30 min under these conditions. As the contents of the lower oligomers decrease with increasing nominal degree of ethoxylation, the maxima of the molecular mass distributions of both sulphated and non-sulphated OEGNPEs are shifted to lower elution volumes (compare Fig. 1A and C), so that distinct resolution of the two groups is possible without significant overlapping for mixtures containing oligomers with up to 12–13 oxyethylene units. To separate mixtures of higher oligomers, the concentration of 2-propanol in the mobile phase can be decreased, but at the cost of longer separation times.

The efficiency of separation is not very high in this example, probably because of the viscosity of the mobile phase used, but it could be possibly increased with a more efficient column, if the pressure limits allow its use. Unfortunately, using less viscous organic modifiers (e.g., methanol or acetonitrile) and tetraalkylammonium salts with shorter alkyl chains failed to improve the separation because the selectivity of separation of the individual oligomers was very low in these mobile phases.

5. Conclusions

The theoretical prediction of the retention of non-ionic oligomers such as OEGNPE surfactants with different degrees of polymerization

can be extended to aqueous–organic mobile phases containing an ion-pairing reagent, the effect of which is similar to that of the concentration of the organic solvent in the mobile phase: it modifies the polarities of the mobile and stationary phases in the chromatographic system used. In these systems, it is possible to calculate the retention (k') as a function of three variables: the number of oligomeric units and the concentrations of the organic solvent and of the ion-pairing reagent in the mobile phase. The ion-pairing reagent does not affect significantly the separation selectivity of the individual oligomers and these calculations would not be of practical value if only non-ionic oligomers are separated, but predictions of this type are potentially useful when mixtures containing both ionic and non-ionic surfactants are chromatographed, as the addition of an ion-pairing reagent is necessary for separations of anionic surfactants.

Cationic ion-pairing reagents with long alkyl chains affect the retention of anionic surfactants in two different ways: the sorption of the large ion-pairing cations on the surface of the stationary phase enhances the sorption of anionic solutes in the form of ion associates at low concentrations of the ion-pairing reagents, whereas at high concentrations the competition of ion-pairing cations in the mobile phase for anionic solutes predominates and decreases the retention. Consequently, maximum retention is observed at a certain concentration of the ion-pairing reagent in the mobile phase. The effect of the concentration of the organic solvent in the mobile phase on the retention of anionic surfactants is similar to that with the non-ionic parent compounds. The retention behaviour of anionic surfactants as a function of the number of oligomeric units and of the concentrations of both the ion-pairing reagent and of the organic solvent in the mobile phase can be described by a simple equation.

Simultaneous separations of the individual sulphated and non-sulphated OEGNPE oligomers can be accomplished on a C_{18} column with mobile phase containing 2-propanol and CTAB in water. The concentrations of 2-propanol and CTAB in the mobile phase can be selected on the basis of the model retention equations to optimize the retention and the selectivity of separation of the individual oligomers. For this purpose, a mobile phase containing 0.04 mol/l CTAB in 45% 2-propanol was found to be the most suitable.

The possibilities of separating sulphated and non-sulphated OEGNPEs on columns packed with silica gel and polar bonded stationary phases will be discussed elsewhere [37].

Acknowledgement

This publication is based on work under Project No. 203/94/1397 sponsored by the Grant Agency of Czech Republic.

References

[1] F.P.B. Van der Maeden, M.E.F. Biemond and P.C.G.M. Janssen, *J. Chromatogr.*, 149 (1978) 539.
[2] M. Ahel and W. Giger, *Anal. Chem.*, 57 (1985) 1577 and 2584.
[3] E. Kunkel, *Tenside Deterg.*, 18 (1981) 301.
[4] A.M. Rothman, *J. Chromatogr.*, 253 (1982) 283.
[5] R.E.A. Escott, S.J. Brinkworth and T.A. Steedman, *J. Chromatogr.*, 282 (1983) 655.
[6] J.A. Pilc and P.A. Sermon, *J. Chromatogr.*, 398 (1987) 375.
[7] I. Zeman, *J. Chromatogr.*, 363 (1986) 223.
[8] K. Levsen, W. Wagner-Redeker, K.H. Schäfer and P. Dobberstein, *J. Chromatogr.*, 323 (1985) 135.
[9] R.H. Schreuder and A. Martin, *J. Chromatogr.*, 435 (1988) 73.
[10] M.S. Holt, E.H. McKerrell, J. Perry and R.J. Watkinson, *J. Chromatogr.*, 362 (1986) 419.
[11] I. Zeman, M. Bareš and J. Šilha, *Tenside Deterg.*, 23 (1986) 181.
[12] W.R. Melander, A. Nahum and Cs. Horváth, *J. Chromatogr.*, 185 (1979) 129.
[13] R.M. Cassidy, *J. Liq. Chromatogr.*, 1 (1978) 241.
[14] J.N. Alexander, M.E. McNally and L.B. Rogers, *J. Chromatogr.*, 318 (1985) 289.
[15] T. Takeuchi, S. Watanabe, N. Kondo, M. Goto and D. Ishii, *Chromatographia*, 25 (1988) 523.
[16] R.E.A. Escott and M. Mortimer, *J. Chromatogr.*, 553 (1991) 423.
[17] S. Brossard, M. Lafosse and M. Dreux, *J. Chromatogr.*, 591 (1992) 149.
[18] P. Jandera, *Chromatographia*, 26 (1988) 417.
[19] P. Jandera, J. Urbánek, B. Prokeš and J. Churáček, *J. Chromatogr.*, 504 (1990) 297.

[20] H. Yoshimura, T. Sugiyama and T. Nagai, *J. Am. Oil Chem. Soc.*, 64 (1987) 550.
[21] A. Nakae and K. Tsuji, *J. Com. Exp. Deterg.*, 14 (1983) 133.
[22] P. Jandera, *J. Chromatogr.*, 449 (1988) 361.
[23] Y. Mengerink, H.C.J. DeMan and S. van der Wal, *J. Chromatogr.*, 552 (1991) 593.
[24] T. Austad and I. Fjelde, *Anal. Lett.*, 25 (1992) 957.
[25] F. Smede, J.C. Kraak, C.F. Werkhoven-Goewie, U.A.Th. Brinkman and R.W. Frei, *J. Chromatogr.*, 247 (1982) 123.
[26] P. Jandera, *J. Chromatogr.*, 314 (1984) 101.
[27] P. Jandera, *J. Chromatogr.*, 449 (1988) 361.
[28] P. Jandera and J. Rozkošná, *J. Chromatogr.*, 362 (1986) 325.
[29] J.-G. Chen, S.G. Weber, L.L. Glavina and F.F. Cantwell, *J. Chromatogr. A*, 656 (1993) 549.
[30] E. Tomlinson, T.M. Jefferies and C.M. Riley, *J. Chromatogr.*, 159 (1978) 281.
[31] J.H. Knox and R.A. Hartwick, *J. Chromatogr.*, 204 (1981).
[32] B.A. Bidlingmeyer, S.N. Deming, W.P. Price, B. Sachok and M. Petrusek, *J. Chromatogr.*, 186 (1979) 419.
[33] J. Stranahan and S.N. Deming, *Anal. Chem.*, 54 (1982) 2251.
[34] J. Stahlberg, *J. Chromatogr.*, 356 (1986) 231.
[35] F.F. Cantwell, *J. Pharm. Biomed. Anal.*, 2 (1984) 153.
[36] J. Fischer and P. Jandera, in preparation.
[37] P. Jandera, J. Urbánek, B. Prokeš and H. Blažková-Brúnová, in preparation.

ELSEVIER

Journal of Chromatography A, 689 (1995) 269–273

JOURNAL OF CHROMATOGRAPHY A

High-performance liquid chromatography of cyanine dyes Multiphase separation, purification, and substitution of the counter ion

D.L. Akins*, V.T. Kumar

Center for Analysis of Structures and Interfaces, Department of Chemistry, The City College, The City University of New York, New York, NY 10031, USA

First received 17 December 1993; revised manuscript received 30 August 1994

Abstract

Multiphase ion-pair chromatography is described for the separation of a mixture of cyanine dyes using CN and C_{18} stationary phases. Radial compression cartridges were combined to form the desired selectivity sequence and to improve chromatographic resolution. Also described is a method for the purification of 1,1′-diethyl-4,4′-cyanine iodide using lithium perchlorate as the ion-pairing agent, as well as a method for substitution of the dye's counter ion with another anion to increase solubility. The relevance of these studies to optical spectroscopy of adsorbed cyanines is also discussed.

1. Introduction

Adsorbed cyanine dyes, in the form of monomers as well as aggregates, have traditionally been used as spectral sensitizers in color photography [1,2], and in recent years have found increasing applications in optical recording devices [3,4] and as non-linear materials [5–8]. Today, the aggregation phenomenon itself is an area of active research, both in terms of understanding the structure of aggregates [9] as well as utilization of the altered spectral and dynamical properties that monomeric species experience in the aggregate environment [8].

The cyanine dyes used in the present study are those whose Raman, UV–Vis absorption and fluorescence spectra, as well as photodynamical properties on a variety of substrates (metal surfaces, vesicle, and colloidal metals) are being investigated in our laboratory, both individually and in presence of other dyes [10,11]. In general, cyanine dyes have two nitrogen heterocyclic rings joined by a conjugated chain of carbon atoms [12]. Table 1 shows the structures of the dyes used in the present study.

We have found that published methods for the HPLC of dyes generally focus on other classes of dyes. As a result, we have found it necessary to develop methods for the separation and analysis of mixtures of cyanine dyes. We have also explored the use of chromatography to improve the purity of commercially purchased cyanine dyes, and to change the counter ion (which in most commercial samples of cyanines is the iodide ion) with the aim of enhancing the dye's solubility in water. Techniques reported here for

* Corresponding author.

0021-9673/95/$09.50
SSDI 0021-9673(94)00849-3

Table 1
Dyes studied

Dye			Capacity factor	
No.	Name	Structure	CN	C_{18}
1	3,3′-Dihexyloxacarbocyanine iodide	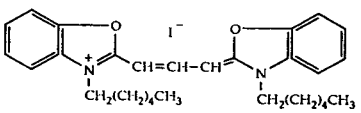	3.25	2.13
2	3,3′-Diethyloxacarbocyanine iodide	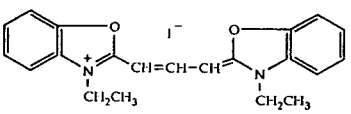	3.88	1.76
3	3,3′-Diethylselenacarbocyanine iodide	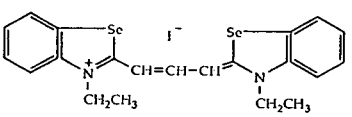	4.18	1.77
4	3,3′-Diethylthiadicarbocyanine iodide	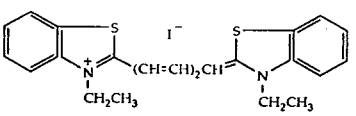	4.27	1.92
5	3,3′-Diethylthiatricarbocyanine iodide	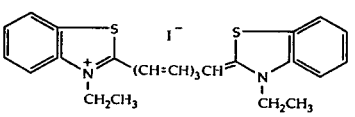	4.30	2.12
6	1,1′-Diethyl-4,4′-cyanine iodide	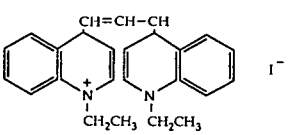	4.60	2.60

replacing the iodide involve a modification of the purification procedure that is advanced as well as application of some non-chromatographic methods.

In this paper we explore the use of octadecylsilane (C_{18}) and cyano (CN) columns for the separation of mixtures of cyanine dyes. We have found, in general, that dyes which are members of the same vinylogous series are easier to separate on the C_{18} column, but remain completely unresolved on the CN column. Also, cyanine dyes in which the heteroatom is varied (e.g., O, S or Se atom), with other structural features unchanged, are found to be better resolved on the polar CN column. Thus a combination of these two stationary phases was expected to lead to better resolution of a mixture of such cyanines. Hence, we joined radial compression cartridges to form the desired selectivity capability. The wide availability of commercial

cartridges allows multiphase chromatography to be performed with minimal changes in instrument setup.

2. Experimental

2.1. Instrumentation

The chromatographic system used is manufactured by Shimadzu (Kyoto, Japan). It consists of two LC-10AD pumps, a SPDM6A photodiode array UV–Vis detector and Nova-Pak CN HP and Nova-Pak C_{18} (100 mm × 8 mm, 4 μm particle size) radial compression cartridges from Waters (Wayland, MA, USA). All experiments were conducted at room temperature (22–25°C).

2.2. Reagents

Cyanine dyes (see Table 1), methanol, methanesulfonic acid, sodium methanesulfonate, *tert.*-butyl methyl ether and methylene chloride were from Aldrich (Milwaukee, WI, USA). Lithium perchlorate was from Ventron (Beverly, MA, USA). All aqueous solutions were made using distilled deionized water.

2.3. Separation of cyanine dyes

Methanol containing 0.002 *M* sodium methanesulfonate was used as the mobile phase. The stationary phase was either CN, C_{18} or a combination of the two. The order of coupling of the cartridges was CN followed by C_{18}. Reversing the order had no effect on the chromatogram. Samples of 20 μl containing nanomolar concentration (ca. 2 nmol) of each dye in pure methanol were injected. A mobile phase flow-rate of 1.0 ml/min was used.

2.4. Purification of 1,1′-diethyl-4,4′-cyanine iodide

The CN cartridge was used in this procedure. The mobile phase was 0.01 *M* lithium perchlorate in methanol, with a flow-rate of 2.0 ml/min. Samples of 0.5 ml containing ca. 0.13 mg of 1,1′-diethyl-4,4′-cyanine iodide in pure methanol were injected. Several fractions containing the dye were combined. The solvent was evaporated under vacuum. The cyanine dye in the residue was extracted using several small portions of methylene chloride, leaving insoluble lithium perchlorate. The methylene chloride solution of the dye was filtered through a sintered glass funnel and concentrated by evaporation. *tert.*-Butyl methyl ether was added to precipitate the dye. The precipitate was centrifuged, washed with more *tert.*-butyl methyl ether and dried in a vacuum oven at 50°C for 30 min. The purity of the dye was calculated from absorbance measurements.

2.5. Substitution of the counter ion

The methylene chloride solution in the above procedure which contained the perchlorate salt of the dye was shaken with a saturated aqueous solution of potassium chloride. The methylene chloride layer was washed with distilled water, dried over anhydrous calcium chloride and filtered through sintered glass. The chloride form of the dye was precipitated by adding *tert.*-butyl methyl ether as in the above procedure.

It might be noted that in the case of 1,1′-diethyl-2,2′-cyanine iodide [also known as pseudoisocyanine (PIC); structure not shown in Table 1], switching the counter ion was easily accomplished without the use of chromatography, due to the high purity of commercial samples. This particular dye is of interest because it is the one most studied in the literature. Its structure is quite similar to that of its 4,4′-cyanine isomer, with the methine linkage occurring at the 2-positions, adjacent to the nitrogen heteroatoms.

For this latter dye, sodium perchlorate was added to the aqueous solution, leading to precipitation of the dye perchlorate. The precipitate was washed with distilled water and dissolved in methylene chloride. The methylene chloride solution was mixed with a saturated potassium chloride solution to substitute the perchlorate with chloride. The remainder of the procedure was identical to that above.

3. Results and discussion

Capacity factors determined for each dye are listed in Table 1. Some of the dyes that have essentially the same capacity factor on the CN column have different values on the C_{18} column, and vice versa. For instance dyes **4** and **5** are unlikely to separate on the CN column under the present conditions. The only difference between the two structures is the length of the polymethine chain joining the heterocyclic rings. This structural difference, however, allows their separation on the C_{18} column. Likewise, dyes **2** and **3** are expected to elute together on the C_{18} column; the oxygen and selenium atoms on the five-membered rings have little influence on retention of the dye on the C_{18} stationary phase. However, these dyes should separate easily on the CN column. Figs. 1 and 2 show chromatograms of a mixture of these on CN column and C_{18} column, respectively. Numbers on the peaks correspond to the numbering of the dyes in Table 1. The identity of the components in each peak was established by comparing the spectrum of the peak species with the spectra of individual dyes. The order of elution and overlapping of peaks in both chromatograms are well in agreement with the data in the table. Combination of the two stationary phases clearly improves separation, as shown in Fig. 3. The iodide counter ion present in all these samples is unretained and can be monitored using UV detection. The identity of this peak was established using the starch test [13].

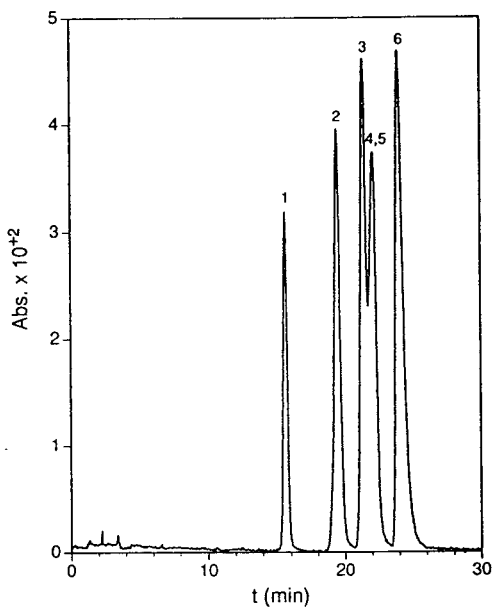

Fig. 1. Chromatogram of the mixture of cyanines using CN stationary phase. Mobile phase: methanol containing 0.002 *M* sodium methanesulfonate. Flow-rate: 1.0 ml/min. $\lambda = 350$–600 nm. Sample: 20 μl solution in methanol containing 0.14, 0.14, 0.28, 0.32, 0.46 and 0.44 μg of dyes **1**, **2**, **3**, **4**, **5** and **6**, respectively. Numbers on the peaks correspond to the numbering of dyes in Table 1.

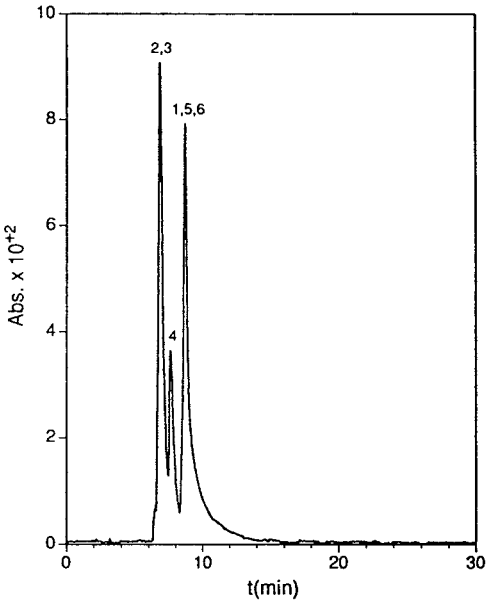

Fig. 2. Chromatogram of the mixture of cyanines using C_{18} stationary phase. Conditions and sample as in Fig. 1.

The commercial sample of 1,1′-diethyl-4,4′-cyanine contained 91.8% dye as determined using its literature reported molar extinction coefficient in methanol of value $8.8 \cdot 10^4\ M^{-1}\ cm^{-1}$ [14]. The purified product contained 96.5% dye. The yield was ca. 60%, some of the dye being lost due to adsorption on the drying agent. The perchlorate counter ion of the dye is easily changed to the chloride when the dye in methylene chloride solution is mixed with a saturated solution of potassium halide. The switching of the counter ion was confirmed by testing with

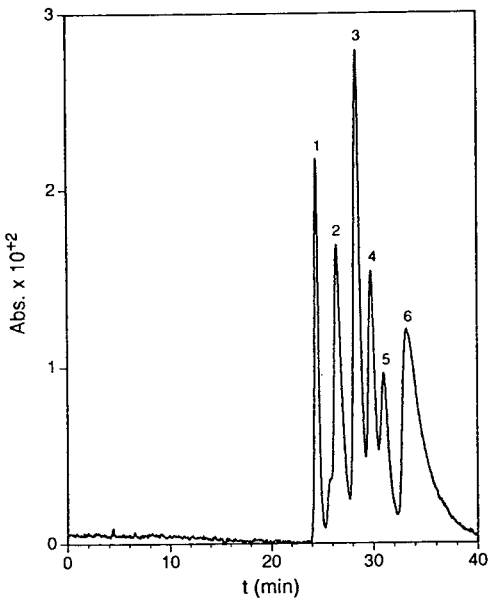

Fig. 3. Chromatogram of the mixture of cyanines on CN–C_{18} multiphase. Conditions and sample as in Fig. 1.

silver nitrate solution. Also, the product was highly soluble in water, unlike the perchlorate form of the dye.

4. Conclusions

Multiple stationary phases can take advantage of the different structural characters of cyanine dyes to accomplish the separation of mixed cyanine samples; however, if the order of elution is different in the two columns the resolution can be adversely affected. The purification procedure described here can be used to enhance dye purity of commercial samples. After chromatography, the perchlorate counter ion of the dye in methylene chloride can be exchanged if mixed with a saturated solution of potassium halide. We find that for 1,1′-diethyl-2,2′-cyanine, a dye which is the focus of many studies in our laboratory, this latter step is a quick and inexpensive way to switch the counter ion without the use of ion-exchange columns (as is often required).

Acknowledgement

Support for this research by the National Science Foundation (NSF) under Grant RII-8802964 is gratefully acknowledged.

References

[1] F.M. Hamer, *The Cyanine Dyes and Related Compounds*, Wiley, New York, 1964.
[2] D.M. Sturmer and D.W. Haseltine, in T.H. James (Editor), *The Theory of the Photographic Process*, Macmillan, New York, 1977, Ch. 8, p. 194.
[3] N. Hiroyuki, *J. Soc. Dyers Colour.*, 104 (1988) 121.
[4] C. Ishimoto, H. Tomimuro and J. Seto, *Appl. Phys. Lett*, 49 (1986) 1677.
[5] E. Hanamura, *Phys. Rev. B*, 37 (1988) 1273.
[6] H. Ishihara and K. Cho, *Phys. Rev. A*, 42 (1990) 1724.
[7] F.C. Spano and S. Mukamel, *Phys. Rev. A*, 40 (1989) 5783.
[8] Y. Wang, *Chem. Phys. Lett.*, 126 (1986) 209.
[9] D.L. Smith, *Photogr. Sci. Eng.*, 18 (1974) 309.
[10] D.L. Akins, J.W. Macklin and H.R. Zhu, *J. Phys. Chem.*, 26 (1992) 4515.
[11] D.L. Akins, S. Ozcelik and J.Q. Liu, presented at the *1994 The Pittsburgh Conference, Chicago, IL, 1994*, abstract 986.
[12] G.E. Ficken, in K. Venkataraman (Editor), *The Chemistry of Synthetic Dyes*, Academic Press, New York, 1971, Ch. 5, p. 212.
[13] G. Svehla, *Vogel's Qualitative Inorganic Analysis*, Wiley, New York, 1987, Ch. 4, p. 180.
[14] L.G.S. Brooker, F.L. White, R.H. Sprague, S.G. Dent, Jr. and G. Van Zandt, *Chem. Rev.*, 41 (1947) 325.

ELSEVIER

Journal of Chromatography A, 689 (1995) 275–284

JOURNAL OF CHROMATOGRAPHY A

Applications of multiplex gas chromatography to the determination of organics in solid samples

Minquan Zhang*, John B. Phillips[1]

Department of Chemical Engineering, Xinjiang Institute of Technology, Urumqi, Xinjiang 830008, China

First received 7 June 1994; revised manuscript received 1 September 1994

Abstract

A multiplex gas chromatographic technique for determining nicotine in cigarettes is described and multiplex gas chromatograms of volatiles from other solid samples are also presented. Direct headspace sampling, which is carried out in a sampler modified from an injector, provides a continuous gas sample stream for multiplex gas chromatography. Volatiles evaporating from the sample are picked up and carried by a carrier gas to a thermal desorption modulator and column. Concentrations to be determined are modulated by the modulator. The thermal desorption modulator is a short section at the head of the capillary column. The modulator section is coated externally with a thin electrically conductive film. An electrical current pulse applied to the thin film heats the modulator section and the stationary phase within it. When the stationary phase is heated and cooled, it releases and adsorbs substances into and from the flowing carrier gas. The signal form resembles a derivative of a chromatographic injection. Large-volume, continuously flowing or headspace samples can be accepted directly. The modulator is simple and effective and is used as both a trap and desorption device. Multiple modulation pulse signals applied during an extended sample introduction period result in a multiplex detector output signal, from which the chromatograms are recovered and computed by applying some fairly simple computational techniques such as cross-correlation. It is possible to determine volatiles in solid samples where the solid material is neither volatile nor soluble in a solvent. No sample pretreatment, preconcentration, extraction or distillation are required. Both the accuracy and precision achieved are fairly good.

1. Introduction

There are many techniques for analysing liquid and solid samples, one of the most attractive being gas chromatographic headspace analysis [1]. By using this method, information on volatiles present in samples can be obtained. When the samples are liquids, it is easy to reach a thermodynamic equilibrium between the volatiles to be determined and the samples. Also, it is easy to obtain quantitative results. However, when solid samples are to be analysed, it is difficult to reach thermodynamic equilibrium between volatiles and solid samples, and quantitative analysis is more difficult. In this case, liquid solvents are often used to extract the volatiles from the matrix, followed by their determination. To achieve complete extraction,

* Corresponding author.

[1] Present address: Department of Chemistry and Biochemistry, Southern Illinois University, Carbondale, IL 62901, USA.

0021-9673/95/$09.50
SSDI 0021-9673(94)00858-2

sometimes multiple extractions are needed, which, however, results in very dilute extracts that cannot be concentrated by evaporation because the volatiles are to be determined. Kolb and co-workers [2–4] used a method called discontinuous gas extraction or multiple headspace extraction to solve this problem. However, some disadvantages still exist, e.g., often an incorrect linear relationship is obtained for log (analyte concentration) vs. analysis number for repeated analyses of the same sample, and the method is time consuming. A dynamic headspace technique or gas–solid extraction was proposed as a solution to these problems [5]. Its main advantage is that no equilibrium between the gas phase and sample is needed, but the problem is that the volatiles are split away from splitter vent, although all of them can be released from the sample.

Recently, we have developed a new technique, multiplex gas chromatography (MGC) with thermal desorption modulation of a fused-silica capillary column [6]. We have reported on the utilization of MGC with rapid concentration to determine trace organics in aqueous samples at below the ppb (v/v) level [7].

In this paper, we describe the use of MGC with direct headspace sampling (DHS) to determine organics in solid samples. As an example, we determined nicotine in cigarettes by this technique. Chromatograms for various other samples have also been obtained. Previously used methods to determine nicotine in smoke involved steam extraction [8], acid–methanol extraction, extraction and subsequent titration [9], steam distillation [10,11], gas chromatographic determination [12] and spectrophotometric determination [13]. Most of the steps in these methods are time consuming and cause some loss of components of interest. In MGC analysis, only a small amount of sample is needed. Prior to analysis, no extra procedure is needed. By using DHS, a continuous gas sample stream can be obtained, which is required in MGC. A concentration pulse generated from modulators which is equivalent to a small-volume injection is of appropriate volume for the column and no extra interfaces are needed. Hence the drawbacks that parts of volatiles are split away or some components of interest are lost can be circumvented. Also, in MGC a series of concentration signals are generated resulting in enhancement of the signal-to-noise ratio due to the multiplex and throughput advantages.

2. Experimental

2.1. Apparatus

The experimental system, is shown in Fig. 1. The experiments were performed on a Model 3920 gas chromatograph (Perkin-Elmer) equipped with a flame ionization detector. The chromatograph was modified as previously reported for MGC [7]. A make-up gas stream was added to sweep the sample emerging from the column to the detector. The laboratory computer system and data acquisition interface between the computer and the chromatograph and the electronic circuitry have been described elsewhere [6].

In these experiments, the injector was modified to be used as a direct headspace sampler for GC. The analytical columns were a Supelcowax 10 fused-silica open-tubular column (25.0 m × 0.250 mm I.D., stationary phase thickness 0.25 μm), an SE-52 fused-silica open-tubular column (6.0 m × 0.250 mm I.D., stationary phase thickness 0.20 μm) and OV-1701 fused-silica open-tubular column (1.0 m × 0.050 mm I.D., stationary phase thickness 0.20 μm). The modulator, which was coated with electrically conductive paint, was 8.0 cm long and its resistance was 2.0 Ω. Its design, shown in Fig. 1B, has been described previously [6]. The modulator was situated outside the oven and kept at room temperature. The computer was used to control the modulator current from a 40 V d.c. power supply using an OPTO 22 (Huntington Beach, CA, USA) Model ODC 5P optically coupled switch. The duration of the current pulse was 120 ms. A 10-Ω resistor was connected in series with the modulator to limit the magnitude of the current through the modulator. In order to

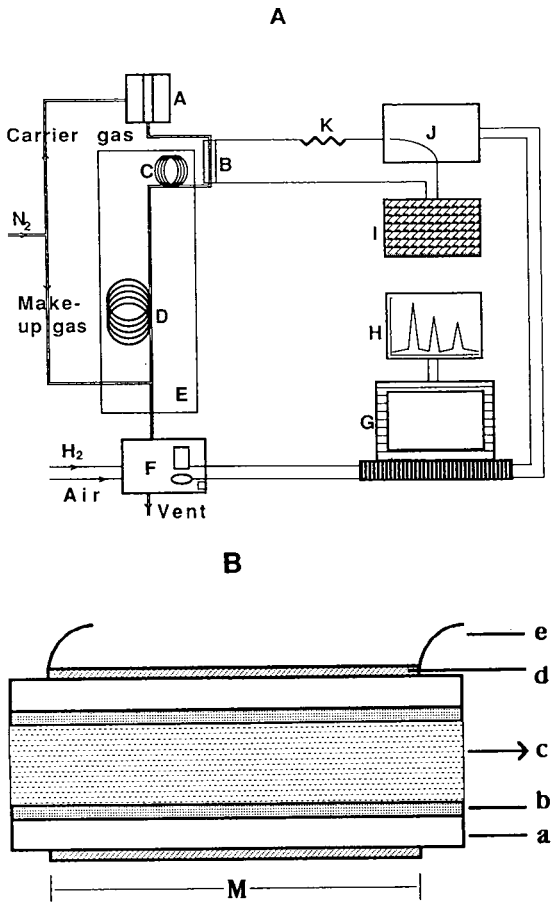

Fig. 1. (A) Schematic diagram of the main components of the multiplex gas chromatographic system. A = Sampler; B = modulator; C = retention gap; D = Supelcowax 10 analytical column; E = oven; F = detector; G = computer; H = plotter; I = power supply; J = electronic switch; K = resistor. (B) Design of thermal desorption modulator prepared on a fused silica open-tubular column. M = Modulator section; a = fused-silica column; b = stationary phase; c = gas stream flow; d = electrically conductive paint; e = electrical contacts.

eliminate peak broadening and peak distortion, a retention gap (an empty fused-silica column, 50 cm × 0.250 mm I.D.) was used ahead of the analytical column. On the other hand, there was no space between the oven and modulator port in order to eliminate peak broadening and to prevent larger molecules from being held in the insulation space.

2.2. Materials

Richland cigarettes (Brown and Williamson Tobacco) purchased from a supermarket were used as the main solid samples. Nicotine (reagent grade) was obtained from Fisher Scientific. The carrier gas was prepurified-grade nitrogen. Hydrogen was obtained from Air Products (Alltown, PA, USA). Soil was taken from the campus. Plastic wrappers for bread and plastic bags originated from a supermarket.

2.3. Procedures

The MGC conditions are given in the figure captions. HDS was carried out in the sampler modified from an injector as illustrated in Fig. 2. A glass tube (12 cm × 5.0 mm I.D.) was installed within the injector. Liquid samples could be placed in the bottom of capillary tubes, which were then inserted into the glass tube. Solid samples were placed in the middle of a smaller glass tube (open at both ends), which was then also inserted into the glass tube. A capped capillary tube or smaller tube containing a num-

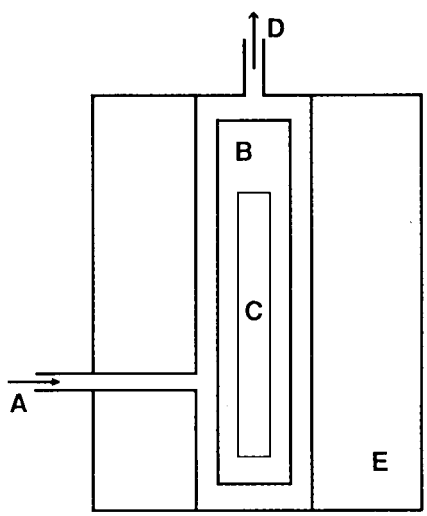

Fig. 2. Direct headspace sampler for MGC. A = Carrier gas inlet; B = glass tubing; C = capillary tube; D = to modulator; E = injector wall.

ber of samples was equilibrated in the sampler for about 5–10 min (it takes slightly longer for liquid samples), then its cap was removed, the capillary tube or the smaller glass tube was inserted and the whole sampler was quickly installed. Generally, the time depends on the state, the properties and the quality of the samples.

By varying the capillary diameter and length or sampler temperature, the sample evaporation rate was adjusted.

We employed the equation $S = x\rho\pi r^2/2L$ [14] to measure S, the diffusion rate of liquids (g/s). Of course, we should obtain x (a constant for the liquid at temperature T, cm/s) before S. In order to obtain x, a plot of L^2 vs. time was made, so a series of L values (depth of the liquid meniscus below the capillary mouth, cm) were measured in an oven with the same temperature as in the MGC sampler at different times. The results are given in Table 1. A plot of L^2 vs. time is shown in Fig. 3.

By MGC, a series of multiplex gas chromatograms of nicotine external standard were obtained. The peak area counts could be plotted against the corresponding concentrations of nicotine calculated from the above equation.

Cigarette samples were placed in the sampler, MGC was run and different chromatograms were obtained as different parts of the cigarettes were tested. The tests on unsmoked cigarettes were repeated at least five times.

After adding a series of nicotine standards to unsmoked cigarettes, MGC was run, giving chromatograms to identify and recover the nicotine.

Multiplex gas chromatograms of other solid samples were also obtained.

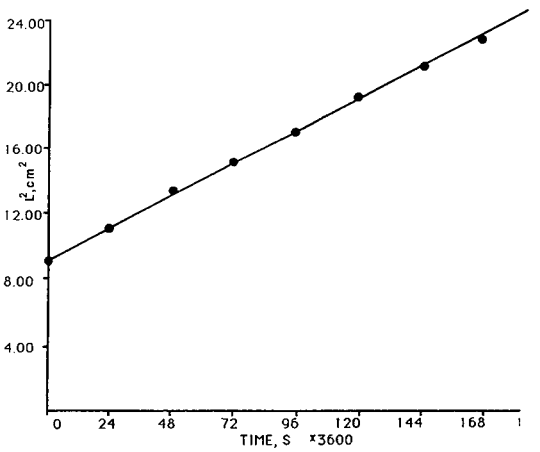

Fig. 3. Plot of L^2 versus time. L = Depth of the liquid meniscus below the capillary mouth; time = corresponding diffusion time of the liquid.

3. Results and discussion

3.1. Multiplex gas chromatograms, calibration, nicotine contents and accuracy

Fig. 4 shows a typical multiplex gas chromatograms obtained at various nicotine concentrations for capillary C in Table 2. The whole concentration series and corresponding peak areas are given in Table 2. In the chromatogram of a nicotine sample, only a single peak is present, although the average time between pulses, equivalent to repeated new injections, is 26 s (1792/69 + 0.120 = 26.09). A series of nicotine peaks would be expected with a distance of about 26 s. For conventional GC, the above conclusion can be drawn without question. However, in the MGC technique, chromatographic peaks from the modulation pulses are severely

Table 1
Diffusion time and corresponding depth of the nicotine meniscus below the capillary mouth (L)

Depth	Time (s × 3600)								
	0	24	49	72	96	120	144	168	192
L (cm)	2.99	3.38	3.69	3.95	4.18	4.42	4.62	4.79	4.95
L^2 (cm^2)	9.00	11.42	13.62	15.60	17.44	19.53	21.34	22.94	24.50

Temperature, 110°C; capillary I.D., 0.150 cm.

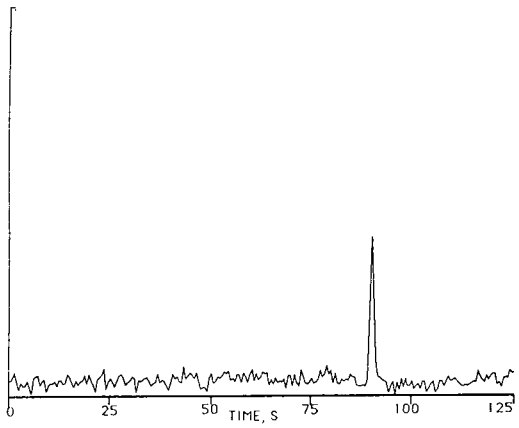

Fig. 4. Typical multiplex gas chromatogram for various nicotine concentrations using capillary C in Table 2. (C) $1.56 \cdot 10^{-6}$ g/ml from capillary of 5.33 cm × 0.150 cm I.D. Supelcowax 10 fused-silica column (25.0 m · 0.250 mm I.D.); stationary phase film thickness, 0.25 μm; modulator length, 8.0 cm; modulator resistance, 2.0 Ω; data acquisition rate, 2 Hz; modulator pulse duration, 0.120 s; modulation signal duration, 1792 data points (30.0 min); average time between pulses, (C) 1792/69 = 26.0 s; others (not shown), (A) 1792/63 = 28.4 s, (B) 1792/83 = 21.6 s, (D) 1792/70 = 25.6 s and (E) 1792/85 = 21.1 s (including a dead time of 4 s); carrier gas flow-rate, 6 ml/min; make-up gas flow-rate, 27 ml/min; sampler temperature, 110°C; column temperature, 220°C; detector temperature, 250°C.

overlapped at the detector, resulting in an output that is not directly interpretable, but a greater information content can be recovered with computer and presented in the form of a chromatogram by a computational technique such as cross-correlation or deconvolution. The computation required to recover the chromatogram is a very effective signal-averaging procedure that compensates for the decrease in sensitivity and dynamic range due to the small volume of each concentration pulse.

Fig. 5 shows multiplex gas chromatograms of different parts of cigarettes. Their nicotine contents are given in Table 3. From these, several attributes of nicotine contents in cigarettes are clear. First, by comparing the retention times of samples with that of the nicotine standard and by adding nicotine as an internal standard, one can identify the nicotine in the cigarettes (see Figs. 5E and 4C). Second, before smoking, the cigarette filter tip contains no nicotine, but after smoking, it contains a fairly high concentration of nicotine, i.e., ca. $4.5 \cdot 10^{-7}$ g/ml in a 0.0204-g cigarette filter tip. It can be concluded that cigarette filter tips play a good role of adsorbing nicotine. Third, in the part of a cigarette remaining after smoking, there is a high concentration of nicotine, showing that it also plays a role in adsorbing nicotine in cigarettes. Concerning the nicotine content, as the total mass of one cigarette is 0.7297 g (0.760 g of smoke and 0.1694 g of filter tip), the total amount of nicotine in an unsmoked cigarette is $2.57 \cdot 10^{-5}$ g/ml [$(0.7603/0.0204 \cdot 6.90 \cdot 10^{-7}$ g/ml] and the total amount of nicotine in a filter tip is $3.74 \cdot 10^{-6}$ g/ml [$(0.1694/0.0204 \cdot 4.50 \cdot 10^{-7}$ g/ml)]. It is more convenient to use this kind of concentration for monitoring the volatiles from solid samples and to prevent workers from being exposed to harmful chemicals. We have already used MGC and related techniques to determine trace organics in aqueous samples, using the quantitative concentration in ppb (v/v) [7].

Table 2
Peak areas obtained for various nicotine concentrations from different capillaries

Capillary I.D. (cm)	Length (cm)	Nicotine concentration		Peak area (cm^2)
		g/s	g/ml[a]	
(A) 0.053	2.00	$5.18 \cdot 10^{-8}$	$5.18 \cdot 10^{-7}$	44.7
(B) 0.150	8.00	$1.04 \cdot 10^{-7}$	$1.04 \cdot 10^{-6}$	75.0
(C) 0.150	5.33	$1.56 \cdot 10^{-7}$	$1.56 \cdot 10^{-6}$	111.2
(D) 0.150	4.00	$2.08 \cdot 10^{-7}$	$2.08 \cdot 10^{-6}$	149.5
(E) 0.150	3.20	$2.60 \cdot 10^{-7}$	$2.60 \cdot 10^{-6}$	203.2

[a] Carrier gas flow-rate 6.0 ml/min.

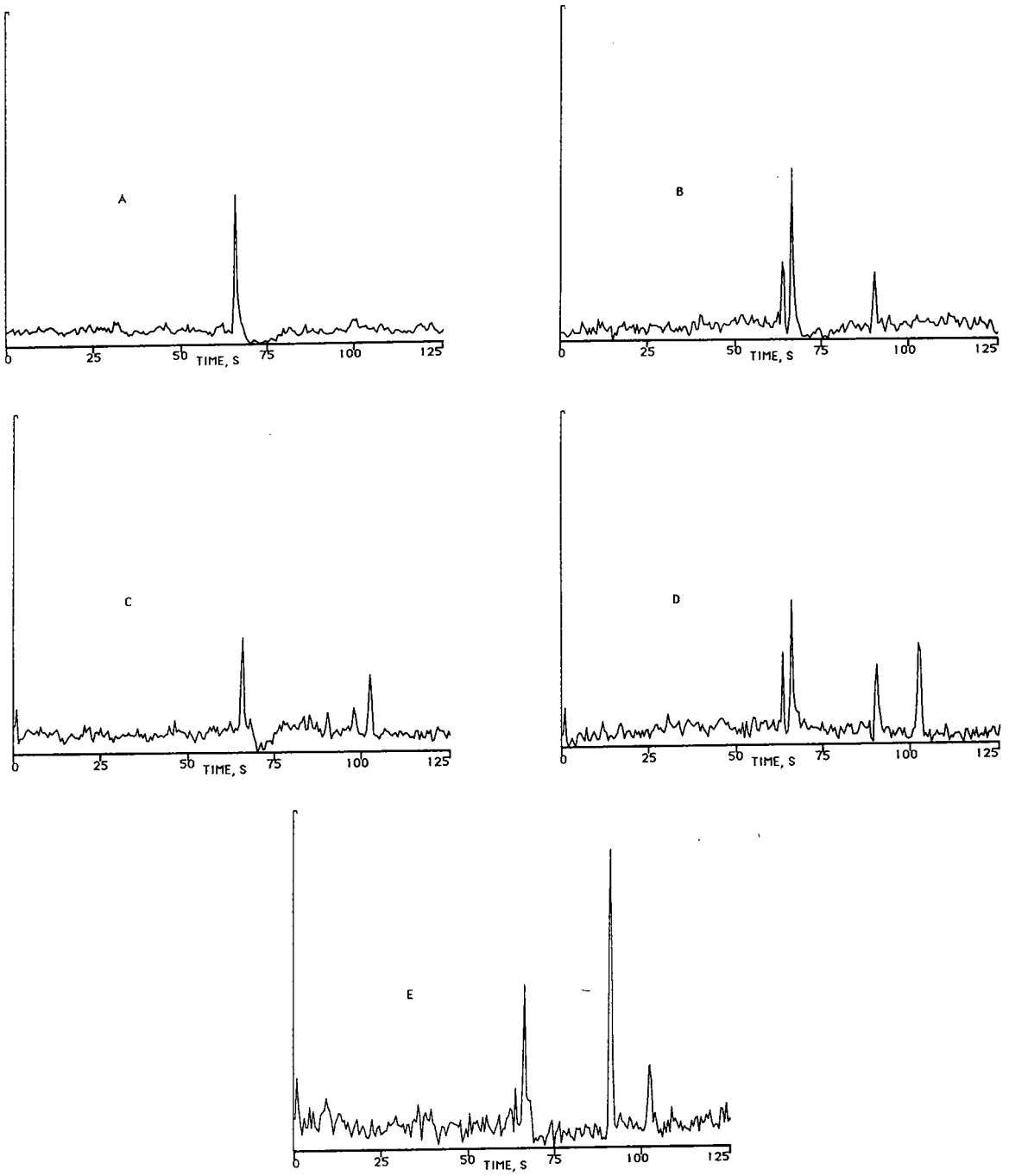

Fig. 5. Multiplex gas chromatograms of different parts of cigarettes. (A) Cigarette filter tip before smoking; (B) cigarette filter tip after smoking; (C) cigarette remaining after smoking; (D) unsmoked cigarette; (E) unsmoked cigarette with nicotine added. Average time between pulses; (A) 1792/80 = 22.4 s; (B) 1792/60 = 29.9 s; (C) 1792/67 = 26.7 s; (D) 1792/91 = 19.7 s; (E) 1792/78 = 23.0 s. Analytical conditions as those in Fig. 4.

Table 3
Nicotine contents of different parts of cigarettes

Part of cigarette	Mass (g)	Peak area (cm^2)	Nicotine concentration (g/ml)
Cigarette filter tip before smoking	0.0204	0	0
Cigarette filter tip after smoking	0.0204	32.3	$4.50 \cdot 10^{-7}$
Cigarette remainder after smoking	0.0204	14.1	$2.00 \cdot 10^{-7}$
Unsmoked cigarette	0.0204	50.3	$6.90 \cdot 10^{-7}$

The recovery of added nicotine was constant to within ±3%, indicating good accuracy (Table 4).

3.2. Reproducibility of nicotine determination by MGC

Table 5 shows that the relative standard deviation among five samples of the same cigarette was less than 3%. This indicates that the precision is comparable to that of other GC techniques.

3.3. Detection limit and sensitivity

By varying the I.D. and the length of capillaries and measuring the peak height, we obtained the detection limit, which is about $1.44 \cdot 10^{-13}$ g/ml (it was obtained using an 8.0 cm × 0.005 mm I.D. column as a capillary tube) and the sensitivity is $3.3 \cdot 10^{-2}$ A s/pulse/g). The detection limit is about two orders of magnitude below the concentration detection limit for a conventional single-injection determination using the same detector and column. This is a direct result of the long modulation signal.

Table 4
Recovery of nicotine added to unsmoked cigarettes

Parameter	First time		Second time		Third time		Fourth time	
	Peak area (mm^2)	Concentration (g/ml)	Peak area (mm^2)	Concentration (g/ml)	Peak area (mm^2)	Concentration (g/ml)	Peak area (mm^2)	Concentration (g/ml)
Unsmoked cigarette	50.3	$6.90 \cdot 10^{-7}$		$6.90 \cdot 10^{-7}$		$6.90 \cdot 10^{-7}$		$6.90 \cdot 10^{-7}$
Nicotine added		$2.08 \cdot 10^{-6}$		$1.04 \cdot 10^{-6}$		$5.18 \cdot 10^{-7}$		$2.59 \cdot 10^{-7}$
Total nicotine found	211.0	$27.1 \cdot 10^{-7}$	134	$17.2 \cdot 10^{-7}$	75.2	$12.2 \cdot 10^{-7}$	70.4	$9.57 \cdot 10^{-7}$
Nicotine recovered		$20.2 \cdot 10^{-7}$		$10.3 \cdot 10^{-7}$		$5.30 \cdot 10^{-7}$		$2.67 \cdot 10^{-7}$
Recovery (%)[a]		97		99		102		103

[a] Range ±3%.

Table 5
Reproducibility of nicotine determination by MGC

Mass of unsmoked cigarette (g)	Peak area (mm^2)	Nicotine concentration (g/ml)	Mean	S.D.	R.S.D. (%)
0.0204	50.3	$6.90 \cdot 10^{-7}$	$6.90 \cdot 10^{-7}$	$0.172 \cdot 10^{-7}$	2.5
0.0204	52.0	$7.11 \cdot 10^{-7}$			
0.0204	49.8	$6.77 \cdot 10^{-7}$			
0.0204	48.8	$6.70 \cdot 10^{-7}$			
0.0204	51.3	$7.04 \cdot 10^{-7}$			

The desorption modulator is a major component of the chromatographic instrumentation on a par with the detector and column. The modulation acts like an automatic and highly reproducible small-volume injection for a continuously flowing sample stream. A thermal desorption modulator has been used in high-speed GC analysis for sample preconcentration and introduction to monitor process streams [15] and in capillary GC for direct headspace sampling to determine the activity coefficients of binary liquids [16]. The multiplex and throughout advantages which have been exploited so successfully in the various Fourier and Hadamard transform spectroscopic methods apply also to MGC. A multiplex advantage exists because each output signal data point contains information encoded from the entire chromatogram; a throughout advantage exists because more sample is passed through the column to the detector per unit time than for batch separation chromatography. The output signal amplitude is directly proportional to the rate of sample flow through the chromatographic system while the amplitude of many noise sources remains constant.

The MGC peaks are very sharp because this modulation technique generates a very sharp injection and is limited by band broadening in the column usually caused by the dead volume, which is often large when a conventional sampling device is used.

The baseline noise is mainly correlation noise caused by approximations in the calculation, and could be eliminated by using a more sophisticated computational procedure. However, the "noise" does not limit detection because it is not random, while a modulation signal is a random signal which is generated by using a pseudo-random number algorithm [17].

3.4. Applications of MGC

The use of MGC in the analysis of real solid samples is reported here for the first time. Previously, we have reported the use of MGC to determine methane in ambient air [18] and trace organics in aqueous samples [7]. MGC with DHS is applicable to the analysis of soil, plastic wrappers for bread, plastic bags, etc. Typical multiplex gas chromatograms are shown in Fig. 6.

4. Conclusions

The use of MGC with DHS to determine nicotine in cigarettes was reported and some chromatograms of solid samples were presented. This technique has the following advantages: simple apparatus and sample introduction, no need for sample pretreatment, preconcentration, extraction or distillation, fairly good accuracy and precision, low detection limit and high sensitivity. It should be easy to carry out automatic analysis if the further modifications of the sampler are made, because the multiple pulses and data acquisition have already been computerized. Further work will be devoted to the

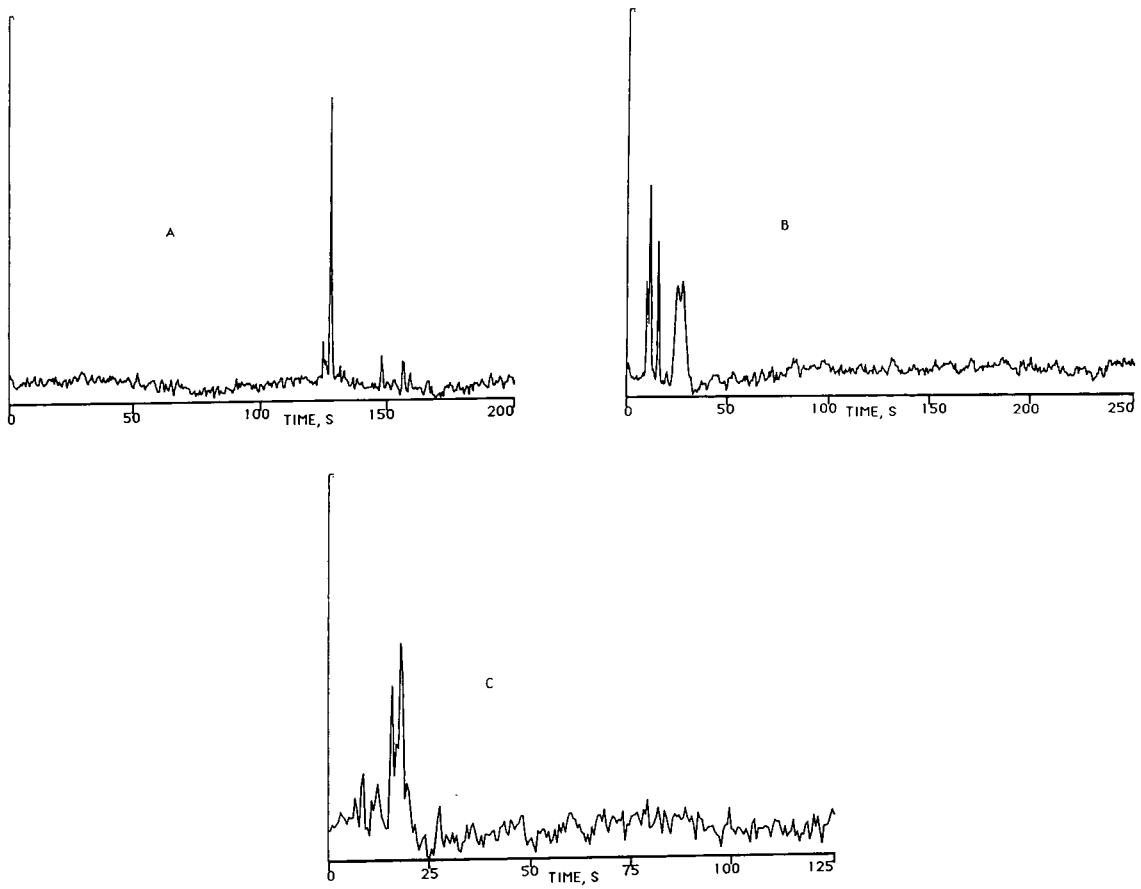

Fig. 6. Multiplex gas chromatograms of other solid samples. (A) Soil. Analytical column as in Fig. 4. Modulation signal duration, 7168 data points; average time between pulses, 7168/267 = 26.8 s; sampler temperature, 120°C; column temperature, 220°C; other conditions as in Fig. 4. (B) Plastic bag. SE-52 fused-silica column (6.0 m × 0.250 mm I.D.); stationary phase film thickness, 0.20 μm; modulator length, 8.0 cm; modulator resistance, 1.8 Ω; average time between pulses, 1792/66 = 27.2 s; carrier gas flow-rate, 3.0 ml/min; make-up gas flow-rate, 20.0 ml/min; sampler temperature, 100°C; column temperature, 120°C; other conditions as in Fig. 4. (C) Plastic wrapper for bread. OV-1701 fused-silica column (1.0 m × 0.050 mm I.D.); stationary phase film thickness, 0.20 μm; modulator length, 5.0 cm; modulator resistance, 1.5 Ω; modulation signal duration, 7168 data points; average time between pulses, 7168/253 = 28.3 s; carrier gas flow-rate, 0.14 ml/min; make-up gas flow-rate, 18.0 ml/min; data acquisition rate, 4 Hz; sampler temperature, 100°C; column temperature, 120°C; other conditions as in Fig. 4.

analysis of other solid samples and real environmental samples, with emphasis on quantitative analysis.

References

[1] H. Hachenberg and A.P. Schmidt, *Gas Chromatographic Headspace Analysis*, Heyden, New York, 1977, p. 37.

[2] B. Kolb and P. Pospisil, *Chromatographia*, 12 (1977) 705.

[3] B. Kolb, P. Pospisil and M. Auer, *J. Chromatogr.*, 204 (1981) 371.

[4] B. Kolb, *Chromatographia*, 9 (1982) 587.

[5] A. Venema, in *7th International Symposium on Capillary Chromatography, Nagara, Gifu, Japan, 11–14 May, 1986*, p. 92.

[6] J.B. Phillips, D. Luu, J.B. Pawliszyn and G.C. Carle, *Anal. Chem.*, 57 (1985) 2779.

[7] M. Zhang and J.B. Phillips, *Chromatographia*, 39 (1994) 294.

[8] C.O. Willits, M.L. Swain, J.A. Connelly and B.A. Brice, *Anal. Chem.*, 22 (1950) 430.
[9] R.H. Cuntiff and P.C. Markunas, *Anal. Chem.*, 27 (1955) 1650.
[10] A.H. Laurene and G.T. Harrell, *Anal. Chem.*, 30 (1958) 1800.
[11] R.B. Griffith and R.N. Jeffrey, *Anal. Chem.*, 20 (1948) 307.
[12] L.D. Quin, *J. Org. Chem.*, 24 (1959) 911.
[13] W. Horwitz (Editor), *Official Methods of Analysis of the Association of Official Agricultural Chemists*, AOAC, Washington, DC, 9th ed., 1960, p. 116.
[14] A.C. Savitsky and S. Siggia, *Anal. Chem.*, 44 (1972) 1712.
[15] Z. Liu, M. Zhang and J.B. Phillips, *J. Chromatogr. Sci.*, 28 (1990) 567.
[16] M. Zhang and J.B. Phillips, *J. Chromatogr.*, 478 (1989) 141.
[17] T.G. Lewis and W.H. Payne, *J. Assoc. Comput. Mach.*, 20 (1973) 456.
[18] J.R. Valentin, G.C. Carle and J.B. Phillips, *Anal. Chem.*, 57 (1985) 1035.

ELSEVIER

Journal of Chromatography A, 689 (1995) 285–304

JOURNAL OF CHROMATOGRAPHY A

Highly enantioselective capillary electrophoretic separations with dilute solutions of the macrocyclic antibiotic ristocetin A

Daniel W. Armstrong*, Mary P. Gasper, Kimber L. Rundlett

Department of Chemistry, University of Missouri–Rolla, Rolla, MO 65401, USA

First received 12 July 1994; revised manuscript received 5 September 1994; accepted 8 September 1994

Abstract

Ristocetin A is one of a series of structurally related amphoteric, glycopeptide, macrocyclic antibiotics. These compounds have several features that make them attractive as chiral selectors. These include spatially oriented functional groups that are known to provide the types of interactions that are conducive to enantio-recognition, a somewhat rigid "pocket" that can provide a site for hydrophobic interactions and polar, flexible arms (*i.e.*, pendent sugar moieties) that can rotate to hydrogen bond and otherwise interact with a variety of chiral analytes. In addition, these compounds are sufficiently soluble in water, aqueous buffers and aqueous–organic solvents that are commonly used in capillary electrophoresis (CE). The use and optimization of ristocetin A as a chiral selector in CE is discussed. Over 120 racemates are resolved including a variety of N-blocked amino acids, non-steroidal anti-inflammatory compounds and a large number of biologically important compounds containing carboxylic acid groups (e.g., mandelic acid derivatives, lactic acid derivatives, folinic acid, tropic acid).

1. Introduction

Recently, several macrocyclic antibiotics and their derivatives have been shown to be exceptional chiral selectors in capillary electrophoresis (CE) [1–3], HPLC [3,4] and TLC [5]. Because of the large number of these compounds and their structural variations, it is expected that they will have a significant impact on many types of enantiomeric separations. For example, ansamycins such as rifamycin B were used to resolve effectively a number of racemic amino alcohols using CE [1]. Conversely, vancomycin, which contains three small macrocyclic rings, effectively resolved over 100 negatively charged analytes, most of which contained at least one carboxylic acid functional group [2]. Vancomycin was also an effective chiral mobile phase additive for the reversed-phase TLC separation of enantiomers [5]. When bonded to 5-μm silica gel and packed in columns, rifamycin B, vancomycin and thiostrepton proved to be effective chiral stationary phases [3,4].

It appears that macrocyclic antibiotics may be more widely effective in CE than most other currently used chiral selectors. A review describing the development of chiral media for CE and future trends appeared recently [6]. Another new CE chiral selector, heparin, was also shown to resolve effectively several cationic compounds [7]. In this paper we describe a different mac-

* Corresponding author.

0021-9673/95/$09.50
SSDI 0021-9673(94)00875-2

rocyclic chiral selector, ristocetin A, and demonstrate that it is very useful in the CE resolution of a variety of racemic analytes.

Ristocetin A is produced as a fermentation product of *Nocardia lurida* [8–10]. As an antibiotic it is very active against Gram-positive bacteria including strains that are resistant to other antibiotics [9,10]. Its action results from selective binding to terminal D-Ala–D-Ala sequences in mucopeptides and inhibiting bacterial cell wall synthesis [11,12]. *Norcardia lurida* also produces a related component referred to as ristocetin B, which differs in the number of sugars in the side-chains. Ristocetin A has a molecular mass of 2066 and consists of an aglycone portion with four joined macrocyclic rings (two having sixteen members, one with fourteen members and one with twelve members) to which several sugars (e.g., arabinose, glucose, mannose and rhamnose) are covalently attached. The structure of ristocetin A is shown in Fig. 1. The ristocetins are related to other known macrocyclic antibiotics including vancomycin, β-avoparcin and teicoplanin [2,12]. As can be seen, ristocetin A has the functionalities and geometry that tend to accentuate chiral recognition between molecules in solution. This includes 38 stereogenic centers, seven aromatic rings, six amide bonds, 21 hydroxyl groups, two primary amine groups and one methyl ester. Together the four macrocyclic rings form a "basket"-like structure. This amphoteric compound is soluble in acidic aqueous solutions and less soluble at neutral pH. It is fairly soluble in polar aprotic solvents such as dimethyl sulfoxide (DMSO) and dimethylformamide (DMF), but insoluble in non-polar organic solvents.

In this work, we evaluated the chiral recognition properties of ristocetin A using CE. Its suitability as a chiral selector for enantiomeric separations and its similarities to and differences from other related chiral selectors are discussed.

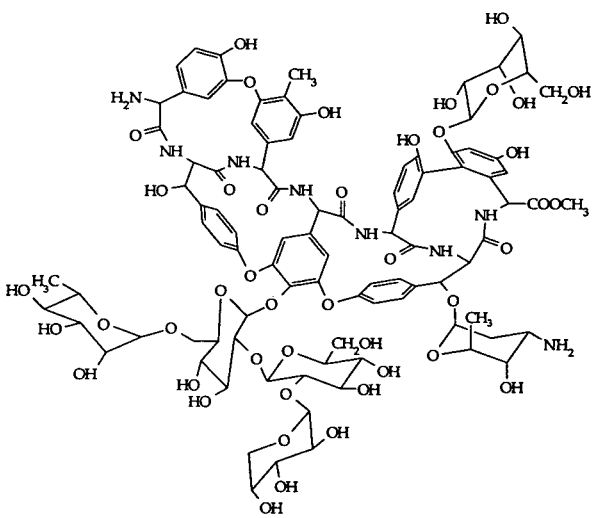

Fig. 1. Structure of ristocetin A ($M_r = 2066$) showing the "pocket" formed by the four fused macrocyclic rings and the polar, pendent carbohydrate moieties.

2. Experimental

2.1. Materials

All commercially prepared amino acids, amino acid derivatives, non-steroidal anti-inflammatory compounds, sodium dihydrogenphophate, potassium hydroxide, sodium hydroxide, amethopterin, folinic acid and ristocetin sulfate salt were purchased from Sigma (St. Louis, MO, USA). *p*-Chloromandelic acid was obtained from Chem Service (West Chester, PA, USA). All other chiral carboxylic acid compounds were purchased from Aldrich (Milwaukee, WI, USA). 6-Aminoquinolyl-N-hydroxysuccinimidyl carbamate (AQC) derivatizing reagent was supplied by Waters (Milford, MA, USA). 2-Propanol was of HPLC grade from Fisher Scientific (St. Louis, MO, USA).

2.2. Methods

Waters provided the Quanta 4000 capillary electrophoresis apparatus equipped with a fixed-wavelength UV lamp. All chiral separations were performed using a 32.5 cm (25 cm to the detector × 50 μm I.D.) fused-silica capillary obtained from Quadrex (New Haven, CT, USA) and detected at 254 nm. The capillary was prepared daily by conditioning with 0.1 *M* potassium hydroxide solution for 10 min. Next, the

capillary was purged with distilled water for 5 min followed by the appropriate concentration and pH of the running buffer for an additional 5 min. The 0.1 *M* sodium phosphate buffer solutions were prepared in a volumetric flask and adjusted to the desired pH with sodium hydroxide. Ristocetin solution was prepared in a volumetric flask, dissolved in the appropriate phosphate buffer and degassed by sonication. The aqueous buffer–organic modifier (2-propanol) mixture was prepared by volume. All samples were dissolved in distilled water and filtered with a 0.45-μm nylon syringe filter purchased from Alltech (Deerfield, IL, USA) prior to injection. The run voltage for all separations was +5 kV. Samples were hydrostatically injected for 3 or 5 s. Chiral separations were achieved with solutions of 0.1 mg/ml and at ambient temperature (22°C). The derivatization procedure for AQC amino acid compounds has been described previously [13]. The absorbance spectra were measured using a Hitachi Model U-2000 double-beam UV–Vis spectrophotometer.

3. Results and discussion

Ristocetin A has some structural similarities to vancomycin, which was shown previously to be an effective chiral selector in CE, HPLC and TLC [2,4,5]. The aglycone of ristocetin A consists of four fused macrocyclic rings rather than three [2,12]. In addition, ristocetin A has more pendant sugar moieties than vancomycin (Fig. 1). Hence the overall molecular mass of ristocetin A is about 36% more than that of vancomycin. However, vancomycin has two chloro-substituted phenyl rings in the central part of the aglycone that are not present in ristocetin A. As shown in Fig. 2, ristocetin A has zero electrophoretic mobility at pH $\approx$ 7.5 in 0.1 *M* phosphate buffer. This is only slightly higher than that found for vancomycin [2]. Hence at pH < 7.5 ristocetin A is positively charged and migrates in the same direction as the electroosmotic flow. Also, it would tend to interact electrostatically with anionic species.

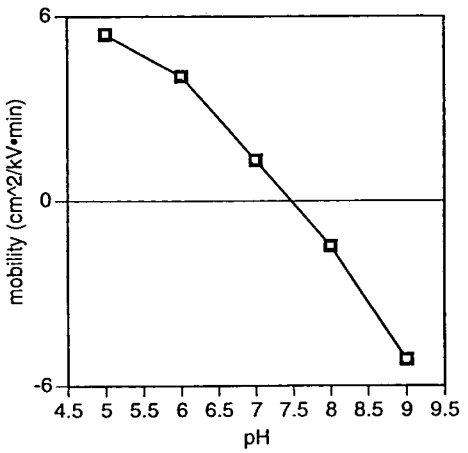

Fig. 2. Plot showing the electrophoretic mobility of ristocetin A at different pH. All runs were performed in 0.1 *M* phosphate buffer (see Experimental) with a 32.5 cm (25 cm to the detector) ×50 μm i.d. fused-silica capillary at a run voltage of +5 kV.

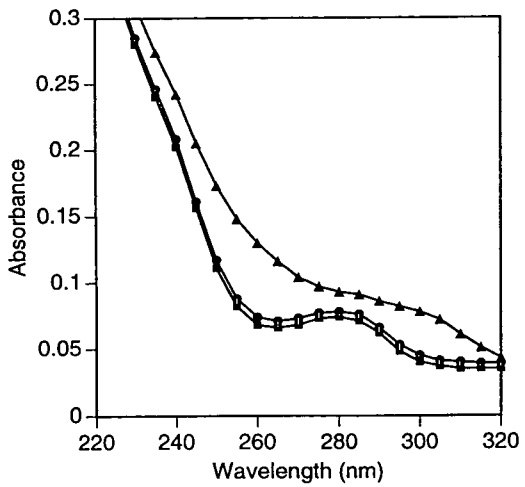

Fig. 3. UV absorbance spectra of ristocetin A (at a concentration of 7.2 $\cdot 10^{-3}$ mg/ml in 0.1 *M* phosphate buffer) at pH 4.0 (□), pH 7.0 (○) and pH 9.9 (▲).

Fig. 3 shows UV spectra of ristocetin A at pH between 4.0 and 9.9. Ristocetin A does not absorb light in the visible region to any significant extent. It is a weak absorber between 250 to 380 nm with a small maximum at ca. 282 nm (Fig. 3). Below 250 nm its absorbance increases significantly. Direct UV detection of aromatic

analytes can be used at wavelengths ≥254 nm. This is because of a combination of two factors: (a) the relatively low absorbance of the chiral selector at these wavelengths and (b) the very low concentrations of the chiral selector needed for the separations (i.e., between 1 and 5 m*M*). At alkaline pH there appears to be a slight red shift of the entire spectrum and a slight levelling of the spectral peaks and troughs (Fig. 3).

Table 1 lists the separation data for over 120 racemic compounds that were resolved using dilute solutions of ristocetin A. This includes all types of N-blocked amino acids (Fig. 4) and a variety of other acidic or anionic compounds. Non-steroidal anti-inflammatory compounds are particularly easy to resolve. The enantioselectivity of ristocetin A appears to be similar to that of vancomycin [2]. However, several chiral compounds containing carboxylic acid functional groups were resolved with ristocetin A that could not be separated with vancomycin. These include mandelic acid, 2-methoxymandelic acid, hexahydromandelic acid, 3-hydroxy-4-methoxymandelic acid, *o*-acetylmandelic acid, 3-methoxymandelic acid, *β*-phenyllactic acid, tropic acid, 2-bromo-3-methylbutyric acid, 1-benzocyclobutenecarboxylic acid and *p*-chloromandelic acid (Fig. 5). Ristocetin A appears to be complementary to

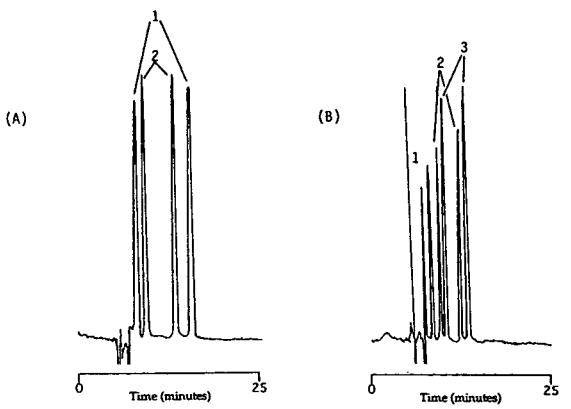

Fig. 4. (A) Electropherogram showing the resolution of racemic (1) N-benzoylalanine and (2) N-benzoylmethionine (B) electropherogram showing the resolution of racemic (1) AQC methionine, (2) AQC *α*-aminopimellic acid and (3) AQC serine. The running buffer was 0.1 *M* phosphate buffer (pH 6)–2 m*M* ristocetin A. The run voltage was 5 kV. See Experimental for further details.

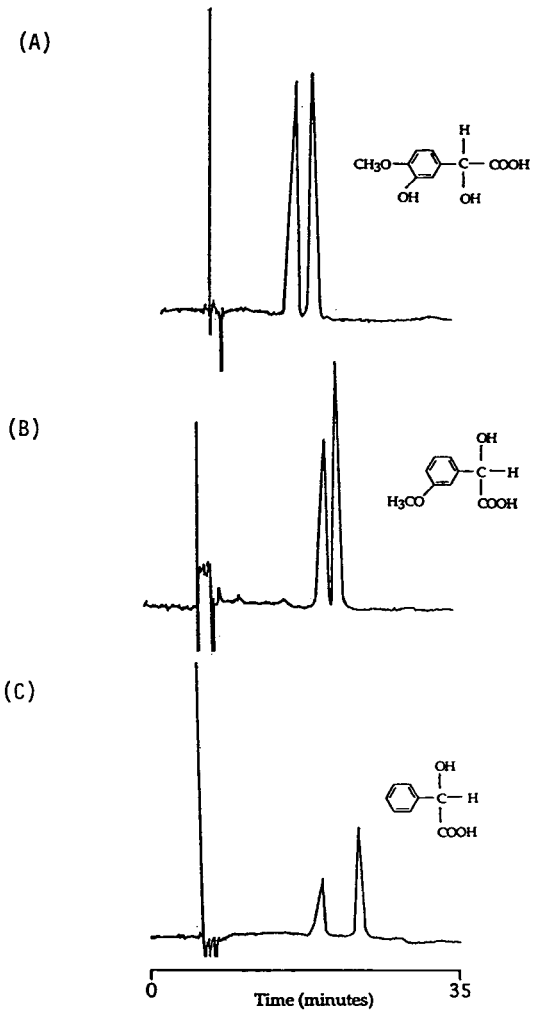

Fig. 5. Electropherograms showing the resolution of racemic (A) 3-hydroxy-4-methoxymandelic acid, (B) 3-methoxymandelic acid and (C) mandelic acid. The running buffer was of 0.1 *M* phosphate buffer (pH 6)–2 m*M* ristocetin A. The run voltage was 5 kV. See Experimental for further details.

rifamycin B and heparin (which resolve cationic compounds) when used as a CE chiral selector [1,7].

There are at least four other distinguishing features of ristocetin A-based CE separations compared with previous vancomycin-based separations. First, at all concentrations between 2 and 5 m*M* ristocetin A (without added organic co-solvent modifiers) the separation times were significantly less than those obtained using van-

Table 1
Enantiomeric resolutions, migration times and apparent and effective mobilities of enantiomers of amino acid derivatives, non-steroidal anti-inflamatory compounds and carboxylic acids separated with ristocetin

Compound	pH	Resolution	Time (1)[a]	Time (2)[b]	$\mu_e(1)$[c]	$\mu_e(2)$[c]
AQC Amino acids[d]						
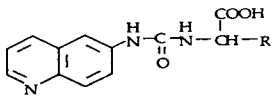						
Alanine CH_3-	7.0	9.4	8.8 (D)	12.6 (L)	−2.5	−8.0
Valine 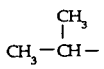	7.0	6.0	10.5	12.6	−5.4	−8.0
Leucine 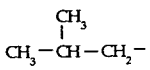	7.0	5.4	9.5 (D)	11.3 (L)	−3.9	−6.5
Isoleucine 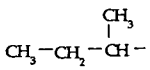	7.0	3.8	9.0	10.6	−2.8	−5.6
Isoserine 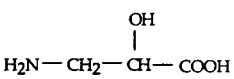	6.0	1.2	13.1	13.7	−8.6	−9.1
Homoserine[e] $HO-CH_2-CH_2-$	6.0	11.1	12.3	16.7	−0.9	−4.4
Norvaline[f] $CH_3-CH_2-CH_2-$	7.0	11.3	13.6	19.0	−1.9	−5.3
α-Amino-n-butyric acid CH_3-CH_2-	7.0	11.3	8.7 (D)	13.2 (L)	−2.2	−8.6
Proline[e] 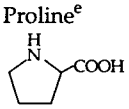	7.0	2.5	18.1	19.4	−4.9	−5.6
3,4-Dehydroproline 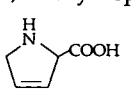	6.0	4.8	11.0	13.1	−6.2	−8.5
α-Aminopimelic acid $COOH-CH_2-CH_2-CH_2-CH_2-$	7.0	4.6	13.0	17.1	−8.4	−11.5

(Continued on p. 290)

Table 1 *(continued)*

Compound	pH	Resolution	Time (1)[a]	Time (2)[b]	$\mu_e(1)$[c]	$\mu_e(2)$[c]
α-Aminoadipic acid 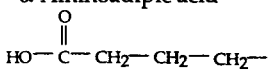	6.0	9.8	13.0	18.1	−5.2	−8.7
Asparagine 	6.0	5.8	11.1	13.6	−6.3	−9.0
Threonine 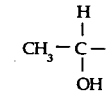	6.0	4.2	12.1	13.9	−4.6	−6.4
Ornithine[g] 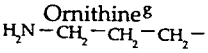	7.0	5.3	17.0	19.1	−4.3	−5.3
Phenlyalanine 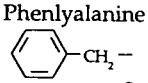	7.0	8.4	8.6	10.1	−2.1	−6.1
Tryptophan[g] 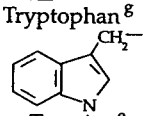	7.0	12.3	17.0	23.2	−4.3	−6.8
m-Tyrosine[e] 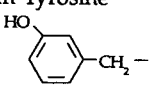	7.0	12.6	12.1	16.2	−0.3	−3.8
Serine[e] 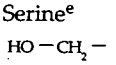	6.0	10.8	14.6 (D)	19.7 (L)	−2.1	−5.0
Norleucine 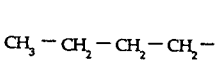	7.0	4.9	9.4	11.3	−1.8	−4.7
Methionine 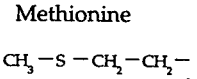	7.0	4.0	9.5	11.1	−3.8	−6.3
Indolelactic acid[d] 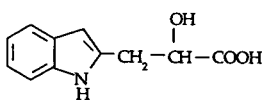	7.0	3.5	30.8	35.3	−4.0	−4.7
Nipecotic acid[h] 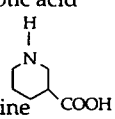	7.0	2.0	30.9	32.2	−4.0	−4.2
Citrulline 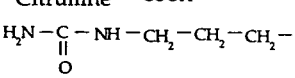	7.0	7.2	8.7	11.8	−2.3	−7.1

Table 1 *(continued)*

Compound	pH	Resolution	Time (1)[a]	Time (2)[b]	$\mu_e(1)$[c]	$\mu_e(2)$[c]
3-Fluorophenylglycine[f] 	7.0	11.2	12.8	18.0	−1.1	−4.8
3-Fluorophenylalanine[f] 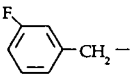	7.0	10.7	12.8	17.9	−1.1	−4.8
DOPA (Dihydroxyphenylalanine) 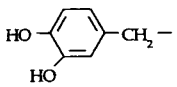	6.0	1.2	12.1	12.5	−7.5	−7.9
3-Amino-3-phenylpropionic acid[f] 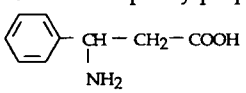	7.0	5.1	11.7	17.4	−2.7	−4.5
4-Chlorophenylalanine[h] 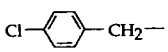	7.0	15.7	20.2	28.0	−1.2	−3.5
FMOC Amino acids[d]						
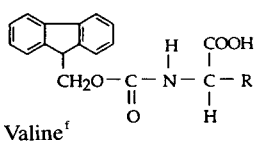 Valine[f] 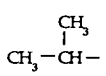	7.0	9.0	12.1	16.6	−3.6	−7.3
Alanine[f] 	7.0	0.4	14.7	15.0	−6.0	−6.2
DOPS (3,4-Dihydroxyphenylserine)[f] 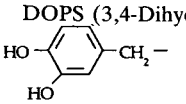	7.0	13.8	11.4	18.6	−2.8	−8.4
Citrulline 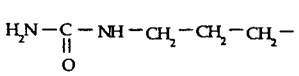	7.0	2.6	9.1	10.0	−1.3	−2.8

(Continued on p. 292)

Table 1 *(continued)*

Compound	pH	Resolution	Time (1)[a]	Time (2)[b]	$\mu_e(1)$[c]	$\mu_e(2)$[c]
Norleucine						
$CH_3-CH_2-CH_2-CH_2-$	7.0	0.7	7.4	7.6	−3.1	−3.7
Serine						
$HO-CH_2-$	7.0	2.4	10.9	12.1	−4.2	−5.6
Proline						
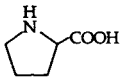	7.0	7.1	9.4	9.9	−1.7	−2.7
Homoserine[f]						
$HO-CH_2-CH_2-$	7.0	4.4	11.9	13.9	−3.5	−5.5
Isoserine[f]						
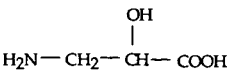	7.0	0.7	15.8	16.0	−6.8	−7.0
α-Amino-adipic acid						
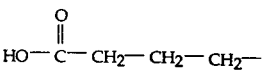	7.0	3.4	14.5	16.1	−5.9	−7.0
α-Amino-pimelic acid						
$COOH-CH_2-CH_2-CH_2-CH_2-$	7.0	4.9	16.2	18.7	−7.1	−8.4
Threonine[f]						
	7.0	0.9	16.2	16.6	−7.0	−7.3
β-Amino-isobutyric acid[f]						
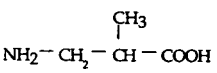	7.0	0.9	16.6	17.0	−7.3	−7.6
3,4-Dehydroproline						
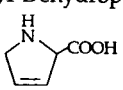	7.0	1.1	15.1	15.6	−8.4	−8.7
Dansyl Amino acids[d]						
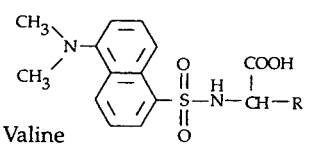						
Valine						
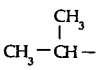	6.0	2.0	13.8	14.6	−5.8	−6.5

Table 1 *(continued)*

Compound	pH	Resolution	Time (1)[a]	Time (2)[b]	$\mu_e(1)$[c]	$\mu_e(2)$[c]
Leucine 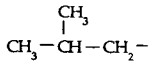	6.0	3.9	11.3	15.6	−3.3	−7.2
Aspartic acid 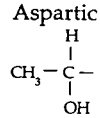	6.0	5.6	37.2 (D)	46.5 (L)	−13.3	−14.1
Phenylalanine 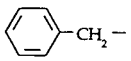	6.0	9.9	10.1	13.3	−1.6	−5.4
Tryptophan 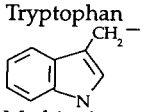	6.0	7.1	11.6	14.3	−3.6	−6.2
Methionine $CH_3-S-CH_2-CH_2-$	6.0	5.3	12.5 (D)	14.6 (L)	−4.7	−6.5
Norleucine $CH_3-CH_2-CH_2-CH_2-$	6.0	5.3	13.0	15.7	−5.1	−7.3
Norvaline $CH_3-CH_2-CH_2-$	6.0	4.7	12.9	14.6	−5.0	−6.5
α-Amino-n-butyric acid CH_3-CH_2-	6.0	3.9	12.6	14.1	−4.7	−6.1
α-Amino-n-caprylic acid $CH_3-CH_2-CH_2-CH_2-CH_2-CH_2-$	6.0	7.6	10.9	12.9	−2.7	−5.1
Serine $HO-CH_2-$	6.0	1.3	21.1	21.7	−6.2	−6.4

2,4-Dinitrophenyl Amino acids[d]

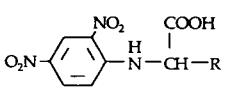

Methionine $CH_3-S-CH_2-CH_2-$ | 7.0 | 7.1 | 8.2 | 11.0 | −1.0 | −6.2

(Continued on p. 294)

Table 1 *(continued)*

Compound	pH	Resolution	Time (1)[a]	Time (2)[b]	$\mu_e(1)$[c]	$\mu_e(2)$[c]
Norleucine[h]						
$CH_3-CH_2-CH_2-CH_2-$	7.0	15.2	22.6	33.1	−2.1	−4.3
Norvaline[h]						
$CH_3-CH_2-CH_2-$	7.0	12.4	20.6	37.6	−1.4	−5.0
α-Amino-n-butyric acid[f]						
CH_3-CH_2-	7.0	3.1	19.0	20.0	−5.1	−5.7
Amino-n-caprylic acid[h]						
$CH_3-CH_2-CH_2-CH_2-CH_2-CH_2-$	7.0	14.7	22.5	29.1	−2.1	−3.7
Glutamic acid						
$HO-\overset{O}{\overset{\|}{C}}-CH_2-CH_2-$	7.0	10.8	12.3	22.8	−4.4	−10.5
Ethionine[f]						
$CH_3-CH_2-S-CH_2-CH_2-$	7.0	16.8	22.0	32.5	−2.7	−5.1
N-3,5-Dinitropyridyl Amino acids[d]						
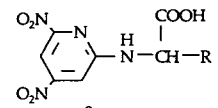						
Alanine[e]						
CH_3-	6.0	0.4	18.4	20.2	−5.3	−6.1
Leucine						
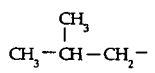	6.0	9.0	9.2	13.4	−3.2	−8.8
Serine						
$HO-CH_2-$	7.0	3.1	14.0	15.4	−9.4	−10.4
Tryptophan						
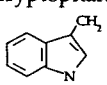	7.0	9.9	8.9	13.6	−2.7	−5.8
Methionine						
$CH_3-S-CH_2-CH_2-$	7.0	0.8	13.2	13.6	−8.7	−9.0
Carbobenzyloxy Amino acids[d]						
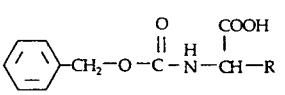	6.0	6.2	12.6	17.1	−4.7	−8.1
Alanine						
CH_3-						

Table 1 *(continued)*

Compound	pH	Resolution	Time (1)[a]	Time (2)[b]	$\mu_e(1)$[c]	$\mu_e(2)$[c]
Valine 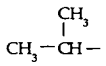	6.0	7.9	10.9 (D)	16.0 (L)	−2.7	−7.5
Leucine 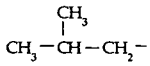	6.0	3.9	10.4	12.0	−2.0	−4.0
Serine 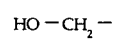	6.0	4.8	15.7	18.0	−7.3	−8.6
Glutamic acid 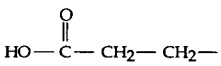	6.0	2.7	13.6	15.7	−5.7	−7.3
Methionine 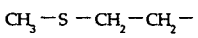	6.0	8.6	11.1 (D)	15.2 (L)	−3.0	−6.9
PHTH Amino acids[d] 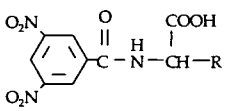						
α-Amino-n-butyric acid 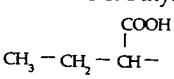	6.0	0.1	14.1	14.5	−6.1	−6.4
Methionine 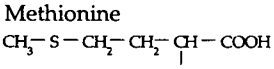	6.0	2.7	11.7	13.0	−3.8	−5.1
Valine 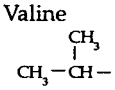	6.0	0.8	15.0	15.4	−6.8	−7.1
N-Benzoyl Amino acids[d] 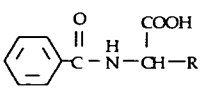	6.0	6.1	11.0	20.9	−2.9	−9.9
Alanine 						

(Continued on p. 296)

Table 1 *(continued)*

Compound	pH	Resolution	Time (1)[a]	Time (2)[b]	$\mu_e(1)$[c]	$\mu_e(2)$[c]
Valine 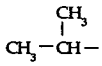	6.0	5.5	10.9	20.6	−2.7	−9.8
Methionine 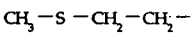	6.0	6.8	12.1	18.1	−1.3	−5.8
Leucine 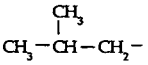	6.0	3.7	11.0	13.6	−6.3	−9.0
N-Formyl Amino acids[d]						
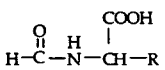 Tryptophan 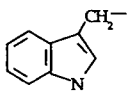	6.0	5.2	8.1	10.9	−4.9	−6.2
Phenylalanine 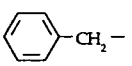	6.0	0.7	14.0	14.6	−3.9	−4.3
N-Acetyl Amino acids[d]						
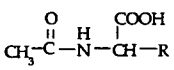 4-Fluorophenylalanine 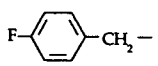	7.0	6.7	8.2	13.5	−1.0	−9.0
Phenylalanine 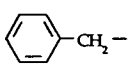	6.0	0.6	14.2	15.0	−4.0	−4.6
Non-steriodal anti-inflammatory drugs[d]						
Flurbiprofen 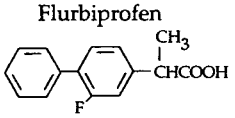	6.0	1.7	27.2	28.1	−8.8	−9.0
Indoprofen 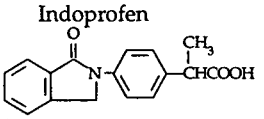	6.0	1.3	12.7	13.1	−4.8	−5.2

Table 1 *(continued)*

Compound	pH	Resolution	Time (1)[a]	Time (2)[b]	$\mu_e(1)$[c]	$\mu_e(2)$[c]
Carprofen 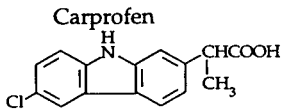	6.0	1.2	12.1	12.3	−7.4	−7.8
Ketoprofen 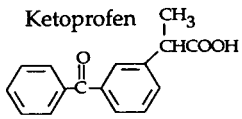	6.0	5.7	12.3	14.3	−4.4	−6.2
Suprofen 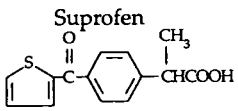	6.0	1.4	17.0	17.4	−8.1	−8.7
Fenoprofen 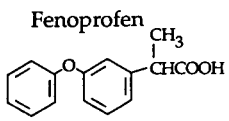	6.0	0.9	16.1	16.5	−7.6	−7.8
Naproxen 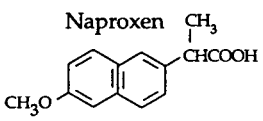	6.0	5.8	11.1	12.6	−3.0	−4.7
Other carboxylic acid compounds						
2-Phenoxypropionic acid[d] 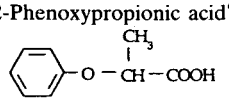	6.0	0.8	21.0	21.7	−13.2	−13.5
2-(2-Chlorophenoxy)propionic acid[d] 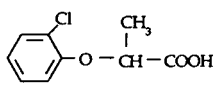	6.0	2.1	19.5	21.4	−12.6	−13.4
2-(3-Chlorophenoxy)propionic acid[d] 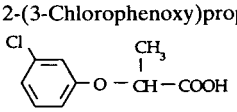	6.0	8.9	11.2	21.4	−3.1	−10.0
2-(4-Chlorophenoxy)propionic acid[d] 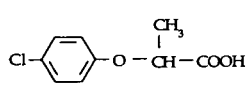	6.0	1.8	15.5	16.9	−10.6	−11.5

(Continued on p. 298)

Table 1 *(continued)*

Compound	pH	Resolution	Time (1)[a]	Time (2)[b]	$\mu_e(1)$[c]	$\mu_e(2)$[c]
Proglumide[d] 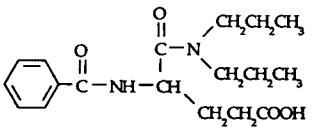	6.0	1.5	14.1	14.5	−9.4	−9.8
±-Dibromohydrocinnamic acid[e] 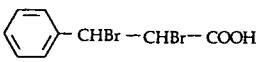	6.0	5.0	20.5	23.4	−6.9	−7.8
Indolelactic acid[d] 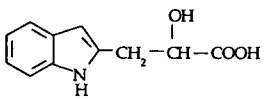	6.0	3.4	12.5	17.1	−8.0	−11.5
±-trans-4-Cotinine carboxylic acid[e] 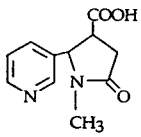	6.0	1.6	20.1	21.6	−6.7	−7.3
Iopanoic acid[e] 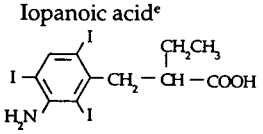	6.0	12.3	8.6	11.1	−2.3	−6.5
Iophenoxic acid[e] 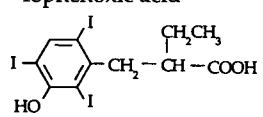	6.0	12.5	10.9	13.4	−6.2	−9.1
2-(4-Hydroxyphenoxy)propionic acid[f] 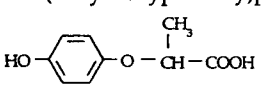	7.0	1.0	27.0	29.1	−9.1	−9.2
β-Phenyllactic acid[e] 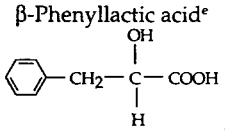	6.0	0.7	16.2	16.8	−4.7	−5.1
3-Phenylbutyric acid[d] 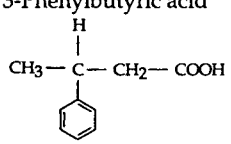	6.0	2.6	15.5	18.7	−10.7	−12.4

Table 1 *(continued)*

Compound	pH	Resolution	Time (1)[a]	Time (2)[b]	$\mu_e(1)$[c]	$\mu_e(2)$[c]
Tropic acid[d] 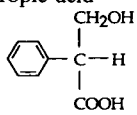	6.0	0.2	21.4	21.8	−13.4	−13.5
2-Bromo-3-methylbutyric acid[d] 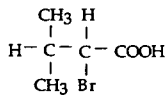	6.0	1.5	25.5	29.0	−14.8	−15.5
p-Chloromandelic acid[g] 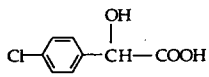	7.0	1.4	17.14	18.4	−11.5	−12.1
3-Hydroxy-4-methoxymandelic acid[d] 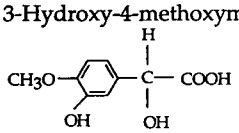	6.0	1.2	24.3	25.8	−11.0	−11.3
Hexahydromandelic acid[e] 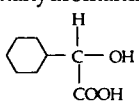	6.0	3.5	23.7	30.1	−10.8	−12.3
2-Methoxymandelic acid[d] 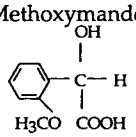	6.0	0.8	21.0	23.0	−13.2	−13.8
3-Methoxymandelic acid[d] 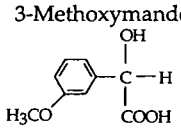	6.0	1.5	16.8	20.2	−11.5	−13.0
RS-O-Acetylmandelic acid[d] 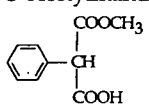	6.0	0.30	22.2	22.5	−13.6	−13.7
Mandelic acid[d] 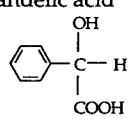	6.0	2.0	23.0	28.4	−13.9	−15.2
Benzocyclobutenecarboxylic acid[d] 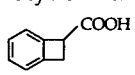	6.0	1.1	21.0	22.5	−13.2	−13.7

(Continued on p. 300)

Table 1 *(continued)*

Compound	pH	Resolution	Time (1)[a]	Time (2)[b]	$\mu_e(1)$[c]	$\mu_e(2)$[c]
3-Oxo-2-indancarboxylic acid[d] 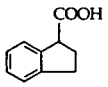	6.0	2.6	27.3	32.5	−10.3	−11.3
1,1′-Binaphthyl-2,2′-diyl hydrogen phosphate[d] 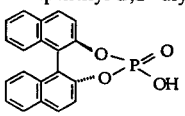	6.0	4.11	17.4	19.5	−5.4	−5.6
3-[4-Carbonyl]-PROXYL[d] 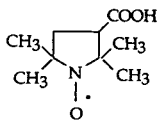	6.0	9.1	26.1	34.3	−12.9	−14.4
3-Methyl-2-phenylbutyric acid[d] 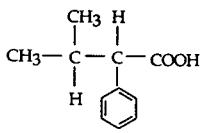	6.0	6.4	25.0	30.6	−8.3	−9.5
2-Phenylbutyric acid[f] 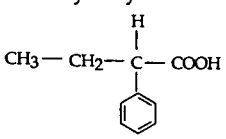	7.0	1.24	30.8	32.2	−9.5	−9.7
Di-0,0′-1-Toluoyl tartaric acid[d] 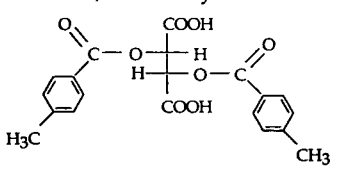	6.0	8.1	25.8	34.3	−8.5	−10.0
α-Aminothiophenacetic acid[d] 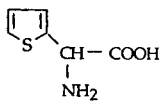	6.0	9.1	39.2	57.8	−13.9	−15.2
Hydroxymandelic acid[f] 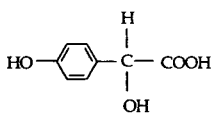	7.0	5.2	24.0	29.2	−11.3	−12.5

Table 1 *(continued)*

Compound	pH	Resolution	Time (1)[a]	Time (2)[b]	$\mu_e(1)$[c]	$\mu_e(2)$[c]
1,4-Dihydro-2-methylbenzoic acid[d] 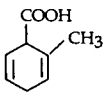	6.0	0.51	36.7	37.6	−10.3	−10.5
2-(4-Nitrophenyl)propionic acid[d] 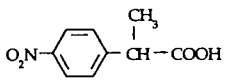	6.0	1.6	16.0	16.7	−4.6	−5.1
Amephoterin[g] 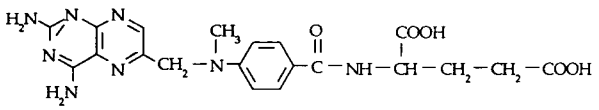	6.0	2.1	32.9	34.6	−6.7	−6.9
Folinic Acid[d,i] 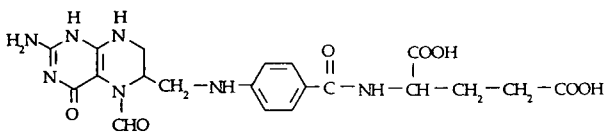	6.0	1.3	14.8	16.8	−10.0	−11.3
Atrolactic acid[d] 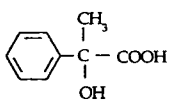	6.0	0.4	28.6	29.1	−15.3	−15.4

The run voltage for all separations was +5 kV. The pH and concentration of vancomycin are indicated. See the Experimental section for further details.

[a] Migration time (in minutes) of the first-eluting enantiomer.

[b] Migration time (in minutes) of the second eluting enantiomer.

[c] $\mu_e(1)$ and $\mu_e(2)$ are the effective electrophoretic mobilities of the first and second eluting enantiomer in $cm^2\ kV^{-1}\ min^{-1}$.

[d] 2m*M* ristocetin added to run buffer.

[e] 5m*M* ristocetin added to run buffer.

[f] 2m*M* ristocetin added to run buffer with 10% 2-propanol.

[g] 2m*M* ristocetin added to run buffer with 20% 2-propanol.

[h] 2m*M* ristocetin added to run buffer with 30% 2-propanol

[i] This is a diastereomeric separation of folinic acid.

comycin. Separation times with vancomycin as a chiral selector and using analogous conditions were typically between 40 and 70 min [2]. Second, as will be shown, organic modifiers can be used to enhance enantioresolutions substantially when using ristocetin A, but less so with vancomycin [2]. Third, aqueous solutions of ristocetin A appear to decompose more slowly than those of vancomycin [2]. Finally, the current cost of vancomycin is much less than that of ristocetin A.

As shown in Table 2, the concentration of ristocetin A in the running buffer can have a significant effect on the CE separation. In general, higher concentrations of the chiral selector produce higher enantioresolutions and longer

Table 2
Effect of ristocetin concentration on the migration times, effective mobilities and resolution of enantiomers

Ristocetin concentration (m*M*)	Compound	R_s	$t(1)^a$	$t(2)^a$	$t(EOF)^b$	$\mu_e(1)^c$	$\mu_e(2)^c$
2	2-(3-Chlorophenoxy)-propionic acid	8.9	11.2	21.4	7.6	−3.1	−10.0
	Ketoprofen	5.7	12.3	14.3	7.5	−4.4	−6.2
	3-Methoxymandelic acid	1.5	16.8	20.2	7.6	−11.5	−13.0
	1-Benzocyclobutene-carboxylic acid	1.1	21.0	22.4	7.5	−13.2	−13.7
5	2-(3-Chlorophenoxy)-propionic acid	22.1	11.6	29.3	11.5	−0.2	−8.7
	Ketoprofen	7.4	15.7	27.5	11.5	−3.8	−5.5
	3-Methoxymandelic acid	4.7	19.2	29.9	11.5	−5.8	−8.8
	1-Benzocyclobutene-carboxylic acid	1.8	42.5	49.6	11.5	−10.3	−10.9

The running buffer was 0.1 *M* phosphate buffer (pH 6) containing the indicated concentration of ristocetin.
[a] The migration times of the enantiomers, $t(1)$ and $t(2)$ are given minutes.
[b] The time corresponding to the electroosmotic flow, $t(EOF)$, is given in minutes. Note that a decrease in the EOF velocity results in an increase in $t(EOF)$.
[c] The effective mobilities, $\mu_e(1)$ and $\mu_e(2)$, are given in $cm^2\ kV^{-1}\ min^{-1}$.

separation times. The reason for the increase in analyte elution time is that higher concentrations of ristocetin tend to slow the electroosmotic flow (Table 2). This is because at these pHs the positively charged ristocetin tends to interact with the wall of the capillary. Increasing the phosphate buffer concentration lessens the wall interactions. However, there is a "trade-off", since increasing buffer concentration also increases heat generation and baseline noise and

Table 3
Effect of pH on the migration times, effective mobilities and resolution of enantiomers with ristocetin as a chiral selector

pH	Compound	R_s	$t(1)^a$	$t(2)^a$	$t(EOF)^b$	$\mu_e(1)^c$	$\mu_e(2)^c$
6	2-(3-Chlorophenoxy)-propionic acid	8.9	11.2	21.4	7.6	−3.1	−10.0
	Ketoprofen	5.7	12.3	14.3	7.5	−4.4	−6.2
	3-Methoxymandelic acid	1.5	16.8	20.2	7.6	−11.5	−13.0
	1-Benzocyclobutene-carboxylic acid	1.1	21.0	22.4	7.5	−13.2	−13.7
7	2-(3-Chlorophenoxy)-propionic acid	5.1	10.1	13.8	7.5	−4.9	−9.2
	Ketoprofen	2.6	12.6	13.7	7.5	−8.1	−9.1
	3-Methoxymandelic acid	1.1	18.1	20.2	7.4	−5.8	−6.7
	1-Benzocyclobutene-carboxylic acid	0.4	21.6	22.0	7.5	−13.4	−13.6

All separations were performed using 2m*M* ristocetin in 0.1 *M* phosphate buffer.
[a] The migration times of the enantiomers, $t(1)$ and $t(2)$, are given in minutes.
[b] The time corresponding to the electroosmotic flow, $t(EOF)$, is given in minutes. Note that a decrease in the EOF velocity results in an increase in $t(EOF)$.
[c] The effective mobilities, $\mu_e(1)$ and $\mu_e(2)$, are given in $cm^2\ kV^{-1}\ min^{-1}$.

usually requires a decrease in the run voltage. The buffer concentration used throughout this work (i.e., 0.1 *M* phosphate, see Experimental) was a compromise after taking into account all of the aforementioned factors. A similar "wall-interaction effect" was noted previously for vancomycin [2]. The wall adsorption does not seem to affect the run-to-run reproducibility as long as all experimental conditions are held constant.

The effective mobilities (μ_e) of the analytes (which have electromigrations opposite to the direction of the electroosmotic flow) decrease with increasing concentration of ristocetin A (Table 2). This is because a greater amount of the analyte is associated with the ristocetin A when the concentration of the chiral selector is increased. Hence the improvement in the enantiomeric separations at higher ristocetin A concentrations seems to be the result of two factors: (1) a greater time of association between the chiral selector and analytes due to mass action and (2) a greater time of association between the chiral selector and analyte due to the decrease in the electroosmotic flow.

Table 3 shows the effect of pH on the enantioseparation of typical racemic analytes in this study. In general, lower pHs give better enantioresolution. However, there is a limit to this

Table 4
Effect of concentration of 2-propanol as an organic additive on the migration times, effective mobilities and resolution of enantiomers with ristocetin as chiral selector

Organic solvent	Compound	R_s	$t(1)^a$	$t(2)^a$	$t(\mathrm{EOF})^b$	$\mu_e(1)^c$	$\mu_e(2)^c$
None	2-(3-Chlorophenoxy)-propionic acid	5.1	10.1	13.8	7.5	−4.9	−9.2
	Ketoprofen	2.6	12.6	13.7	7.5	−8.1	−9.1
	3-Methoxymandelic acid	1.1	18.1	20.2	7.4	−5.8	−6.7
	1-Benzocyclobutene-carboxylic acid	0.4	21.6	22.0	7.5	−13.4	−13.6
10% 2-Propanol	2-(3-Chlorophenoxy)-propionic acid	5.8	14.6	21.3	11.5	−3.0	−6.5
	Ketoprofen	4.5	19.6	21.8	11.5	−5.8	−6.7
	3-Methoxymandelic acid	1.8	28.0	33.2	11.5	−8.3	−9.2
	1-Benzocyclobutene-carboxylic acid	0.7	40.2	40.6	11.5	−10.1	−10.1
20% 2-Propanol	2-(3-Chlorophenoxy)-propionic acid	7.6	21.4	30.8	11.8	−2.7	−6.2
	Ketoprofen	5.7	26.3	29.8	11.8	−7.6	−8.4
	3-Methoxymandelic acid	2.3	39.6	47.5	11.8	−9.7	−10.4
	1-Benzocyclobutene-carboxylic acid	1.1	55.0	57.9	11.7	−10.9	−11.0
30% 2-Propanol	2-(3-Chlorophenoxy)-propionic acid	10.0	26.6	47.7	14.5	−2.4	−5.1
	Ketoprofen	5.79	37.6	43.1	14.6	−4.2	−4.8
	3-Methoxymandelic acid	5.22	63.5	89.6	14.5	−6.0	−6.7
	1-Benzocyclobutene-carboxylic acid	1.23	70.1	73.7	14.6	−11.3	−11.6

All separations were performed using 2 m*M* ristocetin in 0.1 *M* phosphate buffer (pH7) with the indicated volume percentage of organic solvent.

[a] The migration times of the enantiomers, $t(1)$ and $t(2)$, are given in minutes.

[b] The time corresponding to the electroosmotic flow, $t(\mathrm{EOF})$, is given in minutes. Note that a decrease in the EOF velocity results in an increase in $t(\mathrm{EOF})$.

[c] The effective mobilities, $\mu_e(1)$ and $\mu_e(2)$, are given in $\mathrm{cm^2\ kV^{-1}\ min^{-1}}$.

effect as decreasing the pH will significantly decrease the electroosmotic flow (thereby increasing analysis times) and eventually protonate the analytes, making them neutral species. At sufficiently low pH, these two effects inhibit or negate the CE enantioseparation.

Data showing the effects of using an organic modifier in the running buffer are given in Table 4. As found with another macrocyclic antibiotic (rifamycin B), the use of organic modifiers can significantly alter the enantioresolution in some instances [1]. The addition of 2-propanol to the running buffer tended to enhance the enantioresolution for most analytes. Also, the organic modifier greatly increased the analysis (elution) times as a result of the decreased electroosmotic flow velocity. The effect of enhancing the enantioresolution by adding an organic modifier varies with the analyte. Eventually a level of organic modifier is reached that decreases the enantioresolution [1]. Also, when using aqueous–organic solvent mixtures in CE for longer periods of time, one must take precautions to prevent differential evaporation of the solution which will affect reproducibility, analysis times, resolution, etc.

Ristocetin A can decompose with time in aqueous solution. This process is accelerated at acidic or basic pHs and at elevated temperatures. For example, acid hydrolysis removes the sugars and an amine-containing fragment from the molecule [10]. Interestingly, the degradation product remains active against Gram-positive bacteria. However, the overall stability of ristocetin A under typical CE operating conditions (e.g., pH 5–7 and temperatures of 15–25°C) seems to exceed that of vancomycin [2]. We have used solutions of ristocetin A for up to 4 weeks provided that they are refrigerated (ca. 4°C) overnight or when otherwise not in use.

4. Conclusions

Ristocetin A is clearly a highly useful chiral selector for resolving a variety of enantiomers. Most of the racemic analytes in this study contained a free carboxylic acid moiety somewhere in their structure. Several experimental factors can be adjusted to optimize the enantioresolution and analyses times. These include the concentration of the chiral selector, the pH of the running buffer and the addition of moderate amounts of organic modifiers to the running buffer. Direct UV detection at wavelengths >250 nm is feasible because of the low concentrations of ristocetin A needed to achieve enantioresolution and its modest absorbance at those wavelengths. Electrostatic interactions between the racemic analyte and the chiral selector appear to be important in achieving enantioselective association. Extensive mechanistic studies on this and related systems are in progress.

Acknowledgement

Support of this work by the National Institute of Health (NIH Grant BMT 2R01 GM36292-07) is gratefully acknowledged.

References

[1] D.W. Armstrong, K. Rundlett and G.L. Reid, III, *Anal. Chem.*, 66 (1994) 1690.
[2] D.W. Armstrong, K.L. Rundlett and J.-R. Chen, *Chirality*, 6 (1994) 496.
[3] D.W. Armstrong, presented at the *1994 Pittsburgh Conference*, Abstracts, No. 572.
[4] D.W. Armstrong, Y. Tang, S. Chen, Y. Zhou, C. Bagwill and J.-R. Chen, *Anal. Chem.*, 66 (1994) 1473.
[5] D.W. Armstrong and Y. Zhou, *J. Liq. Chromatogr.*, 17 (1994) 1695.
[6] T.J. Ward, *Anal. Chem.*, 66 (1994) 633A.
[7] A.M. Stalcup and N. Hgyei, *Anal. Chem.*, 66 (1994) 3054.
[8] J.E. Philip, J.R. Schrenk and M.P. Hargie, *Antibiot. Annu.*, (1956–57) 669.
[9] M.J. Ramansky, B.M. Limson and J.E. Hawkins, *Antibiot. Annu.*, (1956–57) 706.
[10] D.C. Jordan, in D. Gottlieb and P. Shaw (Editors), *Antibiotics*, Vol. 1, Springer, New York 1967, p. 84.
[11] M. Nieto and H.R. Perkins, *Biochem. J.*, 123 (1971) 789.
[12] D.L. Boger, Y. Nomoto and B.R. Teegarden, *J. Organ. Chem.*, 58 (1993) 1425.
[13] M. Pawlowska, S. Chen and D.W. Armstrong, *J. Chromatogr.*, 641 (1993) 257.

ELSEVIER

Journal of Chromatography A, 689 (1995) 305–311

JOURNAL OF CHROMATOGRAPHY A

Simultaneous determination of organic and inorganic anions in the sub-μmol/l range in rain water by capillary zone electrophoresis

A. Röder, K. Bächmann*

Fachbereich Chemie, Technische Hochschule Darmstadt, Hochschulstrasse 10, D-64289 Darmstadt, Germany

First received 6 July 1994; revised manuscript received 13 September 1994

Abstract

An electrolyte system using *p*-aminobenzoate was developed to determine anions in individual and size-classified rain drops. In comparison with other electrolyte systems it was found to be the most favourable for the analysis of organic acids with low mobility. Using a cationic additive, inorganic anions with high mobility could also be separated. Limits of detection lower than 50 nmol l^{-1} are attainable when sample stacking for enrichment is used.

1. Introduction

For the examination of scavenging processes in the atmosphere, rain drops can be collected in size classes and short time intervals with a Guttalgor [1,2]. The Guttalgor mainly consists of a dewar vessel filled with liquid nitrogen. Rain drops falling into the liquid nitrogen maintain their spherical shape during the freezing process. Consequently, it is possible to separate individual rain drops of different sizes using sieves of different mesh widths. Because of this special technique, the sample volume for chemical analysis is only about 5 μl.

To achieve a detailed understanding of the chemistry in rain, it is necessary to determine as many components as possible. However, owing to the low concentrations and the small sample volumes, only the main ionic components in rain could be determined, e.g., the anions chloride, nitrate, sulphate, formate and acetate [3]. The concentrations range from 10 to 100 μmol l^{-1}. The determination of dicarboxylic acids at low concentrations (<1 μmol l^{-1}) [4] is not yet possible. For inorganic anions and mono- and dicarbonic acids, several methods of determination have been reported, such as capillary zone electrophoresis (CZE), and ion chromatography [5–8]. Organic acids are mainly determined by GC [9–11]. However, no method fulfils all the necessary requirements: simultaneous determination of organic and inorganic anions; low limits of detection for the dicarboxylic acids; enrichment of the dicarboxylic acids in the presence of relatively high concentrations of inorganic anions; and analysis in small sample volumes (<5 μl).

This paper describes the development of a new electrolyte system for indirect UV detection in CZE that satisfies all these requirements.

* Corresponding author.

0021-9673/95/$09.50
SSDI 0021-9673(94)00895-7

2. Experimental

The experiments were performed on a SpectraPhoresis 1000 unit. The length of the untreated fused-silica capillary (I.D. 75 and 50 μm) was 70 cm and 63 cm to the detector window.

The exchange of bromide for hydroxide in a solution of 10 mmol l^{-1} tetradecyltrimethylammonium bromide (TTAB) was performed with the ion exchanger Amberlite IRA-904 (Serva, Heidelberg, Germany).

p-Aminobenzoate (p-AB) electrolyte was prepared from 3 mmol l^{-1} *p*-aminobenzoic acid (Merck) and 4.5 mmol l^{-1} sodium *p*-aminobenzoate (Aldrich), 0.76 mmol l^{-1} barium hydroxide (Merck) and 55 μmol l^{-1} tetradecyltrimethylammonium hydroxide (TTAH) in water purified with a Milli-Q system (Millipore). The acid solution was degassed under vacuum for 30 min in order to remove carbon dioxide, then the pH was adjusted to 9.6 with dilute ammonia solution.

Frozen rain drops were handled in an inert-gas box. With laboratory-made sieves it is possible to transfer the drops quickly into closable receptacles of appropriate size and controlled purity.

3. Results and discussion

3.1. Choice of electrolyte

The most important aspects of the electrolyte for indirect UV detection are its mobility and the limit of detection (LOD) that is attainable. The electrophoretic mobility can be calculated from the equivalent conductance at infinite dilution [12] and the LOD can be calculated by using the equation of Yeung [13].

To compare some frequently used electrolytes, including p-AB, a run with a standard consisting of 1 mmol/l of each dicarboxylic acid was carried out. The parameters that describe the electrolyte system are given in Table 1. Fig. 1 shows as an example three typical electropherograms from electrolyte systems with (A) high mobility (chromate), (B) medium mobility [*p*-hydroxybenzoate (p-HB)] and (C) low mobility [*p*-aminobenzoate (p-AB)]. In the chromate system (A) the peak height of the analytes decreases whereas the peak width increases with decreasing mobility. This system is not suitable for slow analytes.

The mobility of p-HB (Fig. 1B) is expected to be almost as low as that of p-AB. However,

Table 1
Comparison of chosen electrolyte systems for the determination of anions

Parameter	Chromate[a]	Phthalate[a]	Borate/phthalate[b]	p-HB[a]	Salicylate	p-AB	p-AB[50] [c]
Wavelength (nm)	266	254	200	254	232	264	250
Molar absorptivity, ε[d] (l mol^{-1} cm^{-1})	3900	1900	−25 000	15 100	2500	13 600	7000
Mobility[e] (cm^2 V^{-1} s^{-1} · 10^{-4})	8.8	5.5	5.3/5.5	3.5	3.7	3.1	3.1
Observed mobility (cm^2 V^{-1} s^{-1} · 10^{-4})	8.8	4.5	5.3	5.8	3.7	2.1	2.1
Electrolyte concentration (mmol l^{-1})	5	5	5/1	5	5	7.5	20
Current at 30 kV (μA)[f]	95	25	30	20	10	15	10
Working pH	8.0	5.4	9.0	9.4	9.6	9.6	9.6
LOD[g] (μmol l^{-1})	3.6	4.8	2.1	1.7	3.8	0.6	3.1

[a] Waters application note.
[b] Thermo Separation Products application note.
[c] High-concentration p-AB electrolyte using a capillary of 50 μm I.D.
[d] Ref. [12].
[e] Calculated from equivalent conductance at infinite dilution.
[f] Capillary 70 cm × 75 μm I.D.
[g] Calculated using equation of Yeung [13].

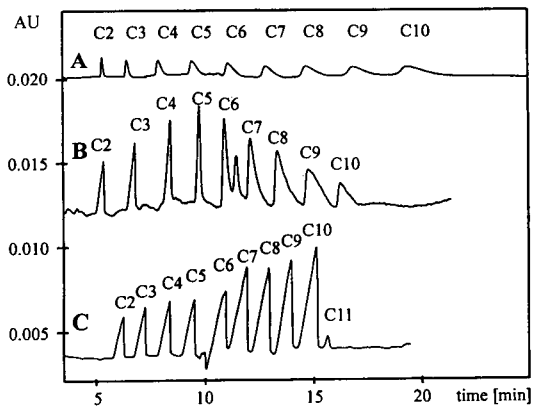

Fig. 1. Comparison of the chosen electrolytes. The run conditions are identical for all electrolyte systems: untreated fused-silica capillaries (70 cm × 75 μm I.D.) with detector window at 63 cm; separation voltage, −30 kV; temperature, 25°C; injection, 1 mmol/l of each dicarboxylic acid (C2–C10) for 1 s under vacuum (1.5 p.s.i.; 1 p.s.i. = 6894.76 Pa). (A) 5 mmol l^{-1} chromate, 55 μmol l^{-1} TTAH, pH 8.0; (B) 5 mmol l^{-1} p-HB, 55 μmol l^{-1} TTAH, pH 9.4; (C) 7.5 mmol l^{-1} p-AB, 55 μmol l^{-1} TTAH, pH 9.6. Peaks: C2 = oxalate; C3 = malonate; C4 = succinate; C5 = glutarate; C6 = adipate; C7 = pimelate; C8 = suberate; C9 = azelate; C10 = sebacate; C11 = undecanedioate.

because of the partly dissociated hydroxy group at pH 9.4, the mobility of phthalate is reached. The electropherogram indicates clearly that for analytes with mobility lower than that of the electrolyte, the peak broadening is larger than for analytes which are faster than the electrolyte. The peaks in the electropherograms of both phthalate systems show the same shape as that in the electropherogram obtained with the p-HB system.

The p-AB system (Fig. 1-C) shows increasing peaks up to the slowest analyte owing to the increasing transfer ratio [14], so that even undecanedioic acid (C11), which exists only as a trace contamination in the standard, was detected. Even for the analysis of rain samples this is advantageous because the fast inorganic anions show higher concentrations than slow organic acids. The peaks in the electropherogram of the salicylate system show the same shape as those in the electropherogram of the p-AB system, but the peak areas in the salicylate system are about five times smaller, as predicted from Yeung's equation, owing to the smaller molar absorptivity (see Table 1). The p-AB system is the optimum system for the determination of the dicarboxylic acids in rain samples, because the LOD decreases with decreasing analyte mobility (Table 2).

3.2. Concentration of electrolyte

High electrolyte concentrations result in a high enrichment factor and a large number of plates. The Joule heating and, for a high molar absorptivity, the linear range of the detector limited the concentration of the electrolyte. With a concentration of 7.5 mmol l^{-1} of p-AB in a capillary of 75 μm I.D., the maximum signal-to-noise ratio and the minimum LOD are obtained. This system is used to determine anions at trace levels in rain samples with small volumes (Fig. 2). Applying a capillary of 100 μm I.D., the concentration of the electrolyte had to be decreased

Table 2
LODs for anions

Anion	LOD[a] (nmol l^{-1})
Chloride	40
Sulphate	30
Nitrite	40
Nitrate	40
Formate	30
Acetate	20
Propionate	20
Methanesulphonate	30
Oxalate	30
Malonate	30
Maleate	20
Succinate	20
Glutarate	20
Adipate	20
Pimelate	10
Suberate	10
Azelate	10
Sebacate	10

[a] Evaluated from calibration graph [15].

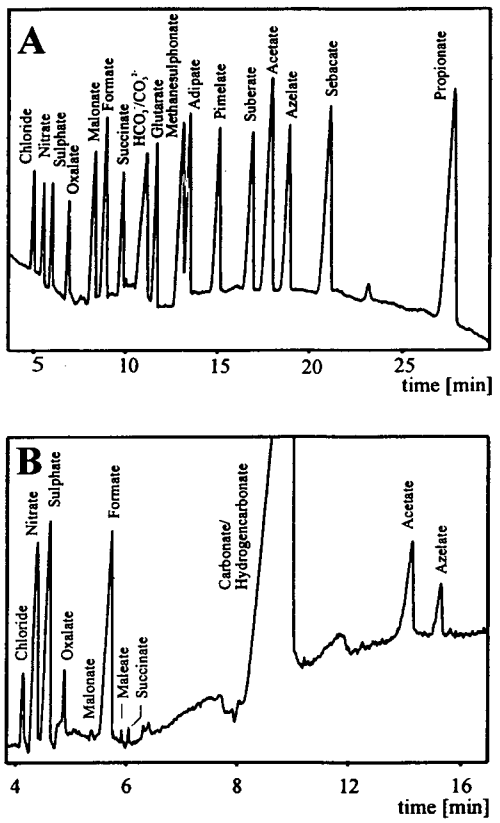

Fig. 2. Electropherograms of (A) a standard (10–25 μmol l^{-1}) and (B) a rain water sample. 7.5 mmol l^{-1} p-AB, 0.76 mmol l^{-1} $Ba(OH)_2$, 55 μmol l^{-1} TTAH (pH 9.4). Untreated fused-silica capillaries (70 cm × 75 μm I.D.) with detector window at 63 cm. Separation voltage, −30 kV; temperature, 25°C; hydrodynamic sample injection for 30 s under vacuum (1.5 p.s.i.).

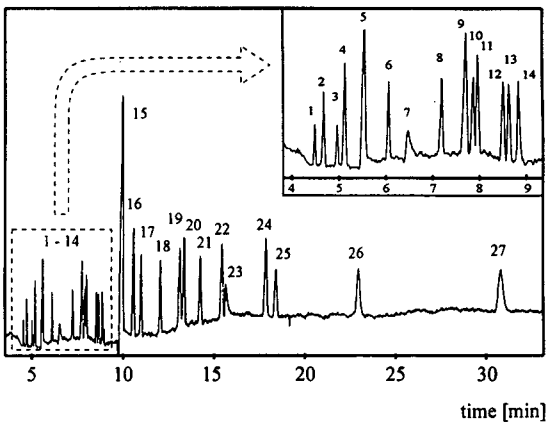

Fig. 3. Electropherogram of a standard with 27 anions (25–50 μmol l^{-1}). 20 mmol l^{-1} p-AB, 0.4 mmol l^{-1} $Ba(OH)_2$, 70 μmol l^{-1} TTAH (pH 9.6). Untreated fused-silica capillaries (70 cm × 50 μm I.D.) with detector window at 63 cm. Separation voltage, −30 kV; temperature 25°C; hydrodynamic sample injection for 3 s under vacuum (1.5 p.s.i.). Peaks: 1 = bromide; 2 = chloride; 3 = nitrite; 4 = nitrate; 5 = sulphate; 6 = oxalate; 7 = sulphite; 8 = malonate; 9 = formate; 10 = fumarate; 11 = maleate; 12 = succinate; 13 = malate; 14 = tartrate; 15 = carbonate; 16 = methanesulphonate; 17 = adipate; 18 = pimelate; 19 = acetate; 20 = suberate; 21 = azelate; 22 = sebacate; 23 = citronate; 24 = propionate; 25 = lactate; 26 = benzoate; 27 = mandelate.

to prevent thermal effects. In this case the resolution decreased. Using a capillary of 50 μm I.D. the efficiency of the separation was improved but the LOD increased. This trend can be enhanced by increasing the electrolyte concentration. Fig. 3 shows the electropherogram of a standard consisting of 27 anions performed with the p-AB[50] system (p-AB 20 mmol l^{-1}, capillary I.D. 50 μm, $\lambda = 250$ nm). That this system gives a two to three times better resolution and a five times higher LOD compared with the p-AB system with the lowest LOD (7.5 mmol l^{-1} p-AB, capillary I.D. 75 μm, $\lambda = 264$ nm).

3.3. Cationic additives

The separation of nitrate and sulphate was not possible without the addition of cations (Fig. 4), which decreased the mobility of sulphate by forming ion pairs. In addition, the mobility of dicarboxylic acids was also affected, especially for oxalate. It can be seen from Table 3 that barium is an optimum cationic additive, based on the solubility product of the different salts. Because of the good solubility of barium hydroxide it is possible to work at a high pH, which increases the dissociation of the organic acids and gives a low LOD. In Fig. 4B the effect of barium ions on the separation is shown. Sulphate is separated from nitrate and, further, the

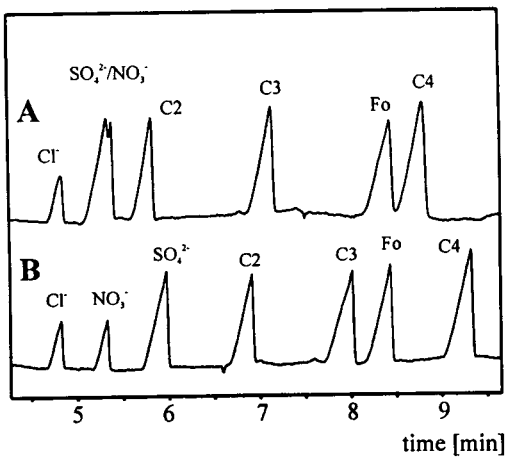

Fig. 4. Effect of a cationic additive on the separation. (A) Without additive; (B) with 0.76 mmol l^{-1} barium. Peaks: C2 = oxalate; C3 = malonate; C4 = succinate; Fo = formate.

mobility of the dicarboxylic acids decreases. The other cations listed in Table 3 influenced the mobility of the dicarboxylic acids more than that of sulphate.

3.4. Electroosmotic flow (EOF) modifier

At pH 9.6 the EOF is so fast that analytes which are slower than oxalate cannot reach the detection window at the anode side. A concentration of 55 μmol/l of TTAH in the electrolyte is sufficient to lower the EOF. Because the EOF is not reversed, sample stacking is possible. The use of TTAB would cause a positive system peak in the position where the bromide peak is expected. This interferes at higher chloride concentrations. By exchanging bromide in TTAB for the hydroxide ion this interference is eliminated.

Table 3
Comparison of the pK_L values (negative logarithm of the solubility product) of some cationic additives

Cation	Sulphate	Oxalate	Hydroxide
Calcium	4.21	8.75	8.33
Strontium	6.12	7.17	3.38
Barium	9.97	6.82	2.37
Lead	7.80	10.56	14.38

3.5. Sample injection and enrichment

Electrokinetic sample injection discriminates ions with low mobilities. This means for the analysis of rain samples that the higher concentration inorganic acids with high mobilities are enriched compared with the dicarboxylic acids, which are only partly dissociated in rain samples. This becomes obvious when the peak of phosphate (No. 11) is compared with that of methanesulphonate (No. 13) in Fig. 5. Both peaks have nearly the same size with hydrodynamic sample injection whereas the phosphate peak does not even reach half of the size of the

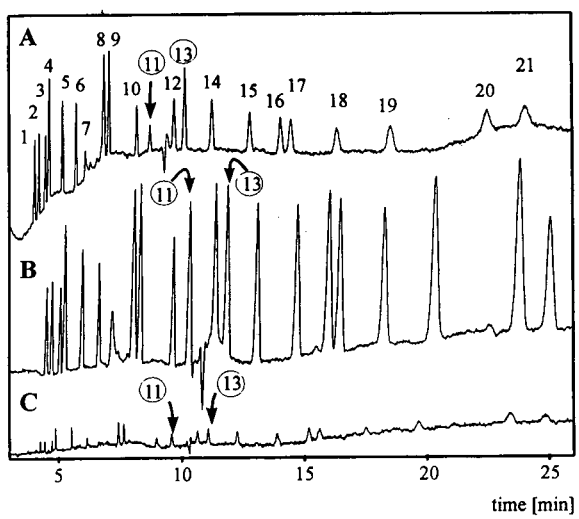

Fig. 5. Comparison of injection methods. (A) Electrokinetic sample injection, 5 s, 10 kV; (B) Hydrodynamic sample injection (sample stacking), 30 s, vacuum (1.5 p.s.i.); (C) Hydrodynamic sample injection, 1 s, vacuum (1.5 p.s.i.). Conditions: untreated fused-silica capillaries (70 cm × 50 μm I.D.) with detector window at 63 cm; separation voltage, −30 kV; temperature, 25°C. Peaks: 1 = bromide; 2 = chloride; 3 = nitrite; 4 = nitrate; 5 = sulphate; 6 = oxalate; 7 = sulphite; 8 = malonate; 9 = formate; 10 = succinate; 11 = phosphate; 12 = glutarate; 13 = methanesulphonate; 14 = adipate; 15 = pimelate; 16 = acetate; 17 = suberate; 18 = azelate; 19 = sebacate; 20 = propionate; 21 = lactate.

methanesulphonate peak with electrokinetic sample injection. The dissociation equilibrium of phosphoric acid in the sample (pH 4.5) differs from that in the electrolyte (pH 9.6), whereas methanesulphonic acid as a strong acid is completely dissociated in both the sample and the electrolyte. Therefore, the determination of weak acids in real samples is difficult and requires a lot of work and time. Electrokinetic sample injection is unfavourable for the determination of dicarboxylic acids in rain samples with small volumes.

With sample stacking no effects of discrimination arise and therefore the quantification is just as simple as with normal hydrodynamic sample injection. However, the migration time shift becomes stronger because of EOF variations caused by wall effects in the sample zone. The normally used correction of the peak area by migration time is sufficient for evaluation.

The high content of carbon dioxide in rain samples causes an interfering carbonate peak, but its migration time can be influenced by changing the pH of the electrolyte.

With 10% filling of the capillary, which corresponds to a sample volume of about 300 nl, the LOD given in Table 2 can be reached. With a higher sample volume the baseline noise becomes worse.

3.6. Results of the analysis of size-classified rain samples

As Fig. 6 demonstrates, the dicarboxylic acids show a different concentration–radius dependence than the monocarboxylic acids because of different scavenging processes, which will be studied in further investigations.

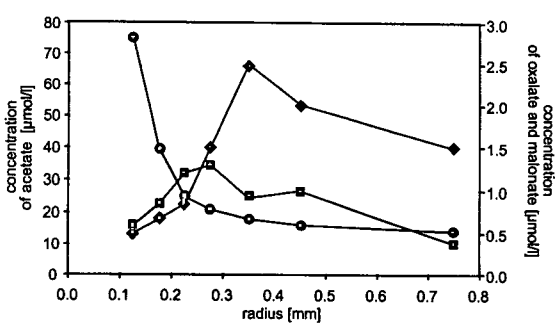

Fig. 6. Concentration of organic acids vs. droplet radius in rain samples. ○ = Acetate; □ = oxalate; ◇ = malonate.

4. Conclusions

The p-AB electrolyte system is suitable for determining simultaneously inorganic and the organic acids in small-volume rain samples. The separation of the inorganic anions is facilitated by the addition of barium ions. Using sample stacking as an on-line enrichment technique, low-concentration dicarboxylic acids can also be detected. With an injection of 300 nl the limits of detection are between 30 nmol l^{-1} for oxalate and 10 nmol/l for sebacinate. Because the EOF is decreased with TTAH, the running time is less than 30 min. In contrast to conventional electrolyte systems, the limit of detection decreases with decreasing mobility using the p-AB system.

Acknowledgements

We are grateful to Thermo Separation Products for supporting this work with a SpectraPhoresis 1000 unit. We also thank the DFG (Deutsche Forschungsgemeinschaft) for financial support as part of the SFB 233.

References

[1] K. Bächmann, A. Röder and I. Haag, *Atmos. Environ.*, 26A (1992) 1795.
[2] K. Bächmann, I. Haag and A. Röder, *Atmos. Environ.*, 27A (1993) 1951.
[3] K. Bächmann, I. Haag, T. Prokop, A. Röder and P. Wagner, *J. Chromatogr.*, 643 (1993) 181.
[4] G.E. Likens, E.S. Edgerton and J.N. Galloway, *Tellus*, 35B (1983) 16.
[5] K. Bächmann, K.-H. Steeg, T. Groh, A. Röder, I. Haumann and J. Boden, *Int. J. Environ. Anal. Chem.*, 49 (1992) 87.
[6] P. Jandik and W.R. Jones, *J. Chromatogr. A*, 546 (1991) 431.
[7] X. Huang, J.A. Lickey, M.J. Gordon and R.N. Zare, *Anal. Chem.*, 61 (1989) 766.

[8] W. Dannecker and K. Selker, *Fresenius' Z. Anal. Chem.*, 335 (1989) 966.
[9] K. Kawamura and I.R. Kaplan, *Environ. Sci. Technol.*, 21 (1987) 105.
[10] Y. Yokouchi and Y. Ambe, *Atmos. Environ.*, 20 (1986) 1727.
[11] H. Satsumabayashi, H. Kurita, Y. Yokouchi and H. Ueda, *Atmos. Environ.*, 24A (1990) 1443.
[12] D.R. Lide (Editor), *CRC Handbook of Chemistry and Physics*, CRC Press, Boca Raton, FL, 71st ed., 1990–91.
[13] E.S. Yeung, *Acc. Chem. Res.*, 22 (1989) 125.
[14] S.M. Cousins, P.R. Haddad and W. Buchberger, *J. Chromatogr. A*, 671 (1994) 397.
[15] *DIN 38402-A43, Ermittlung der Nachweis- und Bestimmungsgrenze von Kalibrierbedürftigen Analysenverfahren*, Beut, Berlin, 1984.

ELSEVIER

Journal of Chromatography A, 689 (1995) 312

JOURNAL OF CHROMATOGRAPHY A

Book Review

Aqueous Two-Phase Systems (*Methods in Enzymology*, Vol. 228), edited by H. Walter and G. Johansson, Academic Press, San Diego, CA, 1994, XXX + 725 pp., price US$ 99.00, ISBN 0-12-182129-3.

Partitioning in aqueous two-phase systems has been revealed as a useful technique for the purification and analytical studies of macromolecules, subcellular components and whole cells. The use of two-phase systems is simple and does not require sophisticated equipment in most instances.

Since the first systematic studies by Albertsson on partitioning of biomaterials in aqueous two-phase systems, this methodology has contributed to enriching the technical alternatives for a large number of preparative or analytical processes. Moreover, it has been possible to use phase partitioning to study complex biological phenomena, such as protein–protein interactions, and to incorporate into the basic principle of partitioning novel advanced techniques such as countercurrent distribution, magnetic-enhanced or affinity separation techniques. Lately this methodology has offered new insights into the large-scale liquid–liquid extraction of proteins of commercial interest. However, the well known reluctance of scientists to use novel methods in which they do not consider themselves to be experts has prevented a broader spread of this methodology.

This book is a very serious attempt to offer easily comprehensible and reproducible protocols for techniques dealing with a wide variety of isolation, characterization and analytical studies of biomaterials.

The volume consists of six sections. The first part deals with the fundamentals, general methodology and descriptions of the most commonly employed apparatus in two-phase systems separation. The next two parts contain selected techniques of conventional or affinity partitioning devoted to the extraction, separation and purification of macromolecules (proteins and nucleic acids) and particulates (cells, organelles, membranes and membrane domains). A specific section is devoted to studies on the interaction, characterization and conformational changes of proteins. Finally, after a minor section on biologically occurring two-phase systems, the book ends with a part on large-scale processes of interest in biotechnology, including downstream processing for extraction of specific proteins, concentration of viruses and removal of wastes.

The clear and detailed description of the techniques included in this book reflect good editorial work and an evident interest to facilitate the spreading of partitioning methodology. In conclusion, this is a valuable technical book for those who wish to apply this versatile methodology to their own technical problems.

Zaragoza, Spain M.J. López-Pérez

SSDI 0021-9673(94)00940-6

ELSEVIER

Journal of Chromatography A, 689 (1995) 313

JOURNAL OF CHROMATOGRAPHY A

Book Review

Introduction to Open-Tubular Column Gas Chromatography, by J.V. Hinshaw and L.S. Ettre, Advanstar Communications, Cleveland, OH, 1994, X + 190 pp., price US$ 24.95, ISBN 0-929870-25-5.

This small work is a revision of a publication entitled *Open Tubular Columns* which was published by the Perkin-Elmer Corporation in 1973. Since this time the technique has developed and matured and this is evident in that the current work has more than doubled in size. The work consists of seven major parts with two final minor parts which list the literature of open-tubular columns and a list of symbols that are used in the preceding parts.

The Introduction (Part I) is largely historical and effectively establishes that the early workers were aware of the potential of the technique which has simply been refined over the ensuing years.

Part II concerns the carrier gas and indicates the manner in which the mobile phase flows through the open-tubular column. Aspects of the pressure drop, the linear velocity, flow-rate and compression correction factors are included.

Part III concerns the separations achieved and considers the distribution process and the quantitative expression of the retention factor and phase ratio. The effect of the thickness of the stationary phase and the methods of expressing retention or separation are discussed.

Part IV considers band broadening and resolution and the influence of the individual terms in the Van Deemter Equation are outlined. Part V, entitled the Stationary Phase, considers first the role of the stationary phase before describing the wide variety of phases available and the several types of open-tubular columns.

The variables of open-tubular columns forms Part VI and a comparison with packed columns commences the part. The effect of the actual variables namely column inner diameter, column length, film thickness, carrier gas and temperature on separation are clearly explained.

Part VII considers the sample inlet system and following the sample introduction process the available types of inlets are each described. In Part VIII the major types of detectors as applicable to both packed and open-tubular column chromatography are considered. The particular detector requirements for use with open-tubular columns being included.

The work is well prepared by two acknowledged experts in the field. The fundamentals of gas chromatography applied to open-tubular columns is presented in a logical and clear sequential manner. The work is recommended as an addition to the bookshelf of both students and practising chromatographers who require a rapid insight into this extremely important area of chromatography.

Kensington, Australia J.K. Haken

SSDI 0021-9673(94)01082-X

Author Index

Carbohydrate Analysis

High Performance Liquid Chromatography and Capillary Electrophoresis

Edited by **Z. El Rassi**

Journal of Chromatography Library, Volume 58

The objective of the present book is to provide a comprehensive review of carbohydrate analysis by HPLC and HPCE by covering analytical and preparative separation techniques for all classes of carbohydrates including mono- and disaccharides; linear and cyclic oligosaccharides; branched heterooligosaccharides (e.g., glycans, plant-derived oligosaccharides); glycoconjugates (e.g., glycolipids, glycoproteins); carbohydrates in food and beverage; compositional carbohydrates of polysaccharides; carbohydrates in biomass degradation; etc.

The book will be of interest to a wide audience, including analytical chemists and biochemists, carbohydrate, glycoprotein and glycolipid chemists, molecular biologists, biotechnologists, etc. It will also be a useful reference work for both the experienced analyst and the newcomer as well as for users of HPLC and HPCE, graduates and postdoctoral students.

Contents: Part I. The Solute.

©1995 692 pages Hardbound
Price: Dfl. 425.00 (US$250.00)
ISBN 0-444-89981-2

ELSEVIER
An imprint of Elsevier Science

ORDER INFORMATION

ELSEVIER SCIENCE B.V.
P.O. Box 330
1000 AH Amsterdam
The Netherlands
Fax: +31 (20) 485 2845

For USA and Canada:
P.O. Box 945, New York
NY 10159-0945
Fax: +1 (212) 633 3680

US$ prices are valid only for the USA & Canada and are subject to exchange rate fluctuations; in all other countries the Dutch guilder price (Dfl.) is definitive. Customers in the European Union should add the appropriate VAT rate applicable in their country to the price(s). Books are sent postfree if prepaid.

Quality Assurance for Environmental Analysis

Method Evaluation within the Measurements and Testing Programme (BCR)

Edited by **Ph. Quevauviller, E.A. Maier** and **B. Griepink**

Techniques and Instrumentation in Analytical Chemistry, Volume 17

Quality assurance (QA) for environmental analysis is a growing feature of the nineties as is illustrated by the number of QA guidelines and systems which are being implemented nowadays. This book focuses on the technical aspects of quality assurance. The techniques used in different analytical fields are critically reviewed and existing tools for evaluating their performance are described. Particular reference is made to the activities of the Measurements and Testing Programme (BCR) of the European Commission towards the improvement of quality control of environmental analysis.

Contents: 1. Quality assurance for environmental analysis (Ph. Quevauviller *et al.*). 2. Development of ICPMS and ID-ICPMS with the determination of Pb and Hg in environmental matrices as an example (M. Campbell). 3. Detection of sources of error in the determination of Cr in environmental matrices by FAAS and ETAAS (G. Rauret *et al.*). 4. Analysis of environmental and biological samples by atomic spectroscopic methods (M. Hoenig, M.F. Gunn). 5. Validation of neutron activation analysis techniques (K. Heydorn). 6. Flow-through (bio)chemical sensors in environmental analysis (M.D. Luque de Castro, M. Válcarcel). 7. Fiber optical sensors applied to field measurements (C. Cámara *et al.*). 8. Chromium speciation in environmental and biological samples (K. Vercoutere, R. Cornelis). 9. Determination of aluminium species in natural waters (B. Fairman, A. Sanz-Medel). 10. Selenium speciation analyses in water and sediment matrices (C. Cámara *et al.*). 11. Antimony speciation in water (M.B. de la Calle- Guntiñas *et al.*). 12. Arsenic speciation in environmental matrices (A. Amran *et al.*). 13. Mercury speciation in biological matrices (I. Drabæk, Å Iverfeldt). 14. Speciation analysis of organolead compounds. Status and future prospects (R. Lobinski *et al.*). 15. Speciation analysis of organotin by GC-AAS and GC-AES after extraction and derivatization (W.M.R. Dirkx *et al.*). 16. High performance liquid chromatography - isotope dilution - inductively coupled plasma - mass spectrometry for lead and tin speciation in environmental samples (S.J. Hill *et al.*). 17. Speciation of organotin compounds in environmental samples by GC-MS (R. Morabito *et al.*). 18. Development of supercritical fluid extraction procedures for the determination of organotin compounds in sediment (J.M. Bayona). 19. Hydride generation for speciation analyses using GC/AAS (R. Ritsema *et al.*). 20. Single and sequential extraction schemes for trace metal speciation in soil and sediment (A.M. Ure *et al.*). 21. Methods for the determination of chlorinated biphenyls in air (M. Morosini, K. Balschmitter). 22. Sample handling and determination of carbamate pesticides and their transformation products in various matrices (M. Honing *et al.*). 23. Method development for the determination of polycyclic aromatic hydrocarbons (PAHs) in environmental matrices (J. Jacob). 24. Method validation for the determination of dioxins (T. Rymen). Subject index.

©1995 670 pages Hardbound
Price: Dfl. 475.00 (US$279.50)
ISBN 0-444-89955-3

ELSEVIER
An imprint of Elsevier Science

ORDER INFORMATION

ELSEVIER SCIENCE B.V.
P.O. Box 330
1000 AH Amsterdam
The Netherlands
Fax: +31 (20) 485 2845

For USA and Canada:
P.O. Box 945, New York
NY 10159-0945
Fax: +1 (212) 633 3680

US$ prices are valid only for the USA & Canada and are subject to exchange rate fluctuations; in all other countries the Dutch guilder price (Dfl.) is definitive. Customers in the European Union should add the appropriate VAT rate applicable in their country to the price(s). Books are sent postfree if prepaid.

PUBLICATION SCHEDULE FOR THE 1995 SUBSCRIPTION

Journal of Chromatography A and *Journal of Chromatography B: Biomedical Applications*

MONTH	O 1994	N 1994	D 1994	J 1995	
Journal of Chromatography A	683/1 683/2 684/1	684/2 685/1 685/2 686/1	686/2 687/1 687/2 688/1 + 2	689/1 689/2 690/1 690/2	The publication schedule for further issues will be published later.
Bibliography Section					
Journal of Chromatography B: Biomedical Applications				663/1 663/2	

INFORMATION FOR AUTHORS

(Detailed *Instructions to Authors* were published in *J. Chromatogr. A*, Vol. 657, pp. 463–469. A free reprint can be obtained by application to the publisher, Elsevier Science B.V., P.O. Box 330, 1000 AH Amsterdam, Netherlands.)

Types of Contributions. The following types of papers are published: Regular research papers (full-length papers), Review articles, Short Communications and Discussions. Short Communications are usually descriptions of short investigations, or they can report minor technical improvements of previously published procedures; they reflect the same quality of research as full-length papers, but should preferably not exceed five printed pages. Discussions (one or two pages) should explain, amplify, correct or otherwise comment substantively upon an article recently published in the journal. For Review articles, see inside front cover under Submission of Papers.

Submission. Every paper must be accompanied by a letter from the senior author, stating that he/she is submitting the paper for publication in the *Journal of Chromatography A* or *B*.

Manuscripts. Manuscripts should be typed in **double spacing** on consecutively numbered pages of uniform size. The manuscript should be preceded by a sheet of manuscript paper carrying the title of the paper and the name and full postal address of the person to whom the proofs are to be sent. As a rule, papers should be divided into sections, headed by a caption (*e.g.*, Abstract, Introduction, Experimental, Results, Discussion, etc.). All illustrations, photographs, tables, etc., should be on separate sheets.

Abstract. All articles should have an abstract of 50–100 words which clearly and briefly indicates what is new, different and significant. No references should be given.

Introduction. Every paper must have a concise introduction mentioning what has been done before on the topic described, and stating clearly what is new in the paper now submitted.

Experimental conditions should preferably be given on a *separate* sheet, headed "Conditions". These conditions will, if appropriate, be printed in a block, directly following the heading "Experimental".

Illustrations. The figures should be submitted in a form suitable for reproduction, drawn in Indian ink on drawing or tracing paper. Each illustration should have a caption, all the *captions* being typed (with double spacing) together on a *separate sheet*. If structures are given in the text, the original drawings should be provided. Coloured illustrations are reproduced at the author's expense, the cost being determined by the number of pages and by the number of colours needed. The written permission of the author and publisher must be obtained for the use of any figure already published. Its source must be indicated in the legend.

References. References should be numbered in the order in which they are cited in the text, and listed in numerical sequence on a separate sheet at the end of the article. Please check a recent issue for the layout of the reference list. Abbreviations for the titles of journals should follow the system used by *Chemical Abstracts*. Articles not yet published should be given as "in press" (journal should be specified), "submitted for publication" (journal should be specified), "in preparation" or "personal communication".

Vols. 1–651 of the *Journal of Chromatography*; *Journal of Chromatography, Biomedical Applications* and *Journal of Chromatography, Symposium Volumes* should be cited as *J. Chromatogr.* From Vol. 652 on, *Journal of Chromatography A* (incl. Symposium Volumes) should be cited as *J. Chromatogr. A* and *Journal of Chromatography B: Biomedical Applications* as *J. Chromatogr. B.*

Dispatch. Before sending the manuscript to the Editor please check that the envelope contains four copies of the paper complete with references, captions and figures. One of the sets of figures must be the originals suitable for direct reproduction. Please also ensure that permission to publish has been obtained from your institute.

Proofs. One set of proofs will be sent to the author to be carefully checked for printer's errors. Corrections must be restricted to instances in which the proof is at variance with the manuscript.

Reprints. Fifty reprints will be supplied free of charge. Additional reprints can be ordered by the authors. An order form containing price quotations will be sent to the authors together with the proofs of their article.

HPLC'95: Innsbruck, Austria

19th International Symposium on Column Liquid Chromatography

May 28–June 2, 1995

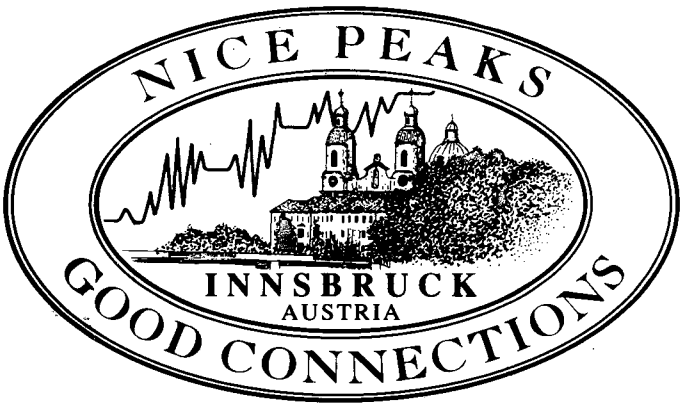

Chairman: **W. Lindner**
University of Graz
Austria

Honorary Chairman: **J.F.K. Huber**
University of Vienna
Austria

FORMAT: The HPLC'95 Symposium in Innsbruck follows the eighteen successful meetings held earlier in this series in Europe and the U.S.A. The format will be similar, covering a broad range of topical issues in Separation Science by oral and poster presentations, together with a series of Poster Discussion Sessions. An International Technical Exhibition on instrumentation, accessories and services will form an integral part of the scientific program.

TOPICS: The broad spectrum of Lecture and Poster Sessions will highlight recent advances in:
o Separation Methods, HPLC, SFC, HP-Affinity Chromatography, etc. o Capillary Electrophoresis o Hyphenated Techniques, Mass Spectrometry o Separation of Stereoisomers and Chiral Recognition o Separation Techniques in Biotechnology o New Developments of Sorption Materials o Preparative Techniques in Chromatography o Sample Preparation and Derivatization o Selective and Sensitive Detection Principles o Clinical, Pharmaceutical, Environmental Applications and Implications o Applications in Food Analysis o Chemometrics in Separation Science, Validation and Regulatory Issues.

The central core of the Symposium will focus on the **Poster Sessions**, which will provide a unique forum for lively discussions on recent research and new developments and for the exchange of ideas together with an informal opportunity to meet colleagues from all over the world. To facilitate a wider discussion of current research and its implications Poster Presenters will be invited to make short oral presentations in discussion group format.

HPLC'95 POSTER AWARD: To acknowledge the major input of Poster Presentations to the continuing success of these Symposia, a number of "HPLC'95 Poster Awards" have been established in order to recognize outstanding contributions to Separation Sciences. The First Prize will be US$ 3000.- to enable the winner to attend the next meeting in the series, HPLC'96 in San Francisco. Scientific calculators will be presented as second and third prizes. This endowment has been make possible by courtesy of Hewlett-Packard and will continue for subsequent Symposia in the series.

LAST MINUTE CONTRIBUTIONS: In view of the rapid development taking place in separation science, the Organisers will be happy to receive *last minute contributions* as **POSTER PRESENTATIONS**, if an Abstract is submitted by **May 10, 1995**

KEY DATES:	January/February 1995	Preliminary Program
	April 20, 1994	Deadline for early registration

ENQUIRIES: If you are interested in attending HPLC'95, please contact:
HPLC'95 Secretariat, Tyrol Congress, Marktgraben 2, A-6020 Innsbruck, Austria
Tel.: +43-512-575600, Fax.: +43-512-575607
or: Professor W. Lindner, Institute of Pharmaceutical Chemistry, Karl-Franzens-University of Graz, A-8010 Graz, Austria, Tel.: +43-316-380-5373, Fax: +43-316-384-6324.

0021-9673(19951213)689:2;1-H